

A hexagonal collision model for the numerical solution of the Boltzmann equation

*Von der Fakultät für
Mathematik und Naturwissenschaften
der Technischen Universität Ilmenau
zur Erlangung des akademischen Grades*

Doctor rerum naturalium (Dr. rer. nat.)

genehmigte Dissertation

vorgelegt von

M.Sc. Laek Sazzad Andallah

*geb. am 12.07.1967
in Nilphamari, Bangladesch*

Referenten:

Prof. Dr. rer. nat. habil. H. Babovsky
Prof. Dr. rer. nat. habil. A. Klar
Prof. Dr. rer. nat. habil. M. Junk

Tag der Einreichung: 10. November 2004
Tag der wissenschaftlichen Aussprache: 14. April 2005

*To my wife Fahmina, and to my mother and specially to the
memories of my father Late S. A. Nazlul Awal who passed away
on 24 March, 2005*

Contents

Introduction	5
1 The Boltzmann equation	13
1.1 The Liouville-equation	13
1.2 Particle interaction	15
1.2.1 The Boltzmann collision operator	17
1.3 Basic properties	19
1.3.1 Collision Invariant	19
1.3.2 Equilibrium solutions	21
1.4 The Macroscopic equations	22
1.5 The Linearized Collision Operator	25
1.6 Boundary conditions	26
2 Discrete Boltzmann equation in \mathbb{R}^2	29
2.1 Hexagonal Discretization of \mathbb{R}^2	29
2.2 A N -layer hexagonal model	39
2.2.1 Identification of Class-A and Class-B hexagons	44
2.2.2 Computational costs	54
2.3 Equilibria for a N -layer model	55
3 2D Numerical experiments	61
3.1 Computation of equilibria	61
3.2 Solution of the Boltzmann equation	69

3.2.1	The space homogeneous case	69
3.2.2	The space inhomogeneous case	73
4	Discrete Boltzmann equation in \mathbb{R}^3	77
4.1	Hexagonal discretization of \mathbb{R}^3	77
4.1.1	Hexagonal collision model in \mathbb{R}^3	80
4.2	The local collision model	86
4.2.1	A twelve-velocity model	86
4.2.2	H-Theorem, Equilibrium solutions	89
4.2.3	The linearized system	92
4.3	Collision model in a bounded hexagonal grid	95
4.3.1	Regular collision model	95
4.3.2	Linearizations	103
4.4	Layer-wise construction of symmetric model	106
4.4.1	The 120-velocity model	108
4.5	Model based on only binary collision law	112
4.5.1	H-Theorem, Equilibrium solutions	113
4.5.2	Regular collision model	114
4.5.3	Linearization	117
4.5.4	The 444-velocity model	119
5	3D Numerical experiments	121
5.1	Discrete equilibria	121
5.2	Solution of the Boltzmann equation	124
5.2.1	The space homogeneous case	124
5.2.2	Space inhomogeneous case	127
A	On the equilibria for the 3D model based on both binary and ternary collision law	129
B	On the equilibria for the 3D hexagonal model based on only binary collision law	133

Introduction

Kinetic equations with the nonlinear Boltzmann equation as prototype, describe the evolution of molecules of *rarefied gases* in which the average distance (the so-called *mean free-path*) travelled by a molecule between two subsequent collisions is not negligible in comparison with a length typical of the structure of the flow being considered. The degree of rarefaction of a gas is generally expressed through the *knudsen number*, $kn = \lambda/L$, where λ is the mean free-path and L is the characteristic dimension. The validity of continuum approach is identified with the validity of Navier-Stokes equations and the traditional requirements for this is that the knudsen number should be less than 0.1. In the limit of zero knudsen number the Navier-Stokes equation reduce to the inviscid Euler equation while the opposite limit of infinite knudsen number is the *collision-less* or *free-molecule* flow regime. The intermediate regime between the continuum and the free-molecule flow regime is called the so-called *transitional regime* and most problems in rarefied gas dynamics involve the transitional regime.

For $\mathbf{f} = \mathbf{f}(t, \mathbf{x}, \mathbf{v})$, a non-negative density function depending on the variables, time $t \in \mathbb{R}, t \geq 0$, the molecular velocity $\mathbf{v} \in \mathbb{R}^d$, $d \in \{2, 3\}$, and the space $\mathbf{x} \in \mathbb{R}^m$, $m \in \{1, \dots, d\}$, the nonlinear Boltzmann equation is given by

$$(\partial_t + \mathbf{v} \cdot \nabla_{\mathbf{x}})\mathbf{f}(\mathbf{v}) = \mathbf{J}[\mathbf{f}, \mathbf{f}] \quad (0.1)$$

where

$$\mathbf{J}[\mathbf{f}, \mathbf{f}] := \int_{\mathbb{R}^d} \int_{S^{d-1}} k(\mathbf{v} - \mathbf{w}, \eta) [\mathbf{f}(\mathbf{v}')\mathbf{f}(\mathbf{w}') - \mathbf{f}(\mathbf{v})\mathbf{f}(\mathbf{w})] d^2\eta d^3\mathbf{w} \quad (0.2)$$

is a $(2d - 1)$ -fold integral known as *Boltzmann collision operator*. Here $k(., .)$ is the collision kernel in the operator satisfying some symmetry properties, the post collision velocities \mathbf{v}', \mathbf{w}' result from the pre-collision velocities \mathbf{v}, \mathbf{w} satisfying the collision relations,

$$\text{conservation of momentum} \quad \mathbf{v} + \mathbf{w} = \mathbf{v}' + \mathbf{w}',$$

$$\text{conservation of kinetic energy} \quad (|\mathbf{v}|^2 + |\mathbf{w}|^2) = (|\mathbf{v}'|^2 + |\mathbf{w}'|^2).$$

Such a pair $\mathbf{v}', \mathbf{w}' \mapsto \mathbf{v}, \mathbf{w}$ can be parameterized by unit vectors $\eta \in S^{d-1}$ with the transformation $T_\eta(\mathbf{v}, \mathbf{w})$ as

$$\mathbf{v}' = \mathbf{v} - \langle \mathbf{v} - \mathbf{w}, \eta \rangle \cdot \eta$$

$$\mathbf{w}' = \mathbf{w} + \langle \mathbf{v} - \mathbf{w}, \eta \rangle \cdot \eta$$

Some details of these has been described in Chapter 1.

For the space homogeneous and for some other special cases, there has been several investigations on the general solution of (0.1) (see [51],[1],[9],[14],[31], [35],[49]). In these special cases, there are some information about the existence and uniqueness of the solution of the Boltzmann equation. However, we are concerned with the numerical simulation techniques for the Boltzmann equation.

The field of numerical simulation techniques for the Boltzmann equation has seen a real challenge for the numerical methods. This is due to the complexity of the $(2d - 1)$ -fold integral (the Boltzmann collision operator), which has to be numerically evaluated at each point in the (discretize) six-dimensional space. Moreover, the modelling of the Boltzmann collision operator have to be satisfied the kinetic features of the classical kinetic theory which becomes very crucial for regular grids of the velocity space. When choosing a pair of pre-collision velocities \mathbf{v}, \mathbf{w} belonging to the collision sphere in a regular grid, the pair of post-collision velocities \mathbf{v}', \mathbf{w}' are in general very sparsely populated and therefore one has to choose a very fine grid. Approximating the post-collision pair \mathbf{v}', \mathbf{w}' by some pairs close to the collision sphere might violate the microscopic conservation laws and is not accepted in general.

Most numerical computations of the Boltzmann equation are based on probabilistic Monte Carlo techniques at different levels. e.g. the *direct simulation Monte Carlo method* (DSMC) by Bird [15] and the modified Monte Carlo method by Nanbu [52]. Detailed description of these methods can be seen in ([12], [15], [25], [40], [59]). In the probabilistic method, the computational costs is much reduced and can be considered approximately of the order of the number of points n . The DSMC methods are mathematically well-understood (see [10], [11], [53], [55], [63]) and has been used with good success in many cases.

On the other hand, because of stochastic character, the DSMC method suffers from low accuracy and gives fluctuating results with respect to finite difference or finite volume methods. In general the convergence is slow and in particular for small knudsen number the convergent rate is very slow. But high accuracy is needed for coupling of the Boltzmann and the fluid dynamic domain. Moreover DSMC methods are still not very well-understood for the computation of stationary flows. In contrary to the probabilistic approaches the deterministic methods enable, in principle, an error estimation and calculation of the rate of convergence. In such cases, it is thus necessary to prefer deterministic methods, based on the classical

discretization of the Boltzmann collision operator. Therefore, we are concerned with the numerical computations of the Boltzmann equation based on deterministic method.

Several deterministic computational approaches have been proposed ([29], [32], [39], [56], [64]) to avoid fluctuations which are specially designed for the numerical solution of the problem in which particle methods are expensive to obtain sufficient accuracy. But these works are for the case of linearized Boltzmann equation or for some particular models.

The so-called *discrete velocity models* (DVM) as a deterministic method in which the velocities of molecules are confined to a finite set vectors has been used for solving the Boltzmann equation. The DVMs were introduced in kinetic theory first by Carleman [23] and Broadwell [19], [20] for the better understanding of the solution of the Boltzmann equation. In the past decades a kinetic theory on DVMs has been established, e.g. the classical work of Gatignol [36]. For the mathematical aspects of the theory concerning global existence and fluid dynamic limit we refer the review article of Platkowski and Illner [58]. Results on stability, consistency and convergence of the DVM can be seen in [16], [17], [57]. In [43], Junk and Rao has presented a new DVM based on the methodology of kinetic schemes.

The DVM approximate the $(2d - 1)$ -fold collision integral on a discrete lattice in the velocity space. For a regular grid in $\mathbb{R}^d : \{v_i \in \mathbb{R}^d; i = 1, \dots, M\}$, let $f_i(t, \mathbf{x}) \approx f(t, \mathbf{x}, \mathbf{v}_i)$, $i = 1, \dots, M$, then the standard form discrete velocity model for the Boltzmann equation reads

$$\begin{aligned} (\partial_t + \mathbf{v}_i \cdot \nabla_{\mathbf{x}}) f_i(t, \mathbf{x}) &= \sum_{j,k,l} A_{i,j}^{k,l} [f_k(t, \mathbf{x}) f_l(t, \mathbf{x}) - f_i(t, \mathbf{x}) f_j(t, \mathbf{x})] \\ &=: J[\mathbf{f}, \mathbf{f}]_i, \quad i = 1, \dots, M, \end{aligned} \quad (0.3)$$

for which the (microscopic) momentum and energy are conserved:

$$v_i + v_j = v_k + v_l, \quad v_i^2 + v_j^2 = v_k^2 + v_l^2. \quad (0.4)$$

Here $A_{i,j}^{k,l}$ denotes the probability of transition for the collision $(i, j) \rightarrow (k, l)$ satisfies some symmetry properties, e.g. the so-called micro-reversibility property $A_{i,j}^{k,l} = A_{k,l}^{i,j}$. Then the solution of the system (0.3) satisfies the kinetic features like conservation laws and H-theorem [36]. The derivation of such moment preserving discretization has been done in [13], [16], [22], [22], [54]. It is proved in [62] that the space of summational invariants is reduced to mass, momentum and energy.

A classical operator-splitting method has been used for the computation of the solutions of this system which consists of splitting the equation into transport and collision steps. The first step solves the transport equation during a time step

Δt :

$$\begin{aligned} (\partial_t + \mathbf{v} \cdot \nabla_x) \mathbf{f}^{n+1/2} &= 0 \\ \mathbf{f}^{n+1/2}(0) &= \mathbf{f}^n \end{aligned} \tag{0.5}$$

where \mathbf{f}^n is a given solution from the previous step. The collision step solves the space homogeneous kinetic equation

$$\begin{aligned} \partial_t \mathbf{f}^{n+1} &= J[\mathbf{f}^{n+1}, \mathbf{f}^{n+1}] \\ \mathbf{f}^{n+1}(0) &= \mathbf{f}^{n+1/2} \end{aligned} \tag{0.6}$$

which contains the Boltzmann collision operator. The validity of this operator splitting has been recently shown in [34].

In recent years several numerical techniques have been proposed to deal with the complexity of the Boltzmann collision operator. In [62], Rogier and Schneider proposed a numerical method for solving the Boltzmann equation which is based on a finite difference scheme for the approximation of the collision kernel and a finite element scheme for the transport phase where the properties of the Boltzmann equation are satisfied. But in this method it requires a very small discretization parameter for a reasonable accuracy. In [37], Görsch has made another approach by smearing out the circle onto the grid and calculating weights which guarantee the conservation laws. This shows a good approximation property but the micro-reversibility is lost. Pareschi and Russo in [61] used some spectral Galerkin methods for the approximation of the Boltzmann operator in the velocity space and the complexity of the method is $\mathcal{O}(n^2)$, where n is the total number of discretization points in velocity space. We refer the works [44], [45], [46], [47], [48] due to Junk and Klar (and with collaboration) for further recent investigations based on a lattice Boltzmann-type discrete velocity model.

However, in the transitional regime, not all features of the Boltzmann collision operator have to be modelled in details and it is desirable to construct simplified model of the Boltzmann collision operator satisfying the basic kinetic features like conservation laws, H-Theorem, correct number of invariants, the properties of linearize collision operator etc. In this regard, in ([5],[7]) Babovsky has introduced simplified collision models in rectangular grid, but there appears many artificial invariants which need to be eliminated by further techniques.

Therefore, in [3] we developed a kinetic theory for the discrete Boltzmann equation based on hexagonal grid in \mathbb{R}^2 . The Boltzmann collision sphere can be much more suited in the hexagonal grid than rectangular grid model. The system of binary collisions contains spurious invariants and to avoid the spurious invariant a ternary interaction law is introduced. It is shown that the conservation laws, the H-Theorem, the correct number of invariants, the properties of linearized operator are satisfied for the discrete Boltzmann equation in the hexagonal grid. This work give the motivation of further tasks with the following contributions.

Outline of the contribution

In chapter-1 we present a short discussion on the derivation of the Boltzmann equation and the basic properties of the Boltzmann collision operator.

In chapter-2, we present briefly the main results on the discrete Boltzmann equation based on hexagons in \mathbb{R}^2 which has been developed in [3]. Then we develop a automatic generation of the hexagonal collision model as described in the following.

In order to solve the Boltzmann equation by the hexagonal discrete velocity model it is necessary to generate a hexagonal grid which automatically provide the basic as well as all possible larger hexagons (on which the local hexagonal collision models are based) contained in the grid. To identify all these regular hexagons, we prove that the centers of all regular hexagons constructed by the nodes of the hexagonal grid on \mathbb{R}^2 , is either a center of the regular basic hexagons or an interior node of the grid. We also prove that if we only include binary collision law, then the collision operator based on any size of hexagonal grid in \mathbb{R}^2 provide only one spurious invariant and this only spurious invariant is identified.

We give notion of a N -layer model which is conducive to find general formulae for all possible regular hexagons contained in the grid \mathcal{G}_N of the model and prove the existence of all the regular hexagons in the grid \mathcal{G}_N . We present algorithms to generate hexagonal mesh of the N -layer model for any $N \in \mathbb{N}_0$ and derive general formulae to identify the nodes of all the regular hexagons exist in the model. We also establish the formulae to obtained information like number of nodes, number of hexagons etc. of the hexagonal grid and this leads to determine the computational costs (in floating point operation) for the evaluation of the Boltzmann collision operator based on the N -layer model. The main results of this work is accepted for publication in [4].

At the end of this chapter, we establish a construction of the equilibrium distribution for the generalize N -layer hexagonal model where the equilibria is described by four parameters characterizing mass, (x,y)-momenta and kinetic energy.

In chapter-3, we present numerical results based on the N -layer hexagonal grid in \mathbb{R}^2 . An error estimation by comparing the discrete equilibria with the corresponding maxwellian leads to determine appropriate size N of the N -layer hexagonal grid for given temperature and bulk velocity. In the case of space-homogeneous Boltzmann equation, the numerical solution of the Boltzmann equation (based on the hexagonal grid) is found very close to the exact solution of the Boltzmann equation due to Krook and Wu [51], for maxwell molecules. In the relaxation problem for hard sphere molecules, it is seen that the solution of the space homogeneous Boltzmann equation completely satisfies the conservation laws and the H-Theorem. As a demonstration of steady state solution of the space inhomogeneous Boltzmann equation, we study standard test problem where the results are seen in a good qualitative agreement with the well-known behaviors of the solution.

The second part of the work concerns with the investigation of a 3D hexagonal collision model. In chapter 4, we introduce a hexagonal collision model in \mathbb{R}^3 and for this we consider the hexagonal grid of so-called sphere packing problem. The local collision model in \mathbb{R}^3 is a twelve-velocity model and the inclusion of only binary collision law in the local collision model produces three spurious invariants. Thus ternary collision law is imposed to avoid the spurious invariant. In order to fulfil the requirements of basic kinetic features, we prove that the 3d collision model satisfies the conservation laws, the H-Theorem, the correct number of invariants as well as the correct dimension of equilibria, and the properties of linearized collision operator.

A very remarkable and significant achievement in the investigation of the 3D hexagonal collision model is that **the correct number of invariants as well as the correct dimension of the equilibria is obtained without introducing ternary collision laws**. For this our basic model is a 216-velocity model for which we **get rid of ternary collision laws**. Therefore for the models smaller than 216-velocity model we need to impose ternary collision law otherwise our model based on only binary collision law. We prove that the basic kinetic features: the conservation laws, the H-Theorem, the correct number of invariants as well as correct dimension of equilibria, and the properties of linearized collision operator are satisfied for the 3D hexagonal model based on only binary collision law.

In order to obtain symmetric nature of the model we give notion of layer-wise construction (extension) of the model and present examples of to different size 3D model-(i) a 120-velocity model as a one-layer model which is based on both binary and ternary collision law, (ii) a 444-velocity model as a 2-layer model which is based on only binary collision law.

We present a construction of the discrete equilibria distribution for our 3D hexagonal model which is described by five parameters characterizing the five physical quantities mass, (x, y, z) -momenta and kinetic energy.

In chapter 5, we present numerical results based on the 120-velocity model and the 444-velocity model in \mathbb{R}^3 . A comparison of the discrete equilibria with the corresponding maxwellian leads to calculate error due the boundary cut on the essential part of the distribution. For the space homogeneous case, the numerical solution of the Boltzmann equation is seen very close to the exact solution given by Krook and Wu [51] for maxwell molecules. In the relaxation problem for hard sphere molecules, it is seen that the solution of the Boltzmann equation completely satisfies the conservation laws and the H-Theorem. As a demonstration of the steady state solution of the space inhomogeneous Boltzmann equation we study a standard test problem with different knudsen number (mean-free-path), and we obtain a good qualitative agreement with the well-known behavior of the solution.

Acknowledgement

I would like to express my gratitude to my supervisor Professor Dr. Hans Babovsky, for everything he has done for the realization of the dissertation. I am grateful to him for introducing me the interesting topic and making me familiar with the topic by fruitful discussions in a very attractive manner. I am indebted to him for the valuable advice and helpful suggestions continuously through-out this work. I acknowledge the support of the German Research Foundation (Deutsche Forschungsgemeinschaft), which essentially contributed to the realization of the work.

I express my sincere gratitude to Professor Dr. A. Klar and to Professor Dr. M. Junk for the interest of acting as a referee of the dissertation.

I express my gratitude to Professor Dr. H. Walther for a fruitful discussion and advice. I am grateful to Dr. W. Neundorf for the helpful discussions during my work and I thank him cordially for the technical and organizational cooperations continuously in preparing my dissertation. I thank to all the colleagues in the department of Numerical Mathematics and Computer Science for the pleasant academic atmosphere and I acknowledge the facilities of the Institute of Mathematics and the Faculty of Mathematics and Natural science, TU Ilmenau. It is my pleasure to acknowledge the generous help of Mrs. Masur-Babovsky in my early stage in Ilmenau and providing me many information and advice.

At the last but not least, I would like to express my gratitude to my family. I am indebted to my parents and other family members for their continuous correspondence and inspirations. The warmest thanks go to my beloved wife Fahmina Andallah for accompanying me in Germany with good understanding and cooperations.

Chapter 1

The Boltzmann equation

The Boltzmann equation, a prominent representative of kinetic equations, describes the evolution of rarefied gases. The dynamics of the Boltzmann equation is given by a free flow step and a particle interactions step with the conservation of momentum and energy. The free flow step is modelled by the Liouville-equation and the particle interaction step is modelled by the Boltzmann collision operator which is presented briefly in the following sections. Our presentation is mainly based on (Babovsky, [8]). The basic properties of the Boltzmann collision operator and the boundary conditions of the Boltzmann equation are also discussed.

1.1 The Liouville-equation

The motion of a particle with mass m in a force-field $F(t, x, v)$ is described by the *Newton-equation*

$$\dot{x}(t) = v(t), \quad \dot{v}(t) = \frac{1}{m}F(x(t), v(t), t) \quad (1.1)$$

where $x(t) \in \mathbb{R}^m$, $m \in \{1, \dots, d\}$ and $v(t) \in \mathbb{R}^d$, $d \in \{2, 3\}$ are the spatial and velocity coordinate at time t . If the coordinate of the particle at time t_0 is known as

$$(x(t_0), v(t_0)) = (x_0, v_0) =: q^0 \quad (1.2)$$

then in principle we can calculate the solution of the ordinary differential equation (1.1) for the initial value (1.2) at any time $t \in \mathbb{R}$.

Definition 1.1 If the initial value problem (1.1), (1.2) is uniquely solvable, we denote the solution at any time t with $\Phi^{t_0, t}q^0$ and then the curve $t \rightarrow \Phi^{t_0, t}q^0$ is called trajectory.

We make the following assumption.

Assumption 1.2 For all $t_0, t \in \mathbb{R}$ and initial value $q^0 = (x_0, v_0) \in \Gamma := \mathbb{R}^m \times \mathbb{R}^d$ there exists a unique solution $\Phi^{t_0, t} q^0 =: q(t)$ of the initial value problem (1.1), (1.2). For all $t \in \mathbb{R}$ the mapping

$$q^0 \rightarrow \Phi^{t_0, t} q^0 \quad (1.3)$$

is a diffeomorphism (i.e. invertible and the mapping and the inverse mapping are continuously differentiable).

With the above assumption the inverse mapping is given by

$$(\Phi^{t_0, t})^{-1} = \Phi^{t, t_0}. \quad (1.4)$$

Remark 1.3 The assumption 1.2 contains the requirement - regularity of the force field F . From the classical theory of the ordinary differential equation the requirement fulfill, for example, when F is Lipschitz continuous.

We now consider that the probability of finding a particle at time t_0 in a measurable subset $M_0 \subset \mathbb{R}^m \times \mathbb{R}^d$ is $\mu_0(M_0)$. Then how is the corresponding probability density in another time t ? To answer this question, we would like to derive an equation and the basic principle for this is the principle of the *conservation of probability*. With the assumption 1.2 a family of probability-measure μ_t obviously satisfy the conservation of probability, if for any measurable set M_0 and for any time t

$$\mu_t(\{\Phi^{t_0, t} q^0, \quad q^0 \in M_0\}) = \mu_0(M_0) \quad (1.5)$$

With this and from the equation (1.4) it follows the existence and uniqueness of the corresponding measure-flow $t \rightarrow \mu_t$, and then for any measurable sets $M \in \Gamma$,

$$\mu_t(M) = \mu_0((\Phi^{t_0, t})^{-1} M) = \mu_0(\Phi^{t, t_0} M). \quad (1.6)$$

For μ_0 is absolutely continuous, it gives a measurable function f_0 by

$$\mu_0(M) = \int_M f_0(q) dq \quad (1.7)$$

The Liouville-equation states how the density can be determine in a situation of a divergent-free force field F .

Theorem 1.4 Liouville-equation: *Consider a divergent free force field F , i.e. for $\nabla \cdot F = 0$ for all (t, x, v) . μ_0 is absolute continuous and $f_0 \in C^1(\Gamma)$ is the corresponding density. Then the measure μ_t is also absolute continuous and the corresponding density $f(t)$ is continuously differentiable and constant along the trajectory:*

$$f(t, \Phi^{t_0, t} q^0) = f_0(q^0) \quad (1.8)$$

and fulfill the Liouville-equation

$$\partial_t f + v \cdot \nabla_x f + \frac{1}{m} F \cdot \nabla_v f = 0 \quad (1.9)$$

where ∂_t is the partial differential operator w.r.to t and ∇_x and ∇_v are the gradients corresponding to spatial and velocity vectors x and v .

proof: We refer ([8], p.10)

Adding the *Boltzmann collision operator* $J[f, f]$ to the Liouville equation (in absence of the field of external forces), we obtain the *Boltzmann equation* is in the form

$$(\partial_t + v \cdot \nabla_x)f(t, x, v) = J[f, f] \quad (1.10)$$

The formulation of the collision operator $J[f, f]$ is based on the momentum and energy conserving particle interactions and the collision operator is composed of a *loss term* and a *win term* which is described in the following section.

1.2 Particle interaction

Let v and w be the pre-collision velocities of two particles T^1 and T^2 of masses m_1 and m_2 respectively. We consider the collisions for which the kinetic energy and moments are conserved and our task is to determine the post-collision velocities v' and w' of the particles T^1 and T^2 respectively.

Interaction between two identical particles

Suppose T^1 and T^2 are identical particles of same radii R and of same masses $m_1 = m_2 = 1$. For a two-particles-interaction $(v, w) \rightarrow (v', w')$, conservation of momentum and energy must hold. Thus the velocities of the two particles satisfy momentum conservation law:

$$v + w = v' + w' \quad (1.11)$$

and energy conservation law:

$$\frac{1}{2}(v^2 + w^2) = \frac{1}{2}(v'^2 + w'^2) \quad (1.12)$$

We choose v' as $v' = v - A\eta$ with a unite vector η , then it follows from the momentum conservation $w' = w + A\eta$, and from the energy conservation $A = \langle v - w, \eta \rangle$.

Theorem 1.5 *a) Two velocity pairs (v, w) and (v', w') for which the equations (1.11) and (1.12) holds, is described with the relation*

$$\begin{pmatrix} v' \\ w' \end{pmatrix} = T_\eta(v, w), \quad (1.13)$$

where η is a unite vector and $T_\eta = (T_\eta^{(1)}, T_\eta^{(2)})^\top$ is defined as

$$T_\eta^{(1)}(v, w) = v - \langle v - w, \eta \rangle \cdot \eta \quad (1.14)$$

$$T_\eta^{(2)}(v, w) = w + \langle v - w, \eta \rangle \cdot \eta \quad (1.15)$$

- b) $T_\eta = T_{-\eta}$ and $T_\eta \circ T_\eta = id$
 c) T_η is differentiable w. r. to (v, w) ; and

$$\left| \frac{\partial(v', w')}{\partial(v, w)} \right| = 1 \quad (1.16)$$

particularly satisfy the integral transformation

$$dv dw = dv' dw' \quad (1.17)$$

- d) The conservation equations

$$|v' - w'| = |v - w| \quad \text{and} \quad \langle v - w, \eta \rangle = \langle v' - w', \eta \rangle \quad (1.18)$$

are satisfied.

proof: Choosing $v' = v - A\eta$ with a unite vector η , it follows from the momentum conservation $w' = w + A\eta$ and from the energy conservation $A = \langle v - w, \eta \rangle$. The statements b) and d) follows from elementary calculations and the statement c) immediately follows from the fact that T_η is an involution.

The impact parameters

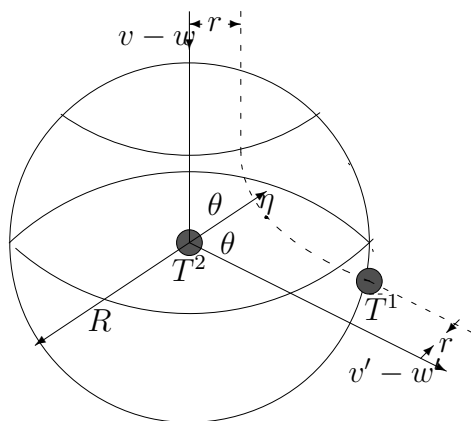


Fig. 1.1 The impact parameters

Apart from the translational velocities of the two collision partners, two *impact parameters* are required to completely specify a collision between spherically symmetric molecules. The first is the distance of closest approach r of the undisturbed trajectories in the center of mass frame of reference. The plane in which the trajectories lie in the center of mass frame is called the collision plane. The second impact parameter is chosen as the angle θ between the collision plane and some

reference plane. The direction η of the change of momentum depends on the impact parameters. As shown in the Fig.1.1, we consider that the particle T^1 is moving with pre-collision and post-collision velocities $(v - w)$ and $(v' - w')$ respectively relative to the particle T^2 . We now choose our co-ordinate system so that $(v - w)$ is in the direction of canonical unit-vector e_3 i.e. $v = (0, 0, |v - w|)^\top$. Then T^1 is moving nearer and nearer to T^2 on the trajectory $\tau \rightarrow (r \cos \phi, r \sin \phi, \tau |v - w|)^\top$, so that by the law of classical mechanics

$$\begin{pmatrix} v' \\ w' \end{pmatrix} = T_\eta(v, w), \quad (1.19)$$

with a unit vector $\eta = (\sin \theta \cos \phi, \sin \theta \sin \phi, \cos \theta)^\top$, $\theta \in [0, \pi/2]$, $\phi \in [0, 2\pi]$; where θ depends on the impact parameter r and velocity $|v - w| = |v' - w'|$:

$$\theta = \theta(r, |v - w|). \quad (1.20)$$

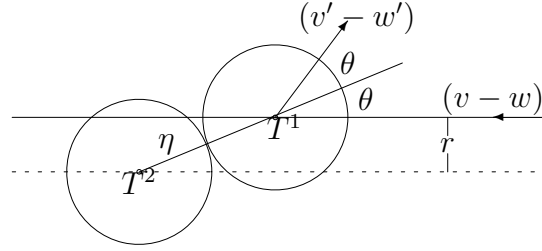


Fig. 1.2 Hard sphere interaction

The Fig.1.2 shows the interaction of two hard spheres. From the geometry it is evident that

$$r = 2R \sin \theta \quad (1.21)$$

We assume that θ is smooth and r is strictly monotonically increasing function and $\theta(0, |v - w|) = 0$ as well as $\theta(2R, |v - w|) = \pi/2$.

1.2.1 The Boltzmann collision operator

On the basis of the previous discussion of particle interactions, we briefly describe here the formulation of the Boltzmann collision operator. Let a particle of velocity v meets another particle of velocity w within a time interval Δt . By the translation of a co-ordinate system, if we suppose that the second particle is at rest, then the first particle moves with the velocity $v - w$. We consider N numbers of the second particles as a field particles in a volume unit. Then the probability of finding the test particle (the first particle) of velocity $(v - w)$ meets a field particle at a point

x_0 in a time interval Δt , is equal to the probability of finding the middle point of the field particle in the collision-cylinder

$$Z_{\Delta t} = \{x \mid \inf_{t \in [0, \Delta t]} |x - (x_0 + t(v - w))| < 2R\} \quad (1.22)$$

The collision cylinder $Z_{\Delta t}$ has the volume $Vol_{\Delta t} = 4\pi R^2 |v - w| \Delta t$. But in a small volume ΔX , the collision between two pre-selected particles is a rather rare event. By searching a two-particle-density $f^{(2)}(v, w)$ for a system of finitely many particles can solve the problem. Following the argument, one can consider a most general probability density and the particle evolution can be described only through a hierarchy of equation (BBGKY-Hierarchy), which is not meaningful for practical consideration. One way-out is in the *Boltzmann-Grad limit*: in a volume element the number of particles $N \rightarrow \infty$ and at the same time the radius $R \rightarrow 0$ so that $NR^2 = \text{const}$. Then two particles that happen to collide can be thought of as two randomly chosen particles, and it make sense to assume that the probability density $f^{(2)}(v, w)$ of finding the first particle with velocity v and the second particle with the velocity w is the product of the probability density of finding the first particle with velocity v and the probability density of finding the second particle with velocity w . With this assumption of *molecular chaos* we write

$$f^{(2)}(v, w) = f(v)f(w) \quad (1.23)$$

Then the probability of meeting a particle with velocity v to another particle with velocity w within a time interval Δt is proportional to $N \cdot \Delta X$, and so equal to

$$N\sigma\Delta X = 4\sigma\pi R^2 N\Delta t |v - w| \cdot f(w) \quad (1.24)$$

Then $\sigma_0 = \lim_{N \rightarrow \infty} 4\pi\sigma NR^2$ provide a loss-term of the collision operator in the form

$$-\sigma_0 |v - w| f(t, x, v) f(t, x, w) \quad (1.25)$$

With the assumption that $\theta(r/R)$ is an diffeomorphism and for $r_0 = r/(2R)$, the probability $P_{(v')}(\Delta V)$ of finding the test particle with the velocity v' in the domain ΔV is

$$P_{v'}(\Delta V) := \sigma_0 \int_{w' \in \mathbb{R}^d} \int_{\eta \in S_+^{d-1}: T_\eta^{(1)}(v', w') \in \Delta v} r_0(\theta) \frac{dr_0}{d\theta} d\theta d\phi |v' - w'| f(w') dw' \quad (1.26)$$

Then from the involution property of T_η (theorem 1.5(b))

$$\int_{\mathbb{R}^d} P_{v'}(\Delta V) f(v') dv' \approx \sigma_0 \int_{\mathbb{R}^d} \int_{\eta \in S_+^{d-1}} k(|v - w|, \theta) f(v') f(w') d\omega(\eta) dw \quad (1.27)$$

the R.H.S. is the win-term, where

$$k(|v - w|, \theta) = 4|v - w| \frac{r_0(\theta)}{\sin\theta} \frac{dr_0}{d\theta} \quad (1.28)$$

and $d\omega$ is the surface element of the unite sphere:

$$d\omega(\eta) = \frac{1}{4\pi} \sin\theta d\theta d\phi \quad (1.29)$$

The Boltzmann collision operator is then given by the sum of the loss-term and win-term:

$$J[f, f] := \sigma_0 \int_{\mathbb{R}^d} \int_{\eta \in S_+^{d-1}} (f(t, x, v')f(t, x, w') - f(t, x, v)f(t, x, w))k(|v - w|, \theta) d\eta dw \quad (1.30)$$

where θ is the angle between η and $v - w$. But since $T_\eta = T_{-\eta}$ (theorem 1.5) we can make the integration over the full surface S^2 and we obtain the Boltzmann collision operator as

$$J[f, f] = \frac{\sigma_0}{2} \int_{\mathbb{R}^d} \int_{\eta \in S^{d-1}} (f(t, x, v')f(t, x, w') - f(t, x, v)f(t, x, w))k(|v - w|, \theta) d\eta dw \quad (1.31)$$

For hard sphere model

As given by the equation (1.21), in particular, for hard sphere molecules

$$r = 2R\sin\theta,$$

therefore,

$$r_0 dr_0 = \sin\theta \cos\theta d\theta$$

and thus with a constant α , it turns out that the Boltzmann collision operator for a hard sphere gas is given by

$$J[f, f] = \alpha \int_{\mathbb{R}^d} \int_{\eta \in S^{d-1}} (f(t, x, v')f(t, x, w') - f(t, x, v)f(t, x, w))|v - w| \cos\theta d\eta dw. \quad (1.32)$$

1.3 Basic properties

We discussed here the basic properties of the Boltzmann collision operator $J[f, f]$.

1.3.1 Collision Invariant

Definition 1.6 Collision invariant: A locally integrable function $\phi : \mathbb{R}^d \rightarrow \mathbb{R}$ is called *collision invariant* of the collision-operator $J[., .]$, if for each $f \in L^1(\mathbb{R}^d)$, ϕJ is integrable, and satisfy

$$\int_{\mathbb{R}^d} \phi(v) J[f, f](v) dv = 0 \quad (1.33)$$

A necessary criteria for collision-invariants is the following.

Lemma 1.7 *A local integrable function ϕ is collision-invariant, if for any $v, w \in \mathbb{R}^d$ and for any unit vector $\eta \in S^{d-1}$, ϕ satisfies*

$$\phi(v) + \phi(w) = \phi(v') + \phi(w') \quad (1.34)$$

proof: By the interchange of v and w we have

$$\begin{aligned} & \int_{\mathbb{R}^d} \phi(v) J[f, f](v) dv \\ &= \int_{\mathbb{R}^d} \int_{\mathbb{R}^d} \int_{S^{d-1}} k(|v-w|, \eta) \{f(v')f(w') - f(v)f(w)\} \phi(v) d\eta dw dv \quad (1.35) \end{aligned}$$

$$= \int_{\mathbb{R}^d} \int_{\mathbb{R}^d} \int_{S^{d-1}} k(|v-w|, \eta) \{f(v')f(w') - f(v)f(w)\} \phi(w) d\eta dw dv \quad (1.36)$$

With the involution property $T_\eta^2 = \text{id}$ and the relation $dv dw = dv' dw'$ we have

$$\begin{aligned} & \int_{\mathbb{R}^d} \phi(v) J[f, f](v) dv \\ &= - \int_{\mathbb{R}^d} \int_{\mathbb{R}^d} \int_{S^{d-1}} k(|v-w|, \eta) \{f(v')f(w') - f(v)f(w)\} \phi(v') d\eta dw dv \quad (1.37) \end{aligned}$$

$$= - \int_{\mathbb{R}^d} \int_{\mathbb{R}^d} \int_{S^{d-1}} k(|v-w|, \eta) \{f(v')f(w') - f(v)f(w)\} \phi(w') d\eta dw dv \quad (1.38)$$

It follows from the equations from (1.36) to (1.38) that

$$\begin{aligned} 4 \times \int_{\mathbb{R}^d} \phi(v) J[f, f](v) dv &= \int_{\mathbb{R}^d} \int_{\mathbb{R}^d} \int_{S^{d-1}} k(|v-w|, \eta) \times \\ & \{f(v')f(w') - f(v)f(w)\} \{\phi(v) + \phi(w) - \phi(v') - \phi(w')\} d\eta dw dv. \quad (1.39) \end{aligned}$$

Then with the definition 1.6, the proof is completed. \square

Definition 1.8 *Basis-collision-invariant:* We call a collision invariant ϕ a *basis-collision-invariant* if for any $v, w \in \mathbb{R}^d$ and for any $\eta \in S^{d-1}$

$$\phi(v) + \phi(w) = \phi(v') + \phi(w') \quad (1.40)$$

Due to the conservation of mass, momenta and energy during the interaction, the functions $\phi_0(v) \equiv 1$ (mass), $\phi_i(v) := v_i, i = 1, \dots, d$ (momenta) and $\phi_4(v) := \frac{1}{2}\|v\|^2$ (kinetic energy) are conservative. The following theorem shows that these are the only collision invariants with certain regularity properties.

Theorem 1.9 *Basis-collision-invariant:* A continuous function $\phi : \mathbb{R}^d \rightarrow \mathbb{R}$ is basis-collision-invariant if and only if

$$\phi(v) = a + \langle b, v \rangle + c\|v\|^2 \quad (1.41)$$

with $a, c \in \mathbb{R}$ and $b \in \mathbb{R}^d$.

proof: see page 50 [8].

1.3.2 Equilibrium solutions

We introduce a function $f : \mathbb{R}^d \rightarrow \mathbb{R}$ satisfying $J[f, f] \equiv 0$. It will be evident that the solution of the space homogeneous Boltzmann equation converge to the equilibrium solution.

Definition 1.10 Equilibrium solution: A function $f \in L^1(\mathbb{R}^d) \cap C(\mathbb{R}^d)$ with the properties

- (a) $f(v) > 0$ for all $v \in \mathbb{R}^d$,
- (b) $\ln(f)J[f, f] \in L^1(\mathbb{R}^d)$

is called *equilibrium solution* of the Boltzmann equation for which $J[f, f] \equiv 0$.

Defining the so-called *H-functional* $H[f] := \int_{\mathbb{R}^d} \ln(f(v))f(v)dv$ we have the following properties of the solution $f(t, v)$ of the space homogeneous Boltzmann equation.

Theorem 1.11 H-theorem: *If the collision kernel $k(|v - w|, \eta) > 0$ almost everywhere then*

- (a) *For the solution $f(t, v)$ of the space homogeneous Boltzmann equation*

$$\frac{dH}{dt} \leq 0,$$

- (b) *$f(\cdot)$ is an equilibrium solution if and only if*

$$f(v) = \exp(a + \langle b, v \rangle + c\|v\|^2). \quad (1.42)$$

proof: It follows from the equation (1.39) that

$$\begin{aligned} 4 \times \int_{\mathbb{R}^d} \ln(f(v))J[f, f](v)dv &= \int_{\mathbb{R}^d} \int_{\mathbb{R}^3} \int_{S^{d-1}} k(|v - w|, \eta) \times \\ &\{f(v')f(w') - f(v)f(w)\} \{\ln(f(v)) + \ln(f(w)) - \ln(f(v')) - \ln(f(w'))\} d\eta dw dv \\ &= \int_{\mathbb{R}^d} \int_{\mathbb{R}^{d-1}} \int_{S^{d-1}} k(|v - w|, \eta) f(v')f(w') \left\{ 1 - \frac{f(v)f(w)}{f(v')f(w')} \right\} \ln\left(\frac{f(v)f(w)}{f(v')f(w')}\right) d\eta dw dv \end{aligned} \quad (1.43)$$

where for $x > 0$, $x \rightarrow (1 - x)\ln(x)$ is a non-positive function and thus

$$\int_{\mathbb{R}^d} \ln(f(v))J[f, f](v)dv \leq 0 \quad (1.44)$$

and as 1 is a collision invariant, it follows immediately that

$$\frac{dH}{dt} = \int_{\mathbb{R}^d} (1 + \ln(f(v)))J[f, f](v)dv \leq 0 \quad (1.45)$$

and the equality sign holds if and only if $f(v)f(w) = f(v')f(w')$ for any $v, w \in \mathbb{R}^d$, $\eta \in S^{d-1}$ and so when $\ln(f)$ is a collision invariant. Then from the theorem 1.9 it follows that

$$\ln(f(v)) = a + \langle b, v \rangle + c\|v\|^2 \quad (1.46)$$

with $a, c \in \mathbb{R}$ and $b \in \mathbb{R}^d$. \square

Remark 1.12 (a) With the above theorem all equilibrium functions can be represented in the form

$$f(v) = M[\rho, \bar{v}, T](v) := \frac{\rho}{(2\pi T)^{d/2}} \exp\left(-\frac{(v - \bar{v})^2}{2T}\right) \quad (1.47)$$

These functions are also called *Maxwell-functions*. The quantities ρ, \bar{v} and T are given by

$$\rho = \int_{\mathbb{R}^d} M[\rho, \bar{v}, T](v) dv \quad (1.48)$$

$$\rho \bar{v} = \int_{\mathbb{R}^d} v M[\rho, \bar{v}, T](v) dv \quad (1.49)$$

$$\rho T = \frac{1}{d} \int_{\mathbb{R}^d} \|v - \bar{v}\|^2 M[\rho, \bar{v}, T](v) dv \quad (1.50)$$

and called the density, bulk-velocity, and temperature of the Maxwell-distribution.

(b) From the theorem 1.11(b), $t \rightarrow H[f(t)]$ decreases monotonically unless f is a maxwellian and this concludes that f tends to maxwellian as $t \rightarrow \infty$. We refer [18], [2], for some further approaches on this topic.

1.4 The Macroscopic equations

Let us now describe the evaluation of macroscopic quantities from the density function f and the relationship between them. Because of the significance of the density function we need to take averages with respect to all the possible velocities for local information, (e.g. density, bulk-velocity at some point of spatial space), while an additional integration with respect to space coordinates is required to obtain global quantities (e.g., total mass of the gas).

Definition 1.13 Moments: For a given non-negative integrable function $f : \mathbb{R}^d \rightarrow \mathbb{R}$, we define the (mass) density ρ by

$$\rho := \int_{\mathbb{R}^d} f(v) dv, \quad (1.51)$$

the bulk-velocity $\bar{v} = (\bar{v}_i)_{i=1}^d$ which is the average of the molecular velocities v by

$$\bar{v}_i := \frac{1}{\rho} \int_{\mathbb{R}^d} v_i f(v) dv, \quad (1.52)$$

the stress tensor $\mathbf{P} = (p_{ij})_{i,j=1}^d$ by

$$p_{i,j} := \int_{\mathbb{R}^d} v_i v_j f(v) dv - \rho \bar{v}_i \bar{v}_j, \quad (1.53)$$

the pressure \mathbf{p} by

$$\mathbf{p} := \frac{1}{d} \text{trace}(\mathbf{P}) = \frac{1}{d} \sum_{i=1}^d p_{ii}, \quad (1.54)$$

the energy density \mathbf{E} by

$$\mathbf{E} := \frac{1}{2} \int_{\mathbb{R}^d} \|v\|^2 f dv, \quad (1.55)$$

the density of the internal energy \mathbf{e} by

$$\mathbf{e} := \frac{1}{2\rho} \int_{\mathbb{R}^d} \|v - \bar{\mathbf{v}}\|^2 f dv = \frac{d\mathbf{p}}{2\rho}, \quad (1.56)$$

and the temperature T by

$$\mathbf{T} := \frac{\mathbf{p}}{\rho} = \frac{2\mathbf{e}}{d}. \quad (1.57)$$

Definition 1.14 Moment-flow: The flow $\mathcal{F}[\Phi]$ of $\Phi[f] := \int_{\mathbb{R}^d} \phi(v) f(v) dv$ is defined by

$$\mathcal{F}[\Phi] := \int_{\mathbb{R}^d} v \phi(v) f(v) dv, \quad (1.58)$$

e.g., the flow of the energy density is given by

$$\mathcal{F}[\mathbf{E}] := \frac{1}{2} \int_{\mathbb{R}^d} v \|v\|^2 f(v) dv. \quad (1.59)$$

Like a flow with respect to the relative velocity $v - \bar{\mathbf{v}}$, the heat-flux vector is defined by

$$\mathbf{q} := \int_{\mathbb{R}^d} (v - \bar{\mathbf{v}}) \|v - \bar{\mathbf{v}}\|^2 f(v) dv, \quad (1.60)$$

then the energy-density with the help of the heat-flux vector can be written in the form

$$\mathcal{F}[\mathbf{E}] = \rho \left(\frac{1}{2} \|v\|^2 + e \right) \bar{\mathbf{v}} + \mathbf{P} \cdot \bar{\mathbf{v}} + \mathbf{q}. \quad (1.61)$$

As a simple mathematical consequence of the Boltzmann equation

$$(\partial_t + v \cdot \nabla_x) f(t, x, v) = J[f, f], \quad (1.62)$$

one can derive five differential relations satisfied by the macroscopic quantities introduced above. These relations describe the balance of mass, momentum and energy and have the same form as in continuum mechanics. To this end let us multiply the Boltzmann equation with collision invariant ϕ and then with $\Phi(t, x) := \int_{\mathbb{R}^d} \phi(v) f(t, x, v) dv$ we have

$$\partial_t \Phi(t, x) + \nabla_x \cdot \mathcal{F}[\Phi](t, x) = 0. \quad (1.63)$$

Then taking ϕ_i , $i = 0, \dots, 4$ as defined in the definition 1.8, we have the following five relations

$$\partial_t \rho + \nabla_x \cdot (\rho \bar{\mathbf{v}}) = 0 \quad (1.64)$$

$$\partial_t(\rho \bar{\mathbf{v}}) + \nabla_x \cdot (\rho \bar{\mathbf{v}} \otimes \bar{\mathbf{v}} + \mathbf{P}) = 0 \quad (1.65)$$

with the tensor product $(\bar{\mathbf{v}} \otimes \bar{\mathbf{v}})_{i,j} := \bar{v}_i \bar{v}_j$,

$$\partial_t \mathbf{E} + \nabla_x \cdot \left(\rho \left(\frac{1}{2} \|v\|^2 + e \right) \bar{\mathbf{v}} + \mathbf{P} \cdot \bar{\mathbf{v}} + \mathbf{q} \right) = 0. \quad (1.66)$$

Remark 1.15 We remark here that in the so-called space-homogeneous case, the various quantities do not depend on \mathbf{x} , then all the space derivatives disappear from the equations (1.64-1.66) and then the quantities $\rho, \rho v, \mathbf{E}$ are conserved, i.e. do not change with time.

We mention here that the number of unknowns in the equation (1.64-1.66) are larger than the number of equations. i.e. the set of equations are not in a closed form. An important modelling problem remains with the formation of closed relations. We give here two examples of the relations of closed form.

1. Euler-equation: $\rho, \bar{\mathbf{v}}$ as well as E and \mathbf{T} are defined as in the definition 1.13 and all other moments are defined through the Maxwell-density $M[\rho, \bar{\mathbf{v}}, \mathbf{T}]$. For Maxwell-functions it can be shown that $\mathbf{P} = \mathbf{p} \cdot \mathbf{I}$ (\mathbf{I} is the unit matrix), and $\mathbf{q} = 0$. With this we obtain the *Euler-equation* as a closed system of 5 equations with 5 unknowns as

$$\partial_t \rho + \nabla_x \cdot (\rho \bar{\mathbf{v}}) = 0 \quad (1.67)$$

$$\partial_t(\rho \bar{\mathbf{v}}) + \nabla_x \cdot (\rho \bar{\mathbf{v}} \otimes \bar{\mathbf{v}} + \mathbf{p}) = 0, \quad (1.68)$$

$$\partial_t \mathbf{E} + \nabla_x \cdot \left(\left(\frac{\rho}{2} \|v\|^2 + \rho e + \mathbf{p} \right) \bar{\mathbf{v}} \right) = 0 \quad (1.69)$$

2. Navier-Stokes-equations: These equations are obtained through the correction of terms \mathbf{P} and \mathbf{q} :

$$\mathbf{P} := (\mathbf{p} + \sigma \nabla_x \cdot \bar{\mathbf{v}}) \mathbf{I} - \mu (\mathbf{D}\bar{\mathbf{v}} + \mathbf{D}\bar{\mathbf{v}}^\top) \quad (1.70)$$

with the functional matrix $\mathbf{D}\bar{\mathbf{v}}$ with the coefficients $(\mathbf{D}\bar{\mathbf{v}})_{ij} = \partial \bar{v}_i / \partial x_j$, and

$$\mathbf{q} = -\kappa \nabla_x \mathbf{T}. \quad (1.71)$$

The quantities σ and μ are called the *viscosity coefficients* and κ is called the *coefficient of heat conduction*.

1.5 The Linearized Collision Operator

We introduced here the linearize collision operator and study some properties of the operator as described in Cercignani, [25]. For M denote the equilibrium solution and with a new unknown h and $\epsilon > 0$, inserting the ansatz

$$f = M + \epsilon M^{\frac{1}{2}} h \quad (1.72)$$

to the non-linear Boltzmann equation (given by equation 1.10) we have:

$$\partial_t h + v \cdot \nabla_x h = Lh + \epsilon \Gamma(h, h). \quad (1.73)$$

Here L is the linearized collision operator defined by

$$Lh = 2M^{-\frac{1}{2}} J[M^{\frac{1}{2}} h, M], \quad (1.74)$$

where J is the bilinear operator associated with $J[f, f]$ i.e.

$$J[f, g] = \frac{1}{2} \int_{\mathbb{R}^d} \int_{S^{d-1}} (f' g'_* + g' f'_* - f g_* - g f_*) k(|v-w|, \theta) d\eta dw \quad (1.75)$$

and $\Gamma(h, h)$ is the non-linear part, and is given by

$$\Gamma(g, h) = M^{-\frac{1}{2}} J[M^{\frac{1}{2}} g, M^{\frac{1}{2}} h] \quad (1.76)$$

with $g = h$. A more explicit form of Lh is as follows

$$Lh = \int_{\mathbb{R}^d} \int_{S^{d-1}} (h' R'_* + R' h'_* - R h_* - h R_*) R_* k(|v-w|, \theta) d\eta dw \quad (1.77)$$

where for convenience R denotes $M^{\frac{1}{2}}$ and $M' M'_* = M M_*$. It has been shown in ([25], chap. 3, eq. 1.10) that

$$\int_{\mathbb{R}^d} J[f, g] \phi(v) dv = \frac{1}{8} \int_{\mathbb{R}^d} \int_{\mathbb{R}^d} \int_{S^{d-1}} (f' g'_* + g' f'_* - f g_* - g f_*) (\phi + \phi_* - \phi' - \phi'_*) k(|v-w|, \theta) d\eta dw dw_* \quad (1.78)$$

Substituting f by Rh , g by M and ϕ by g/R , it follows from the equation (1.78) that

$$\begin{aligned} \int_{\mathbb{R}^{d-1}} g Lh dv &= -\frac{1}{4} \int_{\mathbb{R}^d} \int_{S^{d-1}} (h' R'_* + R' h'_* - R h_* - h R_*) \\ &\quad \times (g' R'_* + R' g'_* - R g_* - g R_*) k(|v-w|, \theta) d\eta dw dw_* \end{aligned} \quad (1.79)$$

Now introducing the Hilbert space of square summable functions of v endowed with the scalar product

$$(g, h) = \int_{\mathbb{R}^d} \bar{g} h dv, \quad (1.80)$$

where the bar denote the complex conjugation, equation (1.79) gives

$$(g, Lh) = (Lg, h). \quad (1.81)$$

Furthermore

$$(h, Lh) \leq 0, \quad (1.82)$$

and the equality sign holds if and only if

$$h'/R' + h'_*/R'_* - h/R - h*/R* = 0, \quad (1.83)$$

i.e., if and only if h/R is a collision invariant. Thus from the above we have the following properties of the Linearized collision operator.

Theorem 1.16 *The linearized collision operator is self-adjoint and non-positive, with a $(d+2)$ -fold null eigenspace spanned by $M^{1/2}\phi_i$, where ϕ_i , $i = 0, \dots, d+1$ are the collision invariants.*

1.6 Boundary conditions

The Boltzmann equation is appended by boundary conditions, which describe the interaction of the gas molecules with the solid walls. The details of the boundary conditions has been described in the corresponding chapters in ([8], [24]). Among the possible boundary conditions described in the above two references, in practice there are mainly two classes of reflection laws which we described here as in [8].

Definition 1.17 (i) *Deterministic reflection law* is formulated through bijective mapping

$$R(a; \cdot) : \{v : \langle n(a), v \rangle < 0\} \rightarrow \{v : \langle n(a), v \rangle > 0\} \quad (1.84)$$

where a molecule striking a wall at 'a' with velocity v reemerges from the wall with a new velocity $w = R(a; \cdot)$. The corresponding boundary condition reads

$$|\langle n(a), v \rangle| f(t, a, v) = |\langle n(a), R(a; v) \rangle| f(t, a, R(a; v)) \quad (1.85)$$

for all v with $\langle n(a), v \rangle < 0$.

(ii) *Stochastic refection law* describes through a family of probability mass $\{R_a(\cdot|v) : \langle n(a), v \rangle < 0\}$ in the set $\{w \in \mathbb{R}^3 : \langle n(a), w \rangle > 0\}$. A molecule striking with the velocity v at a point $a \in \partial\Omega$ in the wall reemerge randomly in accordance with $R_a(\cdot|v)$. Then $R_a(\cdot|v)$ is the velocity density of all the molecules after the impact with the wall. The mass R_a is absolute continuous i.e. $R_a(dw|v) = r_a(w|v)dw$ so that the corresponding boundary condition for $\langle n(a), w \rangle > 0$ reads

$$\langle n(a), w \rangle f(t, a, w) = \int_{\langle n(a), v \rangle < 0} r_a(w|v) |\langle n(a), v \rangle| f(t, a, v) dv \quad (1.86)$$

Example 1.18 (i) The *specular (elastic) reflection* law is described by

$$R_{el}(a; v) = v - 2\langle n(a), v \rangle n(a) \quad (1.87)$$

By the specular reflection the kinetic energy $E_{kin} := mv^2/2$ of the particles do not change. The component of the momenta $p := mv$ orthogonal to $n(a)$ is unchanged while the component parallel to $n(a)$ change in sign. With the help of the distribution-notation, the specular reflection can be formally written in the form of stochastic reflection law as

$$r_a(\cdot|w) = \delta_{R_{el}(a;w)}(\cdot). \quad (1.88)$$

(ii) The diffuse reflection with wall temperature T is described through the stochastic reflection law. The corresponding probability masses are absolute continuous and independent of the out going velocity w . Defining the diffuse reflection with the requirement that the post-collision velocity is independent of the pre-collision velocity and that the equilibrium densities

$$M_T(v) = \frac{1}{(2T)^{5/2}} \exp\left(-\frac{|v|^2}{2T}\right) \quad (1.89)$$

are invariant w. r. to the diffusion reflection, i.e.

$$\langle n(a), v \rangle M_T(v) = \int_{\langle n(a), w \rangle < 0} r_T(v|w) |\langle n(a), w \rangle| M_T(w) dw \quad (1.90)$$

With this $r_T(v|w) \sim \langle n(a), v \rangle M_T(v)$ and after multiplying with the normalization constant

$$r_T(v|w) = \frac{2}{\pi} \sqrt{2T} \langle n(a), v \rangle M_T(v). \quad (1.91)$$

(iii) The *maxwellian reflection law* with accommodation coefficient $\lambda \in [0, 1]$ is a combination of the above two examples:

$$r_T^{(\lambda)}(v|w) = \lambda \delta_{R_{el}(a;w)}(v) + (1 - \lambda) r_T(v|w). \quad (1.92)$$

(iv) Another example is the *reverse reflection law* which is given by

$$R(a; v) := -v \quad (1.93)$$

The only law guaranteeing no-slip condition is the reverse reflection. In both the deterministic laws above, there is no exchange of energy between the fluid and wall. i.e. the deterministic laws are *adiabatic*, while the diffusive law is not adiabatic. The only law with vanishing shear stress is the specular reflection law.

Chapter 2

Discrete Boltzmann equation in \mathbb{R}^2

In this chapter first we briefly describe the main results of the discrete Boltzmann equation based on hexagonal collision model in \mathbb{R}^2 , which has been developed in [3]. Then in order to identify all the regular hexagons we prove that the centers of all regular hexagons constructed by the nodes of the hexagonal grid in \mathbb{R}^2 , is either a center of the regular basic hexagons or an interior node of the grid. We also prove that the system of binary collision law based on bounded hexagonal grid produces only one spurious invariant. We give notion of a N -layer model and prove the existence of all possible regular hexagons belonging to the grid \mathcal{G}_N of the N -layer model. We develop a mesh generator of the N -layer model which automatically provides the basic as well as all possible larger hexagons (on which the local hexagonal collision model are based) and leads to determine computational costs of the Boltzmann collision operator in floating point operation. At the end, we present the construction of the discrete equilibrium distribution for any larger size model based on the hexagonal grid.

2.1 Hexagonal Discretization of \mathbb{R}^2

Define the points

$$\mathbf{c}_\alpha = (c_{\alpha,x}, c_{\alpha,y}), \quad \alpha = (i, j) \in \mathbb{Z}^2 \quad (2.1)$$

by

$$c_{\alpha,x} := \begin{cases} 3hi & \text{for } j \text{ even} \\ (1.5 + 3i)h & \text{for } j \text{ odd} \end{cases} \quad (2.2)$$

$$c_{\alpha,y} := \frac{\sqrt{3}h}{2}j \quad (2.3)$$

where h is a discretization parameter, and the set

$$\mathcal{C} := \{c_\alpha | \alpha \in \mathbb{Z}^2\}. \quad (2.4)$$

The elements $c_\alpha \in \mathcal{C}$ are the centers of the hexagons H_α and the nodes of H_α are given by

$$\mathcal{G}_\alpha := c_\alpha + h \left(\sin\left(\frac{2\pi}{6}(k+0.5)\right), \cos\left(\frac{2\pi}{6}(k+0.5)\right) \right)_{k=0}^5 \in (\mathbb{R}^2)^6 \quad (2.5)$$

The set

$$\mathcal{G} := \bigcup_{\alpha \in \mathbb{Z}^2} \mathcal{G}_\alpha \quad (2.6)$$

of nodes of all hexagons H_α yields the grid by which we discretize \mathbb{R}^2 .

The Fig. 2.1 shows the hexagonal discretization of \mathbb{R}^2 .

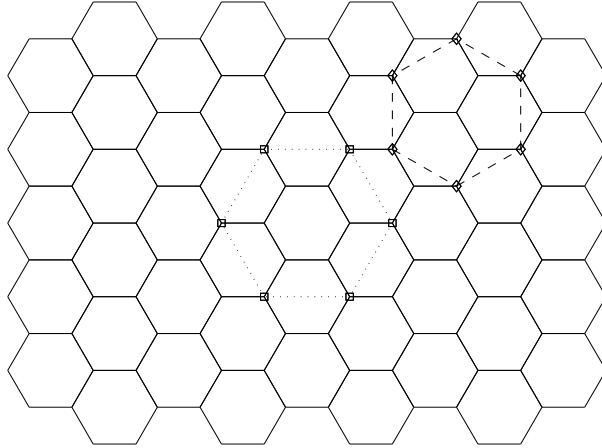


Fig. 2.1 Hexagonal discretization of \mathbb{R}^2 .

Each of the hexagons H_α defined above is called a *basic hexagon* of \mathcal{G} . However, \mathcal{G} contains many larger regular hexagons as indicated by the dotted and dashed line in the Fig. 2.1. The set of all regular hexagons with vertices in \mathcal{G} is denoted by \mathcal{H} . For each $H \in \mathcal{H}$ a numbering $\pi^H = (\pi_0^H, \dots, \pi_5^H)$ is given which lists all nodes of H consecutively in clockwise ordering.

For a given real-valued function $\mathbf{f} \in \mathbb{R}^{|\mathcal{G}|}$ on \mathcal{G} we denote by $\mathbf{f}_H = P_H \mathbf{f}$ the restriction of \mathbf{f} on H , i.e.

$$P_H \mathbf{f} = (f_{\pi_0^H}, \dots, f_{\pi_5^H}) \in \mathbb{R}^6 \quad (2.7)$$

For $H := (\pi_0^H, \dots, \pi_5^H) \in \mathcal{H}$ and $\mathbf{f}_H \in \mathbb{R}_+^6$, a *local collision operator* is introduced as

$$J_H[\mathbf{f}_H, \mathbf{f}_H] = \gamma_{bin} J_{bin}[\mathbf{f}_H, \mathbf{f}_H] + \gamma_{ter} J_{ter}[\mathbf{f}_H, \mathbf{f}_H] \quad (2.8)$$

where

$$\begin{aligned} J_{bin}[\mathbf{f}_H, \mathbf{f}_H]_l &= J_{bin}[\mathbf{f}_H, \mathbf{f}_H]_{l+3} = S[\mathbf{f}, \mathbf{f}] - 3f_l f_{l+3}; \\ S[\mathbf{f}, \mathbf{f}] &:= f_0 f_3 + f_1 f_4 + f_2 f_5, \quad l = 0, 1, 2 \end{aligned} \quad (2.9)$$

and

$$J_{ter}[\mathbf{f}_H, \mathbf{f}_H]_l = (-1)^l T[\mathbf{f}, \mathbf{f}]; \quad T[\mathbf{f}, \mathbf{f}] := f_1 f_3 f_5 - f_0 f_2 f_4; \quad l = 0, \dots, 5, \quad (2.10)$$

The inclusion of only binary collision operator $J_{bin}[\mathbf{f}, \mathbf{f}]$ yields an artificial invariant $\langle a_H, f_H \rangle$,

$$a_H = (1, -1, 1, -1, 1, -1)^\top, \quad (2.11)$$

and therefore to avoid this artificial invariant we included the ternary collision operator $J_{ter}[\mathbf{f}, \mathbf{f}]$.

Then the space homogeneous kinetic equation as an evolution equation for densities $\mathbf{f} = \mathbf{f}(t)$ on \mathcal{G} takes the form

$$\partial_t \mathbf{f} = J[\mathbf{f}, \mathbf{f}], \quad (2.12)$$

where the *global collision operator* $J[\mathbf{f}, \mathbf{f}]$ is given in its weak formulation as

$$\langle \phi, J[\mathbf{f}, \mathbf{f}] \rangle = \sum_{H \in \mathcal{H}} \gamma_H \sum_{l=0}^5 \phi(\pi_i^H) J_H[\mathbf{f}_H, \mathbf{f}_H]_l. \quad (2.13)$$

In a bounded hexagonal grid \mathcal{G}_b , we call (\mathcal{H}_b, γ) the *regular collision model* (see Def. 4.4, [3]) which has the four invariants

$$\begin{aligned} \text{mass} \quad \rho &= \sum f_l, \\ x\text{-momentum} \quad \rho \bar{v}_x &= \sum v_{l,x} f_l, \\ y\text{-momentum} \quad \rho \bar{v}_y &= \sum v_{l,y} f_l, \\ \text{kinetic energy} \quad \frac{1}{2} |\mathbf{v}|^2 &= \frac{1}{2} \sum (v_{l,x}^2 + v_{l,y}^2) f_l \end{aligned}$$

which are conserved in each collision event.

We summarize the results satisfying the common features of kinetic theory which has been developed in [3] as follows.

Let (\mathcal{H}_b, γ) be a regular collision model. Then we have

• **H-Theorem:** Let $\mathbf{f}(t)$ be a solution of the space-homogeneous kinetic equation (2.12) for (\mathcal{H}_b, γ) with all components f_l are strictly positive. Then for the H-functional

$$H[\mathbf{f}] := \sum_l f_l \ln(f_l),$$

$$d_t H[\mathbf{f}] \leq 0$$

and $d_t H[\mathbf{f}] = 0$ if and only if \mathbf{f} is an equilibrium solution (see theorem 4.1, [3]).

- A vector \mathbf{f} is an equilibrium solution if and only if for all regular hexagons $H \in \mathcal{H}_b$, the six-tupel \mathbf{f}_H is an equilibrium solution of the six-velocity model.

- The set \mathcal{E} of equilibria is a smooth four-dimensional manifold (see proposition 4.5 [1]).

- The set of collision invariants is spanned by mass, momenta and kinetic energy (see proposition 4.5 [3]).

The weak formulation of the full linearized operator L on (\mathcal{H}_b, γ) is given by

$$\begin{aligned} \langle \psi, L\phi \rangle &= \sum_{H \in \mathcal{H}_b} \gamma_H \sum_{l=0}^{11} \psi(\pi_l^H) (L_H \phi_H)_l \\ &= \sum_{H \in \mathcal{H}_b} \gamma_H \langle P_H \psi, L_H P_H \phi \rangle \end{aligned} \quad (2.14)$$

and thus

$$L = \sum_{H \in \mathcal{H}_b} \gamma_H P_H^T L_H P_H \quad (2.15)$$

$$\text{where } (P_H)_{l,m} = \begin{cases} 1 & \text{if } l \leq 5 \text{ and } m = \pi_l^H \\ 0 & \text{else} \end{cases} \quad (2.16)$$

- L is a symmetric operator, its null space is four-dimensional and given by

$$N(L) = D^{-\frac{1}{2}} E = D^{\frac{1}{2}} \text{span}(\mathbb{1}, \mathbf{v}_x, \mathbf{v}_y, \mathbf{E}_{kin})$$

and all of its non-zero eigenvalues are negative.

- At the end, the above results were generalized for unbounded hexagonal grid. In a further work in [6], Babovsky has shown that the ternary collision terms imposed in the hexagonal collision model don't exist any more in the continuum limit and the binary collision operator then converges weakly to the true Boltzmann collision operator. \square

Now, for the calculation of the collision operator in a bounded hexagonal grid, we need in advance a list \mathcal{L} of all sixtupels $(\pi_l^H)_{l=0}^5$ of nodes of regular hexagons $H \in \mathcal{H}$.

Therefore, the task of [3] gives the motivation to generate a hexagonal grid which provide all the regular hexagons automatically.

In order to identify all the regular hexagons, we re-write the definition of hexagonal grid \mathcal{G} as well as the center points as follows.

For $\alpha = (i, j) \in \mathbb{Z}^2$, denote $\mathbf{g}_\alpha^t = (g_{\alpha,x}^t, g_{\alpha,y}^t)$, $t = 0, \dots, 3$ by

$$\begin{aligned} g_{\alpha,x}^0 &:= (3i + \frac{1}{2})h, & g_{\alpha,y}^0 &:= (2j + 1)\frac{\sqrt{3}}{2}h \\ g_{\alpha,x}^1 &:= (3i + 1)h, & g_{\alpha,y}^1 &:= 2j\frac{\sqrt{3}}{2}h \\ g_{\alpha,x}^2 &:= (3i + 2)h, & g_{\alpha,y}^2 &:= 2j\frac{\sqrt{3}}{2}h \\ g_{\alpha,x}^3 &:= (3i + \frac{5}{2})h, & g_{\alpha,y}^3 &:= (2j + 1)\frac{\sqrt{3}}{2}h \end{aligned} \quad (2.18)$$

Then for

$$\begin{aligned} \mathcal{G}^t &:= \{\mathbf{g}_\alpha^t | \alpha \in \mathbb{Z}^2\}, \quad t = 0, \dots, 3 \\ \mathcal{G} &:= \bigcup_t \mathcal{G}^t \end{aligned} \quad (2.19)$$

is the set of grid points of the hexagonal discretization on \mathbb{R}^2 . Again we denote $\mathbf{c}_\alpha^s = (c_{\alpha,x}^s, c_{\alpha,y}^s)$ $s = 0, 1$ by

$$\begin{aligned} c_{\alpha,x}^0 &:= 3ih, & c_{\alpha,y}^0 &:= 2j\frac{\sqrt{3}}{2}h \\ c_{\alpha,x}^1 &:= (3i + \frac{3}{2})h, & c_{\alpha,y}^1 &:= (2j + 1)\frac{\sqrt{3}}{2}h \end{aligned} \quad (2.20)$$

and then for

$$\begin{aligned} \mathcal{C}^s &:= \{\mathbf{c}_\alpha^s | \alpha \in \mathbb{Z}^2\}, \quad s = 0, 1 \\ \mathcal{C} &:= \bigcup_s \mathcal{C}^s \end{aligned} \quad (2.21)$$

is the set of center points of the hexagons in \mathbb{R}^2 . With the grid points given by equations (2.18), one can construct many other larger regular hexagons (as indicated by the dotted and dashed line in the Fig. 2.1) in addition to the basic hexagons. In order to identify all the regular hexagons $H \in \mathcal{H}$, we are going to prove that the centers of all the regular hexagons can be either, the grid-points given by equations 2.18, or the center-points given by the equations 2.20. With this ends we discuss the followings properties.

Proposition 2.1 *If $P_1(x_1, y_1)$ and $P_2(x_2, y_2)$ are any two consecutive nodes of a regular hexagon H , then the center $C(x, y)$ of H is given by*

$$x = \frac{1}{2}(x_1 + x_2) \pm \frac{\sqrt{3}}{2}(y_2 - y_1) \quad (2.22)$$

$$y = \frac{1}{2}(y_1 + y_2) \mp \frac{\sqrt{3}}{2}(x_2 - x_1) \quad (2.23)$$

proof:

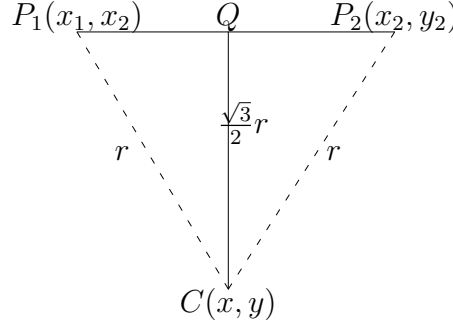


Fig. 2.2 Center point $C(x, y)$.

$P_1C = P_2C$ yields

$$2(x_2 - x_1)x + 2(y_2 - y_1)y + x_1^2 + y_1^2 - x_2^2 - y_2^2 = 0 \quad (2.24)$$

The equation of the line P_1P_2 is given by

$$y = m(x - x_1) + y_1, \quad m = \frac{y_2 - y_1}{x_2 - x_1}, \quad x_1 \neq x_2 \quad (2.25)$$

Then $CQ \perp P_1P_2$ yields

$$y - mx + mx_1 - y_1 = \pm \frac{\sqrt{3}}{2}r\sqrt{1 - m^2} \quad (2.26)$$

Then solving equations (2.24) & (2.26) with $r = |P_1P_2|$ we obtain x, y as in the statement. \square

Lemma 2.2 *Let \mathbb{Z}_e and \mathbb{Z}_o denote the set of even and odd integers respectively. Then for any $i_1, i_2 \in \mathbb{Z}$ (set of integers), $(i_1 + i_2) \in \mathbb{Z}_e(\mathbb{Z}_o)$ if and only if $(i_2 - i_1) \in \mathbb{Z}_e(\mathbb{Z}_o)$*

proof: For any $i_1, i_2 \in \mathbb{Z}$ with $(i_1 + i_2) \in \mathbb{Z}_e$ we assume $(i_2 - i_1) \in \mathbb{Z}_o$. Then we write

$$i_1 + i_2 = 2k, \quad i_2 - i_1 = 2l + 1, \quad k, l \in \mathbb{Z}$$

which contradicts the fact that $i_1, i_2 \in \mathbb{Z}$. Thus $(i_2 - i_1) \in \mathbb{Z}_e$. Similarly, we can proof the other cases. \square .

We use the above two properties to proof the following lemma.

Lemma 2.3 *Let P_1 and P_2 are any two consecutive nodes of a regular hexagon H and the coordinates of both of the nodes belong to the set \mathcal{G}^t (given by the equation (2.19)), $t = 0, \dots, 3$. Then the coordinates of the center C of the hexagon H belongs to either \mathcal{G}^t or $\mathcal{G}^{\tilde{t}}$, $\tilde{t} = t + 2 \pmod{4}$.*

proof: Suppose $P_1(x_1, y_1), P_2(x_2, y_2) \in \mathcal{G}^0$ i.e.

$$P_1 = \left(\left(3i_1 + \frac{1}{2}\right)h, (2j_1 + 1)\frac{\sqrt{3}}{2}h \right), \quad P_2 = \left(\left(3i_2 + \frac{1}{2}\right)h, (2j_2 + 1)\frac{\sqrt{3}}{2}h \right)$$

for some $(i_1, j_1), (i_2, j_2) \in \mathbb{Z}^2$. Then by proposition 2.1, the center $C(x, y)$ of hexagon H is given by

$$x = \left(\frac{3}{2}(i_1 + i_2) + \frac{1}{2} \right)h \pm (j_2 - j_1)\frac{3}{2}h \quad (2.27)$$

$$y = (j_1 + j_2 + 1)\frac{\sqrt{3}}{2}h \mp 3(i_2 - i_1)\frac{\sqrt{3}}{2}h \quad (2.28)$$

We have to consider the following four cases:

1. In the first case, we consider both $(i_1 + i_2), (j_1 + j_2) \in \mathbb{N}_e$. Then by lemma 2.2 we have

$$(i_1 + i_2) = 2k_1, \quad (i_2 - i_1) = 2k_2, \quad (j_1 + j_2) = 2l_1, \quad (j_2 - j_1) = 2l_2$$

for some $(k_1, l_1), (k_2, l_2) \in \mathbb{Z}^2$. Then the the center $C(x, y)$ is given by

$$\begin{aligned} x &= \left(3(k_1 \pm l_2) + \frac{1}{2} \right)h \equiv (3\tilde{i} + \frac{1}{2})h \\ y &= \left(2(l_1 \mp 3k_2) + 1 \right)\frac{\sqrt{3}}{2}h \equiv (2\tilde{j} + 1)\frac{\sqrt{3}}{2}h \end{aligned}$$

for some $(\tilde{i}, \tilde{j}) \in \mathbb{Z}^2$ and thus $(x, y) \in \mathcal{G}^0$.

2. Here we consider $(i_1 + i_2) \in \mathbb{N}_e, (j_1 + j_2) \in \mathbb{N}_o$. Then by lemma 2.2 we have

$$(i_1 + i_2) = 2k_1, \quad (i_2 - i_1) = 2k_2, \quad (j_1 + j_2) = 2l_1 + 1, \quad (j_2 - j_1) = 2l_2 + 1$$

for some $(k_1, l_1), (k_2, l_2) \in \mathbb{Z}^2$. Then the center $C(x, y)$ is given by

$$\begin{aligned} x &= \left(3(k_1 \pm l_2) + \frac{1}{2} \pm \frac{3}{2} \right)h \equiv (3\tilde{i} + 2)h \\ y &= \frac{\sqrt{3}}{2}h \left(2(l_1 \mp 3k_2 + 2) \right) \equiv 2\tilde{j}\frac{\sqrt{3}}{2}h \end{aligned}$$

for some $(\tilde{i}, \tilde{j}) \in \mathbb{Z}^2$ and thus $(x, y) \in \mathcal{G}^2$.

3. In this case we consider $(i_1 + i_2) \in \mathbb{N}_o$, $(j_1 + j_2) \in \mathbb{N}_e$. Then by lemma 2.2 we write

$$(i_1 + i_2) = 2k_1 + 1, \quad (i_2 - i_1) = 2k_2 + 1, \quad (j_1 + j_2) = 2l_1, \quad (j_2 - j_1) = 2l_2$$

for some $(k_1, l_1), (k_2, l_2) \in \mathbb{Z}^2$. Then the center $C(x, y)$ is given by

$$\begin{aligned} x &= \left(3(k_1 \pm l_2) + \frac{3}{2} + \frac{1}{2}\right)h \equiv (3\tilde{i} + 2)h \\ y &= \frac{\sqrt{3}}{2}h \left(2(l_1 \mp 3k_2 \mp 3)\right) \equiv 2\tilde{j} \frac{\sqrt{3}}{2}h \end{aligned}$$

for some $(\tilde{i}, \tilde{j}) \in \mathbb{Z}^2$ and thus $(x, y) \in \mathcal{G}^2$.

4. This is the case of both $(i_1 + i_2), (j_1 + j_2) \in \mathbb{N}_o$. Then by lemma 2.2 we write

$$(i_1 + i_2) = 2k_1 + 1, \quad (i_2 - i_1) = 2k_2 + 1, \quad (j_1 + j_2) = 2l_1 + 1, \quad (j_2 - j_1) = 2l_2 + 1$$

for some $(k_1, l_1), (k_2, l_2) \in \mathbb{Z}^2$. Then the center $C(x, y)$ is given by

$$\begin{aligned} x &= \left(3(k_1 \pm l_2) + \frac{3}{2} + \frac{1}{2} \pm \frac{3}{2}\right)h \equiv \left(3\tilde{i} + \frac{1}{2}\right)h \\ y &= \frac{\sqrt{3}}{2}h \left(2(l_1 \mp 3k_2) + 2 \mp 3\right) \equiv (2\tilde{j} + 1) \frac{\sqrt{3}}{2}h \end{aligned}$$

for some $(\tilde{i}, \tilde{j}) \in \mathbb{Z}^2$ and thus $(x, y) \in \mathcal{G}^0$.

The proof of the other cases for $t = 1, 2, 3$ are similar. \square

Lemma 2.4 *Let P_1 and P_2 be any two consecutive nodes of a regular hexagon H where $P_1(x_1, x_2) \in \mathcal{G}^t$ & $P_2(x_2, y_2) \in \mathcal{G}^{t'}$ ($\mathcal{G}^t, t = 0, \dots, 3$ given by (2.19), $t' \in \{0, \dots, 3\} - \{t\}$), then*

1. *For $|t - t'| = 2$, the coordinates of the center $C(x, y)$ of the hexagon H belongs to either \mathcal{G}^t or $\mathcal{G}^{t'}$;*
2. *For $|t - t'| \neq 2$, the coordinates of the center $C(x, y)$ of the hexagon H belongs to either \mathcal{C}^0 or \mathcal{C}^1 ($\mathcal{C}^s, s = 0, 1$, is given by 2.21).*

proof: First we choose $t = 0, t' = 1$, i.e.

$$P_1 = \left((3i_1 + \frac{1}{2})h, \frac{\sqrt{3}}{2}h(2j_1 + 1) \right), \quad P_2 = \left((3i_2 + 1)h, 2j_2 \frac{\sqrt{3}}{2}h \right)$$

for any $(i_1, j_1), (i_2, j_2) \in \mathbb{Z}^2$. Then by proposition 2.1, the center $C(x, y)$ of hexagon H is given by

$$x = \left(\frac{3}{2}(i_1 + i_2) + \frac{3}{4}\right)h \pm \frac{3}{2}h\left(j_2 - j_1 - \frac{1}{2}\right) \quad (2.29)$$

$$y = \frac{\sqrt{3}}{2}h\left(j_1 + j_2 + \frac{1}{2}\right) \mp \frac{\sqrt{3}}{2}h\left(3(i_2 - i_1) + \frac{1}{2}\right) \quad (2.30)$$

For all the four different cases of $(i_1 + i_2), (j_1 + j_2)$ be even or odd, as in proof of the lemma 2.3, we obtained (x, y) as

$$(x, y) \equiv \left(3\tilde{i}h, 2\tilde{j}\frac{\sqrt{3}}{2}h\right) \in \mathcal{C}^0 \text{ or } \left(\left(3\tilde{i} + \frac{3}{2}\right)h, (2\tilde{j} + 1)\frac{\sqrt{3}}{2}h\right) \in \mathcal{C}^1$$

for $(\tilde{i}, \tilde{j}) \in \mathbb{Z}^2$ and thus $(x, y) \in \mathcal{C}^s, s = 0, 1$. Proof of other cases can be shown by similar straight forward calculation. \square

Theorem 2.5 *The centers of all regular hexagons constructed by any six-tupel nodes of hexagonal grid on \mathbb{R}^2 is either a node of the hexagonal grid or a center of the regular basic hexagon of the hexagonal grid.*

proof: The proof follows from the lemmas (2.3-2.4). \square

Definition 2.6 Class-A, Class-B hexagons: Following Theorem 2.5, the hexagonal grid contains two different classes of regular hexagons with center at the centers of regular basic hexagons and with centers at the interior grid points. We call these two classes of regular hexagons as *class-A* and *class-B* respectively (in Fig. 2.1 they are marked by dotted and dashed line respectively).

Now let $\mathbf{g}_l \in \mathcal{G}, l = 0, 1$ be any two neighboring nodes of the hexagonal grid in \mathbb{R}^2 i.e $|\mathbf{g}_0 - \mathbf{g}_1| = h$. We introduce a *sign*-function (as in [6])

$$\text{sign}: \mathcal{G} \rightarrow \{-1, 1\} \quad (2.31)$$

such that

$$\text{sign}(\mathbf{g}_0)\text{sign}(\mathbf{g}_1) = -1 \quad (2.32)$$

Then for $\alpha = (0, 0)$, if we consider $\text{sign}(\mathbf{g}_\alpha^0) := 1$, for any $\alpha = (i, j) \in \mathbb{Z}^2$ we have

$$\text{sign}(\mathbf{g}_\alpha^t) = (-1)^t \text{ for } t = 0, \dots, 3 \quad (2.33)$$

where \mathbf{g}_α^t is defined by equation (2.18).

Thus with the above definition of *sign*-function,

$$\text{sign}(\mathbf{g}) = (-1)^t, \forall \mathbf{g} \in \mathcal{G}^t, \text{ for } t = 0, \dots, 3. \quad (2.34)$$

$$(2.35)$$

We have the following properties.

Theorem 2.7 *Let $(\mathbf{g}_0, \dots, \mathbf{g}_5)$ be the six-tupel nodes of any regular hexagon $H \in$ class-A. Then*

$$\text{sign}(\mathbf{g}_l)\text{sign}(\mathbf{g}_m) = -1, \quad m = l + 1 \pmod{6}, \quad l = 0, \dots, 5 \quad (2.36)$$

proof: Lemma 2.4(2) is the case of class-A hexagons where the pair $(\mathbf{g}_l, \mathbf{g}_m)$ is such that either

$$\mathbf{g}_l \in \mathcal{G}^0 \ \& \ \mathbf{g}_m \in \mathcal{G}^1, \implies \text{sign}(g_l) = 1, \text{sign}(g_m) = -1 \text{ (by def. (2.33))} \quad (2.37)$$

$$\text{or } \mathbf{g}_l \in \mathcal{G}^0 \ \& \ \mathbf{g}_m \in \mathcal{G}^3, \implies \text{sign}(g_l) = 1, \text{sign}(g_m) = -1 \quad (2.38)$$

$$\text{or } \mathbf{g}_l \in \mathcal{G}^1 \ \& \ \mathbf{g}_m \in \mathcal{G}^2, \implies \text{sign}(g_l) = -1, \text{sign}(g_m) = 1 \quad (2.39)$$

$$\text{or } \mathbf{g}_l \in \mathcal{G}^2 \ \& \ \mathbf{g}_m \in \mathcal{G}^3, \implies \text{sign}(g_l) = 1, \text{sign}(g_m) = -1 \quad (2.40)$$

In all the four cases,

$$\text{sign}(\mathbf{g}_l)\text{sign}(\mathbf{g}_m) = -1. \quad \square$$

Theorem 2.8 *For $\mathbf{g}_l \in \mathcal{G}, l = 0, 1$; let $(\mathbf{g}_0, \dots, \mathbf{g}_5)$ denote the six-tupel nodes and $\bar{\mathbf{g}} \in \mathcal{G}$ denote the center of any regular hexagon $H \in$ class-B. Then*

$$\text{sign}(\mathbf{g}_l) \cdot \text{sign}(\mathbf{g}_m) = 1, \quad m = l + 1 \pmod{6}, \quad l = 0, \dots, 5 \text{ and} \quad (2.41)$$

$$\text{sign}(\mathbf{g}_l) \cdot \text{sign}(\bar{\mathbf{g}}) = 1, \quad l = 0, \dots, 5 \quad (2.42)$$

proof: Again with the definition (2.33), the proof follows from the lemma 2.3 and lemma 2.4 (1). \square

If we exclude the ternary collision operator from the global collision operator given by the equation (2.8), then we have the following result.

Corollary 2.9 *Let \mathbf{f} be a strictly positive density function on \mathcal{G} . Then*

$$\langle \text{sign}(\mathbf{g}), \mathbf{f} \rangle = \text{invariant}$$

and it is the only spurious invariant.

proof: From theorem 2.7 and theorem 2.8 it follows respectively that $\langle \text{sign}(\mathbf{g}_H), \mathbf{f}_H \rangle$ is the spurious invariant $\langle a_H, \mathbf{f}_H \rangle$ (a_H is given by equation 2.11) for $H \in$ class-A and the physical invariant $\pm \rho_H = \langle \pm(1, 1, 1, 1, 1, 1)^\top, \mathbf{f}_H \rangle$ for $H \in$ class-B. Then the proof is completed from the definition (given by equation 2.13) of the global collision operator.

If we consider only binary collision law, then it is seen that the equilibria is a five-dimensional manifold and thus $\langle \text{sign}(\mathbf{g}), \mathbf{f} \rangle$ is the only spurious invariant \square

Remark 2.10 Thus to assure the correct number of invariants of the system it is sufficient to include ternary collision law for a single basic hexagon. However, in order to use shift operator it is necessary to include the ternary collision law for all the basic hexagons but we can exclude it for the class-A and class-B hexagons.

Now to collect all the class-A and class-B hexagons $H \in \mathcal{H}$ from the grid \mathcal{G} , we need a more systematic approach, a layer-wise construction of the model that can be called a N -layer model which is described in the next section.

2.2 A N -layer hexagonal model

Fig. 2.3 shows a 54-velocity model which is constructed by adding two-layers of hexagons centering to a central one and thus called a two-layer model. Similarly by adding one more layer of regular basic hexagons, one can obtain a 3-layer model and so on. In general, we may call such models the N -layer model (as a regular collision model defined in [3]) which can be divided into six symmetric partition as shown in the Fig. 2.3

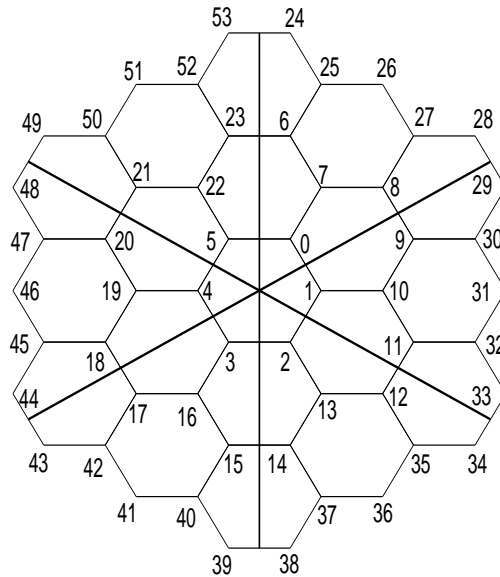


Fig. 2.3 A 54-velocity model as a two-layer model.

In order to generate a hexagonal mesh for the N -layer model, first we collect the centers of all basic hexagons ordered layer-wise and partition-wise as shown in algorithm 2.1.

For a given $N \in \mathbb{N}$,
 INITIALIZE $c_x = 0; c_y = 0$;
 FOR $n = 1$ TO N

$$\begin{aligned}
 c_{x_{0,n}} &= (0, \dots, n-1) \frac{3}{2}h \\
 c_{x_{1,n}} &= \underbrace{\left(n \frac{3}{2}h, \dots, n \cdot \frac{3}{2}h\right)}_n \\
 c_{x_{2,n}} &= \left(n \cdot \frac{3}{2}h - (0, \dots, n-1) \frac{3}{2}h\right) \\
 c_{x_{3,n}} &= -(0, \dots, n-1) \cdot \frac{3}{2}h \\
 c_{x_{4,n}} &= \underbrace{\left(-n \cdot \frac{3}{2}h, \dots, -n \cdot \frac{3}{2}h\right)}_n \\
 c_{x_{5,n}} &= \left(-n \cdot \frac{3}{2}h + (0, \dots, n-1) \frac{3}{2}h\right) \\
 c_{x_n} &= \left(c_{x_{0,n}}, c_{x_{1,n}}, c_{x_{2,n}}, c_{x_{3,n}}, c_{x_{4,n}}, c_{x_{5,n}}\right) \\
 c_x &= (c_x, c_{x_n}) \\
 c_{y_{0,n}} &= (2n - (0, \dots, n-1)) \cdot \frac{\sqrt{3}}{2}h \\
 c_{y_{1,n}} &= (n - 2(0, \dots, n-1)) \frac{\sqrt{3}}{2}h \\
 c_{y_{2,n}} &= -(n + (0, \dots, n-1)) \cdot \frac{\sqrt{3}}{2}h \\
 c_{y_{3,n}} &= (-2n + (0, \dots, n-1)) \cdot \frac{\sqrt{3}}{2}h \\
 c_{y_{4,n}} &= (-n + 2(0, \dots, n-1)) \frac{\sqrt{3}}{2}h \\
 c_{y_{5,n}} &= (n + (0, \dots, n-1)) \cdot \frac{\sqrt{3}}{2}h \\
 c_{y_n} &= \left(c_{y_{0,n}}, c_{y_{1,n}}, c_{y_{2,n}}, c_{y_{3,n}}, c_{y_{4,n}}, c_{y_{5,n}}\right) \\
 c_y &= (c_y, c_{y_n})
 \end{aligned}$$

END

Indices i, n in $(c_{x_{i,n}}, c_{y_{i,n}})$ are for layer and partition respectively.

Algorithm 2.1 Centers of basic hexagons.

By the above algorithm, we obtain the vectors c_x, c_y for the (x, y) -coordinate of the centers of all regular basic hexagon of the N -layer model. The (x, y) -coordinates of

nodes of the basic hexagons are given by

$$\mathbf{G} = \mathbf{c} + h \cdot \left(\sin\left(\frac{2\pi}{6}(k - 0.5)\right), \cos\left(\frac{2\pi}{6}(k - 0.5)\right) \right)_{k=1}^6 \quad (2.43)$$

where h is the discretization parameter, $\mathbf{c} = (c_x, c_y)$ is already obtained by the above algorithm 2.1. The following algorithm 2.2 provides the vectors G_x, G_y respectively for the the x, y -coordinates of the nodes of a N -layer grid and plots the hexagonal mesh as seen in Fig. 2.4.

```

INITIALIZE VECTORS  $G_x, G_y$ 
FOR  $i = 1$  TO  $|c_x|$ 
  INITIALIZE VECTORS  $g_x, g_y$ 
  FOR  $k = 1$  TO 6
     $g_{x_k} = \left( g_x, c_{x_i} + h \left( \sin\left(\frac{2\pi}{6}(k - 0.5)\right) \right) \right)$ 
     $g_{y_k} = \left( g_y, c_{y_i} + h \left( \cos\left(\frac{2\pi}{6}(k - 0.5)\right) \right) \right)$ 
   $g_x = (g_x, g_{x_k})$ 
   $g_y = (g_y, g_{y_k})$ 
  END
   $G_x = (G_x, g_x)$ 
   $G_y = (G_x, g_y)$ 
  FOR  $k = 1$  TO 6
     $l = 1 + \text{mod}(j, 6)$ 
     $x = (g_{x_k}, g_{x_l})$ 
     $y = (g_{y_k}, g_{y_l})$ 
    PLOT  $(x, y)$ 
  END
END

```

Algorithm 2.2 Grid points.

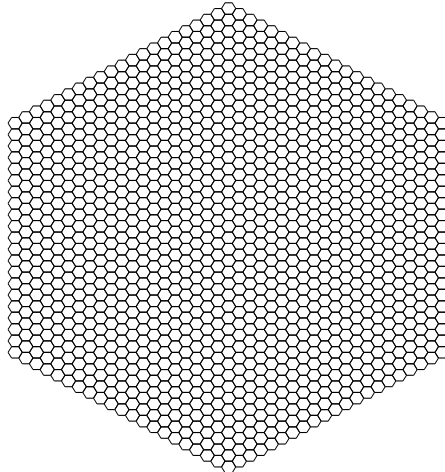


Fig. 2.4 A 20-layer hexagonal mesh.

It can be considered that the 20-layer mesh (Fig. 2.4) consists of 1261 regular basic

hexagons and 2646 nodes but the formulae for this information are given by the lemmas, lemma 2.11 and lemma 2.12 respectively .

The vectors G_x, G_y give, respectively, the (x, y) -co-ordinates of $6 \times |c_x|$ nodes many of which are common. Unique velocity vectors for unique nodes of the N -layer model enumerated as in Fig. 2.3 can be obtained as shown in Algorithm 2.3.

```

INITIALIZE VECTOR  $U = (0, \dots, 5)$ 
FOR  $n = 1$  TO  $N$  (For each  $n$ -th layer)
  INITIALIZE  $W$ 
  FOR  $k = 1$  TO  $6$  (for each  $k$ -th partition)
     $l = 1 + \text{mod}(k, 6)$ 
    INITIALIZE  $v$ 
    FOR  $j = 1$  TO  $n$  (for each  $j$ -th hexagon)
      †  $v_1 = (3(n-1)n + 1 + n(k-1) + j - 1) \times 6 - 1 + k$ 
      †  $v_2 = (3(n-1)n + 1 + n(k-1) + j - 1) \times 6 - 1 + l$ 
       $v = (v, v_1, v_2)$ 
    END
     $v_f = (3(n-1)n + 1 + nk) \times 6 - 1 + k$  (( $2n+1$ )-th node)
    IF  $k=6$ 
       $v_f = (3(n-1)n + 1 + 1) \times 6 - 1$ 
    END
     $V = (v, v_f)$ 
     $W = (W, V)$ 
  END
   $U = (U, W)$ 
END
INITIALIZE VECTORS  $v_x, v_y$  (unique velocity vector)
FOR  $i = 1$  TO  $|U|$ 
   $v_{x_i} = G_x(U_i)$ 
   $v_{y_i} = G_y(U_i)$ 
   $v_x = (v_x, v_{x_i})$ 
   $v_y = (v_y, v_{y_i})$ 
END

```

Algorithm 2.3 Re-enumeration.

The vectors v_x, v_y in the above algorithm represent, respectively, the (x, y) -component velocity vectors of length $6(N+1)^2$ of the N -layer model enumerated as in Fig. 2.3.

† In Algorithm 2.3

$$v_1 = \left(3(n-1)n + 1 + n(k-1) + j - 1 \right) \times 6 - 1 + k$$

$$v_2 = \left(3(n-1)n + 1 + n(k-1) + j - 1 \right) \times 6 - 1 + l, \quad l = 1 + \text{mod}(k, 6)$$

are the indices of G for the $(k, k + 1)$ -th pair of nodes of each j -th ($j = 1, \dots, n$) hexagon of k -th ($k = 1, \dots, 6$) partition of each n -th ($n = 1, \dots, N$) layer, where $3(n - 1)n + 1$ is the number of hexagon up to $(n - 1)$ -th layer, $n(k - 1)$ is the number of hexagon up to $(k - 1)$ -th partition of n -th layer. With (v_1, v_2) we collect the first $2n$ -th indices of each k -th partition of each n -st layer. Finally we collect $(2n + 1)$ -th index

$$v_f = \left(3(n - 1)n + 1 + nk\right) \times 6 - 1 + k \quad \text{and in particular for } k = 6$$

$$v_f = \left(3(n - 1)n + 1 + 1\right) \times 6 - 1 \quad \square$$

The centers of a N -layer model is given in algorithm 2.1. The lines passing through the centers of each n th layer produce N number of hexagons H_c as shown in the figure below. The thick dots in the figure indicate the centers of regular basic hexagons of a 3-layer model.

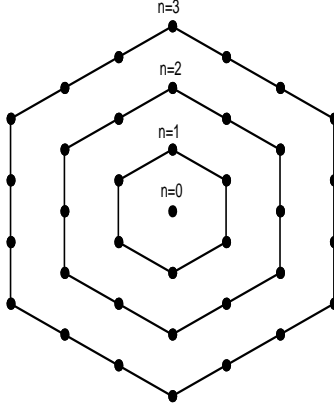


Fig. 2.5 Hexagons H_c passing through the centers at different layers.

Lemma 2.11 *There are $6n$ number of regular basic hexagons in the n -th ($n = 1, \dots, N$) layer of a N -layer grid and the total number of regular basic hexagons of a N -layer grid is given by $3N(N + 1) + 1$.*

Proof: From the definition of center points (as given in algorithm 2.1) of a N -layer grid, the length of each side of a n -th layer hexagon H_c (Fig. 2.5), is given by

$$L = \left(\left(n\frac{3}{2}h\right)^2 + \left(n\frac{\sqrt{3}}{2}h\right)^2 \right)^{1/2} = n\sqrt{3}h,$$

and the distance between any two neighboring centers is given by

$$l = \sqrt{3}h.$$

Thus the number of center points lies on each side is given by

$$\frac{L}{l} = n + 1.$$

That is, the number center points lies on each H_c is $6n$. In other words, the total number of hexagons in the n -th layer is $6n$. Thus,

$$\begin{aligned} \#(\text{regular basic hexagons in a } N\text{-layer grid}) &= 1 + 6(1 + 2 + \cdots + N) \\ &= 3N(N + 1) + 1 \quad \square \end{aligned}$$

Lemma 2.12 *There are $6(2n + 1)$ number of nodes in the n -th ($n = 0, \dots, N$) layer of a N -layer grid, and the total number of nodes in a N -layer grid is given by $6(N + 1)^2$.*

Proof: In 0-st layer, the grid has 6 nodes. For each n -th layer, the grid provides $6n(6 - 2) = 24n$ number of nodes which include the nodes of the $(n - 1)$ -st layer too. e.g.

In 1st-layer, the grid provides $(24 \times 1 - 6) = 18 = 6(2 \times 1 + 1)$ number of nodes.

In 2nd-layer, it provides $(24 \times 2 - 18) = 30 = 6(2 \times 2 + 1)$ number of nodes.

In 3rd-layer, it provides $(24 \times 3 - 30) = 42 = 6(2 \times 3 + 1)$ number of nodes.

Now let us assume that, in m -th layer the grid provides $6(2m + 1)$ number of nodes. Then in the $(m + 1)$ -th layer, it provides

$$\begin{aligned} (24 \times (m + 1) - 6(2m + 1)) &= 12m + 18 \\ &= 6(2 \times (m + 1) + 1) \end{aligned}$$

new nodes.

Therefore, in the N -model,

$$\begin{aligned} \#(\text{the total number of nodes}) &= 6 + 6(2(1 + 2 + \cdots + N) + N) \\ &= 6(N + 1)^2 \quad \square \end{aligned}$$

2.2.1 Identification of Class-A and Class-B hexagons

We already know the co-ordinates $(v_x(l), v_y(l))$ of each l -th node ($l = 1, \dots, 6(N + 1)^2$) of the N -layer model. We also know formula 2.43 to identify the nodes of all basic hexagons. We exclude the basic hexagons from 'class-A' and we call them 'class-0' hexagons and the rest of the 'class-A' ones will be known as 'class-A' hexagons. Then we need to identify the nodes of the class-A and class-B hexagons (definition 2.6). To this aim, we write the definition of grid-points and centers for the N -layer model as follows.

Grid points and Centers of N -layer model

For N is even(odd), $k = \frac{N}{2}(\frac{N-1}{2})$, $\alpha = (i, j) \in \mathbb{Z}^2$, denote $\mathbf{g}_\alpha^t = (g_{\alpha,x}^t, g_{\alpha,y}^t)$, $t = 0, \dots, 3$ by

$$\begin{aligned} g_{\alpha,x}^0 &:= (3i + \frac{1}{2})h, & g_{\alpha,y}^0 &:= (2j + 1)\frac{\sqrt{3}}{2}h \quad \text{where for each} \\ & & & i = 0, \dots, k; \quad j = 0, \pm 1, \dots, \pm(N - i), -(N - i + 1) \quad \text{and for each} \\ & & & i = -1, \dots, -(k + 1); \quad j = 0, \pm 1, \dots, \pm(N - |i|), -(N - |i| + 1), \end{aligned} \quad (2.44)$$

$$\begin{aligned} g_{\alpha,x}^1 &:= (3i + 1)h, & g_{\alpha,y}^1 &:= 2j\frac{\sqrt{3}}{2}h \quad \text{where for each} \\ & & & i = 0, \dots, k; \quad j = 0, \pm 1, \dots, \pm(N - i) \quad \text{and for each} \\ & & & i = -1, \dots, -(k + 1); \quad j = 0, \pm 1, \dots, \pm(N - |i| + 1), \end{aligned} \quad (2.45)$$

$$\begin{aligned} g_{\alpha,x}^2 &:= (3i + 2)h, & g_{\alpha,y}^2 &:= 2j\frac{\sqrt{3}}{2}h \quad \text{where for each } i = 0, \dots, (k - 1) \text{ (or } k) \\ & & & \text{(according as } N \text{ is even(or odd)); } \quad j = 0, \pm 1, \dots, \pm(N - i), \\ & & & \text{and for each } i = -1, \dots, -(k + 1); \quad j = 0, \pm 1, \dots, \pm(N - |i| + 1) \end{aligned} \quad (2.46)$$

$$\begin{aligned} g_{\alpha,x}^3 &:= (3i + \frac{5}{2})h, & g_{\alpha,y}^3 &:= (2j + 1)\frac{\sqrt{3}}{2}h \quad \text{where for each } i = 0, \dots, (k - 1) \text{ (or } k) \\ & & & \text{(according as } N \text{ is even(or odd)); } \quad j = 0, \pm 1, \dots, \pm(N - i - 1), -(N - i) \quad \text{and for each} \\ & & & i = -1, \dots, -(k + 1); \quad j = 0, \pm 1, \dots, \pm(N - |i| + 1), -(N - |i| + 2). \end{aligned} \quad (2.47)$$

Then for

$$\begin{aligned} \mathcal{G}_N^t &:= \{ \mathbf{g}_\alpha^t | \alpha \in \mathbb{Z}^2 \}, \quad t = 0, \dots, 3 \\ \mathcal{G}_N &:= \bigcup_t \mathcal{G}_N^t \end{aligned} \quad (2.48)$$

is the set of grid points of the N -layer hexagonal mesh on \mathbb{R}^2 . Again we denote $\mathbf{c}_\alpha^s = (c_{\alpha,x}^s, c_{\alpha,y}^s)$ $s = 0, 1$ by

$$\begin{aligned} c_{\alpha,x}^0 &:= 3ih, & c_{\alpha,y}^0 &:= 2j\frac{\sqrt{3}}{2}h \quad \text{where for each} \\ & & & i = 0, \pm 1, \dots, \pm k; \quad j = 0, \pm 1, \dots, \pm(N - |i|) \end{aligned} \quad (2.49)$$

$$\begin{aligned} c_{\alpha,x}^1 &:= (3i + \frac{3}{2})h, & c_{\alpha,y}^1 &:= (2j + 1)\frac{\sqrt{3}}{2}h \quad \text{where for each} \\ & & & i = 0, \dots, k; \quad j = 0, \pm 1, \dots, \pm(N - i - 1), -(N - i) \quad \text{and for each} \\ & & & i = -1, \dots, -(k + 1); \quad j = 0, \pm 1, \dots, \pm(N - |i|), -(N - |i| + 1) \end{aligned} \quad (2.50)$$

$$(2.51)$$

and then for

$$\begin{aligned} \mathcal{C}_N^s &:= \{ \mathbf{c}_\alpha^s | \alpha \in \mathbb{Z}^2 \}, \quad s = 0, 1 \\ \mathcal{C}_N &:= \bigcup_s \mathcal{C}_N^s \end{aligned} \quad (2.52)$$

is the set of center points of the basic hexagons of the N -layer hexagonal grid on \mathbb{R}^2 .

Hexagons of Class-A

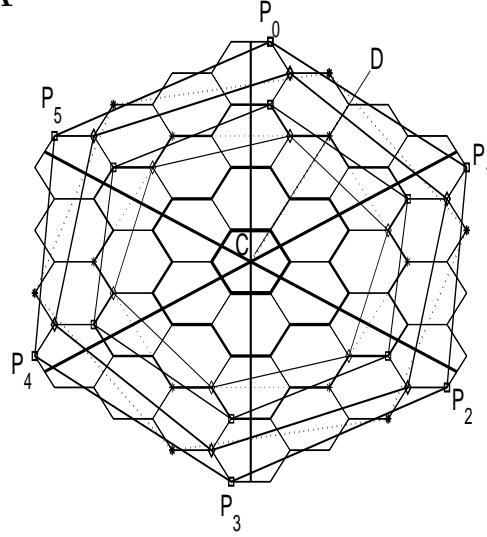


Fig. 2.6 Class-A hexagons.

Fig. 2.6 shows a 3-layer model, where the nodes $0, \dots, 5$ (enumeration is shown in Fig. 2.3) belongs to the 0-th layer (marked by thickest line segments), the nodes $6, \dots, 23$ belongs to the 1st layer (marked by 2nd thickest line segments), and so on. By the three solid straight lines the model is divided into six symmetric partitions and the partition immediately right to the positive y -axis is called as *first partition*. Each partition in the n -th ($n = 0, \dots, N$) layer contains $2n + 1$ number of nodes and have symmetry about the divider line CD . If the center $C(x, y)$ of a regular class-A hexagon H is given together with a node $P_0(x_0, y_0)$, then we can find the all other nodes $P_m(x_m, y_m)$, $m = 1, \dots, 5$ of H by the following formulae.

$$(x_3, y_3) = (2x - x_0, 2y - y_0), \quad (2.53)$$

$$(x_1(x_5), y_1(y_5)) = \left(\frac{1}{2}(x_0 + x) \pm \frac{\sqrt{3}}{2}(y_0 - y), \frac{1}{2}(y_0 + y) \mp \frac{\sqrt{3}}{2}(x_0 - x) \right) \quad (2.54)$$

$$(x_2(x_4), y_1(y_5)) = \left(\frac{1}{2}(x_3 + x) \pm \frac{\sqrt{3}}{2}(y_3 - y), \frac{1}{2}(y_3 + y) \mp \frac{\sqrt{3}}{2}(x_3 - x) \right) \quad (2.55)$$

We may call the pair (C, P_0) as a generator of H .

Proposition 2.13 *Let the origin of the grid \mathcal{G}_N be the center $C(0, 0)$, and $P_0(x_0, y_0)$ be any node in the n th layer of the first partition. Then with generator (C, P_0) , there exist always a regular hexagon $H \in \mathcal{G}_N$.*

proof: Let $P_0(x_0, y_0)$ be any node in the n th layer of the first partition. Then $P_0 \in \mathcal{G}_N^t$ for any $t = 0, \dots, 3$. Thus we have to go through with all this four cases for $t = 0, \dots, 3$.

Case-0: Let $P_0(x_0, y_0) \in \mathcal{G}^0$ in the first partition of the n -th layer. Then

$$(x_0, y_0) = \left((3i + \frac{1}{2})h, (2j + 1)\frac{\sqrt{3}}{2}h \right) \text{ for each } i = 0, \dots, k; \quad j = (n - i)$$

Using the equation (2.53), we find

$$\begin{aligned} x_3 &= -(3i + \frac{1}{2})h = \left(-3(i + 1) + \frac{5}{2} \right)h \equiv \left(3\tilde{i} + \frac{5}{2} \right)h \\ y_3 &= -\left(2(n - i) + 1 \right)\frac{\sqrt{3}}{2}h = \left(-2(n - i - 1) + 1 \right)\frac{\sqrt{3}}{2}h \equiv (2\tilde{j} + 1)\frac{\sqrt{3}}{2}h \end{aligned}$$

where $\tilde{i} = -(k + 1), \dots, -1$ respectively with $\tilde{j} = -(n - k - 1), \dots, -(n - 1)$ guarantee that $(x_3, y_3) \in \mathcal{G}_N^3$.

We show now $P_1(x_1, y_1), P_5(x_5, y_5)$ belongs to \mathcal{G}_N . Using the formula 2.54, we find

$$\begin{aligned} (x_1, y_1) &= \left(\left(\frac{3}{2}n + 1 \right)h, (n - 4i)\frac{\sqrt{3}}{2}h \right) \\ (x_5, y_5) &= \left(\left(3i - \frac{3}{2}n - \frac{1}{2} \right)h, (n + 2i + 1)\frac{\sqrt{3}}{2}h \right) \end{aligned}$$

For n is even we have $n = 2k$, then

$$\begin{aligned} (x_1, y_1) &= \left((3k + 1)h, 2(k - 2i)\frac{\sqrt{3}}{2}h \right) \equiv \left((3\tilde{i}_1 + 1)h, 2\tilde{j}_1\frac{\sqrt{3}}{2}h \right) \\ (x_5, y_5) &= \left(\left(3(i - k - 1) + \frac{5}{2} \right)h, (2(k + i) + 1)\frac{\sqrt{3}}{2}h \right) \equiv \left((3\tilde{i}_5 + \frac{5}{2})h, (2\tilde{j}_5 + 1)\frac{\sqrt{3}}{2}h \right) \end{aligned}$$

where $\tilde{i}_1 = k$ with $\tilde{j}_1 = -k, \dots, k$ and $\tilde{i}_5 = -(k + 1), \dots, -1$ respectively with $\tilde{j}_5 = k, \dots, 2k$ guarantee that $P_1(x_1, y_1) \in G_N^1$ and $P_3(x_5, y_5) \in G_N^3$.

For n is odd, $n = 2k + 1$, then we have

$$\begin{aligned} (x_1, y_1) &= \left(\left(3k + \frac{5}{2} \right)h, (2(k - 2i) + 1)\frac{\sqrt{3}}{2}h \right) \equiv \left(\left(3\tilde{i}_1 + \frac{5}{2} \right)h, (2\tilde{j}_1 + 1)\frac{\sqrt{3}}{2}h \right) \\ (x_5, y_5) &= \left(\left(3(i - k - 1) + 1 \right)h, 2(k + i + 1)\frac{\sqrt{3}}{2}h \right) \equiv \left((3\tilde{i}_5 + 1)h, 2\tilde{j}_5\frac{\sqrt{3}}{2}h \right) \end{aligned}$$

where $\tilde{i}_1 = k$ with $\tilde{j}_1 = -k, \dots, k$ and $\tilde{i}_5 = -(k + 1), \dots, -1$ respectively with $\tilde{j}_5 = (k + 1), \dots, (2k + 1)$ guarantee that $P_1(x_1, y_1) \in \mathcal{G}_N^1$ and $P_3(x_5, y_5) \in \mathcal{G}_N^3$. Thus $P_1(x_1, y_1), P_5(x_5, y_5)$ belongs to \mathcal{G}_N . Similarly using the formulae (2.55), it is seen that $P_2(x_1, y_1), P_2(x_5, y_5)$ also belongs to \mathcal{G}_N .

Case-(1,2,3): In these three cases for $P_0(x_0, y_0) \in \mathcal{G}_N^t, t = 1, 2, 3$, similar arguments holds and it is seen that all the rest nodes $P_m(x_m, y_m) \in \mathcal{G}_N, m = 1, \dots, 5$. \square

Thus each l -th ($l = 1 \cdots, 2n + 1$) nodes from each six partitions of n -th ($n = 1, \dots, N$) layer produce $(2n + 1)$ number of distinct class-A hexagons. Here we exclude $n = 0$, as it is the case for the basic hexagons which we exclude from class-A and we will call the class of all basic hexagons as "class-0". Since the N -layer model can be decompose into $3n(n + 1) + 1$ number of $(N - n)$ -layer model for $n = 1, \dots, N - 1$, therefore for $n = N - 1$, the same $(2(N - 1) + 1)$ distinct hexagons exists for the six centers in the 1-layer, in addition to the center $C(0, 0)$; and for $n = N - 2$ the same $(2(N - 2) + 1)$ distinct hexagons exists for the centers up to the centers in the 2-layer and so forth. In Fig. 2.6, we observe the situation as

1. there are seven distinct hexagons with centers at origin and all seven nodes from each six partition of the $n = 3$ -rd layer,
2. there are five distinct hexagons with center at origin and all five nodes from each six partitions of the $n = 2$ -st layer and in addition, we have the similar five distinct hexagons with center at each 6 centers of the basic hexagons in the 1-st layer,
3. similarly if we consider the hexagons centering to the origin with nodes from the 1-st layer we find three distinct hexagons but we have the similar three distinct hexagons for each centers of the basic hexagons up to the 2-layer.

Thus the total number of class-A hexagons for this $N = 3$ -layer model is given by

$$\#(H_3^A) = 7 \times 1 + 5 \times 7 + 3 \times 19$$

and in general the total number of class-A hexagons H_N^A of a N -layer model is given by

$$\#(H_N^A) = \sum_{n=1}^N (2n + 1) \left(3(N - n)(N - n + 1) + 1 \right).$$

Now in order to derive formula to identify the class-A hexagons, we need to find their radii $R_{n,l}^A$, $l = 1, \dots, (2n + 1)$ and the initial angles $\theta_{n,l}$ for each n -th layer. However the radii are symmetric about the dividing line CD (see Fig. 2.6) of the partition and therefore we need to find the radii for $l = 1, \dots, n + 1$ only and for each $l = 1, \dots, n + 1$ we have to find two initial angles $\theta_{n,l}^m$, $m = 0, 1$. One can easily verify the following proposition.

Proposition 2.14 *In each partition of n -th layer of a N -layer grid, the radii of class-A hexagons are symmetric about the dividing line CD in Fig. 2.6 and are given by*

$$R_{n,l \in [1, n+1]}^A := \left\{ R_{n,2k-1}, R_{n,2k} \right\} \quad (2.56)$$

where

$$R_{n,2k-1}^2 := \left(\frac{1 + 3(k-1)}{2} h \right)^2 + \left(\frac{2n + 2 - k}{2} \sqrt{3} h \right)^2$$

for

$$k = 1, \dots, \frac{n+1}{2} \quad \text{when } n \text{ is odd; } \quad k = 1, \dots, \frac{n+2}{2} \quad \text{when } n \text{ is even}$$

and

$$R_{n,2k}^2 := \left(\frac{2 + 3(k-1)}{2} h \right)^2 + \left(\frac{2n+1-k}{2} \sqrt{3} h \right)^2$$

for

$$k = 1, \dots, \frac{n+1}{2} \quad \text{when } n \text{ is odd; } \quad k = 1, \dots, \frac{n}{2} \quad \text{when } n \text{ is even.}$$

With the radii as given in the above proposition, we give the general formulae to identify the class-A regular hexagons as follows.

Nodes of class-A hexagons H_N^A

If $\mathcal{C}_n \in \mathbb{R}^2$ denotes the centers of the regular basic hexagons up to n -th layer with successive layer ordering $n = 1, \dots, N$ then the nodes $G_{l,n}^{A,m} \in (\mathbb{R}^2)^6$ of the hexagons $H_N^A = \{H_{l,n}^{A,m}\}$ is given as

$$G_{l,n}^{A,m} := \mathcal{C}_{N-n} + R_{n,l}^A \left(\cos \left(\left(\frac{2\pi}{6} \right) k + \theta_{n,l}^m \right), \sin \left(\left(\frac{2\pi}{6} \right) k + \theta_{n,l}^m \right) \right)_{k=1}^6 \in (\mathbb{R}^2)^6, \\ n = 1, \dots, N; \quad m = 0, 1 \text{ for } l = 1, \dots, n \text{ and } m = 0 \text{ for } l = n+1 \quad (2.57)$$

where

$$\theta_{n,l}^m = \sin^{-1} \left(\frac{P_{n,l}^m}{R_{n,l}^A} \right)$$

in which $P_{n,l}^m$ is given by

$$P_{n,l}^0 := (n - (l-1)) \frac{\sqrt{3}}{2} h \quad \text{for } 1 \leq l \leq n+1$$

and

$$P_{n,l}^1 := \left\{ P_{2k-1,n}^2, P_{2k,n}^2 \right\}$$

with

$$P_{2k-1,n}^2 := \frac{n+k}{2} \sqrt{3} h, \quad k = 1, \dots, \frac{n+1}{2} \left(\frac{n}{2} \right) \quad \text{when } n \text{ is odd (even)}$$

$$P_{2k,n}^2 := \frac{n+k}{2} \sqrt{3} h, \quad k = 1, \dots, \frac{n-1}{2} \left(\frac{n}{2} \right) \quad \text{when } n \text{ is odd (even)}.$$

Hexagons of Class-B

It has been seen that the N -layer grid has six symmetric partitions and each partition of the n th ($n = 0, \dots, N$) layer contains $(2n + 1)$ number of nodes. If the center $C(x, y)$ of a regular hexagon H is given together with a node $P_0(x_0, y_0)$, then we can find the all other nodes $P_m(x_m, y_m), m = 1, \dots, 5$ of H by equations (2.53, 2.54, 2.55).

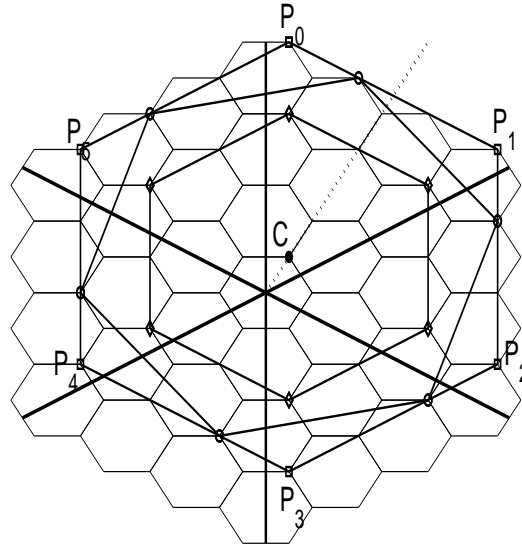


Fig. 2.7 Class-B hexagons.

We then called the pair (C, P_0) as a generator of H .

Proposition 2.15 *Let us consider the first node of the grid \mathcal{G}_N as a center C , i.e. $C \equiv C(\frac{1}{2}h, \frac{\sqrt{3}}{2}h)$ and let $P_0(x_0, y_0)$ be a node in the n -th layer of the first partition. Then with generator (C, P_0) ,*

1. *no regular hexagon exist, if $P_0(x_0, y_0)$ be an even node in the n -th layer.*
2. *there exists a regular hexagon $H \in \mathcal{G}_N$ if $P_0(x_0, y_0)$ be a odd node in the n -th layer.*

proof: 1. Let $P_0(x_0, y_0)$ be an even node in any n -th layer. Then (x_0, y_0) belongs to either in \mathcal{G}_N^1 or in \mathcal{G}_N^3 . Using the formula 2.53, for $(x_0, y_0) \in \mathcal{G}_N^1$ we find

$$\begin{aligned} x_3 &= h - (3i + 1)h = -3ih \equiv 3\tilde{i}h, \\ y_3 &= 2\frac{\sqrt{3}}{2}h - 2j\frac{\sqrt{3}}{2}h \equiv (2\tilde{j})\frac{\sqrt{3}}{2}h, \end{aligned}$$

and for $(x_0, y_0) \in \mathcal{G}_N^3$, we find

$$\begin{aligned} x_3 &= h - (3i + \frac{5}{2})h = (-3i + \frac{3}{2})h \equiv (3\tilde{i} + \frac{3}{2})h \\ y_3 &= 2y - y_0 = 2\frac{\sqrt{3}}{2}h - (2j + 1)\frac{\sqrt{3}}{2}h \equiv (2\tilde{j} + 1)\frac{\sqrt{3}}{2}h \end{aligned}$$

Thus from the definition of the N -layer grid given by the equation (2.48), $(x_3, y_3) \notin \mathcal{G}_N$.

2. If $P_0(x_0, y_0)$ be an odd node in any n th layer, then (x_0, y_0) belongs either to \mathcal{G}_N^0 or to \mathcal{G}_N^2 .

For $(x_0, y_0) \in \mathcal{G}_N^0$, using the formula (2.53), we find

$$\begin{aligned} x_3 &= h - (3i + \frac{1}{2})h = (-3i + \frac{1}{2})h \equiv (3\tilde{i} + \frac{1}{2})h, \\ y_3 &= 2\frac{\sqrt{3}}{2}h - (2j + 1)\frac{\sqrt{3}}{2}h \equiv (2\tilde{j} + 1)\frac{\sqrt{3}}{2}h, \end{aligned}$$

where for $i = 0, \dots, k$; $j = (n - i)$ implies $\tilde{i} = -i, \tilde{j} = -((n - i) - 1)$ which guarantee that $(x_3, y_3) \in \mathcal{G}_N^0$.

For $(x_0, y_0) \in \mathcal{G}_N^2$, we find

$$\begin{aligned} x_3 &= h - (3i + 2)h = (-3i - 1)h \equiv (3\tilde{i} + 2)h, \\ y_3 &= 2\frac{\sqrt{3}}{2}h - (2j)\frac{\sqrt{3}}{2}h \equiv (2\tilde{j})\frac{\sqrt{3}}{2}h, \end{aligned}$$

where for $i = 0, \dots, k$; $j = (n - i)$ implies $\tilde{i} = -(i + 1), \tilde{j} = -((n - i) - 1)$ which guarantee that $(x_3, y_3) \in \mathcal{G}_N^2$. That is, the node $P_3(x_3, y_3) \in \mathcal{G}_N$.

Now we show that $P_1(x_1, x_2), P_5(x_5, y_5)$ belongs to the grid \mathcal{G}_N .

For $P_0(x_0, y_0) \in \mathcal{G}_N^0$, i.e. for

$$(x_0, y_0) = \left((3i + \frac{1}{2})h, (2(n - i) + 1)\frac{\sqrt{3}}{2}h \right),$$

using the formula (2.54), we find that

$$\begin{aligned} (x_1, y_1) &= \left((\frac{3}{2}n + \frac{1}{2})h, (n - 4i + 1)\frac{\sqrt{3}}{2}h \right), \\ (x_5, y_5) &= \left((3i - \frac{3}{2}n + \frac{1}{2})h, (n + 2i + 1)\frac{\sqrt{3}}{2}h \right). \end{aligned}$$

Then in case of $n \in \mathbb{N}_e$, $n = 2k, i = 0, \dots, k$

$$\begin{aligned} (x_1, y_1) &= \left((3k + \frac{1}{2})h, (2(k - 2i) + 1)\frac{\sqrt{3}}{2}h \right) \equiv \left((3\tilde{i}_1 + \frac{1}{2})h, (2\tilde{j}_1 + 1)\frac{\sqrt{3}}{2}h \right), \\ (x_5, y_5) &= \left((3(i - k) + \frac{1}{2})h, (2(k + i) + 1)\frac{\sqrt{3}}{2}h \right) \equiv \left((3\tilde{i}_5 + \frac{1}{2})h, (2\tilde{j}_5 + 1)\frac{\sqrt{3}}{2}h \right), \end{aligned}$$

where $\tilde{i}_1 = k$ with $\tilde{j}_1 = -k, \dots, k$ and $\tilde{i}_5 = -k, \dots, 0$ respectively with $\tilde{j}_5 = k, \dots, 2k$ guarantee that $P_m(x_m, y_m) \in \mathcal{G}_N$, $m = 1, 5$.

In case of $n \in \mathbb{N}_o$, $n - 1 = 2k, i = 0, \dots, k$

$$\begin{aligned}(x_1, y_1) &= \left((3k + 2)h, 2(k - 2i + 1) \frac{\sqrt{3}}{2}h \right) \equiv \left((3\tilde{i}_1 + 2)h, (2\tilde{j}_1) \frac{\sqrt{3}}{2}h \right), \\(x_5, y_5) &= \left((3(i - k - 1) + 2)h, 2(k + i + 1) \frac{\sqrt{3}}{2}h \right) \equiv \left((3\tilde{i}_5 + 2)h, (2\tilde{j}_5) \frac{\sqrt{3}}{2}h \right),\end{aligned}$$

where $\tilde{i}_1 = k$ with $\tilde{j}_1 = -(k - 1), \dots, (k + 1)$ and $\tilde{i}_5 = -(k + 1), \dots, -1$ respectively with $\tilde{j}_5 = (k + 1), \dots, (2k + 1)$ guarantee again that $P_m(x_m, y_m) \in \mathcal{G}_N$ $m = 1, 5$.

Now for $(x_0, y_0) \in \mathcal{G}_N^2$, i.e. for

$$(x_0, y_0) = \left((3i + 2)h, 2(n - i) \frac{\sqrt{3}}{2}h \right),$$

using equation 2.54, we have

$$\begin{aligned}(x_1, y_1) &= \left(\left(\frac{3}{2}n + \frac{1}{2} \right)h, (n - 4i - 1) \frac{\sqrt{3}}{2}h \right), \\(x_5, y_5) &= \left(\left(3i - \frac{3}{2}n + 2 \right)h, (n + 2i + 2) \frac{\sqrt{3}}{2}h \right).\end{aligned}$$

In case of $n \in \mathbb{N}_e$, $n = 2k$

$$\begin{aligned}(x_1, y_1) &= \left(\left(3k + \frac{1}{2} \right)h, (2(k - 2i - 1) + 1) \frac{\sqrt{3}}{2}h \right) \quad i = 0, \dots, k \\ &\equiv \left(\left(3\tilde{i}_1 + \frac{1}{2} \right)h, (2\tilde{j}_1 + 1) \frac{\sqrt{3}}{2}h \right), \\(x_5, y_5) &= \left((3(i - k) + 2)h, 2(k + i + 1) \frac{\sqrt{3}}{2}h \right), \quad i = 0, \dots, (k - 1) \\ &\equiv \left((3\tilde{i}_5 + 2)h, (2\tilde{j}_5) \frac{\sqrt{3}}{2}h \right),\end{aligned}$$

where $\tilde{i}_1 = k$ with $\tilde{j}_1 = -(k + 1), \dots, (k - 1)$ and $\tilde{i}_5 = -k, \dots, -1$ respectively with $\tilde{j}_5 = (k + 1), \dots, 2k$ guarantee that $P_m(x_m, y_m) \in \mathcal{G}_N$, $m = 1, 5$.

In case of $n \in \mathbb{N}_o$, $n - 1 = 2k, i = 0, \dots, k$

$$\begin{aligned}(x_1, y_1) &= \left((3k + 2)h, 2(k - 2i) \frac{\sqrt{3}}{2}h \right) \equiv \left((3\tilde{i}_1 + 2)h, (2\tilde{j}_1) \frac{\sqrt{3}}{2}h \right), \\(x_5, y_5) &= \left(\left(3(i - k) + \frac{1}{2} \right)h, (2(k + i + 1) + 1) \frac{\sqrt{3}}{2}h \right), \equiv \left(\left(3\tilde{i}_5 + \frac{1}{2} \right)h, (2\tilde{j}_5 + 1) \frac{\sqrt{3}}{2}h \right),\end{aligned}$$

where, $\tilde{i}_1 = k$ with $\tilde{j}_1 = -k, \dots, k$ and $\tilde{i}_5 = -k, \dots, 0$ respectively with $\tilde{j}_5 = (k + 1), \dots, (2k + 1)$ guarantee that $P_m(x_m, y_m) \in \mathcal{G}_N$, $m = 1, 5$.

By similar arguments it is also seen that $P_2(x_2, y_2) \in \mathcal{G}_N, P_4(x_4, y_4) \in \mathcal{G}_N$. \square

It is observed (Fig.2.7) that the 1-st and the $(2n+1)$ -th nodes (of each n -st layer) are two consecutive node of the same hexagon. Thus there exist $(2n-1)/2 = n$ number of different hexagons for each n odd nodes as P_0 of each n -st layer of a partition. We have the same situation for other five symmetric partitions and in these cases our centers are respectively the $(1, \dots, 5)$ -th nodes of the 0-layer. But since the N -layer model can be decompose into $(N-n)$ -layer model for each $(n = 1, \dots, N)$, therefore, for P_0 belongs to n th layer $(n = 1, \dots, N-1)$, the same n number of hexagons exist for all the nodes (as center C) up to $(N-n)$ -th layer. e.g. for P_0 belongs to $n = 1$ -st layer there exists a regular hexagon for each nodes up to $(N-1)$ -th layer as centers, i.e. for the first $6(N-1+1)^2$ nodes of the grid as centers. Similarly, for P_0 belongs to $n = 2$ -th layer there exist two regular hexagons for each nodes up to $(N-2)$ -st layer as centers i.e. for the first $6(N-2+1)^2$ nodes of the grid as centers and so forth.

Thus in general, for P_0 belongs to n th $(n = 1, \dots, N)$ layer there exist n regular hexagons for each nodes up to $(N-n)$ -th layer as centers, i.e. for the first $6(N-n+1)^2$ nodes of the grid as centers. Thus the total number of regular hexagons of class-B of a N -layer model is given by

$$\#(H_N^B) = \sum_{n=1}^N 6(N-n+1)^2 \times n.$$

Now in order to collect the six nodes of all these hexagons of class-B, we need to know the radii R and initial angles θ for the n different hexagons with center $C(\frac{1}{2}h, \frac{\sqrt{3}}{2}h)$ for each n th $(n = 1, \dots, N)$ layer. However the radii are symmetric about the dividing line of the partition as shown in the Fig. 2.7, e.g. $R_1 = R_{2n+1}, R_2 = R_{2n}$ etc. Then we need to find only $(n/2 + 1)$ or $(n + 1)/2$ number of radii $R_{n,l}$ ($l = 1, \dots, (n/2 + 1)$ or $(n + 1)/2$) in each n th layer according as n is even or odd and for each radius $R_{n,l}$ we have to find two initial angles $\theta_{n,l}^m, m = 0, 1$. Then we obtained all the hexagons by shifting the center C to all nodes up to $(N-n)$ th layer.

Nodes of class-B hexagons H_N^B

If $\tilde{G}_n \in (\mathbb{R}^2)^{6(n+1)^2}$ denotes the nodes up to n -th layer for $n = 1, \dots, N$ successively of the N -layer hexagonal grid, then the nodes $G_{l,n}^{B,m}$ of the hexagons $H_N^B = \{H_{l,n}^{B,m}\}$ ($n = 1, \dots, N$) of radii $R_{n,l}$ is given by

$$\begin{aligned} G_{l,n}^{B,m} : &= \tilde{G}_{N-n} + R_{n,l}^B \left(\cos \left(\left(\frac{2\pi}{6} \right) k + \theta_{n,l}^j \right), \sin \left(\left(\frac{2\pi}{6} \right) k + \theta_{n,l}^j \right) \right)_{k=1}^6 \in (\mathbb{R}^2)^6, \quad n = 1, \dots, N \\ & \quad m = 0, 1 \text{ for each } l = 0, \dots, (n-1)/2 \text{ (} n/2 - 1 \text{) according as } n \in \mathbb{N}_e(\mathbb{N}_o) \quad (2.58) \\ & \quad \text{and } m = 1 \text{ for } l = n/2, \end{aligned}$$

where the radii

$$R_{n,l}^B = \left(\left(\frac{3l}{2}h \right)^2 + \left((2n-l) \frac{\sqrt{3}}{2}h \right)^2 \right)^{\frac{1}{2}}, l = 0, \dots, \frac{n}{2} \left(\frac{n-1}{2} \right) \text{ according as } n \in \mathbb{N}_e(\mathbb{N}_o)$$

and

$$\theta_{n,l}^m = \sin^{-1} \left(\frac{P_{n,l}^m}{R_{n,l}^B} \right)$$

in which $P_{n,l}^m$, $m = 0, 1$ are given by

$$P_{n,l}^0 := (2n-l) \cdot \frac{\sqrt{3}}{2}h \quad \text{for } l = 0, \dots, (n-1)/2 \text{ (} n/2-1 \text{) according as } n \in \mathbb{N}_e(\mathbb{N}_o),$$

and

$$P_{n,l}^1 := (n+l) \frac{\sqrt{3}}{2}h, \quad l = 1, \dots, \frac{n-1}{2} \left(\frac{n}{2} - 1 \right) \text{ according as } n \in \mathbb{N}_e(\mathbb{N}_o).$$

We note that for $P_{n,l}^1$, $l = 0$ in both odd and even n , and $l = \frac{n}{2}$ for even n is already included with $P_{n,l}^0$.

Thus in a N -layer grid, the total number of regular hexagons of all classes, with the regular basic hexagons as "class-0", is given by

$$\begin{aligned} H_N : &= \# \left(H_N^0 + H_N^B + H_N^A \right) \\ &= \left(3N(N+1) + 1 \right) + \sum_{n=1}^N 6(N-n+1)^2 \times n \\ &\quad + \sum_{n=1}^N (2n+1) \left(3(N-n)(N-n+1) + 1 \right) \end{aligned} \quad (2.59)$$

Therefore, as we know, the co-ordinates $(v_x(l), v_y(l))$ of each l th node ($l = 1, \dots, 6(N+1)^2$) of a N -layer grid as well as the formulae for identifying the regular basic hexagons by equation (2.43) and for the class-A, class-B regular hexagons given above, we can easily find the list of all hexagons $H \in \mathcal{H}$. \square

2.2.2 Computational costs

For a point-wise evaluation of the full collision operator $J[\mathbf{f}, \mathbf{f}]$ defined by equation (2.12), first we calculate

$$S := f_{\pi_0^H} f_{\pi_3^H} + f_{\pi_1^H} f_{\pi_4^H} + f_{\pi_2^H} f_{\pi_5^H} \text{ and } T := f_{\pi_0^H} f_{\pi_2^H} f_{\pi_4^H} - f_{\pi_1^H} f_{\pi_3^H} f_{\pi_5^H},$$

then we calculate

$$J_{\pi_i^H} := \gamma_{\text{bin}}^H (S - 3 * f_{\pi_i^H} f_{\pi_j^H}) - \gamma_{\text{ter}}^H (-1)^i T, \quad i = 0, \dots, 5, \quad j = i + 3 \text{ mod } 6$$

for all basic hexagons $H \in H_N^O$, but for all $H \in H_N^A$ and for all $H \in H_N^B$ we exclude the ternary collision term T . Then it is seen that it requires 14×6 floating point operations (FLOPS) for the calculation of the collision operator restricted to each $H \in H_N^O$ and 7×6 FLOPS for the calculation of the collision operator restricted to each $H \in H_N^A$ and $H \in H_N^B$. Therefore, for the calculation of the collision operator $J[\mathbf{f}, \mathbf{f}]$, we define the total computational cost (in FLOPS)

$$C_J := 6 \times \left(14 \times |H_N^O| + 7 \times |(H_N^A + H_N^B)| \right).$$

Using the general formulae for the N -layer grid, we make a list of the number of grid points, number of basic hexagons, number of class-A and class-B hexagons and the computational cost C_J for a N -layer model, ($N = 0, \dots, 10$) as in the following table.

N	0	1	2	3	4	5	6	7	8	9	10
#(nodes)	6	24	56	96	150	216	294	384	486	600	726
#(H_N^O)	1	7	19	37	61	91	127	169	217	271	331
#(H_N^B)	0	6	36	120	300	630	1176	2016	3240	4950	7260
#(H_N^A)	0	3	26	99	264	575	1098	1911	3104	4779	7050
#($H_N^A + H_N^B$)	0	9	62	219	564	1205	2274	3927	6344	9729	14310
#(H_N)	1	16	81	256	625	1296	2401	4096	6561	10000	14641
cost C_J	84	966	4200	12306	28812	58254	106176	179130	284676	431382	628824

Table 2.1: Computational cost for a N -layer model.

2.3 Equilibria for a N -layer model

It has been shown in [3] that the equilibria $\mathbf{f} \in \mathcal{E}$ of the discrete Boltzmann equation can be expressed in terms of four parameters characterizing mass, momenta and energy. In this section we present such equilibrium distribution for a generalized N -layer model for any $N \in \mathbb{N}_0$.

Strictly positive density vectors $\mathbf{f} = (f_i)_{i=0}^{6(N+1)^2-1}$ for which $J[\mathbf{f}, \mathbf{f}] \equiv 0$ is said to be the equilibrium solutions (equilibria) for a N -layer hexagonal model. The set of equilibria for a N -layer hexagonal model is denoted by \mathcal{E}_N . Suppose $\mathbf{f} \in \mathcal{E}_N$ be the equilibria of a N -layer model and the equilibria at the six nodes of 0-st layer (i.e. at the nodes of the central basic hexagon) is given by

$$(f_0, f_1, f_2, f_3, f_4, f_5) = z \cdot (\kappa_{0+}, \kappa_{1+}, \kappa_{2+}, \kappa_{0-}, \kappa_{1-}, \kappa_{2-})^\top$$

where $z, \kappa_{0+}, \kappa_{1+}, \kappa_{2+} > 0$ are arbitrary quantities satisfying $\kappa_{0+}\kappa_{1-}\kappa_{2+} = 1$ (see prop. 3.3 [3]).

For a 3-layer model, the Fig. 2.8 presents the equilibria for the nodes of the partition corresponding to the triple $z \cdot (\kappa_{0+}, \kappa_{1+}, \kappa_{2+})$.

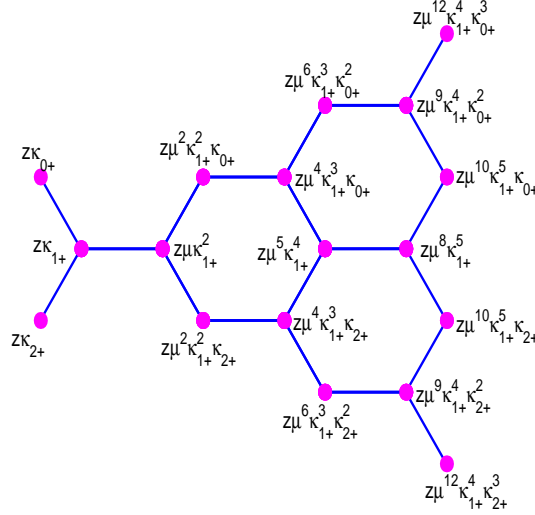


Fig. 2.8 Equilibria restricted to a partition of a 3-layer model.

The values of the equilibria are calculated in a similar way as in Theorem 4.1 in [3], for the layer $n = 1, 2, 3$, respectively as

$$z(\mu^2 \kappa_{1+}^2 \kappa_{0+}, \mu \kappa_{1+}^2, \mu^2 \kappa_{1+}^2 \kappa_{2+}) \in \text{1st layer},$$

$$z(\mu^6 \kappa_{1+}^3 \kappa_{0+}^2, \mu^4 \kappa_{1+}^3 \kappa_{0+}, \mu^5 \kappa_{1+}^4, \mu^4 \kappa_{1+}^3 \kappa_{2+}, \mu^6 \kappa_{1+}^3 \kappa_{2+}^2) \in \text{2nd layer},$$

$$z(\mu^{12} \kappa_{1+}^4 \kappa_{0+}^3, \mu^9 \kappa_{1+}^4 \kappa_{0+}^2, \mu^{10} \kappa_{1+}^5 \kappa_{0+}, \mu^8 \kappa_{1+}^5, \mu^{10} \kappa_{1+}^5 \kappa_{2+}, \mu^9 \kappa_{1+}^4 \kappa_{2+}^2, \mu^{12} \kappa_{1+}^4 \kappa_{2+}^3) \in \text{3rd layer},$$

where z parameterizes mass, $(\kappa_{0+}, \kappa_{2+})$ characterize non-vanishing bulk-velocity, and μ is responsible for kinetic energy. At each n th layer of a partition we have $(2n + 1)$ nodes and the node numbering is from the top to bottom of at each layer. We generalize these values of equilibria for a partition of a N -layer model as in the proposition below.

Proposition 2.16 *For a partition (of a N -layer model) corresponding to the triple $z(\kappa_{0+}, \kappa_{1+}, \kappa_{2+})$, the equilibria is described in-terms of the parameters $\mu, \kappa_{0+}, \kappa_{1+}, \kappa_{2+}$ as in the following three steps.*

1. *Corresponding to the values at the first node (the top one in the figure) of the $(n - 1)$ -th layer ($n = 2, \dots, N$), there obtained two values of equilibria with increments $\kappa_{1+}\mu^n$ and $\kappa_{0+}\kappa_{1+}\mu^{2n}$ which are assigned respectively to the second and first nodes of the n -st layer. Corresponding to the values at the last node (the bottom one in the figure) of the $(n - 1)$ -th layer, there obtained also two values of equilibria with increments $\kappa_{1+}\mu^n$ and $\kappa_{1+}\kappa_{2+}\mu^{2n}$ which are assigned respectively to the $2n$ -th and $(2n + 1)$ -th nodes of the n th layer.*

2. Corresponding to the values of each $2m$ -th (even) node ($m = 1, \dots, n-1$) of the $(n-1)$ -th layer, there obtained values at the $(2m+1)$ -th node of the n -th layer with an increment $\kappa_{1+}^2 \mu^{2n}$.
3. Corresponding to each $(2l+1)$ -th (odd) node ($l = 1, \dots, n-2$) of the $(n-1)$ -th layer, there obtained values of equilibria with an increment $\kappa_{1+} \mu^n$ which is assigned to the $(2l+2)$ -th node of the n th layer.

The equilibria for other partitions as well as for the complete N -layer model is determined by symmetry.

Let the equilibria at the i th ($i = 1, \dots, 2n+1$) node of the n th ($n = 0, \dots, N$) layer is given by

$$f(n, i) = z \mu^{m(n,i)} \kappa_{0+}^{k_0(n,i)} \kappa_{1+}^{k_1(n,i)} \kappa_{2+}^{k_2(n,i)}; \quad (m, k_0, k_1, k_2) \in \mathbb{N}_0 \quad (2.60)$$

Then following the statement of the proposition 2.16, one can calculate the exponents $m(n, i)$, $k_0(n, i)$, $k_1(n, i)$, $k_2(n, i)$; $n = 0, \dots, N$; $i = 1, \dots, 2n+1$ as shown in Algorithm 2.4.

```

INITIALIZE  $m(0, 1) = 0, m(1, 1) = 2,$ 
            $m(1, 2) = 1, m(1, 3) = 2$ 
FOR  $n = 2$  TO  $N$ 
   $m(n, 1) = m(n-1, 1) + 2n$ 
  FOR  $i = 2(2)2n$ 
     $m(n, i) = m(n-1, i-1) + n$ 
  END
  FOR  $j = 3(2)(2n-1)$ 
     $m(n, j) = m(n-1, j-1) + 2n$ 
  END
   $m(n, 2n+1) = m(n-1, 2n-1) + 2n$ 
END

```

```

INITIALIZE  $k_1(1, 1) = 2, k_1(1, 2) = 2,$ 
            $k_1(1, 3) = 2$ 
FOR  $n = 2$  TO  $N$ 
   $k_1(n, 1) = k_1(n-1, 1) + 1$ 
  FOR  $i = 2(2)2n$ 
     $k_1(n, i) = k_1(n-1, i-1) + 1$ 
  END
  FOR  $j = 3(2)(2n-1)$ 
     $k_1(n, j) = k_1(n-1, j-1) + 2$ 
  END
   $k_1(n, 2n+1) = k_1(n-1, 2n-1) + 1$ 
END

```

```

INITIALIZE  $k_0(0, 1) = 1, k_0(1, 1) = 1$ 
FOR  $n = 2$  TO  $N$ 
   $k_0(n, 1) = k_0(n-1, 1) + 1$ 
  FOR  $i = 2$  TO  $n$ 
     $k_0(n, i) = k_0(n-1, i-1)$ 
  END
  FOR  $i = n+1$  TO  $2n+1$ 
     $k_0(n, i) = 0$ 
  END
END

```

```

INITIALIZE  $k_2(0, 1) = 1, k_2(1, 3) = 1$ 
FOR  $n = 2$  TO  $N$ 
   $k_2(n, 2n+1) = k_2(n-1, 2n-1) + 1$ 
  FOR  $i = n+2$  TO  $2n$ 
     $k_2(n, i) = k_2(n-1, i-1)$ 
  END
  FOR  $i = 1$  TO  $n+1$ 
     $k_2(n, i) = 0$ 
  END
END

```

Algorithm 2.4 To calculate the exponents $m(n, i)$, $k_0(n, i)$, $k_1(n, i)$, $k_2(n, i)$.

Now if we substitute κ_{1+} by $\kappa_{0+}\kappa_{2+}$ in equation (2.60) then we have the following statement.

Theorem 2.17 *Let $\mathbb{N}_o, \mathbb{N}_e$ denote respectively the set of odd and even natural numbers. The i -th equilibria in the n -th layer of the partition corresponding to the triple $(\kappa_{0+}, \kappa_{1+}, \kappa_{2+})$ is given by*

$$f(n, i) = z\mu^{m(n,i)}\kappa_{0+}^{\bar{k}_0(n,i)}\kappa_{2+}^{\bar{k}_2(n,i)}; \quad n = 0, \dots, N; \quad i = 1, \dots, 2n + 1 \quad (2.61)$$

where for $i = 1, \dots, n + 1$,

$$\begin{aligned} \bar{m}(n, i) &= n^2 + n - d_i, \quad \text{for } i \in \mathbb{N}_o \quad d_{i=2k+1} = nk - k^2, \\ & \quad k = 0, \dots, \frac{n}{2} \quad \text{if } n \in \mathbb{N}_e \quad \text{and} \quad k = 0, \dots, \frac{n-1}{2} \quad \text{if } n \in \mathbb{N}_o, \\ &= n^2 - d_i \quad \text{for } i \in \mathbb{N}_e \quad d_{i=2k+2} = nk - k(k+1), \\ & \quad k = 0, \dots, \frac{n-2}{2} \quad \text{if } n \in \mathbb{N}_e \quad \text{and} \quad k = 0, \dots, \frac{n-1}{2} \quad \text{if } n \in \mathbb{N}_o; \end{aligned}$$

$$\begin{aligned} \bar{k}_0(n, i) &= 2n + 1 - d_i, \quad \text{for } i \in \mathbb{N}_o \quad d_{i=2k+1} = k, \\ & \quad k = 0, \dots, \frac{n}{2} \quad \text{if } n \in \mathbb{N}_e \quad \text{and} \quad k = 0, \dots, \frac{n-1}{2} \quad \text{if } n \in \mathbb{N}_o, \\ &= 2n - d_i, \quad \text{for } i \in \mathbb{N}_e \quad d_{i=2k+2} = k, \\ & \quad k = 0, \dots, \frac{n-2}{2} \quad \text{if } n \in \mathbb{N}_e \quad \text{and} \quad k = 0, \dots, \frac{n-1}{2} \quad \text{if } n \in \mathbb{N}_o; \end{aligned}$$

$$\begin{aligned} \bar{k}_2(n, i) &= n + 1 + d_i, \quad \text{for } i \in \mathbb{N}_o \quad d_{i=2k+1} = k, \\ & \quad k = 0, \dots, \frac{n}{2} \quad \text{if } n \in \mathbb{N}_e \quad \text{and} \quad k = 0, \dots, \frac{n-1}{2} \quad \text{if } n \in \mathbb{N}_o, \\ &= n + 1 + d_i, \quad \text{for } i \in \mathbb{N}_e \quad d_{2k+2} = k, \\ & \quad k = 0, \dots, \frac{n-2}{2} \quad \text{if } n \in \mathbb{N}_e \quad \text{and} \quad k = 0, \dots, \frac{n-1}{2} \quad \text{if } n \in \mathbb{N}_o. \end{aligned}$$

For the rest $i = n + 2, \dots, 2n + 1$,

$$m(n, i_{(=n+2, \dots, 2n+1)}) = m(n, i_{(=n, \dots, 1)}) \quad \text{respectively,}$$

$$\bar{k}_0(n, i_{(=n+2, \dots, 2n+1)}) = \bar{k}_2(n, i_{(=n, \dots, 1)}) \quad \text{respectively,}$$

$$\bar{k}_2(n, i_{(=n+2, \dots, 2n+1)}) = \bar{k}_0(n, i_{(=n, \dots, 1)}) \quad \text{respectively.}$$

proof: By lemma-3.2 [3], we obtain the values of the equilibria for $n = 2$ and $n = 3$ as shown in the Fig. 2.8 and we see that the statement holds true for $n = 0, \dots, n = 3$. Now let us assume that the statement is true for an arbitrary $n \geq 4$. Then in this n -th layer we consider three consecutive values of equilibria

respectively for $i = (2k + 1), (i + 1), (i + 2)$ for any $k = 0, \dots, (n - 1)/2 - 1$ if n is odd, or, for any $k = 0, \dots, n/2 - 1$ if n is even, as stated in the theorem as

$$\begin{aligned} g_2 &= \mu^{n^2+n+k^2-nk} \kappa_{0+}^{2n-k+1} \kappa_{2+}^{n+k+1} \\ g_1 &= \mu^{n^2-nk+k(k+1)} \kappa_{0+}^{2n-k} \kappa_{2+}^{n+k+1} \\ g_0 &= \mu^{n^2+n+(k+1)^2-n(k+1)} \kappa_{0+}^{2n-k} \kappa_{2+}^{n+k+2} \end{aligned}$$

Choosing these equilibria g_2, g_1, g_0 of three consecutive nodes of the n -th layer, we denote g_3, g_4, g_5 the equilibria at the $(i + 1)$ -th, $(i + 2)$ -th and $(i + 3)$ -th nodes respectively in the $(n + 1)$ -st layer. Then (g_0, \dots, g_5) are the equilibria restricted to a regular basic hexagon and the unknown values g_3, g_4, g_5 are obtain by lemma(3.2) [3], i.e. by

$$\frac{g_0 g_2}{g_1} = \frac{g_1 g_3}{g_2} = \frac{g_2 g_4}{g_3} = \frac{g_3 g_5}{g_4} = \frac{g_4 g_0}{g_5} = \frac{g_5 g_1}{g_0}$$

as,

$$\begin{aligned} g_3 &= \mu^{(n+1)^2-(n+1)k+k(k+1)} \kappa_{0+}^{2(n+1)-k} \kappa_{2+}^{(n+1)+k+1} \\ g_4 &= \mu^{(n+1)^2+(n+1)+(k+1)^2-(n+1)(k+1)} \kappa_{0+}^{2(n+1)-k} \kappa_{2+}^{(n+1)+k+1} \\ g_5 &= \mu^{(n+1)^2-(n+1)(k+1)+(k+1)(k+2)} \kappa_{0+}^{2(n+1)-(k+1)} \kappa_{2+}^{(n+1)+(k+1)+1} \end{aligned}$$

Thus we see that if the theorem is true for any (n, i) then it also holds true for $(n + 1, i + 1)$. \square

Corollary 2.18 *For a regular collision model (\mathcal{H}_b, γ) , let $\mathbf{f} \in \mathcal{E}$ be the equilibria. If we denote the i -th component equilibria as $f_i := z\mu^m \kappa$, and the corresponding radius $r_i := \sqrt{3n + 1}$ where $r_i^2 = v_{x,i}^2 + v_{y,i}^2$, then $m = n$.*

Chapter 3

2D Numerical experiments

In this chapter we present numerical results based on the N -layer hexagonal grid (in \mathbb{R}^2) which has been developed in the previous chapter. A comparison of the discrete equilibria with the corresponding maxwellian leads to determine an appropriate size N of the N -layer hexagonal grid for given temperature and bulk velocity.

In the case of space-homogeneous case, we compare the numerical solution with the exact solution of the Boltzmann equation due to Wu and Krook [51] for maxwell molecules and perform relaxation problem. In the space inhomogeneous case, we present the steady state results of the test problems: Heat transfer between two parallel plates, a 2d vapor deposition problem.

3.1 Computation of equilibria

Here we compute the discrete equilibria establish by theorem 2.17, which is described by the parameters $z, \mu, \kappa_{0+}, \kappa_{2+}$ characterizing respectively mass, temperature, bulk-velocity. It is evident that

$\bar{v}_x = 0, < 0, > 0$ according as $\kappa_{0+}\kappa_{2+} = \kappa_{1+} = 1, < 1, > 1$, and
 $\bar{v}_y = 0, < 0, > 0$ according as $(\kappa_{0+} - \kappa_{2+}) = 0, < 0, > 0$. We have

$$\kappa_{0+} - \kappa_{2+} = \kappa_{0+} - \frac{\kappa_{1+}}{\kappa_{0+}} \tag{3.1}$$

Therefore to obtain a pre-assign pair $(\bar{v}_x, \bar{v}_y) = (p, q)$, we first find the value of κ_{1+} for which $\bar{v}_x = p$ and then we find the value of κ_{0+} for which $\bar{v}_y = q$. Then $q = 0, < 0, > 0$ according as $\kappa_{0+} = \sqrt{\kappa_{1+}}, < \sqrt{\kappa_{1+}}, > \sqrt{\kappa_{1+}}$.

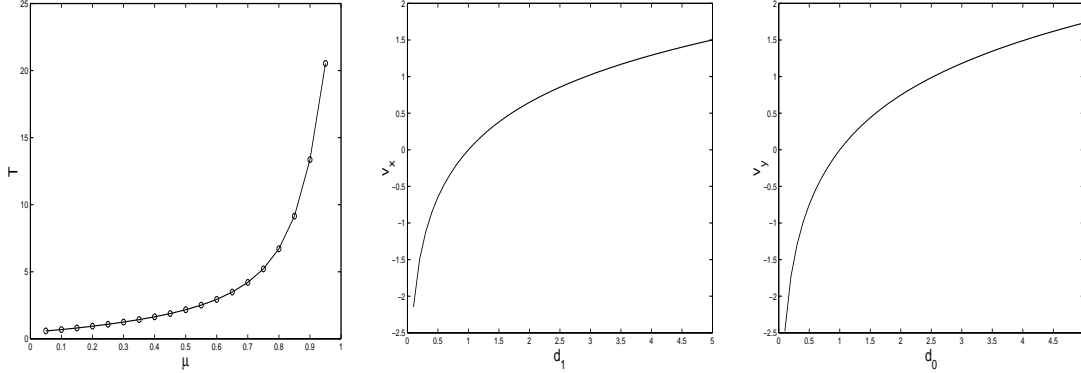


Fig. 3.1 $T(\mu)$, $\bar{v}_x(\kappa_{1+})$, and $\bar{v}_y(\kappa_{0+})$.

Figure 3.1 shows respectively the temperature T for different values of μ in zero bulk velocity, the x-component bulk-velocity \bar{v}_x for different values of d_1 with $\mu = 0.2$, $\kappa_{0+} = \sqrt{\kappa_{1+}}$, and the y-component bulk-velocity \bar{v}_y for different values of κ_{0+} with $\mu = 0.2$, $\kappa_{1+} = 1$. As all these macroscopic quantities (say, $g(k)$) are monotonically increasing with respect to the corresponding parameters (k), thus for a pre-assigned $g = \tilde{g}$ we can easily find the parameter $k = \tilde{k}$ as shown in Algorithm 3.1.

```

Initial guess:  $k = k_0$ 
Calculate  $g(k)$ 
IF  $g = \tilde{g}$ 
     $\tilde{k} = k$ 
    BREAK
ELSE
     $k = k + (\tilde{g} - g)\epsilon$ 
    ( $\epsilon$  depends upon a given accuracy)
END
CONTINUE

```

Algorithm 3.1

Now we compute the discrete equilibria $\tilde{\mathbf{f}}^h \in \mathcal{E}$ given by the theorem 2.17 for the case of zero bulk-velocity on a 4-layer grid (of 150 grid points) with discretization parameter $h = 1$ for three different value of $\mu = 0.05, 0.7, 0.9$ and the corresponding maxwellian given by

$$\tilde{f} = \frac{\rho}{(2\pi T)^{d/2}} \exp\left(\frac{-(\mathbf{v} - \bar{\mathbf{v}})^2}{2T}\right), \quad d = 2$$

where $\rho := \sum_i \tilde{f}_i^h$ is the mass density, $\bar{\mathbf{v}} := (1/\rho) \sum_i \mathbf{v}_i \tilde{f}_i^h$ is defined as the bulk velocity and $T = (1/2\rho) \sum_i (\mathbf{v}_i - \bar{\mathbf{v}})^2 \cdot \tilde{f}_i^h$ is the temperature. We compare the normalize discrete equilibrium state \mathbf{f}^h with the normalize maxwellian $\tilde{\mathbf{f}}$ and calculate the error

$$err =: \|\mathbf{f} - \mathbf{f}^h\|_1 \quad (3.2)$$

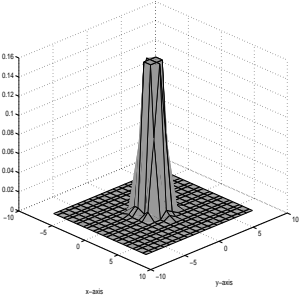
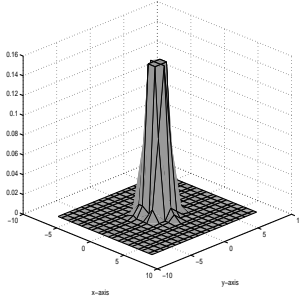
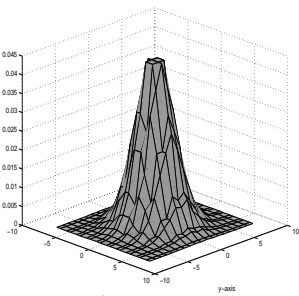
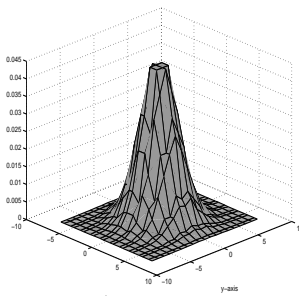
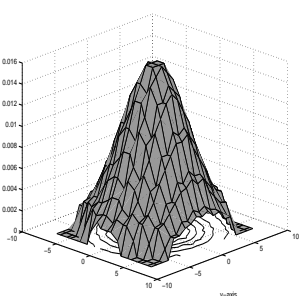
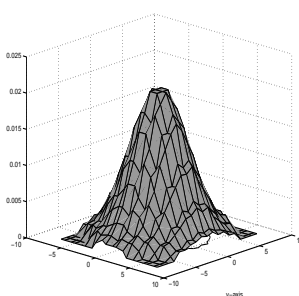
$\mathbf{f}^h =$ Discrete equilibria	$\mathbf{f} =$ Maxwellian	$err = \ \mathbf{f} - \mathbf{f}^h\ _{L_1}$
(1) 		$\rho = 1.000$ $\bar{v}_x = 0$ $\bar{v}_y = 0$ $\mu = 0.05$ $T = 0.5854$ $err = 0.0593$
(2) 		$\rho = 1.000$ $\bar{v}_x = 0$ $\bar{v}_y = 0$ $\mu = 0.7$ $T = 4.1865$ $err = 0.0033$
(3) 		$\rho = 1.000$ $\bar{v}_x = 0$ $\bar{v}_y = 0$ $\mu = 0.9$ $T = 10.2770$ $err = 0.1692$

Table 3.1: Discrete equilibria and Maxwellian in varying temperature on a 4-layer grid.

and the moments, temperature as shown in the table 3.1. Here we present three interesting cases of three different temperatures with zero bulk-velocities.

1. In the first case the calculated temperature $T = 0.5854$ for $\mu = 0.05$. The main part of the configuration is centered at the origin with a small radius and a small part of the mass occurred on the grid. That is the resolution of the grid is too low to present such low temperature and this causes 6% error.
2. This is a good situation because the main part of the mass of the function f lies inside of the domain. In this case it occurs very little error for $\mu = 0.7$ for which the calculated temperature $T = 4.1865$.
3. Here the grid is not large enough to present such high temperature $T = 10.2770$ for a given $\mu = 0.9$ and a significant fraction of the mass of the function f is

cut down the boundary which causes a noticeable 17% error. Thus to avoid this error it requires further extension of the 4-layer grid model.

It is thus seen that for larger temperature we need a larger model to restrict the error to a reasonable range otherwise we obtained a noticeable error due to boundary effect.

Let us now observe the effect of varying bulk-velocity for a constant temperature. For this we choose $\mu = 0.8$ in a 6-layer hexagonal grid (of 294 grid points) and calculate the equilibrium solution for three different cases of bulk-velocities $(\bar{v}_x, \bar{v}_y) = (0, 0), (3, 0),$ and $(3, \sqrt{3})$ by taking (using Algorithm 3.1) respectively

$$\kappa_{0+} = \kappa_{1+} = 1; \kappa_{1+} = 1.5671, \kappa_{0+} = \sqrt{d_1}; \text{ and } \kappa_{1+} = 1.5671; \kappa_{0+} = 1.5673.$$

For these values of the parameters we compute the moments, temperature together with the heat flux components

$$\begin{aligned} q_x^h &= \frac{1}{2} \sum_i f_i \cdot (v_{xi} - \bar{v}_x) ((v_{xi} - \bar{v}_x)^2 + (v_{yi} - \bar{v}_y)^2) \\ q_y^h &= \frac{1}{2} \sum_i f_i \cdot (v_{yi} - \bar{v}_y) ((v_{xi} - \bar{v}_x)^2 + (v_{yi} - \bar{v}_y)^2) \end{aligned}$$

and the stress tensor components

$$\begin{aligned} p_{xx}^h &= \sum_i f_i \cdot (v_{xi} - \bar{v}_x)^2 \\ p_{xy}^h = p_{yx}^h &= \sum_i f_i \cdot (v_{xi} - \bar{v}_x)(v_{yi} - \bar{v}_y) \\ p_{yy}^h &= \sum_i f_i \cdot (v_{yi} - \bar{v}_y)^2 \end{aligned}$$

The table 3.2 illustrates three different situations.

1. In the first case both the bulk-velocity components are zero and $f^h \in \mathcal{E}$ is symmetric about both the axes. In the stress tensor, both the principal diagonal elements are equal to the calculated temperature $T = 6.7144$ and both the off diagonal elements are zero. Here we observe vanishing heat flux components. As the main part of the mass lies inside the domain we obtain a very little error in this case.
2. In the second case, we impose positive x-component bulk-velocity and zero y-component bulk-velocity. In this situation $f^h \in \mathcal{E}$ loses its symmetry property

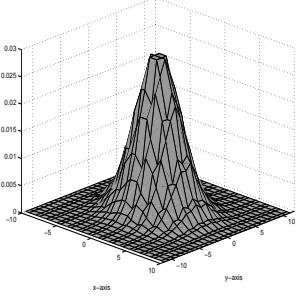
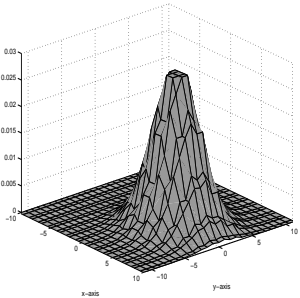
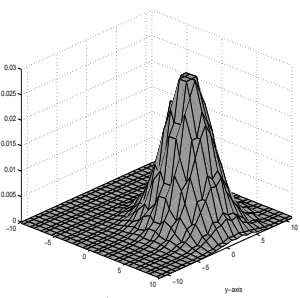
$f^h = \text{Equilibria}$	m^h	p^h		q^h
	$\rho^h = 1.000$ $\bar{v}_x = 0$ $\bar{v}_y = 0$ $T = 6.7144$ $\text{err} = 0.0008$	6.7144	0.0000	0.0000
	$\rho^h = 1.000$ $\bar{v}_x = 3.0000$ $\bar{v}_y = 0$ $T = 6.6465$ $\text{err} = 0.0095$	6.6006	0.0000	-0.4522
	$\rho^h = 1.000$ $\bar{v}_x = 2.9982$ $\bar{v}_y = 1.7320$ $T = 6.6100$ $\text{err} = 0.0139$	6.5853	-0.0430	-0.5441

Table 3.2: Discrete equilibria in varying bulk-velocity on a 6-layer grid.

about the x-axis and we obtain non-zero x-component heat flux. However, the remaining symmetry property in the direction of \bar{v}_y still guarantees the diagonal form of the stress tensor p^h . It is seen that the principal diagonal elements of the stress tensor are not equal anymore. On the other hand, temperature remains almost the same as in the first case which means nonzero bulk-velocity doesn't influence the temperature. In this case we have more error than the first case which is due to a little boundary effect and this cause a little change of the temperature.

3. In the third case, both the components of the bulk-velocity are positive and this causes the non-symmetric nature of $f^h \in \mathcal{E}$ about both the co-ordinate axes of the grid. The diagonal form of the stress tensor p^h is violated and both the components of q^h are negative. The temperature changes is little which is consistent with the little error due the boundary effect.

In all the three cases the main part of the configuration is symmetric about the centers (whose co-ordinates are given by the corresponding bulk-velocity (\bar{v}_x, \bar{v}_y)) of three different basic hexagon of the grid.

The results presented in the table 3.1 and 3.2 are seen good agreement with the similar results presented in [38].

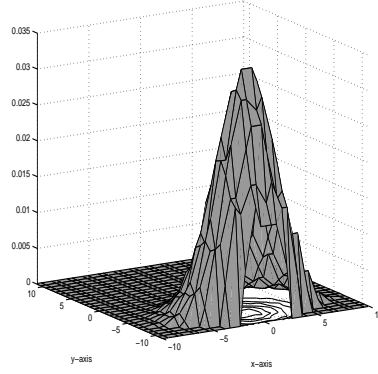


Fig. 3.2 Error occurs due to boundary cut.

We further increase the bulk velocity e.g by imposing $\kappa_{1+} = 1; \kappa_{0+} = 0.37$ for the same temperature by $\mu = 0.8$ on the same 6-layer grid. Then we obtain a large error 17.12% due to the boundary effect as shown in the Fig. 3.2. In this situation of the bulk velocity $\bar{v}_x = 0, \bar{v}_y = -7.1705$, it requires a larger size grid than the 6-layer grid in order to restrict error to a reasonable range. Therefore, an appropriate size N of the grid have to be determined which depends upon the values of temperature T and the magnitude of the bulk-velocity $|\mathbf{v}|$ i.e $N = N(T, |\mathbf{v}|)$ and this is described in the following.

Appropriate grid size

In order to determine the appropriate size grid for a given values of $\mu, \kappa_{0+}, \kappa_{2+}$, we compute the error $err = \|f - f^h\|_1$ for different sizes N of the N -layer model and choose the smallest N as an appropriate size for which the error restricted to a given tolerance.

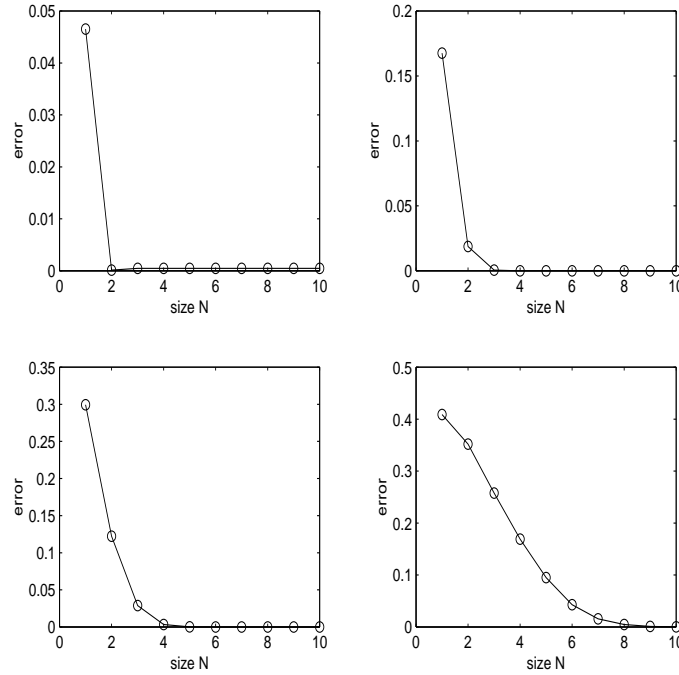


Fig. 3.3 Error w.r.to size N for increasing temperature T in zero bulk-velocity \mathbf{v} .

Fig. 3.3 shows the error with respect to the size N for zero bulk velocity with four increasing values of temperature res for $\mu = 0.3, 0.5, 0.7, 0.9$. In the first case for $\mu = 0.3$, it shows that the error goes below 1% for $N = 2$ and thus for given tolerance 0.01, $N = 2$ is the appropriate size for $\mu = 3$. Similarly the rest three cases shows that $N = 3, 4, 8$ are the appropriate size for given values of $\mu = 0.5, 0.7, 0.9$ respectively. For given temperature and bulk-velocity we can determine the appropriate size (az) of the model by the few steps as shown in Algorithm 3.2

```

Initialize:  $N = 1$ 
Calculate  $err = \|f - f^h\|_{L_1}$ 
IF  $err < tol$ 
     $az = N$ 
    BREAK
ELSE
     $N = N + 1$ 
END
CONTINUE

```

Algorithm 3.2

The table 3.3 lists up appropriate size N for tolerance 0.005 at zero bulk-velocity with some different values of μ .

In table 3.4, we present temperature T corresponding to given values of μ .

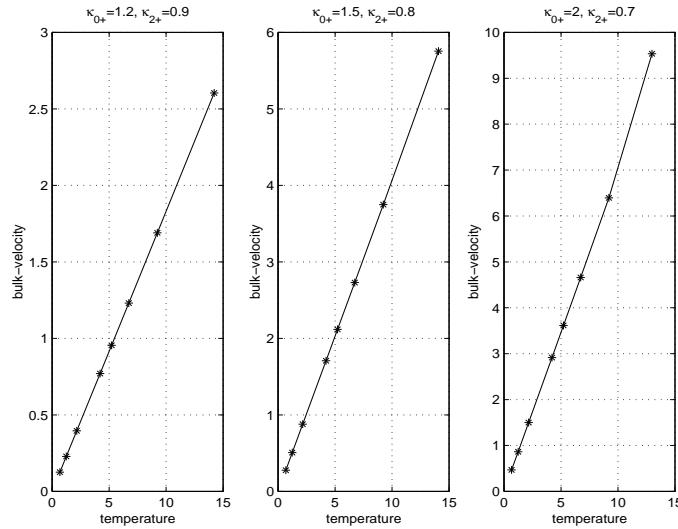
μ	0.2	0.3-0.4	0.45-0.55	0.6-0.7	0.75	0.80	0.85	0.9
N	1	2	3	4	5	6	7	8

Table 3.3: N for $err < 0.005$

μ	0.1	0.2	0.3	0.35	0.4	0.45	0.5	0.55
T	0.6875	0.9384	1.2457	1.4257	1.6275	1.8781	2.1623	2.5026
μ	0.6	0.65	0.7	0.75	0.8	0.83	0.85	0.87
T	2.9357	3.4780	4.1865	5.2053	6.7144	8.0165	9.2136	10.7174
μ	0.88	0.89	0.9	0.91	0.92	93	0.94	0.95
T	11.6369	12.8269	14.1435	15.8485	17.9490	20.5536	24.1173	29.0648

Table 3.4: Temperature T w.r.to μ

Fig. 3.4 shows the calculated bulk-velocity for given $\mu \in [0.1, 0.9]$ at three different choice of $(\kappa_{0+}, \kappa_{2+})$.

**Fig. 3.4** Bulk-velocity depends on $T(\mu)$ and κ 's

As expected, it is clearly seen in the Fig. 3.4 that the modulus of the bulk-velocity $|\mathbf{v}|$ depends upon the choice of temperature as well as the values of the parameters κ_{0+}, κ_{2+} .

Fig. 3.5 below shows appropriate size $N(T, |\mathbf{v}|)$ for two different choices of the pairs (d_0, d_1) and some varying values of μ . For both the cases of $(d_0, d_1) = (2, 2), (3, 3)$ (in figure the upper and lower respectively) we observed that the temperature profiles are the same but the velocity profiles are changing as expected.

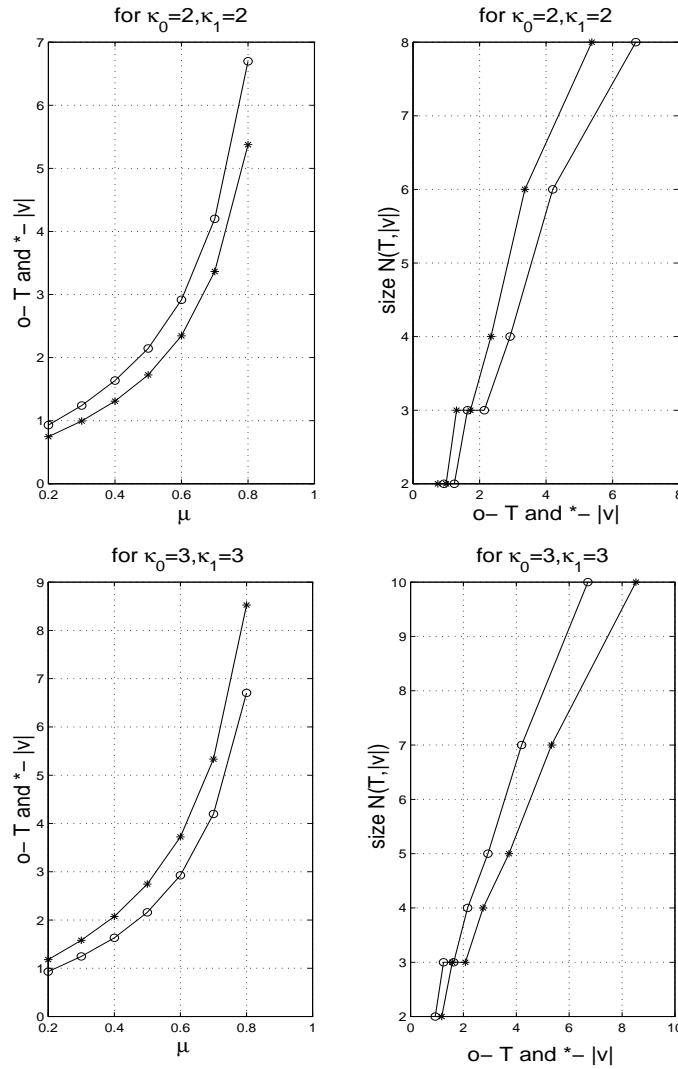


Fig. 3.5 Size $N(T, |\mathbf{v}|)$ depends on temperature T and bulk-velocity \mathbf{v}

3.2 Solution of the Boltzmann equation

3.2.1 The space homogeneous case

As a demonstration of the solution of the space homogeneous Boltzmann equation we present here (A) Comparison of the numerical solution with the exact solution of the Boltzmann equation due to Krook and Wu [51], (B) The relaxation problem.

(A) Comparison with Exact solution

The exact solution of the space homogeneous Boltzmann equation for Maxwell's molecules is due to Krook and Wu [51] and is given by

$$f(v, t) = \frac{\exp(-v^2/2K)}{2(2\pi K)^{3/2}} \left(\frac{(5K-3)}{K} + \frac{(1-K)v^2}{K^2} \right) \quad (3.3)$$

where

$$K = 1 - \exp(-t/6)$$

As a distribution function, f must be nonnegative. Therefore $K \geq \frac{3}{5}$ yields $t \geq t_0 = 5.498$.

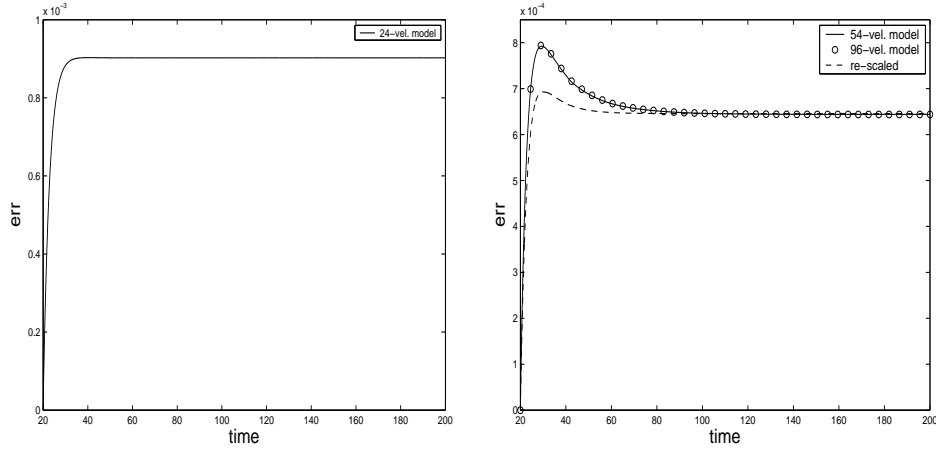


Fig. 3.6 Comparison with exact solution

We compute the solution f_h of space homogeneous Boltzmann equation by using fourth order Runge-Kutta scheme. For three different size model, M1: 24-velocity model as a 1-layer model, M2: 54-velocity model as 2-layer model, M3: 96-velocity model as a 3-layer model we calculated the relative error

$$err = \frac{\|f - f_h\|_1}{\|f\|_1}$$

where f is the exact solution given by equation (3.3).

Fig. 3.6 shows the relative errors for the three models where the error is larger in the case of 1-layer model than the other two cases as because the size of 1-layer model is not enough to include the essential part of the initial distribution. For the other two models M2, M3 error coincide extremely well and in the larger time the errors decreases to 0.00065 which is quite reasonable with the error that has been computed by comparing discrete equilibria and Maxwellian in the previous section. The dashed line in the second figure shows the error err for re-scaled time by a some factor and in this case the maximum of the error reduced significantly and in large time it is the same as before.

(B) The Relaxation problem:

Our test case here concerns the relaxation of a spatially homogeneous distribution to its equilibrium. We consider a gas of identical hard sphere molecules so that the collision frequency for the hexagons H is given by

$$\gamma_H = \pi d^2 \times \text{diam}(H)$$

where d is the diameter of the molecules. The given value of the diameter d is related to determine viscosity coefficient μ given by (see page 67, Bird [15])

$$\mu = (5/16)(T/\pi)^{1/2}(\rho/d^2), \quad (3.4)$$

as well as the mean free-path λ given by (see page 117, Cercignani, [27])

$$\lambda = \frac{\mu(\pi T/2)^{1/2}}{p}, \quad (3.5)$$

where ρ, T, p are the density, temperature, pressure respectively.

We perform here the relaxation of space homogeneous problem and verify the physical properties of the numerical scheme. We consider the initial density (Fig. 3.7a) as a composition of two discrete equilibria centered at two different points on the grid and of the same width. We choose a 6-layer grid (of 294 nodes) which is sufficient to include the essential part of the initial density. (Fig. 3.7b) shows the solution at equilibrium state and (Fig. 3.8c) shows the time evolution of the H-functional.

These results are completely consistent with the basic features of kinetic theory which has been developed in [3]. i.e. Mass, momenta, kinetic energy are invariants and the H -functional is monotonically decreasing w. r. to time.

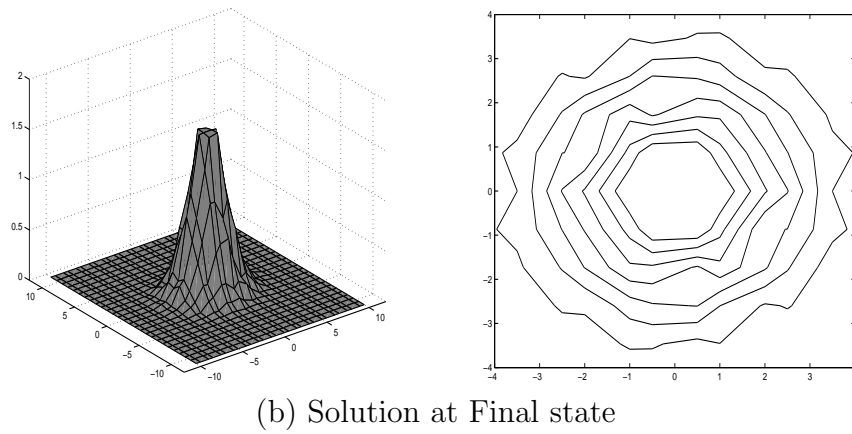
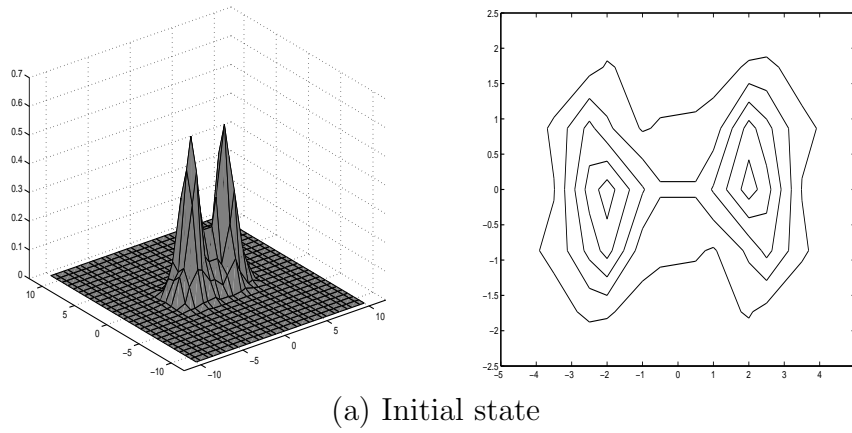


Fig. 3.7 Relaxation problem in a 6-layer grid of 294 nodes

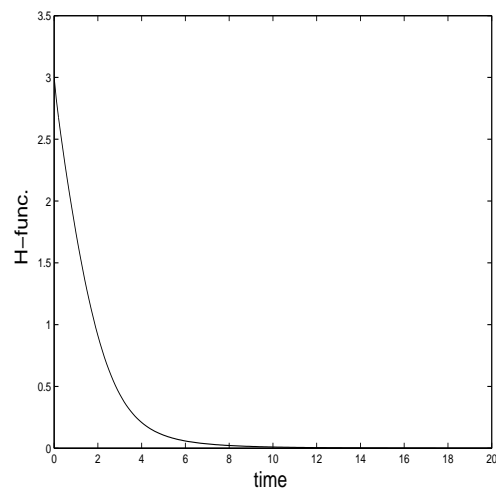


Fig. 3.8 Entropy along time in the relaxation problem

3.2.2 The space inhomogeneous case

As a demonstration of steady flows established at large time, we study the test problems: a) heat transfer between two parallel plates, and b) two-dimensional vapor deposition problem, as an initial value problem. We use the classical operator-splitting method for the computation of the solutions where the equation spilt into transport and collision steps. For the transport step we use a finite difference scheme and for the collision step we use the fourth order Runge-Kutta scheme. We present the results obtained by using three different size discrete velocity models- M2: 54-velocity model, M3: 96-velocity model, M4: 150-velocity model as a 2-layer, 3-layer and 4-layer models respectively.

(a) Heat transfer between two parallel plates

This is a standard test problem in kinetic theory known as "stationary plane Couette flow" and for this we refer [35], [49], [50], [60],[65]. We consider a hard sphere gas between two parallel infinite plates placed at a distance L and having uniform wall temperature $T_0 = 1$ and $T_1 = 1.5$ at $x = 0$ and $x = L$ respectively. We impose diffuse reflection boundary condition on both the walls with density $\rho = 1$ and bulk-velocity $\tilde{\mathbf{v}} = 0$. In our calculation, the discretization parameter of the velocity space $h = 1$, the Knudsen number $Kn = \lambda/L$, where λ is the mean free path.

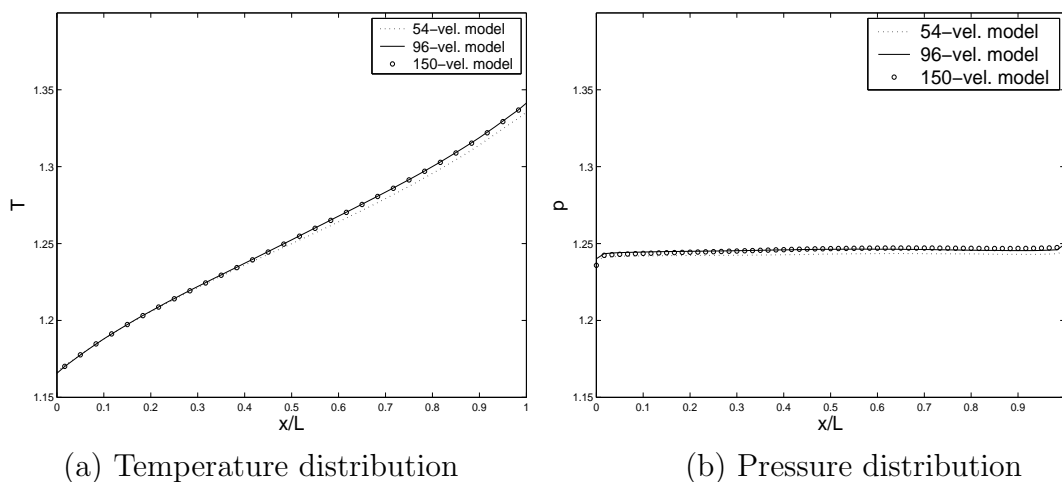


Fig. 3.9 Heat transfer problem for $kn = 0.1$

Fig. 3.9(a) shows the temperature distributions obtained by the three different size models M2, M3, M4. The result by the model M2 differ than the results by the other two models at the high-temperature as because the size of M2 is not enough for the high temperature. We know from the Navier-stokes theory that the temperature

profile between the two plates is a straight line connecting the two wall temperatures T_0 and T_1 . However, due to the description of the considered gas by kinetic equation and boundary conditions, we obtain the expected temperature jump as well as the kinetic boundary layers. As we also know from the theory of steady Couette flow (can be seen in [26], equation (2.3.6)) that the pressure is constant throughout the spatial domain between the plates, Fig. 3.9(b) shows almost a constant pressure profile except little boundary effect.

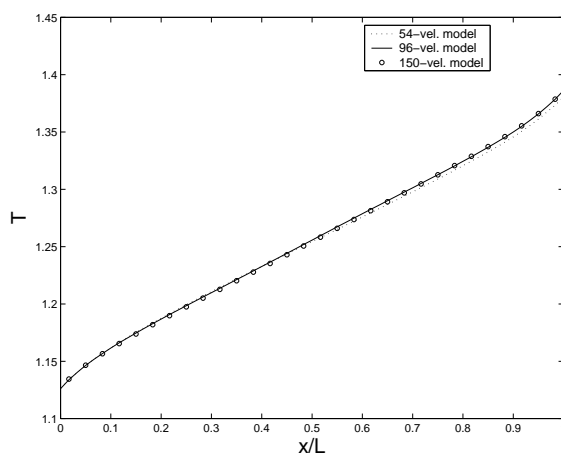


Fig. 3.10 The temperature distribution for $kn = 0.02$

Fig. 3.10 shows the temperature distribution for smaller knudsen number $kn = 0.02$. In this case we obtain less temperature jump than the previous case of larger knudsen number. The Temperature profile from the model M2 differ from that from the models M3 and M4 as before.

(b) Two-dimensional vapor deposition problem

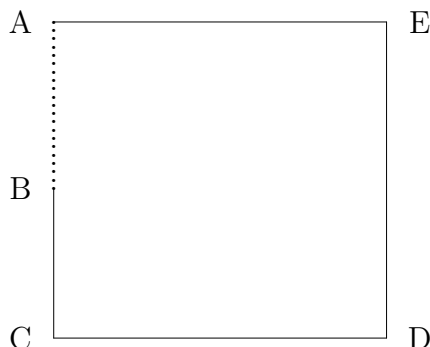
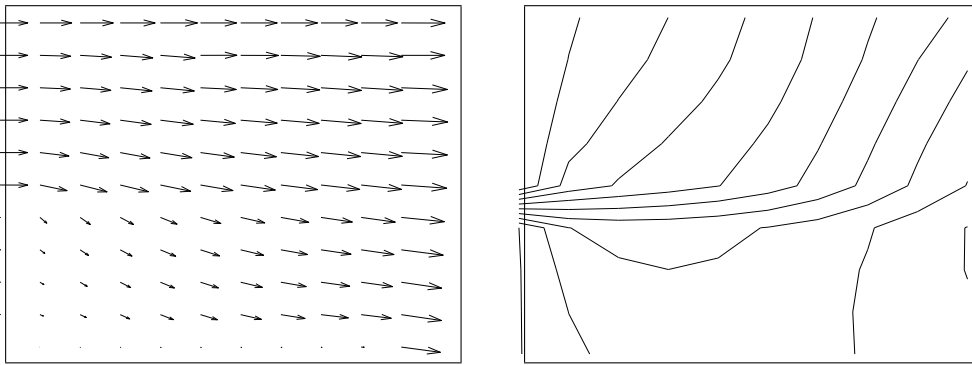


Fig. 3.11 Model chamber of vacuum vapor deposition

We consider a two-dimensional chamber of vacuum deposition as shown in figure 3.11, as a model of a vacuum vapor deposition apparatus [28]. Here AB is the evaporation surface from which molecules reflected are assumed to possess a steady Maxwellian distribution at a surface temperature T_0 . All incident molecules are deposited on the deposition surface DE and the molecules reflect specularly from the surface of symmetry EA . The rest walls BC and CD are diffuse reflection surface at a temperature T_0 . The dimensions of the chamber are $h/l = 1.0$, $b/l = 0.5$.

i) Model M2:



ii) Model M3

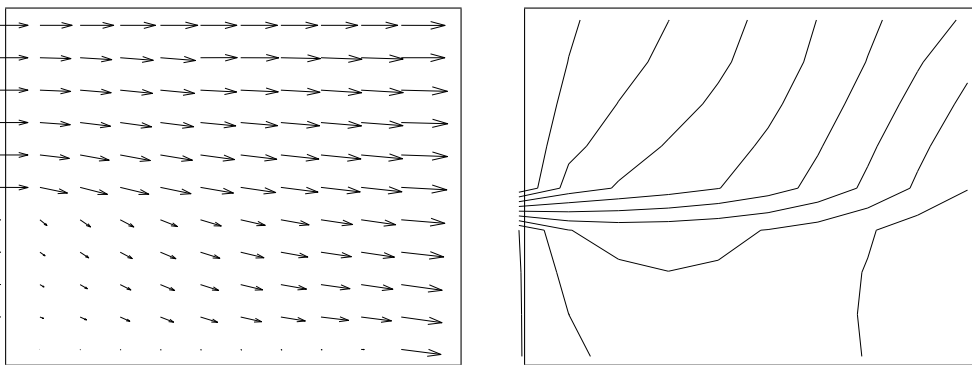


Fig. 3.12 Velocity vectors and density contours

The calculated results are shown in the figure 3.12 and the results are in reasonable qualitative agreement with the results shown in [28]. It is seen that the velocity vectors are similar in the three cases but the density contours differs slightly.

Chapter 4

Discrete Boltzmann equation in \mathbb{R}^3

In this chapter we present the kinetic theory of a discrete Boltzmann equation based on hexagonal discretization of \mathbb{R}^3 . We introduce hexagonal collision model in \mathbb{R}^3 and prove that the model satisfies the basic kinetic features of the classical kinetic theory.

4.1 Hexagonal discretization of \mathbb{R}^3

For the hexagonal discretization of \mathbb{R}^3 , we select the grid of so-called 'sphere-packing' problem. Details about the sphere packing problem can be seen in [30].

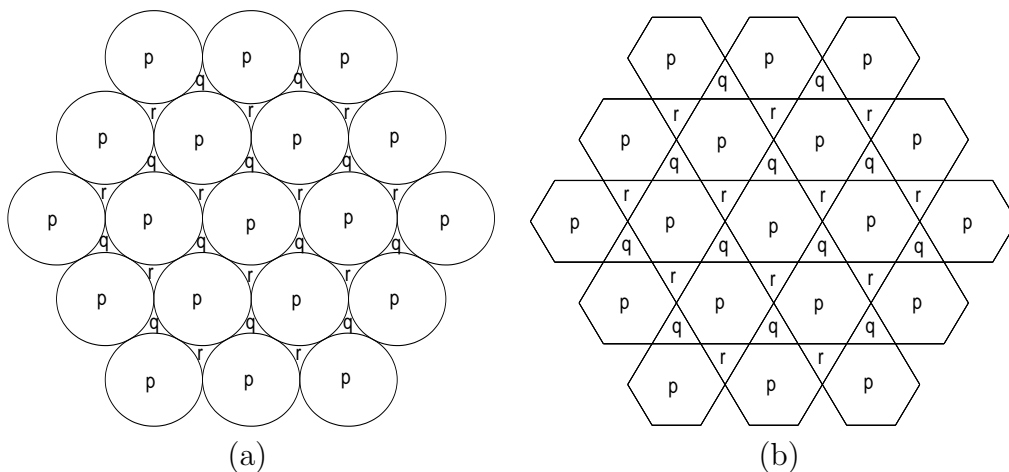


Fig. 4.1 Hexagonal grid in \mathbb{R}^3

The Fig. 4.1a shows a horizontal cut across the middle of unit spheres arranged in a layer and Fig. 4.1b is the corresponding hexagonal grid obtained from the contact points of the spheres. First we take such a layer of spheres with the arrangement as

shown in Fig. 4.1, with the centers at the points marked 'p'. Then above this p-label spheres we place a second layer of spheres with centers marked 'r' as r-label spheres and below the p-label we place another layer of spheres with centers marked 'q' as q-label of spheres. In Fig. 4.1b, the centers of the p-label spheres are the centers of the corresponding hexagons, and the centers of the q-label and r-label spheres are the center of gravity of the corresponding triangles.

Then choosing the labels of spheres as

$$\cdots pqrpqrpqr \cdots$$

we generate a 3d-hexagonal grid where the nodes are the contact points of the spheres (there can be other possibilities too). In this arrangement of spheres, due to the contact points above and below the mid horizontal cuts of the spheres, in between the two consecutive horizontal cuts (along the mid horizontal cuts of the spheres) (r, p) , (p, q) , (q, r) there exists intermediate horizontal cuts q , r , p respectively. Thus, choosing the horizontal cuts with the arrangement as

$$\cdots prqprqprq \cdots$$

we obtain the final grid by which we discretize \mathbb{R}^3 .

Therefore, we can define the hexagonal grid in \mathbb{R}^3 as follows.

For $\alpha = (i, j, k) \in \mathbb{Z}^3$, denote $\mathbf{g}_\alpha^{t,p} = (g_{\alpha,x}^{t,p}, g_{\alpha,y}^{t,p}, g_{\alpha,z}^{t,p})$, $t = 0, \dots, 3$, by

$$\begin{aligned} g_{\alpha,x}^{0,p} &:= 2ih, & g_{\alpha,y}^{0,p} &:= (4j+2)\frac{\sqrt{3}}{2}h; \\ g_{\alpha,x}^{1,p} &:= \left(2i + \frac{1}{2}\right)h, & g_{\alpha,y}^{1,p} &:= (2j+1)\frac{\sqrt{3}}{2}h; \\ g_{\alpha,x}^{2,p} &:= (2i+1)h, & g_{\alpha,y}^{2,p} &:= 4j\frac{\sqrt{3}}{2}h; \\ g_{\alpha,x}^{3,p} &:= \left(2i + \frac{3}{2}\right)h, & g_{\alpha,y}^{3,p} &:= \left(2j+1\right)\frac{\sqrt{3}}{2}h; \end{aligned} \quad (4.1)$$

and $g_{\alpha,z}^{t,p} := 3k\frac{\sqrt{6}}{3}h$ for all $t = 0, \dots, 3$.

Then for

$$\begin{aligned} \mathcal{G}^{t,p} &:= \{\mathbf{g}_\alpha^{t,p} \mid \alpha \in \mathbb{Z}^3\}, \quad t = 0, \dots, 3, \\ \mathcal{G}^p &:= \bigcup_t \mathcal{G}^{t,p} \end{aligned} \quad (4.2)$$

is defined as the set of grid points of the p-label cut.

Denoting

$$g_{\alpha,x}^{t,q} := g_{\alpha,x}^{t,p} + h, \quad g_{\alpha,y}^{t,q} := g_{\alpha,y}^{t,p} + \frac{1}{\sqrt{3}}h, \quad g_{\alpha,z}^{t,q} := (3k+1)\frac{\sqrt{6}}{3}h, \quad (4.3)$$

$$\begin{aligned}\mathcal{G}^{t,q} &:= \{\mathbf{g}_\alpha^{t,q} \mid \alpha \in \mathbb{Z}^3\}, \quad t = 0, \dots, 3, \\ \mathcal{G}^q &:= \bigcup_t \mathcal{G}^{t,q}\end{aligned}\quad (4.4)$$

is defined as the set of grid points of the q-label cut.

Again denoting

$$g_{\alpha,x}^{t,r} := g_{\alpha,x}^{t,p} + h, \quad g_{\alpha,y}^{t,r} := g_{\alpha,y}^{t,p} - \frac{1}{\sqrt{3}}h, \quad g_{\alpha,z}^{t,r} := (3k+2)\frac{\sqrt{6}}{3}h \quad (4.5)$$

$$\begin{aligned}\mathcal{G}^{t,r} &:= \{\mathbf{g}_\alpha^{t,r} \mid \alpha \in \mathbb{Z}^3\}, \quad t = 0, \dots, 3, \\ \mathcal{G}^r &:= \bigcup_t \mathcal{G}^{t,r}\end{aligned}\quad (4.6)$$

is defined as the set of grid points of the r-label cut. Thus finally the set

$$\mathcal{G} := \bigcup_p \mathcal{G}^p \quad (4.7)$$

is defined as the set of grid points of our hexagonal grid in \mathbb{R}^3 .

Now to define the centers of all the basic unit spheres (including the intermediate imaginary spheres) we denote first $\mathbf{c}_\alpha^{s,p} := (c_{\alpha,x}^{s,p}, c_{\alpha,y}^{s,p}, c_{\alpha,z}^{s,p})$, $s = 0, 1$ by

$$\begin{aligned}c_{\alpha,x}^{0,p} &:= 2ih, & c_{\alpha,y}^{0,p} &:= 4j\frac{\sqrt{3}}{2}h; \\ c_{\alpha,x}^{1,p} &:= (2i+1)h, & c_{\alpha,y}^{1,p} &:= (4j+2)\frac{\sqrt{3}}{2}h; \\ \text{and } c_{\alpha,z}^{s,p} &:= 3k\frac{\sqrt{6}}{3}h \quad \text{for both } s = 0, 1;\end{aligned}\quad (4.8)$$

then for

$$\begin{aligned}\mathcal{C}^{s,p} &:= \{\mathbf{c}_\alpha^{s,p} \mid \alpha \in \mathbb{Z}^3\}, \quad s = 0, 1 \\ \mathcal{C}^p &:= \bigcup_s \mathcal{C}^{s,p}\end{aligned}\quad (4.9)$$

is defined the set of center points of the unit spheres corresponding to p-label cut. Now denoting

$$c_{\alpha,x}^{s,q} := c_{\alpha,x}^{s,p} + h, \quad c_{\alpha,y}^{s,q} := c_{\alpha,y}^{s,p} + \frac{1}{\sqrt{3}}h, \quad g_{\alpha,z}^{s,q} := (3k+1)\frac{\sqrt{6}}{3}h \quad (4.10)$$

$$\begin{aligned}\mathcal{C}^{s,q} &:= \{\mathbf{c}_\alpha^{s,q} \mid \alpha \in \mathbb{Z}^3\}, \quad s = 0, 1 \\ \mathcal{C}^q &:= \bigcup_s \mathcal{C}^{s,q}\end{aligned}\quad (4.11)$$

is defined as the set of center points of the unit spheres corresponding to the q-label cuts. Again denoting

$$c_{\alpha,x}^{s,r} := c_{\alpha,x}^{s,p} + h, \quad c_{\alpha,y}^{s,r} := c_{\alpha,y}^{s,p} - \frac{1}{\sqrt{3}}h, \quad c_{\alpha,z}^{s,r} := (3k+2)\frac{\sqrt{6}}{3}h \quad (4.12)$$

$$\begin{aligned} \mathcal{C}^{s,r} &:= \{c_{\alpha}^{s,r} \mid \alpha \in \mathbb{Z}^3\}, \quad s = 0, 1 \\ \mathcal{C}^r &:= \bigcup_s \mathcal{C}^{s,r} \end{aligned} \quad (4.13)$$

is defined as the set of center points of the unit spheres corresponding to the r-label cuts. Then finally

$$\mathcal{C} := \bigcup_p \mathcal{C}^p \quad (4.14)$$

is the set of center points of the spheres placed in the hexagonal grid \mathcal{G} given by the equation (4.7).

4.1.1 Hexagonal collision model in \mathbb{R}^3

Now we investigate the 3D-hexagonal collision model corresponding to a sphere as a local collision model. In the sphere-packing problem, a unit sphere keeps in contact with twelve other neighbouring unit spheres at twelve contact points. Collecting these twelve contact points as nodes, we construct a twelve-velocity collision model as a local collision model corresponding to each single sphere. Connecting these twelve nodes (uniformly distributed on the surface of a unit sphere) as shown in the Fig. 4.2 we obtain a cubic figure which is called as 'cub-octahedron' (archimedean solid) in [33], (p.-82). But for the sake of familiarity with our title 'hexagonal model' (and as one can easily observe that the cubic figure is a composition of four regular hexagons), this cubic figure can be known as '*hexagonal-cube*' or shortly as '*h-cube*'. We call such unit h-cubes (including the h-cubes for the intermediate imaginary spheres) as regular *basic* h-cubes.

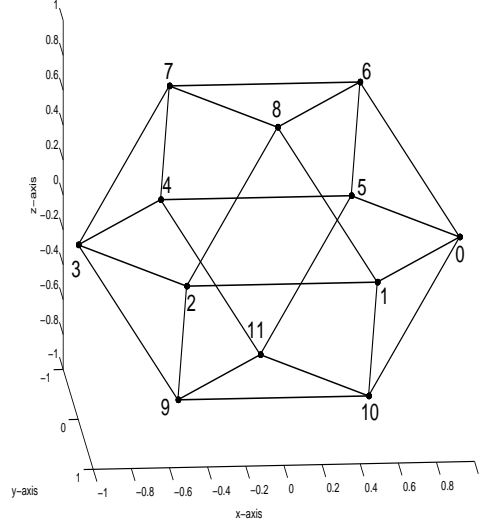


Fig. 4.2 A regular basic hexagonal-cube (h-cube).

The (x,y,z) -coordinates of the twelve nodes of the regular basic h-cube (Fig. 4.2) are defined by

$$\mathbf{v}_x := \frac{1}{2} \begin{pmatrix} 2 \\ 1 \\ -1 \\ -2 \\ -1 \\ 1 \\ 1 \\ -1 \\ 0 \\ -1 \\ 1 \\ 0 \end{pmatrix}, \quad \mathbf{v}_y := \frac{\sqrt{3}}{6} \begin{pmatrix} 0 \\ 3 \\ 3 \\ 0 \\ -3 \\ -3 \\ -1 \\ -1 \\ 2 \\ 1 \\ 1 \\ -2 \end{pmatrix}, \quad \mathbf{v}_z := \frac{\sqrt{6}}{3} \begin{pmatrix} 0 \\ 0 \\ 0 \\ 0 \\ 0 \\ 0 \\ 1 \\ 1 \\ 1 \\ -1 \\ -1 \\ -1 \end{pmatrix} \quad (4.15)$$

In our collision model we impose collision law for each regular basic h-cubes as well as for some other larger regular h-cubes constructed from the hexagonal grid \mathcal{G} defined by the equation (4.7). In order to identify these larger (non-basic) h-cubes, we need to study some properties of the hexagonal grid \mathcal{G} . In Fig. 4.2, the plane hexagon $(0, 1, 2, 3, 4, 5)$ belongs to the p-label cut (p-cut), the upper triangular section $(6, 7, 8)$ belongs to the q-cut and the lower triangular section $(9, 10, 11)$ belongs to the r-cut and the center of the h-cube is the center of the plane hexagon. We consider a p-cut along the plane hexagon $(0, 1, 2, 3, 4, 5)$ and investigate the existence of the regular h-cubes (as in Fig. 4.2), of different radii and centers corresponding to this reference p-cut. To this aim, first we investigate the existence of plane hexagons (of different radii and centers) in the reference cut. For this one can prove the following lemma as in the case of hexagonal grid in \mathbb{R}^2 described in chapter 3.

Lemma 4.1 *Let P_1 and P_2 are any two consecutive nodes of a regular hexagon H of any cut and the coordinates of both of the nodes belong to the set \mathcal{G}^t , $t = 0, \dots, 3$ (\mathcal{G}^t is defined by the equation (4.2)). Then*

1. *for $t = 0, 2$, the coordinates of the center C of the hexagon H belongs to either \mathcal{G}^0 or \mathcal{G}^2 , and*
2. *for $t = 1, 3$, the coordinates of the center C of the hexagon H belongs to either any \mathcal{G}^t , $t = 0, \dots, 3$.*

Lemma 4.2 *Let P_1 and P_2 are any two consecutive nodes of a regular hexagon H of any cut where $P_1(x_1, x_2) \in \mathcal{G}^t$ and $P_2(x_2, y_2) \in \mathcal{G}^{t'}$ ($\mathcal{G}^t, t = 0, \dots, 3$ given by the equation (4.2), $t' \in \{0, \dots, 3\} - \{t\}$), then*

1. *for $|t - t'| = 2$, the center $C(x, y)$ of the hexagon H belongs to either \mathcal{G}^t or $\mathcal{G}^{t'}$;*
2. *for $|t - t'| \neq 2$, the center $C(x, y)$ of the hexagon H belongs to either any \mathcal{C}^s , $s = 0, 1$ or any \mathcal{G}^t , $t = 1, 3$.*

From the above two lemmas we conclude the following theorem.

Theorem 4.3 *The centers of all regular hexagons constructed by any six-tupel nodes of any hexagonal cut (Fig. 4.1b) is either a node of the hexagonal grid or a center of the regular basic hexagon of the hexagonal cut.*

proof: The proof follows from the lemmas 4.1 and 4.2 \square

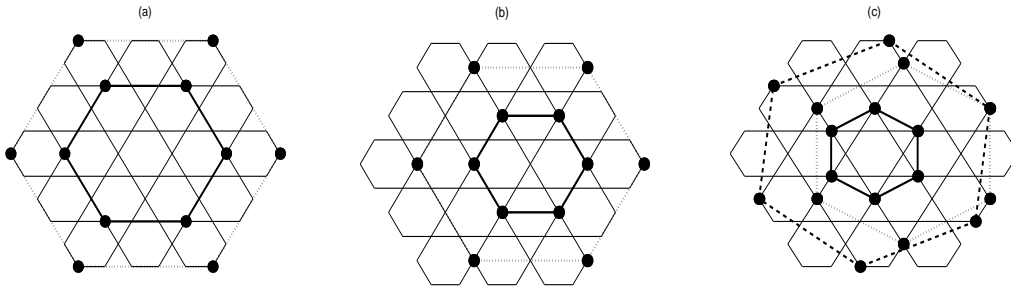


Fig. 4.3 Hexagons of different classes

Following the theorem 4.3, we classify all the possible hexagons of the cut according to their centers and radii.

1. **Class-A:** Fig. 4.3a shows the 'Class-A' hexagons in which the centers are the center of regular basic hexagons and the radii $r_a \in R_a := \{(2i + 1)h, i = 0, 1, 2, \dots\}$.

2. Class-B: Fig. 4.3b shows the 'Class-B' hexagons in which the centers are interior nodes and the radii $r_b \in R_b := \{(2i + 2)h, i = 0, 1, 2, \dots\}$.
3. Class-C: In this class (Fig. 4.3c) the center of the hexagons are either the centers of the regular hexagons or the interior nodes but the radii $r_c \notin \mathbb{N} = R_a \cup R_b$ i.e. $r_c \in (R_a \cup R_b)^c$, the complement of $R_a \cup R_b$.

If we consider a regular h-cube by choosing the class-C hexagons of the cut as a mid horizontal section, then the z -coordinates of the rest six nodes above and below the class-C hexagons are given by

$$v_z = (3k + r_c) \frac{\sqrt{6}}{3} h, \quad k \in \mathbb{Z} \quad (4.16)$$

where $r_c \notin \mathbb{N}$ implies that the z -coordinate $v_z \notin g_{\alpha,z}^{t,n}$, $n = p, q, r$ (defined by the equations (4.1), (4.3), (4.5)). In other words, the regular h-cubes corresponding to the class-C hexagons of the cut do not belong to the hexagonal grid \mathcal{G} .

Therefore our investigation of the 3d collision model based on the class-A and class-B hexagons of the reference cut. The (x, y, z) -coordinates of the twelve nodes of the larger h-cubes corresponding to the class-A and class-B hexagons of the reference cut can be obtained by

$$\tilde{\mathbf{v}} = \mathbf{c} + r\mathbf{v} \quad (4.17)$$

where \mathbf{c} and r are center and radius of the class-A and class-B hexagons of reference cut and $\mathbf{v} = (\mathbf{v}_x, \mathbf{v}_y, \mathbf{v}_z)$ is the (x, y, z) -coordinates of the twelve nodes of a unit h-cube given by the equation (4.15). We have the following property.

Proposition 4.4 *Corresponding to each hexagons of class-A and class-B of the cut, there exists always a regular h-cube where all the twelve nodes of the h-cube belong to the grid \mathcal{G} .*

proof: Following the definitions 4.3 and 4.5, we can write the (x,y,z) -coordinates of the grid of q-cut and r-cut respectively as

$$\begin{aligned} g_{\alpha,x}^{0,q} &:= (2i + 1)h, & g_{\alpha,y}^{0,q} &:= 4(3j + 2) \frac{\sqrt{3}}{6} h; \\ g_{\alpha,x}^{1,q} &:= \left(2i + \frac{3}{2}\right)h, & g_{\alpha,y}^{1,q} &:= (6j + 5) \frac{\sqrt{3}}{6} h; \\ g_{\alpha,x}^{2,q} &:= 2ih, & g_{\alpha,y}^{2,q} &:= (12j + 2) \frac{\sqrt{3}}{6} h; \\ g_{\alpha,x}^{3,q} &:= \left(2i + \frac{1}{2}\right)h, & g_{\alpha,y}^{3,q} &:= (6j + 5) \frac{\sqrt{3}}{6} h; \\ g_{\alpha,z}^{t,q} &:= (3k + 1) \frac{\sqrt{6}}{3} h, & & \text{for all } t = 0, \dots, 3; \end{aligned} \quad (4.18)$$

and

$$\begin{aligned}
g_{\alpha,x}^{0,r} &:= (2i+1)h, & g_{\alpha,y}^{0,r} &:= 4(3j+1)\frac{\sqrt{3}}{6}h \\
g_{\alpha,x}^{1,r} &:= \left(2i + \frac{3}{2}\right)h, & g_{\alpha,y}^{1,r} &:= (6j+1)\frac{\sqrt{3}}{6}h \\
g_{\alpha,x}^{2,r} &:= 2ih, & g_{\alpha,y}^{2,r} &:= (12j-2)\frac{\sqrt{3}}{6}h \\
g_{\alpha,x}^{3,r} &:= \left(2i + \frac{1}{2}\right)h, & g_{\alpha,y}^{3,r} &:= (6j+1)\frac{\sqrt{3}}{6}h \\
g_{\alpha,z}^{t,q} &:= (3k+2)\frac{\sqrt{6}}{3}h, & & \text{for all } t = 0, \dots, 3.
\end{aligned} \tag{4.19}$$

For the center $(c_x, c_y, c_z) \in \mathbf{c}_\alpha^{0,p}$ and radii $r_a \in R_a$, by the equation (4.17), we have for $l = 0, 1, 2, \dots$

$$\begin{aligned}
\tilde{\mathbf{v}}_x &= 2ih + (2l+1)h \cdot \mathbf{v}_x, \\
\tilde{\mathbf{v}}_y &= 4j\frac{\sqrt{3}}{2}h + (2l+1)h \cdot \mathbf{v}_y \\
\tilde{\mathbf{v}}_z &= 3k\frac{\sqrt{6}}{3}h + (2l+1)h \cdot \mathbf{v}_z
\end{aligned} \tag{4.20}$$

Then at the first node, we have

$$\begin{aligned}
\tilde{\mathbf{v}}_{x,0} &= 2ih + (2l+1)h = (2(i+l)+1)h = (2\tilde{i}+1)h, \quad \tilde{i} = (i+l) \in \mathbb{Z} \\
\tilde{\mathbf{v}}_{y,0} &= 4j\frac{\sqrt{3}}{2}h + (2l+1) \times 0 = 4\tilde{j}\frac{\sqrt{3}}{2}h, \quad \tilde{j} = j \in \mathbb{Z} \\
\tilde{\mathbf{v}}_{z,0} &= 3k\frac{\sqrt{6}}{3}h = 3\tilde{k}\frac{\sqrt{6}}{3}h, \quad \tilde{k} = k \in \mathbb{Z} \\
&\implies (\tilde{\mathbf{v}}_{x,0}, \tilde{\mathbf{v}}_{y,0}, \tilde{\mathbf{v}}_{z,0}) \in \mathcal{G}^{2,p}.
\end{aligned}$$

Similarly it is seen that for $i = 1, \dots, 5$,

$$(\tilde{\mathbf{v}}_{x,i}, \tilde{\mathbf{v}}_{y,i}, \tilde{\mathbf{v}}_{z,i}) \in \mathcal{G}^{t,p}, \quad \text{for some } t = 0, \dots, 3$$

Now we have

$$\begin{aligned}
\tilde{\mathbf{v}}_{x,6} &= 2ih + (2l+1)\frac{h}{2} = \left(2\tilde{i} + \frac{1}{2}\right)h \quad \text{or} \quad \left(2\tilde{i} + \frac{3}{2}\right)h \\
&\quad \text{according as } l \in \mathbb{N}_e \quad \text{or} \quad l \in \mathbb{N}_o \quad \text{respectively, for any } \tilde{i} \in \mathbb{Z}; \\
\tilde{\mathbf{v}}_{y,6} &= 4j\frac{\sqrt{3}}{2}h - (2l+1) \cdot \frac{\sqrt{3}}{6}h = (6\tilde{j}+5)\frac{\sqrt{3}}{6}h \in \text{q-cut} \quad \text{for } l=0, \text{ for any } \tilde{j} \in \mathbb{Z} \\
&= (2\tilde{j}+1)\frac{\sqrt{3}}{2}h \in \text{p-cut} \quad \text{for } l=1, \text{ for any } \tilde{j} \in \mathbb{Z} \\
&= (6\tilde{j}+1)\frac{\sqrt{3}}{6}h \in \text{r-cut} \quad \text{for } l=2, \text{ for any } \tilde{j} \in \mathbb{Z} \\
&= (6\tilde{j}+5)\frac{\sqrt{3}}{6}h, \in \text{q-cut} \quad \text{for } l=3, \text{ for } \tilde{j} = \dots - 2, 0, 2, \dots;
\end{aligned}$$

and so forth, and

$$\begin{aligned}
\tilde{\mathbf{v}}_{z,6} &= 3k \frac{\sqrt{6}}{3} h + (2l+1) \frac{\sqrt{6}}{3} h = (3\tilde{k}+1) \frac{\sqrt{6}}{3} h \in \text{q-cut} \quad \text{for } l=0, \text{ for any } \tilde{k} \in \mathbb{Z} \\
&= 3\tilde{k} \frac{\sqrt{6}}{3} h \in \text{p-cut} \quad \text{for } l=1, \text{ for any } \tilde{k} \in \mathbb{Z} \\
&= (3\tilde{k}+2) \frac{\sqrt{6}}{3} h \in \text{r-cut} \quad \text{for } l=2, \text{ for any } \tilde{k} \in \mathbb{Z} \\
&= (3\tilde{k}+1) \frac{\sqrt{6}}{3} h \in \text{q-cut} \quad \text{for } l=3, \text{ for any } \tilde{j} \in \mathbb{Z},
\end{aligned}$$

and so forth. Therefore,

$$(\tilde{\mathbf{v}}_{x,6}, \tilde{\mathbf{v}}_{y,6}, \tilde{\mathbf{v}}_{z,6}) \in \mathcal{G}.$$

Similarly it can be shown that

$$(\tilde{\mathbf{v}}_{x,i}, \tilde{\mathbf{v}}_{y,i}, \tilde{\mathbf{v}}_{z,i}) \in \mathcal{G} \quad \text{for } i = 7, \dots, 11.$$

Similar arguments also holds true for the case of $(c_x, c_y, c_z) \in \mathbf{c}_\alpha^{1,p}$ with radii $r \in R_a$ and for the case of $(c_x, c_y, c_z) \in \mathcal{G}_{\text{int}}$ with radii $r \in R_b$ \square

With the horizontal p, q, r-label cuts in our hexagonal grid, there exists some other (non-horizontal) cuts too, e.g. along the hexagon (1, 10, 11, 4, 7, 8) of the Fig. 4.2, as shown in Fig. 4.7 and by symmetry, the properties given by the theorem 4.3 and proposition 4.4 are also true for these non-horizontal cuts.

Definition 4.5 We call the h-cubes corresponding to the class-A and class-B hexagons (of the cuts) as 'class-A' h-cubes and 'class-B' h-cubes respectively.

The set of all such regular h-cubes with vertices in \mathcal{G} is denoted by \mathcal{H} . For each $H \in \mathcal{H}$ a numbering $\pi^H = (\pi_0^H, \dots, \pi_{11}^H)$ is given which lists all nodes of H as enumerated in Fig. 4.2.

For a given real-valued function $\mathbf{f} \in \mathbb{R}^{|\mathcal{G}|}$ on \mathcal{G} we denote by $\mathbf{f}_H = P_H \mathbf{f}$ the restriction of \mathbf{f} on H , i.e.

$$P_H \mathbf{f} = (f_{\pi_0^H}, \dots, f_{\pi_{11}^H}) \in \mathbb{R}^{12}. \quad (4.21)$$

For $H := (\pi_0^H, \dots, \pi_{11}^H) \in \mathcal{H}$ and $\mathbf{f}_H \in \mathbb{R}_+^{11}$, a *local collision operator*

$$J_H[\mathbf{f}_H, \mathbf{f}_H] = (J_H[\mathbf{f}_H, \mathbf{f}_H]_0, \dots, J_H[\mathbf{f}_H, \mathbf{f}_H]_{11}) \quad (4.22)$$

has been introduced in the next section. Given this, the space homogeneous kinetic equation as an evolution equation for densities $\mathbf{f} = \mathbf{f}(t)$ on \mathcal{G} has the form

$$\partial_t = J[\mathbf{f}, \mathbf{f}] \quad (4.23)$$

where the *global collision operator* $J[\mathbf{f}, \mathbf{f}]$ is given in its weak formulation as

$$\langle \phi, J[\mathbf{f}, \mathbf{f}] \rangle = \sum_{H \in \mathcal{H}} \gamma_H \sum_{i=0}^{11} \phi(\pi_i^H) J_H[\mathbf{f}_H, \mathbf{f}_H]_i. \quad (4.24)$$

Here $\phi : \mathcal{G} \rightarrow \mathbb{R}$ is an appropriate test function and the scalar product is defined by

$$\langle \phi, \mathbf{f} \rangle = \sum_{g \in \mathcal{G}} \phi(g) \mathbf{f}(g). \quad (4.25)$$

Let $\gamma_H \geq 0$ denotes the collision rate corresponding to H and then for (4.24), we denote

$$\mathcal{H}^+ := \{H \in \mathcal{H} | \gamma_H > 0\} \quad (4.26)$$

as the set of all regular hexagons which are involved in the collisions.

4.2 The local collision model

In this section we describe a twelve-velocity collision model as a local collision model and prove that the model satisfies the basic kinetic features of the classical kinetic theory.

4.2.1 A twelve-velocity model

Let $H = (\mathbf{z}_0, \dots, \mathbf{z}_{11})$ denote a regular h-cube enumerated as in Fig. 4.4 and $\mathbf{f} = (f_i)_{i=0}^{11}$ denote a density vector on H with strictly positive components. Our collision model on H consists of *binary* and *ternary* collisions. The binary interaction law states that any pair of velocities $(\mathbf{z}_i, \mathbf{z}_{i+3})$ ($i = i_1 + i_2$; for each $i_1 = 0, 6$; $i_2 = 0, 1, 2$) is transformed into the pairs $(\mathbf{z}_k, \mathbf{z}_{k+3})$ ($k = k_1 + k_2$; for each $k_1 = 0, 6$; $k_2 = 0, 1, 2$) with equal probabilities. This binary interactions yields the collision operator $J_{bin}[\mathbf{f}, \mathbf{f}]$ given by

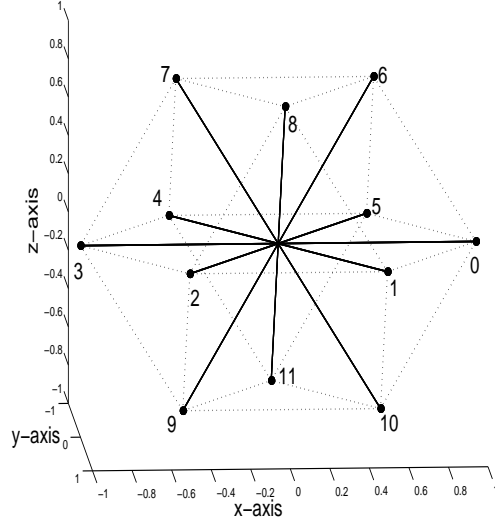


Fig. 4.4 A twelve-velocity local collision model

$$J_{bin}[\mathbf{f}, \mathbf{f}]_i = J_{bin}[\mathbf{f}, \mathbf{f}]_{i+3} = S[\mathbf{f}, \mathbf{f}] - 6f_i f_{i+3}; \quad i = i_1 + i_2; \quad \text{for each } i_1 = 0, 6; \quad i_2 = 0, 1, 2$$

where

$$S[\mathbf{f}, \mathbf{f}] = f_0 f_3 + f_1 f_4 + f_2 f_5 + f_6 f_9 + f_7 f_{10} + f_8 f_{11}.$$

Then the kinetic equation reads

$$\partial_t \mathbf{f} = J_{bin}[\mathbf{f}, \mathbf{f}]. \quad (4.27)$$

Define the vectors

$$\mathbb{1} := \begin{pmatrix} 1 \\ 1 \\ 1 \\ 1 \\ 1 \\ 1 \\ 1 \\ 1 \\ 1 \\ 1 \\ 1 \\ 1 \end{pmatrix}, \quad \mathbf{v}_x := \frac{1}{2} \begin{pmatrix} 2 \\ 1 \\ -1 \\ -2 \\ -1 \\ 1 \\ 1 \\ -1 \\ -1 \\ 0 \\ -1 \\ 1 \\ 0 \end{pmatrix}, \quad \mathbf{v}_y := \frac{\sqrt{3}}{6} \begin{pmatrix} 0 \\ 3 \\ 3 \\ 0 \\ -3 \\ -3 \\ -1 \\ -1 \\ -1 \\ 2 \\ 1 \\ 1 \\ -2 \end{pmatrix}, \quad \mathbf{v}_z := \frac{\sqrt{6}}{3} \begin{pmatrix} 0 \\ 0 \\ 0 \\ 0 \\ 0 \\ 0 \\ 1 \\ 1 \\ 1 \\ 1 \\ -1 \\ -1 \\ -1 \end{pmatrix}, \quad (4.28)$$

$$\mathbf{a}_1 := \begin{pmatrix} 1 \\ 1 \\ 1 \\ 1 \\ 1 \\ -1 \\ -1 \\ -1 \\ -1 \\ -1 \\ -1 \\ -1 \end{pmatrix}, \quad \mathbf{a}_2 := \begin{pmatrix} 1 \\ 1 \\ 1 \\ -1 \\ -1 \\ -1 \\ -1 \\ -1 \\ 1 \\ 1 \\ 1 \\ 1 \end{pmatrix}, \quad \mathbf{a}_3 := \begin{pmatrix} 1 \\ 1 \\ 1 \\ -1 \\ -1 \\ -1 \\ 1 \\ 1 \\ 1 \\ -1 \\ -1 \\ -1 \end{pmatrix}. \quad (4.29)$$

Then it can be verified that the equation (4.27) has the four physically relevant invariants

$$\text{mass} \quad \rho = \langle \mathbf{1}, \mathbf{f} \rangle, \quad (4.30)$$

$$x\text{-momentum} \quad \rho \bar{v}_x = \langle \mathbf{v}_x, \mathbf{f} \rangle, \quad (4.31)$$

$$y\text{-momentum} \quad \rho \bar{v}_y = \langle \mathbf{v}_y, \mathbf{f} \rangle, \quad (4.32)$$

$$z\text{-momentum} \quad \rho \bar{v}_z = \langle \mathbf{v}_z, \mathbf{f} \rangle \quad (4.33)$$

and three artificial collision invariants $\langle \mathbf{a}_l, \mathbf{f} \rangle, l = 1, 2, 3$. In order to eliminate these three artificial invariants, we introduce the *ternary* interaction law

$$(\mathbf{z}_i, \mathbf{z}_{j_p}, \mathbf{z}_{k_p}) \longleftrightarrow (\mathbf{z}_{l_p}, \mathbf{z}_{m_p}, \mathbf{z}_{n_p}) \quad p = 1, 2, \quad (4.34)$$

where for $i = 0, \dots, 11$,

$$\begin{aligned} \{\{i, j_p, k_p\}, \{l_p, m_p, n_p\}\} \in T := & \left\{ \{\{1, 3, 5\}, \{0, 2, 4\}\}, \{\{3, 6, 10\}, \{0, 7, 9\}\}, \right. \\ & \left. \{\{4, 8, 10\}, \{1, 7, 11\}\}, \{\{5, 8, 9\}, \{2, 6, 11\}\} \right\} \end{aligned} \quad (4.35)$$

which results a ternary collision operator

$$\begin{aligned} J_{ter}[\mathbf{f}, \mathbf{f}]_i = \sum_{p=1}^2 (f_{l_p} f_{m_p} f_{n_p} - f_i f_{j_p} f_{k_p}) \quad \text{for each } i = 0, \dots, 11, \quad p = 1, 2 \\ \{\{i, j_p, k_p\}, \{l_p, m_p, n_p\}\} \in T. \end{aligned} \quad (4.36)$$

It can be verified that $J_{ter}[\mathbf{f}, \mathbf{f}]$ has the physically relevant collision invariants (4.30) to (4.33) but the artificial invariants $\langle \mathbf{a}_l, \mathbf{f} \rangle, l = 1, 2, 3$ are no longer.

Thus the *local collision operator* J_H is given by

$$J_H[\mathbf{f}, \mathbf{f}] = \gamma_{bin} J_{bin}[\mathbf{f}, \mathbf{f}] + \gamma_{ter} J_{ter}[\mathbf{f}, \mathbf{f}], \quad (\gamma_{bin}, \gamma_{ter}) > 0, \quad (4.37)$$

and the space homogeneous evolution equation reads

$$\partial_t \mathbf{f} = J_H[\mathbf{f}, \mathbf{f}]. \quad (4.38)$$

4.2.2 H-Theorem, Equilibrium solutions

For a twelve-velocity collision model on a regular h-cube H , we define *equilibrium solutions* (equilibria) as a strictly positive density vector $\mathbf{f} = (f_i)_{i=0}^{11}$ for which $J_H[\mathbf{f}, \mathbf{f}] = 0$ and we denote the set of equilibria by \mathcal{E}_H .

Theorem 4.6 H-Theorem: *For a given strictly positive density vector $\mathbf{f} = (f_i)_{i=0}^{11}$, we define the H-functional*

$$H[\mathbf{f}] := \sum_{i=0}^{11} f_i \ln(f_i). \quad (4.39)$$

If $t \mapsto \mathbf{f}(t)$ denotes a solution of (4.38), then $H[\mathbf{f}](t)$ is monotonically decreasing with t . Moreover, $\partial_t H[\mathbf{f}](t) = 0$ if and only if $\mathbf{f}(t) \in \mathcal{E}_H$.

Proof: It can be shown that

$$\begin{aligned} \partial_t H[\mathbf{f}](t) &= \sum_{i=0}^{11} (1 + \ln(f_i(t))) \partial_t f_i(t) = f_1 f_4 \ln\left(\frac{f_0 f_3}{f_1 f_4}\right) \left(1 - \frac{f_0 f_3}{f_1 f_4}\right) \\ &+ f_2 f_5 \ln\left(\frac{f_0 f_3}{f_2 f_5}\right) \left(1 - \frac{f_0 f_3}{f_2 f_5}\right) + f_6 f_9 \ln\left(\frac{f_0 f_3}{f_6 f_9}\right) \left(1 - \frac{f_0 f_3}{f_6 f_9}\right) \\ &+ f_7 f_{10} \ln\left(\frac{f_0 f_3}{f_7 f_{10}}\right) \left(1 - \frac{f_0 f_3}{f_7 f_{10}}\right) + f_8 f_{11} \ln\left(\frac{f_0 f_3}{f_8 f_{11}}\right) \left(1 - \frac{f_0 f_3}{f_8 f_{11}}\right) \\ &+ f_2 f_5 \ln\left(\frac{f_1 f_4}{f_2 f_5}\right) \left(1 - \frac{f_1 f_4}{f_2 f_5}\right) + f_6 f_9 \ln\left(\frac{f_1 f_4}{f_6 f_9}\right) \left(1 - \frac{f_1 f_4}{f_6 f_9}\right) \\ &+ f_7 f_{10} \ln\left(\frac{f_1 f_4}{f_7 f_{10}}\right) \left(1 - \frac{f_1 f_4}{f_7 f_{10}}\right) + f_8 f_{11} \ln\left(\frac{f_1 f_4}{f_8 f_{11}}\right) \left(1 - \frac{f_1 f_4}{f_8 f_{11}}\right) \quad (4.40) \\ &+ f_6 f_9 \ln\left(\frac{f_2 f_5}{f_6 f_9}\right) \left(1 - \frac{f_2 f_5}{f_6 f_9}\right) + f_7 f_{10} \ln\left(\frac{f_2 f_5}{f_7 f_{10}}\right) \left(1 - \frac{f_2 f_5}{f_7 f_{10}}\right) \\ &+ f_8 f_{11} \ln\left(\frac{f_2 f_5}{f_8 f_{11}}\right) \left(1 - \frac{f_2 f_5}{f_8 f_{11}}\right) + f_7 f_{10} \ln\left(\frac{f_6 f_9}{f_7 f_{10}}\right) \left(1 - \frac{f_6 f_9}{f_7 f_{10}}\right) \\ &+ f_8 f_{11} \ln\left(\frac{f_6 f_9}{f_8 f_{11}}\right) \left(1 - \frac{f_6 f_9}{f_8 f_{11}}\right) + f_8 f_{11} \ln\left(\frac{f_7 f_{10}}{f_8 f_{11}}\right) \left(1 - \frac{f_7 f_{10}}{f_8 f_{11}}\right) \\ &+ f_1 f_3 f_5 \ln\left(\frac{f_0 f_2 f_4}{f_1 f_3 f_5}\right) \left(1 - \frac{f_0 f_2 f_4}{f_1 f_3 f_5}\right) + f_3 f_6 f_{10} \ln\left(\frac{f_0 f_7 f_9}{f_3 f_6 f_{10}}\right) \left(1 - \frac{f_0 f_7 f_9}{f_3 f_6 f_{10}}\right) \\ &+ f_4 f_8 f_{10} \ln\left(\frac{f_1 f_7 f_{11}}{f_4 f_8 f_{10}}\right) \left(1 - \frac{f_1 f_7 f_{11}}{f_4 f_8 f_{10}}\right) + f_5 f_8 f_9 \ln\left(\frac{f_2 f_6 f_{11}}{f_5 f_8 f_9}\right) \left(1 - \frac{f_2 f_6 f_{11}}{f_5 f_8 f_9}\right) \\ &= \sum_{j=1}^{19} \zeta_j \phi(\xi_j) \end{aligned}$$

where $\phi(x) = \ln(x)(1-x)$, and ζ_j, ξ_j are strictly positive numbers. The H-Theorem follows from the fact that ϕ is a non-positive function for $x > 0$ with $\phi(x) = 0 \Leftrightarrow x = 1$. \square

Proposition 4.7 $\mathbf{f} = (f_i)_{i=0}^{11}$ is a equilibria if and only if the following conditions are satisfied.

$$f_0f_3 = f_1f_4 = f_2f_5 = f_6f_9 = f_7f_{10} = f_8f_{11}, \quad (4.41)$$

$$f_0f_2f_4 = f_1f_3f_5, \quad f_0f_7f_9 = f_3f_6f_{10}, \quad f_1f_7f_{11} = f_4f_8f_{10}, \quad f_2f_6f_{11} = f_5f_8f_9. \quad (4.42)$$

Proof: The proof follows from the above H-Theorem. \square

For the characterization of $\mathbf{f} \in \mathcal{E}_H$, we need the following results.

Lemma 4.8 For $\mathbf{f} \in \mathcal{E}_H$ if we denote

$$r^2 := f_0f_3 = f_1f_4 = f_2f_5 = f_6f_9 = f_7f_{10} = f_8f_{11} \quad (4.43)$$

then the following relation holds

$$r^3 = f_0f_2f_4 = f_1f_3f_5 = f_0f_7f_9 = f_3f_6f_{10} = f_1f_7f_{11} = f_4f_8f_{10} = f_2f_6f_{11} = f_5f_8f_9 \quad (4.44)$$

$$\begin{aligned} r &= \underbrace{\frac{f_0f_2}{f_1} = \frac{f_1f_3}{f_2} = \frac{f_2f_4}{f_3} = \frac{f_3f_5}{f_4} = \frac{f_4f_0}{f_5} = \frac{f_5f_1}{f_0}}_{(a)} \\ &= \underbrace{\frac{f_0f_7}{f_6} = \frac{f_3f_6}{f_7} = \frac{f_7f_9}{f_3} = \frac{f_3f_{10}}{f_9} = \frac{f_9f_0}{f_{10}} = \frac{f_{10}f_6}{f_0}}_{(b)} \\ &= \underbrace{\frac{f_2f_6}{f_8} = \frac{f_5f_8}{f_6} = \frac{f_6f_{11}}{f_5} = \frac{f_5f_9}{f_{11}} = \frac{f_2f_{11}}{f_9} = \frac{f_8f_9}{f_2}}_{(c)} \\ &= \underbrace{\frac{f_1f_{11}}{f_{10}} = \frac{f_4f_{10}}{f_{11}} = \frac{f_7f_{11}}{f_4} = \frac{f_4f_8}{f_7} = \frac{f_1f_7}{f_8} = \frac{f_8f_{10}}{f_1}}_{(d)} \end{aligned} \quad (4.45)$$

Proof: As $f_0f_2f_4 = f_1f_3f_5$, therefore,

$$f_0f_2f_4 = \frac{r^6}{f_1f_3f_5}$$

yields

$$r^3 = f_0f_2f_4 = f_1f_3f_5.$$

Similarly, $r^3 = f_3f_6f_{10} = f_0f_7f_9$ and so on.

From (4.43), we find

$$f_3f_6 \frac{r^2}{f_7} = f_3f_6f_{10} = f_0f_7f_9 = f_7 \frac{r^4}{f_3f_6}$$

yields

$$r = \frac{f_3 f_6}{f_7}$$

Similarly the other equalities also hold. \square

Remark 4.9 In the above lemma, the equations (4.45(a)–(d)) are corresponding to the four plane hexagons (0, 1, 2, 3, 4, 5); (0, 10, 9, 3, 7, 6); (6, 5, 11, 9, 2, 8); (1, 10, 11, 4, 7, 8) respectively.

Proposition 4.10 \mathcal{E}_H is a smooth four-dimensional manifold.

Proof: Following the equation (4.45-a) of the above lemma with the proposition 3.3 in [3], the equilibria at the six nodes of the horizontal hexagonal cut of the h-cube H can be presented by

$$(f_i)_{i=0}^5 = r(\kappa_{0+}, \kappa_{1+}, \kappa_{2+}, \kappa_{0-}, \kappa_{1-}, \kappa_{2-})^\top, \quad \kappa_{1+} = \kappa_{0+}\kappa_{2+}, \quad \kappa_{i-} = 1/\kappa_{i+}, \quad i = 0, 1, 2 \quad (4.46)$$

Denoting $f_6 := r\kappa_{3+}$, from the equation (4.45-(b)), i.e from

$$\frac{f_0 f_7}{f_6} = \frac{f_3 f_6}{f_7} = \frac{f_7 f_9}{f_3} = \frac{f_3 f_{10}}{f_9} = \frac{f_9 f_0}{f_{10}} = \frac{f_{10} f_6}{f_0}$$

we have

$$f_7^2 = \frac{f_3 f_6^2}{f_0} \implies f_7 = r\kappa_{0-}\kappa_{3+} =: r\kappa_{4+},$$

$$f_9 = \frac{f_0 f_3}{f_6} = r\kappa_{3-},$$

$$f_{10} = \frac{f_0 f_3}{f_7} = r\kappa_{0+}\kappa_{3-} =: r\kappa_{4-}.$$

Again from (4.45-(d)), i.e. from

$$\frac{f_1 f_{11}}{f_{10}} = \frac{f_4 f_{10}}{f_{11}} = \frac{f_7 f_{11}}{f_4} = \frac{f_4 f_8}{f_7} = \frac{f_1 f_7}{f_8} = \frac{f_8 f_{10}}{f_1}$$

we have,

$$f_8^2 = \frac{f_1 f_7^2}{f_4} \implies f_8 = r\kappa_{2+}\kappa_{3+} =: r\kappa_{5+}$$

and

$$f_{11} = \frac{f_1 f_4}{f_8} = r\kappa_{2-}\kappa_{3-} =: r\kappa_{5-}.$$

Thus the set of equilibria $f \in \mathcal{E}_H$ is given by

$$\mathbf{f} = r(\kappa_{0+}, \kappa_{1+}, \kappa_{2+}, \kappa_{0-}, \kappa_{1-}, \kappa_{2-}, \kappa_{3+}, \kappa_{4+}, \kappa_{5+}, \kappa_{3-}, \kappa_{4-}, \kappa_{5-})^\top \quad (4.47)$$

with $\kappa_{1+} = \kappa_{0+}\kappa_{2+}$, $\kappa_{4+} = \kappa_{0-}\kappa_{3+}$, $\kappa_{5+} = \kappa_{2+}\kappa_{3+}$, $\kappa_{i-} = 1/\kappa_{i+}$, $i = 0, \dots, 5$. \square

4.2.3 The linearized system

Let

$$\mathbf{e} = (e_i)_{i=0}^{11} = r(\kappa_{0+}, \kappa_{1+}, \kappa_{2+}, \kappa_{0-}, \kappa_{1-}, \kappa_{2-}, \kappa_{3+}, \kappa_{4+}, \kappa_{5+}, \kappa_{3-}, \kappa_{4-}, \kappa_{5-})^\top \in \mathcal{E}_H \quad (4.48)$$

be an equilibrium solution of the twelve-velocity model and define

$$D_H := \text{diag}(e_i, i = 0, \dots, 11) \quad (4.49)$$

Inserting the ansatz

$$\mathbf{f} = \mathbf{e} + \epsilon D_H^{\frac{1}{2}} \phi \quad (4.50)$$

into the equation (4.38) and neglecting the terms quadratic in ϵ yields the *linearized equation*

$$\partial_t \phi = L_H \phi := D_H^{-\frac{1}{2}} (\gamma_{bin} L_1 D_1 + \gamma_{ter} (L_2^1 D_2 + L_2^2 D_3)) D_H^{\frac{1}{2}} \phi \quad (4.51)$$

where the diagonal matrices

$$D_1 = \text{diag}(e_3, e_4, e_5, e_0, e_1, e_2, e_9, e_{10}, e_{11}, e_6, e_7, e_8), \quad (4.52)$$

$$D_2 = \text{diag}(e_2 e_4, e_3 e_5, e_0 e_4, e_1 e_5, e_0 e_2, e_1 e_3, e_2 e_{11}, e_0 e_9, e_4 e_{10}, e_5 e_8, e_3 e_6, e_1 e_7), \quad (4.53)$$

$$D_3 = \text{diag}(e_7 e_9, e_7 e_{11}, e_6 e_{11}, e_6 e_{10}, e_8 e_{10}, e_8 e_9, e_3 e_{10}, e_1 e_{11}, e_5 e_9, e_0 e_7, e_4 e_8, e_2 e_6), \quad (4.54)$$

and

$$L_1 = \begin{pmatrix} -5 & 1 & 1 & -5 & 1 & 1 & 1 & 1 & 1 & 1 & 1 & 1 \\ 1 & -5 & 1 & 1 & -5 & 1 & 1 & 1 & 1 & 1 & 1 & 1 \\ 1 & 1 & -5 & 1 & 1 & -5 & 1 & 1 & 1 & 1 & 1 & 1 \\ -5 & 1 & 1 & -5 & 1 & 1 & 1 & 1 & 1 & 1 & 1 & 1 \\ 1 & -5 & 1 & 1 & -5 & 1 & 1 & 1 & 1 & 1 & 1 & 1 \\ 1 & 1 & -5 & 1 & 1 & -5 & 1 & 1 & 1 & 1 & 1 & 1 \\ 1 & 1 & 1 & 1 & 1 & 1 & -5 & 1 & 1 & -5 & 1 & 1 \\ 1 & 1 & 1 & 1 & 1 & 1 & 1 & -5 & 1 & 1 & -5 & 1 \\ 1 & 1 & 1 & 1 & 1 & 1 & -5 & 1 & 1 & -5 & 1 & 1 \\ 1 & 1 & 1 & 1 & 1 & 1 & 1 & -5 & 1 & 1 & -5 & 1 \\ 1 & 1 & 1 & 1 & 1 & 1 & 1 & 1 & -5 & 1 & 1 & -5 \end{pmatrix}, \quad (4.55)$$

$$L_2^1 = \begin{pmatrix} -1 & 1 & -1 & 1 & -1 & 1 & 0 & -1 & 0 & 0 & 1 & 0 \\ 1 & -1 & 1 & -1 & 1 & -1 & 0 & 0 & 1 & 0 & 0 & -1 \\ -1 & 1 & -1 & 1 & -1 & 1 & -1 & 0 & 0 & 1 & 0 & 0 \\ 1 & -1 & 1 & -1 & 1 & -1 & 0 & 1 & 0 & 0 & -1 & 0 \\ -1 & 1 & -1 & 1 & -1 & 1 & 0 & 0 & -1 & 0 & 0 & 1 \\ 1 & -1 & 1 & -1 & 1 & -1 & 1 & 0 & 0 & -1 & 0 & 0 \\ 0 & 0 & 0 & 0 & 0 & 0 & -1 & 1 & 0 & 1 & -1 & 0 \\ 0 & 0 & 0 & 0 & 0 & 0 & 0 & -1 & 1 & 0 & 1 & -1 \\ 0 & 0 & 0 & 0 & 0 & 0 & 1 & 0 & -1 & -1 & 0 & 1 \\ 0 & 0 & 0 & 0 & 0 & 0 & 1 & -1 & 0 & -1 & 1 & 0 \\ 0 & 0 & 0 & 0 & 0 & 0 & 0 & 1 & -1 & 0 & -1 & 1 \\ 0 & 0 & 0 & 0 & 0 & 0 & -1 & 0 & 1 & 1 & 0 & -1 \end{pmatrix}, \quad (4.56)$$

$$L_2^2 = \begin{pmatrix} -1 & 0 & 0 & 1 & 0 & 0 & 1 & 0 & 0 & -1 & 0 & 0 \\ 0 & -1 & 0 & 0 & 1 & 0 & 0 & -1 & 0 & 0 & 1 & 0 \\ 0 & 0 & -1 & 0 & 0 & 1 & 0 & 0 & 1 & 0 & 0 & -1 \\ 1 & 0 & 0 & -1 & 0 & 0 & -1 & 0 & 0 & 1 & 0 & 0 \\ 0 & 1 & 0 & 0 & -1 & 0 & 0 & 1 & 0 & 0 & -1 & 0 \\ 0 & 0 & 1 & 0 & 0 & -1 & 0 & 0 & -1 & 0 & 0 & 1 \\ 1 & 0 & -1 & -1 & 0 & 1 & -1 & 0 & 1 & 1 & 0 & -1 \\ -1 & -1 & 0 & 1 & 1 & 0 & 1 & -1 & 0 & -1 & 1 & 0 \\ 0 & 1 & 1 & 0 & -1 & -1 & 0 & 1 & -1 & 0 & -1 & 1 \\ -1 & 0 & 1 & 1 & 0 & -1 & 1 & 0 & -1 & -1 & 0 & 1 \\ 1 & 1 & 0 & -1 & -1 & 0 & -1 & 1 & 0 & 1 & -1 & 0 \\ 0 & -1 & -1 & 0 & 1 & 1 & 0 & -1 & 1 & 0 & 1 & -1 \end{pmatrix}. \quad (4.57)$$

Denoting $L_2 := L_2^1 + L_2^2$, we have

$$L_2 = \begin{pmatrix} -2 & 1 & -1 & 2 & -1 & 1 & 1 & -1 & 0 & -1 & 1 & 0 \\ 1 & -2 & 1 & -1 & 2 & -1 & 0 & -1 & 1 & 0 & 1 & -1 \\ -1 & 1 & -2 & 1 & -1 & 2 & -1 & 0 & 1 & 1 & 0 & -1 \\ 2 & -1 & 1 & -2 & 1 & -1 & -1 & 1 & 0 & 1 & -1 & 0 \\ -1 & 2 & -1 & 1 & -2 & 1 & 0 & 1 & -1 & 0 & -1 & 1 \\ 1 & -1 & 2 & -1 & 1 & -2 & 1 & 0 & -1 & -1 & 0 & 1 \\ 1 & 0 & -1 & -1 & 0 & 1 & -2 & 1 & 1 & 2 & -1 & -1 \\ -1 & -1 & 0 & 1 & 1 & 0 & 1 & -2 & 1 & -1 & 2 & -1 \\ 0 & 1 & 1 & 0 & -1 & -1 & 1 & 1 & -2 & -1 & -1 & 2 \\ -1 & 0 & 1 & 1 & 0 & -1 & 2 & -1 & -1 & -2 & 1 & 1 \\ 1 & 1 & 0 & -1 & -1 & 0 & -1 & 2 & -1 & 1 & -2 & 1 \\ 0 & -1 & -1 & 0 & 1 & 1 & -1 & -1 & 2 & 1 & 1 & -2 \end{pmatrix}. \quad (4.58)$$

We note that both L_1 and L_2 are symmetric. L_1 has 0 as 7-fold and -12 as 5-fold eigenvalue; L_2 has 0 as 9-fold eigenvalue and -8 as 3-fold eigenvalue. The common null space $\ker(L_1) \cap \ker(L_2)$ is spanned by $\mathbb{1}, \mathbf{v}_x, \mathbf{v}_y, \mathbf{v}_z$ defined in (4.28) which is

because of the conservation of mass and (x,y,z)-momentum. L_1 and L_2 are commutative and thus there exists an orthogonal basis v_0, \dots, v_{11} of \mathbb{R}^{12} of joint eigenvectors of L_1 and L_2 giving rise to the representations

$$L_1 = T \operatorname{diag}(-12, -12, -12, -12, -12, 0, 0, 0, 0, 0, 0, 0)T^{-1}, \quad (4.59)$$

$$L_2 = T \operatorname{diag}(0, 0, 0, 0, 0, 0, 0, 0, 0, -8, -8, -8)T^{-1}. \quad (4.60)$$

$$(4.61)$$

At first we consider the case

$$\mathbf{e} = \frac{\rho}{12}(1, 1, 1, 1, 1, 1, 1, 1, 1, 1, 1, 1)^\top \quad (4.62)$$

in which

$$D_H = D_1 = \frac{\rho}{12} I \quad \text{and} \quad D_2 = D_3 = \frac{\rho^2}{144} I = \frac{\rho}{12} D_1 \quad (4.63)$$

where I denotes the identity matrix. The linearized collision operator is thus given by

$$\begin{aligned} L_H &= \frac{1}{12}(\tilde{\gamma}_{bin}L_1 + \tilde{\gamma}_{ter}L_2) \\ &= T \operatorname{diag}(-\tilde{\gamma}_{bin}, -\tilde{\gamma}_{bin}, -\tilde{\gamma}_{bin}, -\tilde{\gamma}_{bin}, -\tilde{\gamma}_{bin}, 0, 0, 0, 0, -\tilde{\gamma}_{ter}, -\tilde{\gamma}_{ter}, -\tilde{\gamma}_{ter})T^{-1} \end{aligned} \quad (4.64)$$

with the new collision frequencies

$$\tilde{\gamma}_{bin} = \rho \gamma_{bin} \quad (4.65)$$

$$\tilde{\gamma}_{ter} = \frac{\rho^2}{12} \gamma_{ter} \quad (4.66)$$

In the second case we consider the equilibrium \mathbf{e} to be of the general form (4.48). Then we have

$$\operatorname{diag}(\kappa_{0-}, \kappa_{1-}, \kappa_{2-}, \kappa_{0+}, \kappa_{1+}, \kappa_{2+}, \kappa_{3-}, \kappa_{4-}, \kappa_{5-}, \kappa_{3+}, \kappa_{4+}, \kappa_{5+})^\top = r D_H^{-1} \quad (4.67)$$

$$\begin{aligned} D_2=D_3 &= r^2 \operatorname{diag}(\kappa_{0-}, \kappa_{1-}, \kappa_{2-}, \kappa_{0+}, \kappa_{1+}, \kappa_{2+}, \kappa_{3-}, \kappa_{4-}, \kappa_{5-}, \kappa_{3+}, \kappa_{4+}, \kappa_{5+})^\top \\ &= r D_1 = r^3 D_H^{-1} \end{aligned} \quad (4.68)$$

and thus the equation (4.51) yields

$$L_H = D_H^{-\frac{1}{2}}(\tilde{\gamma}_{bin}L_1 + \tilde{\gamma}_{ter}L_2)D_H^{-\frac{1}{2}} \quad (4.69)$$

with

$$\tilde{\gamma}_{bin} = r^2 \gamma_{bin} \quad (4.70)$$

$$\tilde{\gamma}_{ter} = r^3 \gamma_{ter} \quad (4.71)$$

Following the arguments above, $\tilde{\gamma}_{bin}L_1 + \tilde{\gamma}_{ter}L_2$ has a four-fold eigenvalue 0 and eight strictly negative eigenvalues. Thus the same is true for L_H . We collect the results.

Proposition 4.11 *Let \mathbf{e} be an equilibria of the form (4.48). Then the linearization L_H (given by (4.69)) around \mathbf{e} is a symmetric operator, it has four-fold zero eigenvalue. The null-space is*

$$N(L_H) = D_H^{\frac{1}{2}} \text{span}(\mathbb{1}, \mathbf{v}_x, \mathbf{v}_y, \mathbf{v}_z) \quad (4.72)$$

The rest eight eigenvalues are strictly negative, five of which are proportional to r^2 and the other three are proportional to r^3 .

4.3 Collision model in a bounded hexagonal grid

In this section we prove that the basic kinetic features: the conservation laws, correct number of invariants as well as correct dimension of the equilibria, the properties of linearized collision operator are satisfied for the global collision model on bounded hexagonal grid in \mathbb{R}^3 . The bounded hexagonal grid is composed of a finite number of connected basic h-cubes.

4.3.1 Regular collision model

Let \mathcal{G}_b denote the finite restrictions of the infinite grid \mathcal{G} and \mathcal{H}_b denote the set of regular h-cubes contained in \mathcal{G}_b with the assumption $\mathcal{H}_b \neq \emptyset$. Then the collision operator J_b on \mathcal{G}_b is given by the weak formulation

$$\langle \phi, J[\mathbf{f}] \rangle = \sum_{H \in \mathcal{H}_b} \gamma_H \sum_{i=0}^{11} \phi(\pi_i^H) J_b[\mathbf{f}_H]_i \quad (4.73)$$

In the sequel we denote by a *collision model* on \mathcal{G} a pair (\mathcal{H}_b, γ) , where $\mathcal{H}_b \subset \mathcal{H}$ is a bounded set of h-cubes, and $\gamma : \mathcal{H}_b \mapsto [0, \infty)$ denote the collision frequencies for all h-cubes contained in \mathcal{H}_b . \mathcal{H}_+ denotes the set of $H \in \mathcal{H}_b$ with $\gamma_H > 0$.

As an immediate generalization of the twelve-velocity model we find the following H-Theorem.

Theorem 4.12 H-Theorem: *Let $\mathbf{f}(t)$ be a solution of the kinetic equation for a collision model (\mathcal{H}_b, γ) with all components f_i are strictly positive. For the H-functional*

$$H[\mathbf{f}] := \sum_i f_i \ln(f_i), \quad (4.74)$$

$d_t H[\mathbf{f}] \leq 0$ and $d_t H[\mathbf{f}] = 0$ if and only if \mathbf{f} is an equilibrium solution.

proof: For each $H \in \mathcal{H}_b$ and for $f_i := f_{\pi_i^H}$, $i = 0, \dots, 11$ define (as in the proof of Theorem 4.6)

$$\begin{aligned}
\eta_H[\mathbf{f}] : &= f_1 f_4 \ln \left(\frac{f_0 f_3}{f_1 f_4} \right) \left(1 - \frac{f_0 f_3}{f_1 f_4} \right) \\
&+ f_2 f_5 \ln \left(\frac{f_0 f_3}{f_2 f_5} \right) \left(1 - \frac{f_0 f_3}{f_2 f_5} \right) + f_6 f_9 \ln \left(\frac{f_0 f_3}{f_6 f_9} \right) \left(1 - \frac{f_0 f_3}{f_6 f_9} \right) \\
&+ f_7 f_{10} \ln \left(\frac{f_0 f_3}{f_7 f_{10}} \right) \left(1 - \frac{f_0 f_3}{f_7 f_{10}} \right) + f_8 f_{11} \ln \left(\frac{f_0 f_3}{f_8 f_{11}} \right) \left(1 - \frac{f_0 f_3}{f_8 f_{11}} \right) \\
&+ f_2 f_5 \ln \left(\frac{f_1 f_4}{f_2 f_5} \right) \left(1 - \frac{f_1 f_4}{f_2 f_5} \right) + f_6 f_9 \ln \left(\frac{f_1 f_4}{f_6 f_9} \right) \left(1 - \frac{f_1 f_4}{f_6 f_9} \right) \\
&+ f_7 f_{10} \ln \left(\frac{f_1 f_4}{f_7 f_{10}} \right) \left(1 - \frac{f_1 f_4}{f_7 f_{10}} \right) + f_8 f_{11} \ln \left(\frac{f_1 f_4}{f_8 f_{11}} \right) \left(1 - \frac{f_1 f_4}{f_8 f_{11}} \right) \quad (4.75) \\
&+ f_6 f_9 \ln \left(\frac{f_2 f_5}{f_6 f_9} \right) \left(1 - \frac{f_2 f_5}{f_6 f_9} \right) + f_7 f_{10} \ln \left(\frac{f_2 f_5}{f_7 f_{10}} \right) \left(1 - \frac{f_2 f_5}{f_7 f_{10}} \right) \\
&+ f_8 f_{11} \ln \left(\frac{f_2 f_5}{f_8 f_{11}} \right) \left(1 - \frac{f_2 f_5}{f_8 f_{11}} \right) + f_7 f_{10} \ln \left(\frac{f_6 f_9}{f_7 f_{10}} \right) \left(1 - \frac{f_6 f_9}{f_7 f_{10}} \right) \\
&+ f_8 f_{11} \ln \left(\frac{f_6 f_9}{f_8 f_{11}} \right) \left(1 - \frac{f_6 f_9}{f_8 f_{11}} \right) + f_8 f_{11} \ln \left(\frac{f_7 f_{10}}{f_8 f_{11}} \right) \left(1 - \frac{f_7 f_{10}}{f_8 f_{11}} \right) \\
&+ f_1 f_3 f_5 \ln \left(\frac{f_0 f_2 f_4}{f_1 f_3 f_5} \right) \left(1 - \frac{f_0 f_2 f_4}{f_1 f_3 f_5} \right) + f_3 f_6 f_{10} \ln \left(\frac{f_0 f_7 f_9}{f_3 f_6 f_{10}} \right) \left(1 - \frac{f_0 f_7 f_9}{f_3 f_6 f_{10}} \right) \\
&+ f_4 f_8 f_{10} \ln \left(\frac{f_1 f_7 f_{11}}{f_4 f_8 f_{10}} \right) \left(1 - \frac{f_1 f_7 f_{11}}{f_4 f_8 f_{10}} \right) + f_5 f_8 f_9 \ln \left(\frac{f_2 f_6 f_{11}}{f_5 f_8 f_9} \right) \left(1 - \frac{f_2 f_6 f_{11}}{f_5 f_8 f_9} \right)
\end{aligned}$$

Then

$$d_t H[\mathbf{f}](t) = \sum_{H \in \mathcal{H}_b} \gamma_H \eta_H[\mathbf{f}] \leq 0. \quad (4.76)$$

since

$$\eta_H[\mathbf{f}] \leq 0 \quad (4.77)$$

An equilibrium state is achieved if and only if for all $H \in \mathcal{H}_b$ with $\gamma_H > 0$

$$\eta_H[\mathbf{f}] = 0. \quad \square \quad (4.78)$$

The last statement of the previous proof can be restated as follows.

Corollary 4.13 *A vector \mathbf{f} is an equilibrium solution if and only if for all regular h -cubes $H \in \mathcal{H}_+$, the twelve-tupel \mathbf{f}_H is an equilibrium solution of the twelve-velocity model.*

For a collision model (\mathcal{H}_b, γ) , we have the five invariants

$$\text{mass} \quad \rho = \sum f_i, \quad (4.79)$$

$$x\text{-momentum} \quad \rho \bar{v}_x = \sum v_{i,x} f_i, \quad (4.80)$$

$$y\text{-momentum} \quad \rho \bar{v}_y = \sum v_{i,y} f_i, \quad (4.81)$$

$$z\text{-momentum} \quad \rho \bar{v}_z = \sum v_{i,z} f_i, \quad (4.82)$$

$$\text{kinetic energy} \quad \frac{1}{2} |\mathbf{v}|^2 = \frac{1}{2} \sum (v_{i,x}^2 + v_{i,y}^2 + v_{i,z}^2) f_i \quad (4.83)$$

which are conserved in each collision event. Since we want to exclude artefacts we are going to introduce the notion of *regular* collision models. Our *basic model* (A model, with minimum number of h-cubes which satisfies the requirements that the five quantities: mass, (x,y,z)-momenta and kinetic energy are invariant in each collision event) for this is a 81-velocity model.

A 81-velocity model:

Definition 4.14 Following the definition of the center points given by the equation (4.14), a h-cube H^l is called as a *l-level h-cube* if the z-coordinate of the center of H^l is given by

$$c_z := l \frac{2\sqrt{6}}{3} \quad (4.84)$$

We construct a 81-velocity model, which is the composition of

1. five 0-level regular basic h-cubes H_i^0 , $i = 0, \dots, 4$, having centers

$$C^0 = \left\{ (0, 0, 0), (1, -\sqrt{3}, 0), (2, 0, 0), (1, \sqrt{3}, 0), (-1, \sqrt{3}, 0) \right\}$$

respectively (A cut along the horizontal hexagonal sections is shown in the figure 4.5),

2. two 1-level regular basic h-cubes H_i^1 , $i = 0, 1$ and one (-1) -level regular basic h-cubes H_0^{-1} with centers at

$$C^1 = \left\{ \left(1, -\frac{1}{\sqrt{3}}, \frac{2\sqrt{6}}{3} \right), \left(0, \frac{2}{\sqrt{3}}, \frac{2\sqrt{6}}{3} \right) \right\} \quad \text{and} \quad C^{-1} = \left\{ \left(1, \frac{1}{\sqrt{3}}, -\frac{2\sqrt{6}}{3} \right) \right\}$$

respectively,

3. two $(-1/2)$ -level regular basic h-cubes $H_i^{-1/2}$, $i = 0, 1$ and one $(1/2)$ -level regular basic h-cubes $H_0^{1/2}$ with their centers

$$C^{-1/2} = \left\{ \left(1, -\frac{1}{\sqrt{3}}, -\frac{\sqrt{6}}{3} \right), \left(0, \frac{2}{\sqrt{3}}, -\frac{\sqrt{6}}{3} \right) \right\} \quad \text{and} \quad C^{1/2} = \left\{ \left(1, \frac{1}{\sqrt{3}}, \frac{\sqrt{6}}{3} \right) \right\}$$

respectively,

4. In addition to these basic h-cubes of the model, we can also find some other larger class-A and class-B h-cubes. Among those we collect the two class-B h-cubes \tilde{H}_i , $i = 0, 1$ of radii $2h$ centered at the first two nodes 0,1 of H_0^0 , in Fig. 4.5, the six nodes of the hexagons restricted to the 0-level cut of these two class-B h-cubes are marked by 'o' and '*' respectively.

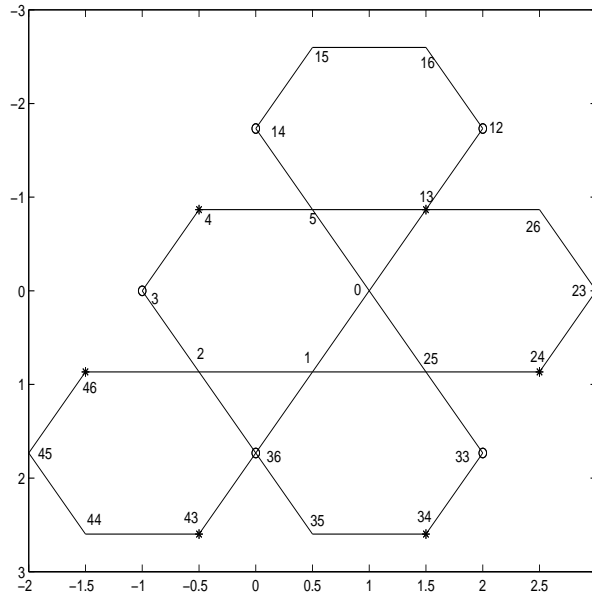


Fig. 4.5 Horizontal cut of the 0-level h-cubes of a
81-velocity model

With the enumeration as shown in Fig. 4.2 for each h-cubes of the 81-velocity model,

the list of h-cubes can be given as,

$$\begin{aligned}
H_0^0 &= (0, 1, 2, 3, 4, 5, 6, 7, 8, 9, 10, 11), \\
H_1^0 &= (12, 13, 5, 14, 15, 16, 17, 18, 19, 20, 21, 22), \\
H_2^0 &= (23, 24, 25, 0, 13, 26, 27, 28, 29, 30, 31, 32), \\
H_3^0 &= (33, 34, 35, 36, 1, 25, 37, 38, 39, 40, 41, 42), \\
H_4^0 &= (36, 43, 44, 45, 46, 2, 47, 48, 49, 50, 51, 52), \\
H_0^{\frac{1}{2}} &= (29, 37, 38, 8, 6, 28, 53, 54, 55, 1, 25, 0), \\
H_0^{-\frac{1}{2}} &= (32, 30, 10, 11, 20, 21, 13, 5, 0, 56, 57, 58), \\
H_1^{-\frac{1}{2}} &= (42, 40, 51, 52, 9, 10, 1, 2, 36, 59, 60, 61), \\
H_0^1 &= (62, 53, 54, 63, 64, 65, 66, 67, 68, 6, 28, 19), \\
H_1^1 &= (55, 69, 70, 71, 72, 54, 73, 74, 75, 47, 38, 8), \\
H_0^{-1} &= (76, 77, 60, 61, 56, 57, 30, 10, 42, 78, 79, 80), \\
\tilde{H}_0 &= (23, 33, 36, 3, 14, 12, 62, 63, 55, 61, 76, 58), \\
\tilde{H}_1 &= (24, 34, 43, 46, 4, 13, 53, 72, 69, 59, 77, 56).
\end{aligned} \tag{4.85}$$

We use this list of h-cubes (with their enumeration) to prove the properties of the model in bounded grid.

Equilibria of the 81-velocity model

Let us re-denote the above set of h-cubes of the 81-velocity model as

$$\begin{aligned}
H^{(i+1)} &:= H_i^0, \quad i = 0, \dots, 4; \quad H^{(6)} := \tilde{H}_0, \quad H^{(7)} := \tilde{H}_1, \quad H^{(8)} := H_0^{\frac{1}{2}}, \quad H^{(9)} := H_0^{-\frac{1}{2}}, \\
H^{(10)} &:= H_1^{-\frac{1}{2}}, \quad H^{(11)} := H_0^1, \quad H^{(12)} := H_1^1, \quad H^{(13)} := H_0^{-1}.
\end{aligned} \tag{4.86}$$

Following the equation (4.47), for $f \in \mathcal{E}_{81}$ we denote

$$\mathbf{f}_{H^{(k)}} := r^{(k)} \left(\kappa_{0+}^{(k)}, \kappa_{1+}^{(k)}, \kappa_{2+}^{(k)}, \kappa_{0-}^{(k)}, \kappa_{1-}^{(k)}, \kappa_{2-}^{(k)}, \kappa_{3+}^{(k)}, \kappa_{4+}^{(k)}, \kappa_{5+}^{(k)}, \kappa_{3-}^{(k)}, \kappa_{4-}^{(k)}, \kappa_{5-}^{(k)} \right), \quad k = 1, \dots, 13, \tag{4.87}$$

where $\kappa_{1+}^{(k)} = \kappa_{0+}^{(k)} \kappa_{2+}^{(k)}$, $\kappa_{4+}^{(k)} = \kappa_{0-}^{(k)} \kappa_{3+}^{(k)}$, $\kappa_{5+}^{(k)} = \kappa_{2+}^{(k)} \kappa_{3+}^{(k)}$ and $\kappa_{i-}^{(k)} = \frac{1}{\kappa_{i+}^{(k)}}$, $i = 0, \dots, 5$.

Then the equilibria $\mathbf{f} \in \mathcal{E}_{|v_z=0}$ restricted to the cut $H^{(k)}|_{v_z=0}$ (Fig. 4.5) are given by

$$\mathbf{f}_{H^{(k)}|_{v_z=0}} = r^{(k)} \left(\kappa_{0+}^{(k)}, \kappa_{1+}^{(k)}, \kappa_{2+}^{(k)}, \kappa_{0-}^{(k)}, \kappa_{1-}^{(k)}, \kappa_{2-}^{(k)} \right), \quad k = 1, \dots, 7, \tag{4.88}$$

where $\kappa_{1+}^{(k)} = \kappa_{0+}^{(k)} \kappa_{2+}^{(k)}$ and $\kappa_{i-}^{(k)} = \frac{1}{\kappa_{i+}^{(k)}}$, $i = 0, 1, 2$.

We prove following lemma as lemma-A.1 in appendix-A.

Lemma 4.15 *The equilibria $\mathbf{f} \in \mathcal{E}_{|v_z=0}$ restricted to the 0-level cut of the 81-velocity model (as given by the equation (4.88)) is a smooth four-dimensional manifold.*

We mention here that in a h-cube H (Fig. 4.2), we can find four hexagons, eight triangles and six squares.

Proposition 4.16 *Suppose $\mathbf{f} \in \mathcal{E}_H$.*

(i) *If three components of \mathbf{f} restricted to any three nodes of any one of the four hexagonal-sections of H are given together with another component of \mathbf{f} restricted to a node which does not belong to this same hexagonal-section, then the rest eight unknown components of \mathbf{f} can be uniquely determined in terms of the given four components.*

(ii) *If the three components of \mathbf{f} restricted to any one of the eight triangular-sections of H are given together with another component of \mathbf{f} restricted to a nodes of the hexagonal-section which is parallel to that triangular section, then all the rest eight unknown components of \mathbf{f} can also be uniquely determined in terms of the given four components.*

Proof: Following the equation (4.47), for $\mathbf{f} \in \mathcal{E}_H$ we have

$$\mathbf{f} = r(\kappa_{0+}, \kappa_{1+}, \kappa_{2+}, \kappa_{0-}, \kappa_{1-}, \kappa_{2-}, \kappa_{3+}, \kappa_{4+}, \kappa_{5+}, \kappa_{3-}, \kappa_{4-}, \kappa_{5-}), \quad (4.89)$$

where $\kappa_{1+} = \kappa_{0+}\kappa_{2+}$, $\kappa_{4+} = \kappa_{0-}\kappa_{3+}$, $\kappa_{5+} = \kappa_{2+}\kappa_{3+}$, $\kappa_{i-} = 1/\kappa_{i+}$, $i = 0, \dots, 5$
(i) For any three of $(f_0, f_1, f_2, f_3, f_4, f_5)$ are given, $r, \kappa_{0+}, \kappa_{2+}$ can be uniquely determined. Then for a given equilibria from any (f_6, f_7, f_8) or (f_9, f_{10}, f_{11}) , the parameter κ_{3+} can also determined. Similar arguments holds for other cases.
(ii) This is an equivalent case of (i). \square

Using the above proposition, we proved the following lemma.

Lemma 4.17 *The set \mathcal{E} of equilibria of 81-velocity model (basic model) is a smooth five dimensional manifold.*

Proof : The equilibria $\mathbf{f} \in \mathcal{E}$ is given by (4.87). In the proof of the lemma 4.15, it has been shown in appendix-A (lemma A.1) that $(r^{(k)}, \kappa_{0+}^{(k)}, \kappa_{2+}^{(k)}, k = 1, \dots, 7)$ can be uniquely parameterized by quadrupel $(\kappa_{0+}^{(1)}, \kappa_{2+}^{(1)}, r^{(1)}, r^{(2)})$ and the the equilibria $\mathbf{f}_{H^{(k)}}|_{v_z=0}$ is a smooth four-dimensional manifold. Now we investigate further for the rest $\mathbf{f} \in \mathcal{E}_{H^{(k)}}|_{v_z \neq 0}$ and we will show that, in addition to the quadrupel, it requires one more parameter ($\kappa_{3+}^{(1)}$) to describe all of $\mathbf{f} \in \mathcal{E}$. As shown in the equation (4.47), the equilibria $\mathbf{f} \in \mathcal{E}_{H^{(1)}}$ can be described by $\left\{(\kappa_{0+}^{(1)}, \kappa_{2+}^{(1)}, \kappa_{3+}^{(1)}, r^{(1)})\right\}$ where it requires an additional parameter $\kappa_{3+}^{(1)}$ with the set $\left\{(\kappa_{0+}^{(1)}, \kappa_{2+}^{(1)}, r^{(1)}, r^{(2)})\right\}$. Thus $\mathbf{f}_{H^{(k)}}|_{v_z=0} \cup \mathbf{f}_{H^{(1)}}$

can be uniquely determined by the five unknowns $\left\{(\kappa_{0+}^{(1)}, \kappa_{2+}^{(1)}, \kappa_{3+}^{(1)}, r^{(1)}, r^{(2)})\right\}$. That is, for the given values of this five parameters, $\mathbf{f}_{H^{(k)}|_{vz=0}} \cup \mathbf{f}_{H^{(1)}}$ are known quantities.

Now we will show that the rest of the components of $f \in \mathcal{E}$ can also be determined by the above five parameters only. With this end, we observe in $H^{(8)} = (29, 37, 38, 8, 6, 28, 53, 54, 55, 1, 25, 0)$ that the three component of $f \in \mathcal{E}_{H^{(8)}}$ restricted to the three nodes $(1, 25, 0)$ of a triangular-section is already obtained together with a equilibria restricted to the node (6) which belongs to the hexagonal-section parallel to the triangular-section. Thus by proposition 4.16 (ii), $\mathbf{f} \in \mathcal{E}_{H^{(8)}}$ are all obtained also in terms of the above five parameters. Then, similarly, the proposition 4.16 (ii) also holds successively for $H^{(9)}, H^{(10)}, H^{(2)}, H^{(3)}, H^{(4)}, H^{(5)}, H^{(11)}, H^{(12)}, H^{(13)}$. It is thus seen that $\mathbf{f} \in \mathcal{E}_{H^{(k)}}$, $k = 1, \dots, 13$ can be determined by five unknowns $\left\{(\kappa_{0+}^{(1)}, \kappa_{2+}^{(1)}, \kappa_{3+}^{(1)}, r^{(1)}, r^{(2)})\right\}$. \square

Thus we define the notion of *basic extension* and *regular* collision model as follows.

Definition 4.18 Let (\mathcal{H}_b, γ) and $(\mathcal{H}'_b, \gamma')$ be two collision models.

(a) $(\mathcal{H}'_b, \gamma')$ is called a *basic extension* of (\mathcal{H}_b, γ) , if there is a basic "l-level" h-cube (Definition 4.14) $H^l \notin \mathcal{H}_b$ such that

(i) the set of basic h-cubes of \mathcal{H}'_b is obtained from those of \mathcal{H}_b by adding H^l and consequently by adding either a pair $(H^{l+\frac{1}{2}}, H^{l-1})$ or $(H^{l-\frac{1}{2}}, H^{l+1})$ (or both the pairs),

(ii) two consecutive vertices of H^l are already contained in the grid generated by \mathcal{H}_b ,

(iii) $\gamma_{H_0} > 0$.

We note that such a basic-extension also provides at least one larger (of radii $2h$) h-cube \tilde{H}^l . The three nodes of the bottom-triangular (top-triangular) section and four consecutive nodes of the horizontal hexagonal-section of $H^{l+\frac{1}{2}} (H^{l-\frac{1}{2}})$ and four consecutive nodes of the horizontal hexagonal-section of \tilde{H}^l are already in \mathcal{H}_b . One of the top (bottom)-triangular node of \tilde{H}^l coincide with top (bottom)-triangular node of $H^{l+\frac{1}{2}} (H^{l-\frac{1}{2}})$.

(b) $(\mathcal{H}'_b, \gamma')$ is called a (non-trivial) extension of (\mathcal{H}_b, γ) , if for some $n \geq 1$, there exists a sequence

$$(\mathcal{H}_b, \gamma) = (\mathcal{H}_b^{(0)}, \gamma^{(0)}), (\mathcal{H}_b^{(1)}, \gamma^{(1)}), \dots, (\mathcal{H}_b^{(n)}, \gamma^{(n)}) = (\mathcal{H}'_b, \gamma') \quad (4.90)$$

such that $(\mathcal{H}_b^{(k+1)}, \gamma^{(k+1)})$ is a basic extension of $(\mathcal{H}_b^{(k)}, \gamma^{(k)})$. In this case we write

$$(\mathcal{H}_b, \gamma) < (\mathcal{H}'_b, \gamma') \quad (4.91)$$

(c) A collision model (\mathcal{H}_b, γ) is called *regular* if it is an extension of the 81-velocity model (basic model).

Proposition 4.19 *Let (\mathcal{H}_b, γ) be a regular collision model. Then*

- (i) *the set \mathcal{E} of equilibria is a smooth 5-dimensional manifold,*
- (ii) *the set of collision invariants is spanned by mass, momenta and kinetic energy.*

Proof: (i): The proof follows by induction over the number of basic extensions. The statement is true for 81-velocity model (see lemma 4.17). By induction hypothesis we assume that it also holds true for a collision model $(\mathcal{H}'_b, \gamma')$. Let (\mathcal{H}_b, γ) is obtained from $(\mathcal{H}'_b, \gamma')$ by a basic extension by adding the set of basic h-cubes $\{H^l, H^{l+\frac{1}{2}}, H^{l-1}\}$ or $\{H^l, H^{l-\frac{1}{2}}, H^{l+1}\}$ or both the sets (Definition 4.18). Let \mathcal{E}' and \mathcal{E} be the respective sets of equilibria. From our assumption \mathcal{E}' is a smooth 5-dimensional manifold, we have to prove that \mathcal{E} is also a smooth 5-dimensional manifold. To this end, we show that $\mathbf{f} \in \mathcal{E}$ can be uniquely determined if its restriction \mathbf{f}' to the smaller grid \mathcal{H}'_b is given. From corollary 4.13, $\mathbf{f} \in \mathcal{E}$ implies that $\mathbf{f}' \in \mathcal{E}'$ and \mathbf{f}_H is an equilibrium solution for $H = H^l, H^{l+\frac{1}{2}}, H^{l-1}$ or for $H = H^l, H^{l-\frac{1}{2}}, H^{l+1}$ or in both the cases. We have to show that these \mathbf{f}_H (for $H = H^l, H^{l+\frac{1}{2}}, H^{l-1}$ or for $H = H^l, H^{l-\frac{1}{2}}, H^{l+1}$ or in both the cases) can be uniquely determined in terms of the given $\mathbf{f}' \in \mathcal{E}'$.

From the definition 4.18 of basic extension

1. The three bottom-triangular(top-triangular) nodes with four consecutive horizontal hexagonal-section nodes of $H^{l+\frac{1}{2}}(H^{l-\frac{1}{2}})$ are already in \mathcal{H}'_b and thus by proposition 4.16, $\mathbf{f}_H^{l+\frac{1}{2}}(\mathbf{f}_H^{l-\frac{1}{2}})$ uniquely determined from the given $\mathbf{f}' \in \mathcal{E}'$.
2. Four consecutive hexagonal-section nodes of the larger (of radii $2h$) h-cube \tilde{H}^l are already in \mathcal{H}'_b and one of the top (bottom)-triangular node of \tilde{H}^l coincide with top (bottom)-triangular node of $H^{l+\frac{1}{2}}(H^{l-\frac{1}{2}})$; thus by proposition 4.16 (i) $\mathbf{f}_{\tilde{H}^l}$ is obtained. Then we find that equilibria at four hexagonal-section nodes (two from \mathcal{H}'_b and two via \tilde{H}^l) and two top (bottom)-section nodes (that coincides with hexagonal-section nodes of $H^{l+\frac{1}{2}}(H^{l-\frac{1}{2}})$) of H^l is known and thus by proposition 4.16 (i), \mathbf{f}_{H^l} can be uniquely determined from the given $\mathbf{f}' \in \mathcal{E}'$.
3. the three triangular-section nodes (two from \mathcal{H}'_b and one via $H^{l+\frac{1}{2}}(H^{l-\frac{1}{2}})$) and two hexagonal section nodes (via \tilde{H}^l) of $H^{l-1}(H^{l+1})$ is known and thus by proposition 4.16 (ii), $\mathbf{f}_{H^{l-1}}(\mathbf{f}_{H^{l+1}})$ can be uniquely determined from the given $\mathbf{f}' \in \mathcal{E}'$ \square .

(ii) This follows from corollary 4.23 below \square .

4.3.2 Linearizations

For a regular collision model (\mathcal{H}_b, γ) denote by

$$\mathcal{G}_b := \bigcup_{\alpha: H_\alpha \in \mathcal{H}_b} =: \{\mathbf{z}_\beta \mid \beta \in \mathbf{I}_b\}, \quad (4.92)$$

the set of all grid points related to \mathcal{H}_b , indexed by some finite set \mathbf{I}_b . We define the following elements (similar to (4.28)) of $\mathbb{R}^{\mathbf{I}_b}$,

$$\mathbb{1} := (1)_{\beta \in \mathbf{I}_b}, \quad \mathbf{v}_x := (\mathbf{z}_{\beta,x})_{\beta \in \mathbf{I}_b} \quad \mathbf{v}_y := (\mathbf{z}_{\beta,y})_{\beta \in \mathbf{I}_b} \quad \mathbf{v}_z := (\mathbf{z}_{\beta,z})_{\beta \in \mathbf{I}_b} \quad (4.93)$$

and in addition

$$\mathbf{E}_{kin} := \frac{1}{2}(|\mathbf{z}_\beta|^2)_{\beta \in \mathbf{I}_b} \quad (4.94)$$

Furthermore we define

$$E := \text{span}(\mathbb{1}, \mathbf{v}_x, \mathbf{v}_y, \mathbf{v}_z, \mathbf{E}_{kin}) \quad (4.95)$$

The restriction of the vectors (4.95) to single h-cube H in \mathcal{H}_b are marked with a lower index H and

$$E_H := \text{span}(\mathbb{1}_H, (\mathbf{v}_x)_H, (\mathbf{v}_y)_H, (\mathbf{v}_z)_H) \quad (4.96)$$

Lemma 4.20 *Let $\phi \in \mathbb{R}^{81}$ be a scalar function on the grid of 81-velocity model and $H^{(i)}, i = 1, \dots, 13$ denotes the h-cubes of the 81-velocity model given by the equation 4.86. If $\phi_{H^{(i)}} \in E_{H^{(i)}}, i = 1, \dots, 13$, then $\phi \in E$.*

Proof: Suppose $\phi \in \mathbb{R}^{81}$ such that $\phi_{H^{(i)}} \in E_{H^{(i)}}, i = 1, \dots, 13$. We construct another function $\psi \in E$ as

$$\psi = \beta_0 \mathbb{1} + \beta_1 \mathbf{v}_x + \beta_2 \mathbf{v}_y + \beta_3 \mathbf{v}_z + \beta_4 \mathbf{E}_{kin}$$

which coincides with ϕ in the nodes 0, 1, 2, 6, 25. This problem is uniquely solvable, since the restrictions of the vectors $\mathbb{1}, \mathbf{v}_x, \mathbf{v}_y, \mathbf{v}_z, \mathbf{E}_{kin}$ to these points are linearly independent. We have to show that $\psi = \phi$. Elementary calculations show that

$$(\mathbf{E}_{kin})_{H^{(i)}} \in \text{span}(\mathbb{1}, \mathbf{v}_x, \mathbf{v}_y, \mathbf{v}_z), \quad i = 1, \dots, 13.$$

We conclude that

$$\phi_{H^{(i)}} \in \text{span}(\mathbb{1}, \mathbf{v}_x, \mathbf{v}_y, \mathbf{v}_z), \quad i = 1, \dots, 13.$$

We observe that $\psi_{H^{(1)}}$ coincides with $\phi_{H^{(1)}}$ at four nodes (0, 1, 2, 6) of $H^{(1)}$. But since the restrictions to $\mathbb{1}, \mathbf{v}_x, \mathbf{v}_y, \mathbf{v}_z$ at these four points are linearly independent, therefore, $\psi_{H^{(1)}} = \phi_{H^{(1)}}$. Similar arguments holds for $H^{(i)}$ successively for $i = 8, 9, 10, 11, 12, 13, 6, 7, 2, 3, 4, 5$. Thus, $\psi_{H^{(i)}} = \phi_{H^{(i)}}$ for all i \square

We generalize this result for any regular collision model as in the following.

Lemma 4.21 *Let (\mathcal{H}_b, γ) be a regular collision model. $E := \text{span}(\mathbf{1}, \mathbf{v}_x, \mathbf{v}_y, \mathbf{v}_z, \mathbf{E}_{kin})$ and $E_H := \text{span}(\mathbf{1}_H, (\mathbf{v}_x)_H, (\mathbf{v}_y)_H, (\mathbf{v}_z)_H)$. Then $\phi \in E$ if and only if $\phi_H \in E_H$ for all $H \in \mathcal{H}_+$.*

Proof: " \implies ": Let

$$\phi = \alpha_0 \mathbf{1} + \alpha_1 \mathbf{v}_x + \alpha_2 \mathbf{v}_y + \alpha_3 \mathbf{v}_z + \alpha_4 \mathbf{E}_{kin} \quad (4.97)$$

and for $H \in \mathcal{H}_b$, we denote the center of H by $\mathbf{c}_H = (c_{H,x}, c_{H,y}, c_{H,z})$. Applying the projection operator P_H and denoting by $\mathbf{v}_{H,i} = \mathbf{c}_H + \mathbf{w}_i$, $|\mathbf{w}_i|^2 = 1$, the twelve vertices of H yields

$$\begin{aligned} P_H \mathbf{E}_{kin} &= \frac{1}{2} (v_{x,i}^2 + v_{y,i}^2 + v_{z,i}^2)_{i=0}^{12} \\ &= \frac{1}{2} (|\mathbf{w}_i|^2 + |\mathbf{c}_H|^2) \mathbf{1} + c_{H,x} (w_{x,i})_{i=0}^{12} + c_{H,y} (w_{y,i})_{i=0}^{12} + c_{H,z} (w_{z,i})_{i=0}^{12} \\ &\in \text{span}(\mathbf{1}_H, (\mathbf{v}_x)_H, (\mathbf{v}_y)_H, (\mathbf{v}_z)_H) \end{aligned} \quad (4.98)$$

and

$$\begin{aligned} P_H \phi &= P_H(\alpha_0 \mathbf{1} + \alpha_1 \mathbf{v}_x + \alpha_2 \mathbf{v}_y + \alpha_3 \mathbf{v}_z + \alpha_4 \mathbf{E}_{kin}) \\ &= \alpha_0 \mathbf{1}_H + \alpha_1 (\mathbf{v}_x)_H + \alpha_2 (\mathbf{v}_y)_H + \alpha_3 (\mathbf{v}_z)_H + \alpha_4 P_H \mathbf{E}_{kin} \\ &\in \text{span}(\mathbf{1}_H, (\mathbf{v}_x)_H, (\mathbf{v}_y)_H, (\mathbf{v}_z)_H). \end{aligned} \quad (4.99)$$

" \longleftarrow ": The proof follows by induction over the number of basic extensions. From previous lemma, the statement is true for 81-velocity model. We assume that the statement holds true for the collision model $(\mathcal{H}'_b, \gamma')$. Let us suppose that by adding a basic hexagon H^l , and consequently, either a pair $(H^{l+\frac{1}{2}}, H^{l-1})$ or $(H^{l-\frac{1}{2}}, H^{l+1})$ or both the pairs, to $(\mathcal{H}'_b, \gamma')$, we obtain collision model (\mathcal{H}_b, γ) . The extension automatically provide at least one larger (of radii $2h$) h-cube \tilde{H}^l . Let ϕ be such that

$$\phi_H \in \text{span}(\mathbf{1}_H, (\mathbf{v}_x)_H, (\mathbf{v}_y)_H, (\mathbf{v}_z)_H) \quad \text{for all } H \in \mathcal{H}_+. \quad (4.100)$$

By ϕ' we denote the restriction of ϕ onto \mathcal{H}'_b and then by induction hypothesis we obtain

$$\phi' = \alpha_0 \mathbf{1}' + \alpha_1 \mathbf{v}'_x + \alpha_2 \mathbf{v}'_y + \alpha_3 \mathbf{v}'_z + \alpha_4 \mathbf{E}'_{kin} \quad (4.101)$$

We have to prove that

$$\phi = \alpha_0 \mathbf{1} + \alpha_1 \mathbf{v}_x + \alpha_2 \mathbf{v}_y + \alpha_3 \mathbf{v}_z + \alpha_4 \mathbf{E}_{kin} \quad (4.102)$$

From the definition of basic extension it follows that three bottom-triangular (top-triangular) nodes, four consecutive hexagonal-section nodes of $H^{l+\frac{1}{2}}$ ($H^{l-\frac{1}{2}}$) and four consecutive hexagonal-section nodes of \tilde{H}^l are already in \mathcal{H}'_b . Since four nodes (three from its hexagonal section one from else) of $H^{l+\frac{1}{2}}$ ($H^{l-\frac{1}{2}}$) say, $\mathbf{z}_i, \mathbf{z}_{i+1}, \mathbf{z}_{i+2}, \mathbf{z}_{i+3}$ are already in \mathcal{H}'_b , thus,

$$\phi(\mathbf{z}_{i+j}) = \phi'(\mathbf{z}_{i+j}) = \alpha_0 + \alpha_1 \mathbf{v}_x(\mathbf{z}_{i+j}) + \alpha_2 \mathbf{v}_y(\mathbf{z}_{i+j}) + \alpha_3 \mathbf{v}_z(\mathbf{z}_{i+j}), \quad j = 0, \dots, 3 \quad (4.103)$$

Furthermore, there are quantities $\alpha_0^H, \alpha_1^H, \alpha_2^H, \alpha_3^H$ such that

$$\phi(\mathbf{z}_{i+j}) = \alpha_0^H + \alpha_1^H \mathbf{v}_x(\mathbf{z}_{i+j}) + \alpha_2^H \mathbf{v}_y(\mathbf{z}_{i+j}) + \alpha_3^H \mathbf{v}_z(\mathbf{z}_{i+j}), \quad j = 0, \dots, 3 \quad (4.104)$$

But since the restrictions to $\mathbb{1}, \mathbf{v}_x, \mathbf{v}_y, \mathbf{v}_z$ at such four nodes are linearly independent, thus

$$\alpha_i^H = \alpha_i, \quad i = 0, 1, 2, 3. \quad \square$$

Let $\mathbf{e} \in \mathcal{E}$ be an equilibrium for a regular collision model (\mathcal{H}_b, γ) . Define the diagonal matrix D as

$$D = \text{diag}(e_\beta \mid \beta \in \mathbf{I}_b) \quad (4.105)$$

Inserting the ansatz

$$\mathbf{f} = \mathbf{e} + \epsilon D^{\frac{1}{2}} \phi \quad (4.106)$$

into (4.73) and neglecting terms quadratic in ϵ yields the *linearized kinetic equation*. From corollary (4.13) we know that for any $H \in \mathcal{H}$, the restriction \mathbf{e}_H is an equilibrium solution of the twelve-velocity model on H . The restriction of the linearize operator L to H is denoted by L_H . Suppose ψ is a test function on \mathcal{G}_b . Then according to the weak formulation (4.73) of the nonlinear collision operator, the weak formulation of the full linearized operator L on (\mathcal{H}_b, γ) is

$$\langle \psi, L\phi \rangle = \sum_{H \in \mathcal{H}_b} \gamma_H \sum_{i=0}^{11} \psi(\pi_i^H) (L_H \phi_H)_i = \sum_{H \in \mathcal{H}_b} \gamma_H \langle P_H \psi, L_H P_H \phi \rangle \quad (4.107)$$

and thus

$$L = \sum_{H \in \mathcal{H}_b} \gamma_H P_H^T L_H P_H \quad (4.108)$$

where, $P_H \in \mathbb{R}^{12 \times |\mathcal{G}_b|}$ is the matrix defined by

$$(P_H)_{i,j} = \begin{cases} 1, & \text{if } i \leq 11 \text{ and } j = \pi_i^H \\ 0, & \text{else} \end{cases} \quad (4.109)$$

Theorem 4.22 *L is a symmetric operator, its null space is five-dimensional and given by*

$$N(L) = D^{-\frac{1}{2}} E = D^{\frac{1}{2}} \text{span}(\mathbb{1}, \mathbf{v}_x, \mathbf{v}_y, \mathbf{v}_z, \mathbf{E}_{kin}) \quad (4.110)$$

and all of its non-zero eigenvalues are negative.

proof: Since all L_H are symmetric and non-positive, therefore L is symmetric and non-positive. Thus the equation

$$\mathbf{x}^T L \mathbf{x} = 0 \quad (4.111)$$

is valid iff $\mathbf{x}_H^T L_H \mathbf{x}_L = 0$ for all $H \in \mathcal{H}_+$. Because of Lemma 4.21 and Proposition 4.11, this is true iff $\mathbf{x} \in D^{\frac{1}{2}} \text{span}(\mathbb{1}, \mathbf{v}_x, \mathbf{v}_y, \mathbf{v}_z, \mathbf{E}_{kin})$. \square

Corollary 4.23 *The set of collision invariants of the nonlinear Boltzmann operator is spanned by $\mathbb{1}, \mathbf{v}_x, \mathbf{v}_y, \mathbf{v}_z, \mathbf{E}_{kin}$.*

Proof: The invariance of $\mathbb{1}, \mathbf{v}_x, \mathbf{v}_y, \mathbf{v}_z, \mathbf{E}_{kin}$ follows from mass, momentum and energy conservation of the local collision event. Suppose ψ is a collision invariant, i.e.

$$\langle \psi, J[\mathbf{f}] \rangle = 0 \quad (4.112)$$

for all non-negative densities on \mathbf{f} . Choosing a small perturbation from equilibrium, $\mathbf{f} = \mathbf{e} + \epsilon\phi$, equation (4.112) yields

$$\epsilon \langle \psi, D^{\frac{1}{2}} L D^{-\frac{1}{2}} \phi \rangle + \mathcal{O}(\epsilon^2) = 0 \quad (4.113)$$

for $0 < \epsilon \leq \epsilon_0$, from which follows

$$\langle L D^{\frac{1}{2}} \psi, D^{-\frac{1}{2}} \phi \rangle = 0 \quad (4.114)$$

Since this has to hold for all ϕ , theorem (4.22) yields $\psi \in \text{span}(\mathbb{1}, \mathbf{v}_x, \mathbf{v}_y, \mathbf{v}_z, \mathbf{E}_{kin})$. \square

4.4 Layer-wise construction of symmetric model

The 81-velocity model which has been introduced in the previous section is not symmetric about the origin but useful only to prove the basic properties with minimum efforts. In order to obtain symmetry about a origin we need to extend the model always in a circular-layer-wise manner which is described in the following.

At each twelve vertices of a regular basic h-cube $H_0 = (0, 1, 2, 3, 4, 5, 6, 7, 8, 9, 10, 11)$, we attach another twelve regular basic h-cubes successively so that any two h-cubes has only one common nodes. Then we obtain a 120-velocity model, say, M^0 originated at $(0, 0, 0)$ which can be known as a *one-layer model*.

Thus a one-layer (a 120-velocity) model is a composition of thirteen regular basic h-cubes H_i , $i = 0, \dots, 12$ and the list of the centers of these regular basic h-cubes at three different levels (Definition 4.14) (1-level, 0-level, and (-1) -level) are given as follows.

$$\begin{aligned} C^0 &= \left\{ (0, 0, 0), (2, 0, 0), (1, \sqrt{3}, 0), (-1, \sqrt{3}, 0), (-2, 0, 0), (-1, -\sqrt{3}, 0), (1, -\sqrt{3}, 0) \right\} \in \text{cut-p} \\ C^1 &= \left\{ \left(1, -\frac{1}{\sqrt{3}}, \frac{2\sqrt{6}}{3}\right), \left(-1, -\frac{1}{\sqrt{3}}, \frac{2\sqrt{6}}{3}\right), \left(0, \frac{2}{\sqrt{3}}, \frac{2\sqrt{6}}{3}\right) \right\} \in \text{cut-p} \\ C^{-1} &= \left\{ \left(-1, \frac{1}{\sqrt{3}}, -\frac{2\sqrt{6}}{3}\right), \left(1, \frac{1}{\sqrt{3}}, -\frac{2\sqrt{6}}{3}\right), \left(0, -\frac{2}{\sqrt{3}}, -\frac{2\sqrt{6}}{3}\right) \right\} \in \text{cut-p} \end{aligned}$$

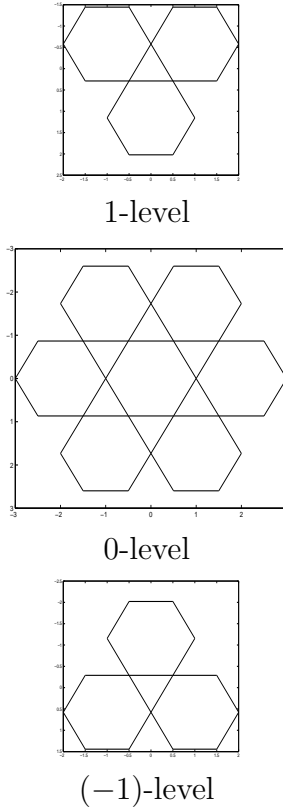


Fig. 4.6 Horizontal hexagonal cuts of the basic h-cubes of a one-layer (120-velocity) model.

These thirteen regular basic h-cubes belong to 'class-A' defined in section 1. From now we exclude the $(\pm 1/2)$ -level regular basic h-cubes from the list of basic h-cubes and we identify these regular basic h-cubes as item-1. Following the proposition 4.4, we identify the class-A and class-B h-cubes in three items where item-2 belongs to class-B and the other two items belong to class-A.

1. item-1: In this item, the list of centers of the $(\pm 1/2)$ -level regular h-cubes of radii h are given by ¹

¹Here the (x, y) -coordinates of the centers are the center points of the six triangles of the 0-level section of the Fig. 4.6 and the z -coordinates are due to the next upper q-cuts and lower p-cuts. This one-layer model also contains three other mid section (non-horizontal) as shown in the Fig. 4.7 as cut-b, cut-c, and cut-d and we can also find six similar centers for each of these three non-horizontal cuts. However, it is verified that the centers of this item-1 corresponding to the non-horizontal cuts are coincide with those belongs to $C^{\frac{1}{2}}, C^{-\frac{1}{2}}$ of the horizontal cut. Thus considering here the h-cubes only due to the horizontal cut includes all possible h-cubes of this item.

$$C^{\frac{1}{2}} = \left\{ \left(1, \frac{1}{\sqrt{3}}, \frac{\sqrt{6}}{3}\right), \left(-1, \frac{1}{\sqrt{3}}, \frac{\sqrt{6}}{3}\right), \left(0, -\frac{2}{\sqrt{3}}, \frac{\sqrt{6}}{3}\right) \right\} \in \text{cut-q}$$

$$C^{-\frac{1}{2}} = \left\{ \left(1, -\frac{1}{\sqrt{3}}, -\frac{\sqrt{6}}{3}\right), \left(-1, -\frac{1}{\sqrt{3}}, -\frac{\sqrt{6}}{3}\right), \left(0, \frac{2}{\sqrt{3}}, -\frac{\sqrt{6}}{3}\right) \right\} \in \text{cut-r}$$

2. item-2: In this item, there are twelve h-cubes \tilde{H}_i , $i = 1, \dots, 12$ of radii $2h$ with center at the twelve nodes $(0, 1, 2, 3, 4, 5, 6, 7, 8, 9, 10, 11)$ of the central regular basic h-cube H_0 .
3. item-3: There is a h-cube of radius $3h$ with center at the center of the central regular basic h-cube H_0 .

The co-ordinates of the twelve nodes of the regular h-cubes of these three items can be obtained by using the formula given by equation (4.17).

Now for further extension of this 120-velocity model M^0 , we add twelve further 120-velocity model M^j , $j = 1, \dots, 12$ with origin at the centers of the twelve exterior basic h-cubes of M^0 , then the composition of thirteen 120-velocity model,

$$\overline{M} = \bigcup_{j,H} M^j, \quad j = 0, \dots, 12 \quad (4.115)$$

can be called a *two-layer model* and so on. In the two-layer model, in addition to the basic h-cubes, we have to collect the h-cubes of all the three items mention above for each 120-model M^j , $j = 0, \dots, 12$ and the further large h-cubes of these three items of radii $2h, 4h, 5h$ respectively.

4.4.1 The 120-velocity model

Fig. 4.6 shows the mid horizontal cuts of the basic h-cubes of a 120-velocity model. The list of all 32 regular h-cubes of the 120-velocity model is given in the appendix-B and are denoted by $H^{(i)}$, $i = 0, \dots, 31$.

Theorem 4.24 *The 120-velocity model is a regular collision model. In particular, the space of collision invariants is spanned by mass, momenta and kinetic energy.*

Proof: The 120-velocity model is obtained by subsequent basic extension of 81-velocity model \square

In order to describe equilibria for the 120-velocity model, we present the four cuts of the 120 velocity model, along the hexagonal-sections $(0,1,2,3,4,5)$, $(0,10,9,3,7,6)$,

(1,10,11,4,7,8) and (6,5,11,9,2,8) of the central basic h-cubes $H^{(0)}$, as in the Fig. 4.7. We call these cuts as 'Cut-a', 'Cut-b', 'Cut-c' and 'Cut-d' respectively. Each four cuts contains 30-nodes but some of which are common. The 24 nodes of radii $\sqrt{5}$ which do not belong to the cuts are (19,22,27,30,38,41,49,52,57,60,67,70,73,76,82,85,89,92,97,100, 107,109,113,114).

The statement of Theorem 4.25 describing the equilibria for a 120-velocity model is easily readable if we go through the four cuts of the Fig. 4.7. e.g. In cut-a, the node 15 lies in the direction in between the nodes 0, 5 for which the bulk-velocity parameters are κ_{0+}, κ_{2-} respectively. Then the bulk velocity parameter for the node 15 reads as the product $\kappa_{0+}\kappa_{2-}$ and for the node 16 the bulk-velocity parameter obtained by multiplying further with κ_{0+} and reads as $\kappa_{0+}^2\kappa_{2-}$ and so on. The kinetic energy parameter μ is also easily readable due to the corollary 4.26.

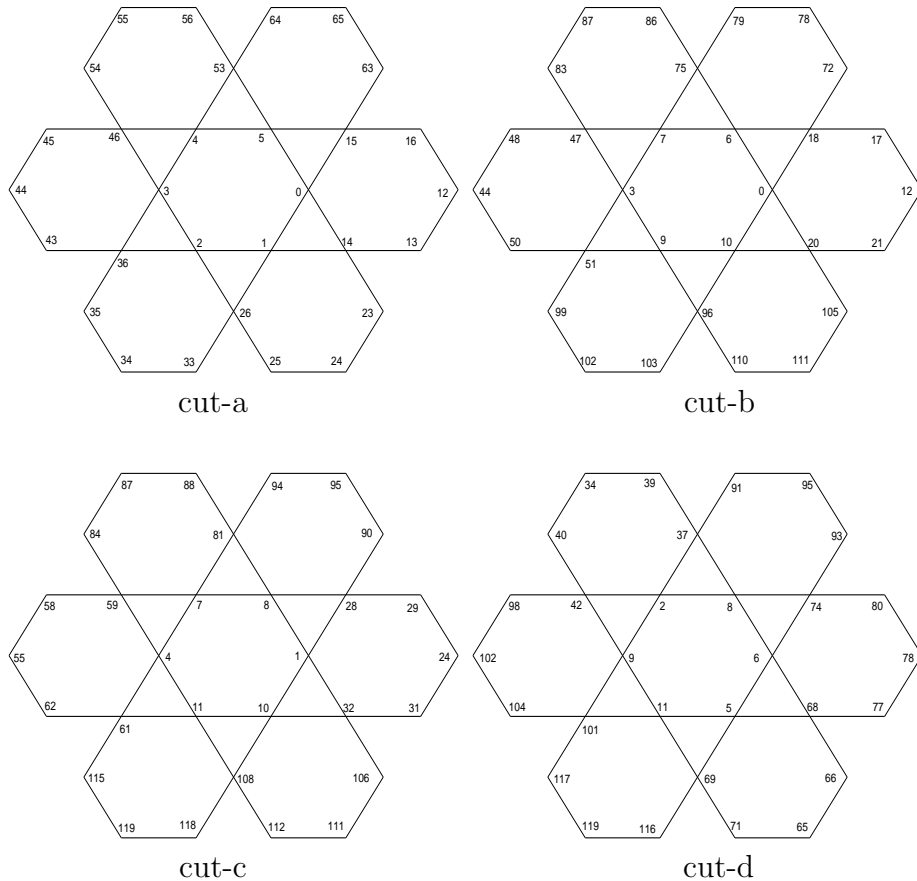


Fig. 4.7 Four cuts of the 120-velocity model

Theorem 4.25 Suppose $\mathbf{f} \in \mathcal{E}_{120}$ and

$$(f_0, f_1, f_2, f_3, f_4, f_5, f_6, f_7, f_8, f_9, f_{10}, f_{11})^\top = z(\kappa_{0+}, \kappa_{1+}, \kappa_{2+}, \kappa_{0-}, \kappa_{1-}, \kappa_{2-}, \kappa_{3+}, \kappa_{4+}, \kappa_{5+}, \kappa_{3-}, \kappa_{4-}, \kappa_{5-})^\top \quad (4.116)$$

with $z, \kappa_{0+}, \kappa_{2+}, \kappa_{3+} > 0$ arbitrary quantities satisfying $\kappa_{1+} = \kappa_{0+}\kappa_{2+}$, $\kappa_{4+} = \kappa_{0-}\kappa_{3+}$, $\kappa_{5+} = \kappa_{2+}\kappa_{3+}$. Then the equilibria of the 120-velocity model is given as follows.

(a) At the nodes of the 'cut-a', the equilibria at (53, 15, 14, 26, 36, 46) of radius $\sqrt{3}$ are given as

$$(f_{53}, f_{15}, f_{14}, f_{26}, f_{36}, f_{46})^\top = z\mu(\kappa_{1-}\kappa_{2-}, \kappa_{2-}\kappa_{0+}, \kappa_{0+}\kappa_{1+}, \kappa_{1+}\kappa_{2+}, \kappa_{2+}\kappa_{0-}, \kappa_{0-}\kappa_{1-})^\top, \quad (4.117)$$

at the next outer nodes of radius $\sqrt{7}$ the equilibria are

$$\begin{aligned} (f_{63}, f_{16})^\top &= z\mu^3\kappa_{2-}\kappa_{0+}(\kappa_{2-}, \kappa_{0+})^\top, & (f_{13}, f_{23})^\top &= z\mu^3\kappa_{0+}\kappa_{1+}(\kappa_{0+}, \kappa_{1+})^\top, \\ (f_{25}, f_{33})^\top &= z\mu^3\kappa_{1+}\kappa_{2+}(\kappa_{1+}, \kappa_{2+})^\top, & (f_{35}, f_{43})^\top &= z\mu^3\kappa_{2+}\kappa_{0-}(\kappa_{2+}, \kappa_{0-})^\top, \\ (f_{45}, f_{54})^\top &= z\mu^3\kappa_{0-}\kappa_{1-}(\kappa_{0-}, \kappa_{1-})^\top, & (f_{56}, f_{64})^\top &= z\mu^3\kappa_{1-}\kappa_{2-}(\kappa_{1-}, \kappa_{2-})^\top, \end{aligned} \quad (4.118)$$

and at the extreme outer nodes they are

$$(f_{12}, f_{24}, f_{34}, f_{44}, f_{55}, f_{65})^\top = z\mu^4(\kappa_{0+}^3, \kappa_{1+}^3, \kappa_{2+}^3, \kappa_{0-}^3, \kappa_{1-}^3, \kappa_{2-}^3)^\top. \quad (4.119)$$

(b) At the nodes of the 'cut-b', the equilibria at (18, 20, 96, 51, 47, 75) of radius $\sqrt{3}$ are given as

$$(f_{18}, f_{20}, f_{96}, f_{51}, f_{47}, f_{75})^\top = z\mu(\kappa_{3+}\kappa_{0+}, \kappa_{0+}\kappa_{4-}, \kappa_{4-}\kappa_{3-}, \kappa_{3-}\kappa_{0-}, \kappa_{0-}\kappa_{4+}, \kappa_{4+}\kappa_{3+})^\top, \quad (4.120)$$

at the next outer nodes of radius $\sqrt{7}$ the equilibria are

$$\begin{aligned} (f_{72}, f_{17})^\top &= z\mu^3\kappa_{3+}\kappa_{0+}(\kappa_{3+}, \kappa_{0+})^\top, & (f_{21}, f_{105})^\top &= z\mu^3\kappa_{0+}\kappa_{4-}(\kappa_{0+}, \kappa_{4-})^\top, \\ (f_{110}, f_{103})^\top &= z\mu^3\kappa_{4-}\kappa_{3-}(\kappa_{4-}, \kappa_{3-})^\top, & (f_{99}, f_{50})^\top &= z\mu^3\kappa_{3-}\kappa_{0-}(\kappa_{3-}, \kappa_{0-})^\top, \\ (f_{48}, f_{83})^\top &= z\mu^3\kappa_{0-}\kappa_{4+}(\kappa_{0-}, \kappa_{4+})^\top, & (f_{86}, f_{79})^\top &= z\mu^3\kappa_{4+}\kappa_{3+}(\kappa_{4+}, \kappa_{3+})^\top, \end{aligned} \quad (4.121)$$

and at the extreme outer nodes they are

$$(f_{12}, f_{111}, f_{102}, f_{44}, f_{87}, f_{78})^\top = z\mu^4(\kappa_{0+}^3, \kappa_{4-}^3, \kappa_{3-}^3, \kappa_{0-}^3, \kappa_{4+}^3, \kappa_{3+}^3)^\top. \quad (4.122)$$

(c) At the nodes of the 'cut-c', the equilibria at (28, 32, 108, 61, 59, 81) of radius $\sqrt{3}$ are given as

$$(f_{28}, f_{32}, f_{108}, f_{61}, f_{59}, f_{81})^\top = z\mu(\kappa_{5+}\kappa_{1+}, \kappa_{1+}\kappa_{4-}, \kappa_{4-}\kappa_{5-}, \kappa_{5-}\kappa_{1-}, \kappa_{1-}\kappa_{4+}, \kappa_{4+}\kappa_{5+})^\top, \quad (4.123)$$

at the next outer nodes of radius $\sqrt{7}$ the equilibria are

$$\begin{aligned} (f_{90}, f_{29})^\top &= z\mu^3\kappa_{5+}\kappa_{1+}(\kappa_{5+}, \kappa_{1+})^\top, & (f_{31}, f_{106})^\top &= z\mu^3\kappa_{1+}\kappa_{4-}(\kappa_{1+}, \kappa_{4-})^\top, \\ (f_{112}, f_{118})^\top &= z\mu^3\kappa_{4-}\kappa_{5-}(\kappa_{4-}, \kappa_{5-})^\top, & (f_{115}, f_{62})^\top &= z\mu^3\kappa_{5-}\kappa_{1-}(\kappa_{5-}, \kappa_{1-})^\top, \\ (f_{58}, f_{84})^\top &= z\mu^3\kappa_{1-}\kappa_{4+}(\kappa_{1-}, \kappa_{4+})^\top, & (f_{88}, f_{94})^\top &= z\mu^3\kappa_{4+}\kappa_{5+}(\kappa_{4+}, \kappa_{5+})^\top, \end{aligned} \quad (4.124)$$

and at the extreme outer nodes they are

$$(f_{24}, f_{111}, f_{119}, f_{55}, f_{87}, f_{95})^\top = z\mu^4(\kappa_{1+}^3, \kappa_{4-}^3, \kappa_{5-}^3, \kappa_{1-}^3, \kappa_{4+}^3, \kappa_{5+}^3)^\top. \quad (4.125)$$

(d) At the nodes of the 'cut-d', the equilibria at (74, 68, 69, 101, 42, 37) of radius $\sqrt{3}$ are given as

$$(f_{74}, f_{68}, f_{69}, f_{101}, f_{42}, f_{37})^\top = z\mu(\kappa_{5+}\kappa_{3+}, \kappa_{3+}\kappa_{2-}, \kappa_{2-}\kappa_{5-}, \kappa_{5-}\kappa_{3-}, \kappa_{3-}\kappa_{2+}, \kappa_{2+}\kappa_{5+})^\top \quad (4.126)$$

at the next outer nodes of radius $\sqrt{7}$ the equilibria are

$$\begin{aligned} (f_{93}, f_{80})^\top &= z\mu^3\kappa_{5+}\kappa_{3+}(\kappa_{5+}, \kappa_{3+})^\top, & (f_{77}, f_{66})^\top &= z\mu^3\kappa_{3+}\kappa_{2-}(\kappa_{3+}, \kappa_{2-})^\top, \\ (f_{71}, f_{116})^\top &= z\mu^3\kappa_{2-}\kappa_{5-}(\kappa_{2-}, \kappa_{5-})^\top, & (f_{117}, f_{104})^\top &= z\mu^3\kappa_{5-}\kappa_{3-}(\kappa_{5-}, \kappa_{3-})^\top, \\ (f_{98}, f_{40})^\top &= z\mu^3\kappa_{3-}\kappa_{2+}(\kappa_{3-}, \kappa_{2+})^\top, & (f_{39}, f_{91})^\top &= z\mu^3\kappa_{2+}\kappa_{5+}(\kappa_{2+}, \kappa_{5+})^\top, \end{aligned} \quad (4.127)$$

and at the extreme outer nodes they are

$$(f_{78}, f_{65}, f_{119}, f_{102}, f_{34}, f_{95})^\top = z\mu^4(\kappa_{3+}^3, \kappa_{2-}^3, \kappa_{5-}^3, \kappa_{3-}^3, \kappa_{2+}^3, \kappa_{5+}^3)^\top. \quad (4.128)$$

Finally the equilibria at the nodes at a distance $\sqrt{5}$ (which do not belongs to the four cuts) are given as

$$\begin{aligned} (f_{19}, f_{22}, f_{27}, f_{30}, f_{38}, f_{41}, f_{49}, f_{52}, f_{57}, f_{60}, f_{67}, f_{70}, f_{73}, f_{76}, f_{82}, f_{85}, f_{89}, f_{92}, f_{97}, f_{100}, f_{107}, f_{109}, f_{113}, f_{114})^\top \\ = z\mu^2(\kappa_{0+}^2\kappa_{5+}, \kappa_{0+}^2\kappa_{5-}, \kappa_{1+}^2\kappa_{3+}, \kappa_{1+}^2\kappa_{3-}, \kappa_{2+}^2\kappa_{4+}, \kappa_{2+}^2\kappa_{4-}, \kappa_{0-}^2\kappa_{5+}, \kappa_{0-}^2\kappa_{5-}, \\ \kappa_{1-}^2\kappa_{3+}, \kappa_{1-}^2\kappa_{3-}, \kappa_{2-}^2\kappa_{4+}, \kappa_{2-}^2\kappa_{4-}, \kappa_{3+}^2\kappa_{1+}, \kappa_{3+}^2\kappa_{1-}, \kappa_{4+}^2\kappa_{2+}, \kappa_{4+}^2\kappa_{2-}, \\ \kappa_{5+}^2\kappa_{0+}, \kappa_{5+}^2\kappa_{0-}, \kappa_{3-}^2\kappa_{1+}, \kappa_{3-}^2\kappa_{1-}, \kappa_{4-}^2\kappa_{2+}, \kappa_{4-}^2\kappa_{2-}, \kappa_{5-}^2\kappa_{0+}, \kappa_{5-}^2\kappa_{0-})^\top. \end{aligned} \quad (4.129)$$

Proof: By using the list of all h-cubes $H^{(i)}$, $i = 0, \dots, 31$ of the 120-velocity model as given in appendix B, the statement of the theorem can be verified as follows.

(a) In the proof of Lemma A.1, denoting

$$(\kappa_{0+}^{(1)}, \kappa_{1+}^{(1)}, \kappa_{2+}^{(1)}, \kappa_{0-}^{(1)}, \kappa_{1-}^{(1)}, \kappa_{2-}^{(1)}) = (\kappa_{0+}, \kappa_{1+}, \kappa_{2+}, \kappa_{0-}, \kappa_{1-}, \kappa_{2-}),$$

$r^{(1)} := z$ and $r^{(2)} := \mu^2 z \kappa_{2-}^{(1)2}$, the 23 components of equilibria

$f_0, f_1, f_2, f_3, f_4, f_5, f_{63}, f_{15}, f_{53}, f_{64}, f_{65}, f_{12}, f_{13}, f_{14}, f_{16}, f_{23}, f_{24}, f_{25}, f_{26}, f_{33}, f_{34}, f_{35}, f_{36}$ (which are the components restricted to the corresponding cut of the 81-velocity (basic) model) are obtained as stated in the theorem. Using the formula (4.45-a) of lemma 4.8 for $H^{(15)}$, we have

$$\frac{f_{46}f_{14}}{f_5} = \frac{f_{25}f_5}{f_{14}},$$

which yields

$$f_{46} = z\mu\kappa_{0-}\kappa_{1-}.$$

Now we see that three equilibria from each hexagons (3, 36, 43, 44, 45, 46) and (53, 4, 46, 54, 55, 56) are already obtained. Therefore again using the formula (4.45-a),

$$\frac{\pi_0\pi_2}{\pi_1} = \frac{\pi_1\pi_3}{\pi_2} = \frac{\pi_2\pi_4}{\pi_3} = \frac{\pi_3\pi_5}{\pi_4} = \frac{\pi_4\pi_0}{\pi_5} = \frac{\pi_5\pi_1}{\pi_0},$$

we obtained the equilibria at the rest nodes (43, 44, 45, 54, 55, 56) as stated in the theorem.

(b), (c), (d) and rest: To determine these, first we denote the equilibria of $H^{(25)} = (19, 27, 28, 8, 6, 18, 73, 74, 89, 1, 14, 0)$ by

$$\mathbf{f}_{H^{(25)}} := r \left(a_0, a_0 a_2, a_2, \frac{1}{a_0}, \frac{1}{a_0 a_2}, \frac{1}{a_2}, a_3, \frac{a_3}{a_0}, a_2 a_3, \frac{1}{a_3}, \frac{a_0}{a_3}, \frac{1}{a_2 a_3} \right). \quad (4.131)$$

The equilibria at (1,14,0,6) are already known as

$$\begin{aligned} \frac{r}{a_3} &= z\kappa_{1+}, \\ \frac{ra_0}{a_3} &= z\mu\kappa_{0+}\kappa_{1+}, \\ \frac{r}{a_2 a_3} &= z\kappa_{0+}, \\ \frac{r}{a_0 a_2} &= z\kappa_{3+}. \end{aligned}$$

Solving the above four equations for the unknowns (r, a_0, a_2, a_3) we obtained the equilibria $\mathbf{f}_{H^{(25)}}$. Similarly we obtained $\mathbf{f}_{H^{(i)}}$ successively for $i = 26, 27, 1, \dots, 9, 28, 29, 30, 10, 11, 12$ as stated in the theorem. \square

In the statement of the above theorem, z parameterize the density, $\lambda_i = \ln(\kappa_i)$, $i = 0, \dots, 3$ denote the eccentricities and are responsible for non-vanishing bulk velocity, μ parameterize kinetic energy.

Corollary 4.26 *Let $\mathbf{f} \in \mathcal{E}$ be the equilibria of a 120-velocity model. If we denote the i -th component equilibria as $f_i := z\mu^m \kappa$, and the corresponding radius $r_i := \sqrt{2n+1}$ where $r_i^2 = v_{x,i}^2 + v_{y,i}^2 + v_{z,i}^2$, then $m = n$.*

proof: The proof follows from the theorem 4.25. ²

4.5 Model based on only binary collision law

In this section we **exclude the ternary collision law** from the local collision operator defined by the equation (4.37) and establish that a 216-velocity model, **based on only binary collision law**, is a basic regular collision model which satisfies the basic requirements of the kinetic theory. We also prove that the basic kinetic features: the conservation laws, the correct number of invariants as well as the correct dimension of the equilibria, the properties of linearized collision operator

²The equilibria stated by the theorem 4.25 as well as by the corollary 4.26 can be (and has been) used as a basis to determined the equilibria for the larger grid model.

are satisfied for a regular collision model, based on only binary collision law, in a bounded hexagonal grid in \mathbb{R}^3 .

As we have already described in the previous section, a further extension of a 120-velocity model can be obtained by composing further 120-velocity models with centers at the center of the twelve exterior h-cubes successively. In this manner, the composition of two 120-velocity model is a 177-velocity model, the composition of three 120-velocity model is a 216-velocity model, and then 255-velocity model, \dots , composition of thirteen 120-velocity model is a 444-velocity model (a two-layer model). We now denote the 120-velocity models by M and the set of all such ordered 120-velocity model by \mathcal{M} .

In absence of ternary collision law, the local collision operator defined by equation 4.37 reduces to

$$J_H[\mathbf{f}] = \gamma_{bin} J_{bin}[\mathbf{f}], \quad \gamma_{bin} > 0, \quad (4.132)$$

and with this the space homogeneous Boltzmann equation on H is

$$\partial_t \mathbf{f} = J_H[\mathbf{f}] \quad (4.133)$$

The global collision operator is defined by the corresponding weak formulation given by the equation (4.24).

4.5.1 H-Theorem, Equilibrium solutions

Following the theorems 4.6 and 4.12, the H-Theorem for this case is the immediate consequences of dropping out the ternary collision terms. Then from the H-Theorem we have the following properties.

Proposition 4.27 $\mathbf{f} \in \mathcal{E}$ is a equilibria if and only if

$$f_{\pi_0^H} f_{\pi_3^H} = f_{\pi_1^H} f_{\pi_4^H} = f_{\pi_2^H} f_{\pi_5^H} = f_{\pi_6^H} f_{\pi_9^H} = f_{\pi_7^H} f_{\pi_{10}^H} = f_{\pi_8^H} f_{\pi_{11}^H} \quad (4.134)$$

for all $H \in \mathcal{H}_+$.

Corollary 4.28 A vector $\mathbf{f} \in \mathcal{E}$ is an equilibrium solution if and only if for all $M \in \mathcal{M}$ the 120-tupel \mathbf{f}_M is an equilibrium solution of the 120-velocity model.

In appendix-B , the propositions B.1, B.2, B.3 state the following properties of equilibria.

Proposition 4.29 The equilibria $\mathbf{f} \in \mathcal{E}_{|M^0}$ of a 120-velocity model is an 11-dimensional manifold.

Proposition 4.30 The equilibria $\mathbf{f} \in \mathcal{E}_{|M^0 \cup M^1}$ of a 177-velocity model is a 7-dimensional manifold.

Proposition 4.31 *The equilibria $\mathbf{f} \in \mathcal{E}_{|M^0 \cup M^1 \cup M^2}$ of a 216-velocity model is a 5-dimensional manifold.*

Remark 4.32 (i) In the proof of the proposition 4.31 in appendix-B, we have shown that the equilibria $\mathbf{f} \in \mathcal{E}_{|M^0 \cup M^1 \cup M^2}$ of a 216-velocity model can be uniquely parameterized by the 5 parameters a_0, a_1, a_2, a_4, b_0 . Making all the subsequent substitutions in the propositions 4.29, 4.30, 4.31 and re-denoting

$$a_0 := z\kappa_{0+}, \quad a_1 := z\kappa_{0-}, \quad a_2 := z\kappa_{1+}, \quad a_4 := z\kappa_{3+}, \quad b_0 := z\mu^4\kappa_{0+}^3,$$

we obtain the equilibria $\mathbf{f} \in \mathcal{E}_{120}$ as stated in theorem 4.25 (in the model which includes the ternary collision law) and the equilibria $\mathbf{f} \in \mathcal{E}_{216}$ is also characterized by the parameters $z, \mu, \kappa_{0+}, \kappa_{1+}, \kappa_{2+}, \kappa_{3+}, \kappa_{4+}, \kappa_{5+}$ with $z, \mu, \kappa_{0+}, \kappa_{2+}, \kappa_{3+} > 0$ arbitrary quantities satisfying $\kappa_{1+} = \kappa_{0+}\kappa_{2+}$, $\kappa_{4+} = \kappa_{0-}\kappa_{3+}$, $\kappa_{5+} = \kappa_{2+}\kappa_{3+}$ where z characterizes density, μ characterizes kinetic energy and $\kappa_{0+}, \kappa_{2+}, \kappa_{3+}$ are responsible for non-vanishing moments.

(ii) We find that the corollary 4.26 also holds true for the equilibria $\mathbf{f} \in \mathcal{E}_{216}$.

4.5.2 Regular collision model

In the case of the **model based on only binary collision law**, we are going to define the notion of regular collision model and our basic model (a model with minimum number of nodes which satisfy the physical requirements that the five quantities, mass, (x,y,z)-momenta and kinetic energy are invariants) for this is 216-velocity model, $\widetilde{M} := M^0 \cup M^1 \cup M^2$ ($M^j \in \mathcal{M}$, $j = 0, 1, 2$). Fig. 4.8 shows the mid horizontal section of all the basic h-cubes of the 216-velocity model \widetilde{M} arranged in three levels.

Remark 4.33 In the proof of the proposition B.3 in appendix-B, the five parameters a_0, a_1, a_2, a_4, b_0 describing the equilibria of 216-velocity model, are corresponding to the nodes (0, 1, 3, 6, 12) which belong to the first two h-cubes H^0, H^1 only. Therefore, if the equilibria restricted to the nodes (0, 1, 3, 6, 12) of a 216-velocity model are given, then the rest components of the equilibria can be uniquely determined.

Thus we define the notion of the *basic extension* as well as the *regular collision model* as in Definition 4.34.

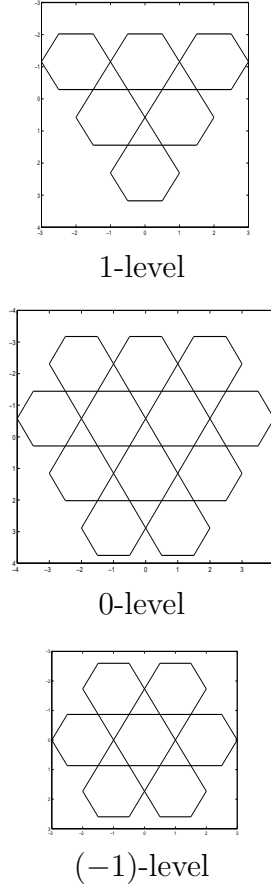


Fig. 4.8 Horizontal hexagonal cuts of the basic h-cubes of a 216-velocity model

Definition 4.34 Let (\mathcal{H}_b, γ) and $(\mathcal{H}'_b, \gamma')$ be two collision models.

(a) $(\mathcal{H}'_b, \gamma')$ is called a **basic extension** of (\mathcal{H}_b, γ) , if there are some regular basic h-cubes $H' \notin \mathcal{H}_b$ such that

- (i) the set of basic h-cubes of \mathcal{H}'_b is obtained from those of \mathcal{H}_b by adding the H' 's,
- (ii) the new h-cubes H' belong to a new 216-velocity model \widetilde{M}' (as constructed in Fig. 4.8) so that the first two h-cubes H'^0, H'^1 of \widetilde{M}' are already contained in the grid generated by \mathcal{H}_b ,
- (iii) $\gamma_{H'} > 0$.

(b) $(\mathcal{H}'_b, \gamma')$ is called a (non-trivial) extension of (\mathcal{H}_b, γ) , if for some $n \geq 1$ there exists a sequence

$$(\mathcal{H}_b, \gamma) = (\mathcal{H}_b^{(0)}, \gamma^{(0)}), (\mathcal{H}_b^{(1)}, \gamma^{(1)}), \dots, (\mathcal{H}_b^{(n)}, \gamma^{(n)}) = (\mathcal{H}'_b, \gamma') \quad (4.135)$$

such that $(\mathcal{H}_b^{(k+1)}, \gamma^{(k+1)})$ is a basic extension of $(\mathcal{H}_b^{(k)}, \gamma^{(k)})$. In this case we write

$$(\mathcal{H}_b, \gamma) < (\mathcal{H}'_b, \gamma') \quad (4.136)$$

(c) A collision model (\mathcal{H}_b, γ) is called *regular* if it is an extension of the 216-velocity model (the basic model, Fig. 4.8).

Corollary 4.35 below follows from the H-Theorem.

Corollary 4.35 *A vector $\mathbf{f} \in \mathcal{E}_{\mathcal{H}_b}$ is an equilibrium solution for a regular collision model (\mathcal{H}_b, γ) if and only if $\mathbf{f}_{\widetilde{M}}$ is an equilibrium solution for all 216-velocity model \widetilde{M} contained in \mathcal{H}_b .*

Proposition 4.36 *Let (\mathcal{H}'_b, γ) be a regular collision model. Then the set \mathcal{E} of equilibria is a smooth 5-dimensional manifold.*

proof: The statement is true for a 216-velocity model (see prop. 4.31). We assume that it holds true for a regular collision model (\mathcal{H}_b, γ) and (\mathcal{H}'_b, γ) is a basic extension of (\mathcal{H}_b, γ) by adding a 216-velocity model \widetilde{M}' . Let \mathcal{E}' and \mathcal{E} be the respective sets of equilibria. From our assumption \mathcal{E} is a smooth 5-dimensional manifold, we have to prove that \mathcal{E}' is also a smooth 5-dimensional manifold. To this end, we show that $\mathbf{f}' \in \mathcal{E}'$ is uniquely determined if its restriction \mathbf{f} to the smaller grid \mathcal{H}_b is given. From corollary 4.35, $\mathbf{f}' \in \mathcal{E}'$ implies that $\mathbf{f} \in \mathcal{E}$ and $\mathbf{f}'_{\widetilde{M}'}$ is an equilibrium in \widetilde{M}' . From the definition 4.34 of basic extension, the first two h-cubes of \widetilde{M}' are already in the grid \mathcal{H}_b and therefore, by remark 4.33 the equilibria $\mathbf{f}'_{\widetilde{M}'}$ can be uniquely determined by the equilibria at the five nodes $(0, 1, 3, 6, 12)_{\widetilde{M}'}$ which are already known from $\mathbf{f} \in \mathcal{E}$. \square

Lemma 4.37 *Let (\mathcal{H}_b, γ) be a regular collision model and $\phi \in \mathbb{R}^{|\mathcal{H}_b|}$ be a scalar function on the grid \mathcal{H}_b . Denote $E := \text{span}(\mathbf{1}, \mathbf{v}_x, \mathbf{v}_y, \mathbf{v}_z, \mathbf{E}_{kin})$ and $E_{\widetilde{M}} := \text{span}(\mathbf{1}_{\widetilde{M}}, (\mathbf{v}_x)_{\widetilde{M}}, (\mathbf{v}_y)_{\widetilde{M}}, (\mathbf{v}_z)_{\widetilde{M}}, (\mathbf{E}_{kin})_{\widetilde{M}})$. Then $\phi \in E$ if and only if $\phi_{\widetilde{M}} \in E_{\widetilde{M}}$ for all $\widetilde{M} \in \mathcal{H}_b$.*

proof: " \implies ": Let

$$\phi = \alpha_0 \mathbf{1} + \alpha_1 \mathbf{v}_x + \alpha_2 \mathbf{v}_y + \alpha_3 \mathbf{v}_z + \alpha_4 \mathbf{E}_{kin} \quad (4.137)$$

Applying the projection operator $P_{\widetilde{M}}$

$$\begin{aligned} \phi_{\widetilde{M}} = P_{\widetilde{M}} \phi &= P_{\widetilde{M}}(\alpha_0 \mathbf{1} + \alpha_1 \mathbf{v}_x + \alpha_2 \mathbf{v}_y + \alpha_3 \mathbf{v}_z + \alpha_4 \mathbf{E}_{kin}) \\ &= \alpha_0 \mathbf{1}_{\widetilde{M}} + \alpha_1 (\mathbf{v}_x)_{\widetilde{M}} + \alpha_2 (\mathbf{v}_y)_{\widetilde{M}} + \alpha_3 (\mathbf{v}_z)_{\widetilde{M}} + \alpha_4 (\mathbf{E}_{kin})_{\widetilde{M}} \\ &\in \text{span}(\mathbf{1}_{\widetilde{M}}, (\mathbf{v}_x)_{\widetilde{M}}, (\mathbf{v}_y)_{\widetilde{M}}, (\mathbf{v}_z)_{\widetilde{M}}, (\mathbf{E}_{kin})_{\widetilde{M}}). \end{aligned} \quad (4.138)$$

" \impliedby ": The proof follows by induction over the number of basic extensions. We assume that the statement holds true for the collision model $(\mathcal{H}'_b, \gamma')$. Let us suppose that by adding a 216-velocity model \widetilde{M}' , we obtain collision model (\mathcal{H}_b, γ) . Let ϕ be such that

$$\phi_{\widetilde{M}} \in \text{span}(\mathbf{1}_{\widetilde{M}}, (\mathbf{v}_x)_{\widetilde{M}}, (\mathbf{v}_y)_{\widetilde{M}}, (\mathbf{v}_z)_{\widetilde{M}}, (\mathbf{E}_{kin})_{\widetilde{M}}) \quad \text{for all } \widetilde{M} \in \mathcal{H}_b. \quad (4.139)$$

By ϕ' we denote the restriction of ϕ onto \mathcal{H}'_b and then by induction hypothesis we obtain

$$\phi' = \alpha_0 \mathbb{1}' + \alpha_1 \mathbf{v}'_x + \alpha_2 \mathbf{v}'_y + \alpha_3 \mathbf{v}'_z + \alpha_4 \mathbf{E}'_{kin} \quad (4.140)$$

We have to prove that

$$\phi = \alpha_0 \mathbb{1} + \alpha_1 \mathbf{v}_x + \alpha_2 \mathbf{v}_y + \alpha_3 \mathbf{v}_z + \alpha_4 \mathbf{E}_{kin} \quad (4.141)$$

Suppose

$$\phi := \beta_0 \mathbb{1} + \beta_1 \mathbf{v}_x + \beta_2 \mathbf{v}_y + \beta_3 \mathbf{v}_z + \beta_4 \mathbf{E}_{kin} \quad (4.142)$$

From the definition 4.34 of basic extension it follows that three are five nodes $(0, 1, 3, 6, 12)_{\widetilde{M}'}$ which are already in \mathcal{H}'_b . Since the restrictions to $\mathbb{1}, \mathbf{v}_x, \mathbf{v}_y, \mathbf{v}_z, \mathbf{E}_{kin}$ at these five nodes are linearly independent, thus

$$\beta_i = \alpha_i, \quad i = 0, \dots, 4. \quad \square$$

4.5.3 Linearization

We recall L_1, D_H as defined in the section 4.2.3, P_H as defined by equation (4.109) and make the linearization ansatz

$$\mathbf{f} = \mathbf{e} + \epsilon D^{1/2} \phi, \quad (4.143)$$

where \mathbf{e}, D are defined as in the section 4.3.2. Then in absence of ternary collision law, equation (4.69) reduces to

$$L_H = D_H^{-\frac{1}{2}} \hat{\gamma}_{bin} L_1 D_H^{-\frac{1}{2}}. \quad (4.144)$$

For all 216-velocity model $\widetilde{M} \in \mathcal{H}_b$, denote

$$L := \sum_{H \in \mathcal{H}_b} P_H^\top L_H P_H \quad (4.145)$$

$$\widetilde{L}_{\widetilde{M}} := \sum_{H \in \widetilde{M}} P_H^\top \hat{\gamma}_{bin} L_1 P_H, \quad (4.146)$$

$$\begin{aligned} L_{\widetilde{M}} &:= \sum_{H \in \widetilde{M}} P_H^\top L_H P_H = \sum_{H \in \widetilde{M}} P_H^\top D_H^{-\frac{1}{2}} \hat{\gamma}_{bin} L_1 D_H^{-\frac{1}{2}} P_H \\ &= D_{\widetilde{M}}^{-\frac{1}{2}} \widetilde{L}_{\widetilde{M}} D_{\widetilde{M}}^{-\frac{1}{2}} \end{aligned} \quad (4.147)$$

Proposition 4.38 $L_{\widetilde{M}}$ is symmetric and non-positive, its null space is five-dimensional and is given by

$$N(L_{\widetilde{M}}) = D_{\widetilde{M}}^{\frac{1}{2}} \text{span}(\mathbb{1}_{\widetilde{M}}, (\mathbf{v}_x)_{\widetilde{M}}, (\mathbf{v}_y)_{\widetilde{M}}, (\mathbf{v}_z)_{\widetilde{M}}, (\mathbf{E}_{kin})_{\widetilde{M}}) \quad (4.148)$$

proof: Since all $L_H \in \widetilde{M}$ are symmetric and non-positive, therefore $L_{\widetilde{M}}$ is symmetric and non-positive. It can be verified that $x_{\widetilde{M}}^\top \widetilde{L}_{\widetilde{M}} x_{\widetilde{M}} = 0$ for all $x_{\widetilde{M}} \in S := \{\mathbb{1}_{\widetilde{M}}, (\mathbf{v}_x)_{\widetilde{M}}, (\mathbf{v}_y)_{\widetilde{M}}, (\mathbf{v}_z)_{\widetilde{M}}, (\mathbf{E}_{kin})_{\widetilde{M}}\}$ and the vectors $(\mathbb{1})_{\widetilde{M}}, (\mathbf{v}_x)_{\widetilde{M}}, (\mathbf{v}_y)_{\widetilde{M}}, (\mathbf{v}_z)_{\widetilde{M}}, (\mathbf{E}_{kin})_{\widetilde{M}}$ are linearly independent. Thus

$$N(\widetilde{L}_{\widetilde{M}}) = \text{span}(\mathbb{1}_{\widetilde{M}}, (\mathbf{v}_x)_{\widetilde{M}}, (\mathbf{v}_y)_{\widetilde{M}}, (\mathbf{v}_z)_{\widetilde{M}}, (\mathbf{E}_{kin})_{\widetilde{M}}) \quad (4.149)$$

via equation 4.147 yields

$$N(L_{\widetilde{M}}) = D^{\frac{1}{2}} \text{span}(\mathbb{1}_{\widetilde{M}}, (\mathbf{v}_x)_{\widetilde{M}}, (\mathbf{v}_y)_{\widetilde{M}}, (\mathbf{v}_z)_{\widetilde{M}}, (\mathbf{E}_{kin})_{\widetilde{M}}) \quad \square \quad (4.150)$$

Theorem 4.39 *L is symmetric and non-positive, its null space is five-dimensional and is given by*

$$N(L) = D^{\frac{1}{2}} \text{span}(\mathbb{1}, \mathbf{v}_x, \mathbf{v}_y, \mathbf{v}_z, \mathbf{E}_{kin}) \quad (4.151)$$

Since all L_H are symmetric and non-positive, therefore L is symmetric and non-positive. Thus

$$\begin{aligned} x^\top Lx &= 0 \\ \iff x_H^\top L_H x_H &= 0, \text{ for all } H \in \mathcal{H}_+ \\ \iff x_{\widetilde{M}}^\top L_{\widetilde{M}} x_{\widetilde{M}} &= 0, \text{ for all } \widetilde{M} \in \mathcal{H}_b \end{aligned}$$

Then by proposition 4.38, this is valid iff

$$x_{\widetilde{M}} \in D^{\frac{1}{2}} \text{span}(\mathbb{1}_{\widetilde{M}}, (\mathbf{v}_x)_{\widetilde{M}}, (\mathbf{v}_y)_{\widetilde{M}}, (\mathbf{v}_z)_{\widetilde{M}}, (\mathbf{E}_{kin})_{\widetilde{M}})$$

Then by lemma 4.37, this is true iff

$$x \in D^{\frac{1}{2}} \text{span}(\mathbb{1}, \mathbf{v}_x, \mathbf{v}_y, \mathbf{v}_z, \mathbf{E}_{kin})$$

Corollary 4.40 *The set of collision invariants of the nonlinear Boltzmann operator is spanned by $\mathbb{1}, \mathbf{v}_x, \mathbf{v}_y, \mathbf{v}_z, \mathbf{E}_{kin}$.*

Proof: The invariance of $\mathbb{1}, \mathbf{v}_x, \mathbf{v}_y, \mathbf{v}_z, \mathbf{E}_{kin}$ follows from mass, momentum and energy conservation of the local collision event. Suppose ψ is a collision invariant, i.e.

$$\langle \psi, J[\mathbf{f}] \rangle = 0 \quad (4.152)$$

for all non-negative densities on \mathbf{f} . Choosing a small perturbation from equilibrium by the ansatz $\mathbf{f} = \mathbf{e} + \epsilon \phi$ equation (4.152) yields

$$\epsilon \langle \psi, D^{\frac{1}{2}} L D^{-\frac{1}{2}} \phi \rangle + \mathcal{O}(\epsilon^2) = 0 \quad (4.153)$$

for $0 < \epsilon \leq \epsilon_0$, from which follows

$$\langle L D^{\frac{1}{2}} \psi, D^{-\frac{1}{2}} \phi \rangle = 0. \quad (4.154)$$

Since this has to hold for all ϕ , therefore, we conclude from Theorem (4.39) that $\psi \in \text{span}(\mathbb{1}, \mathbf{v}_x, \mathbf{v}_y, \mathbf{v}_z, \mathbf{E}_{kin}) \quad \square$

4.5.4 The 444-velocity model

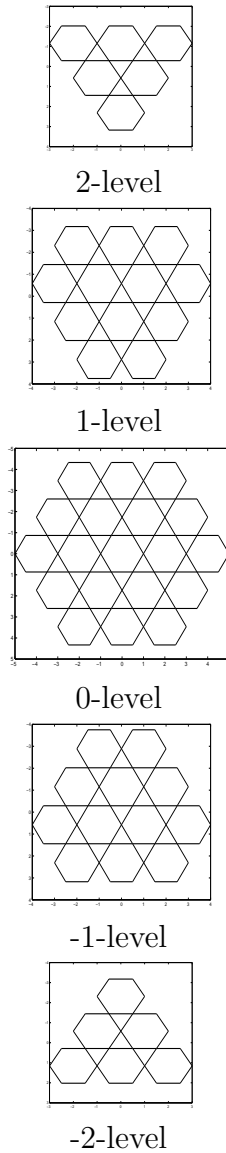


Fig. 4.9 Horizontal hexagonal cuts of the basic h-cubes of a 444-velocity model

The 444-velocity model is obtained by a composition of thirteen 120-velocity model which can be known as a two-layer model as already mentioned in section 4.4. First we consider a 120-velocity model M^0 with origin at $(0, 0, 0)$. Then our 444-velocity model is obtained by adding twelve other 120-velocity models M^j , $j = 1, \dots, 12$ with M^0 , having origins at the center of the twelve exterior h-cubes of M^0 . The horizontal hexagonal cuts of the basic h-cubes is shown in the Fig. 4.9 at five different levels (Definition 4.14). This two-layer model is the composition of 55 basic h-cubes which

provides 52 further class-A h-cubes and 132 class-B h-cubes. The mesh generation, enumeration and the listing of all h-cubes is done automatically.

Theorem 4.41 *The 444-velocity model is a regular collision model for which the space of collision invariants is spanned by $\rho, \rho\bar{v}_x, \rho\bar{v}_y, \rho\bar{v}_z$, and \mathbf{E}_{kin} .*

proof: The 444-velocity model can be obtained by subsequent basic extension (as defined in definition 4.34) of the basic 216-velocity model (as shown in Fig. 4.8).

Equilibria of the 444-velocity model:

Let $\mathbf{f} \in \mathcal{E}_{444}$ be the equilibria of the 444-velocity model. Then by the corollary 4.28, $\mathbf{f}_M \in \mathcal{E}_M$ for all 120-velocity model $M \in \mathcal{H}_{444}$. By choosing the equilibria $\mathbf{f} \in \mathcal{E}_{120}$ of the 120-velocity models (which has been given by theorem 4.25) as basis, we can determine the equilibria of 444-velocity model. Denote the equilibria $\mathbf{f}_{M^0} \in \mathcal{E}_{M^0}$ of the central 120-velocity model (which has been given by theorem 4.25) by

$$\mathbf{f}_{M^0} := z\mu^{\mathbf{m}_{|M^0}} \kappa_{|M^0} \quad (4.155)$$

and the equilibria of the other twelve 120-velocity model by

$$\mathbf{f}_{M^j} := z\mu^{\mathbf{m}_{|M^j}} \kappa_{|M^j}, \quad j = 1, \dots, 12 \quad (4.156)$$

Now we have to find the exponents $\mathbf{m}_{|M^j}$ of μ and $\kappa_{|M^j}$ for $j = 1, \dots, 12$. From the remark 4.33, since the corollary 4.26 is holds true for the basic 216-velocity model, then by symmetry of the 444-velocity model, the corollary 4.26 also holds true for the 444-velocity model. Thus by using the corollary 4.26 we can easily find the exponent $\mathbf{m}_{|M^j}$ of μ for $j = 1, \dots, 12$. From the construction of the 444-velocity model, it is evident that

$$\kappa_{|M^j} = \kappa_{|M^0} \times r^j$$

where for $j = 1, \dots, 12$,

$$r^j = \kappa_{0+}^2, \kappa_{1+}^2, \kappa_{2+}^2, \kappa_{0-}^2, \kappa_{1-}^2, \kappa_{2-}^2, \kappa_{3+}^2, \kappa_{4+}^2, \kappa_{5+}^2, \kappa_{3-}^2, \kappa_{4-}^2, \kappa_{5-}^2$$

respectively. Then the equilibria $\mathbf{f} \in \mathcal{E}_{444}$ is given by

$$\mathbf{f} = \bigcup_M \mathbf{f}_M \quad \text{for all } M \in \{M^0, \dots, M^{12}\}. \quad (4.157)$$

Chapter 5

3D Numerical experiments

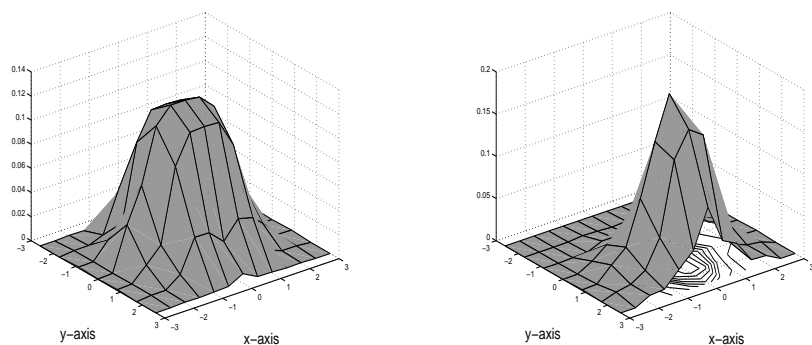
We present numerical results based on the hexagonal grid model in \mathbb{R}^3 by using the 120-velocity model (M_1) and the 444-velocity model (M_2), described in the previous chapter. We mention here that the 120-velocity model is based on both binary and ternary collision law whereas the 444-model is based on only binary collision law.

In the first section we compute the equilibria for both the models M_1 and M_2 and compare the discrete equilibria with the corresponding maxwellian which leads to calculate errors due to boundary cuts.

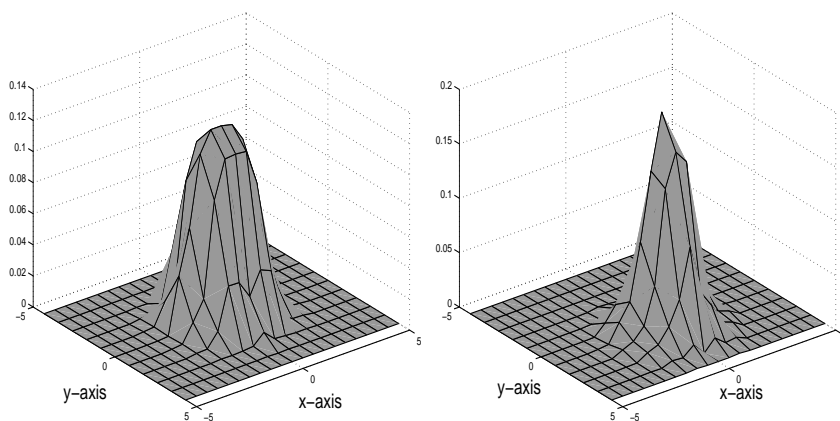
In the next section, we demonstrate the numerical solution of the Boltzmann equation. In the case of space homogeneous case, for maxwell molecule, we compare the numerical solutions with the exact solution due to Wu and Krook [51] and perform relaxation problem. For the space inhomogeneous case, we present the steady state solution for a standard test problem.

5.1 Discrete equilibria

We compute the equilibria \mathbf{e} for the models M_1 and M_2 given respectively by Theorem 4.25 and by equation (4.157). Figure 5.1(a,b) show the equilibria restricted to the mid horizontal cut of the models M_1, M_2 respectively. In a constant temperature ($\mu = 0.23$), for both the models M_1, M_2 , the first figures are showing equilibrium distribution \mathbf{e} for zero bulk velocities (i.e. for $\kappa_{0+} = \kappa_{2+} = \kappa_{3+} = 1$) but in the second figures we consider $\kappa_{2+} = 5, \kappa_{0+} = \kappa_{3+} = 1$.



a) For the 120-velocity model



b) For the 444-velocity model

Fig. 5.1 Equilibria restricted to the mid horizontal cut

We compare this discrete equilibria e with the corresponding maxwellian

$$m = \frac{\rho}{(2\pi T)^{3/2}} \exp\left(\frac{-(\mathbf{v} - \bar{v})^2}{2T}\right) \quad (5.1)$$

by computing the error

$$err := \|e - m\|_1. \quad (5.2)$$

In order to restrict the error $err < 0.01$, in the case of zero bulk velocity ($\kappa_{0+} = \kappa_{2+} = \kappa_{3+} = 1$), we find the range of the temperature T as shown in the table 5.1.

Model	μ	T
M_1	0.19-0.24	0.61-0.69
M_2	0.19-0.50	0.61-1.47

Table 5.1: For $err < 0.01$

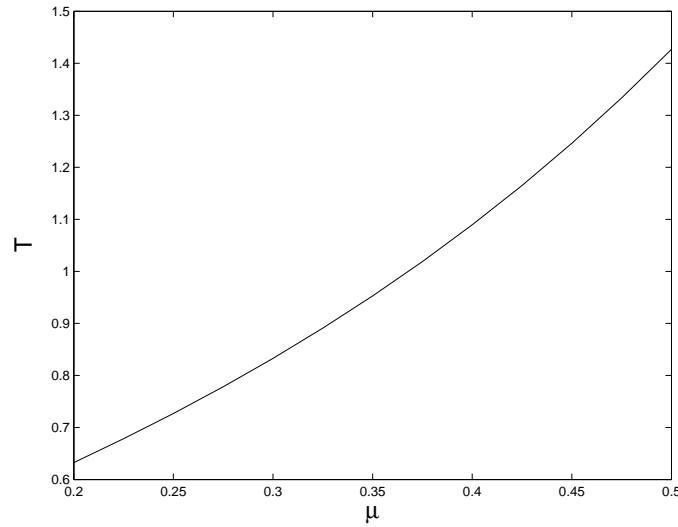


Fig. 5.2 Temperature $T(\mu)$ at zero bulk-velocity

Fig. 5.2 and Table 5.1 shows the temperature T corresponding to some given values of μ , for the model M_2 .

μ	0.2	0.225	0.250	0.275	0.300	0.325	0.350	0.375	0.400	0.425	0.450	0.475	0.5
T	0.6325	0.678	0.727	0.778	0.833	0.89	0.95	1.02	1.09	1.165	1.246	1.333	1.427

Table 5.2: Temperature $T(\mu)$ at zero bulk-velocity

Now for the fixed temperature $T(0.2) = 0.63$ we observe the change of bulk-velocity w.r.to $\kappa_{0+}, \kappa_{2+}, \kappa_{3+}$. It is evident that

- (i) $\bar{v}_x < 0, = 0, > 0$, according as $\kappa_{0+} < 1, = 1, > 1$ respectively.
 - (ii) $\bar{v}_y < 0, = 0, > 0$, according as $\kappa_{2+} < 1/\sqrt{\kappa_{0+}}, = 1/\sqrt{\kappa_{0+}}, > 1/\sqrt{\kappa_{0+}}$ respectively.
 - (iii) $\bar{v}_z < 0, = 0, > 0$, according as $\kappa_{3+} < \sqrt{\kappa_{0+}}, = \sqrt{\kappa_{0+}}, > \sqrt{\kappa_{0+}}$ respectively.
- Thus, for required values of $(\bar{v}_x, \bar{v}_y, \bar{v}_z)$, first fixing the value of κ_{0+} we can fix the values of κ_{2+}, κ_{3+} .

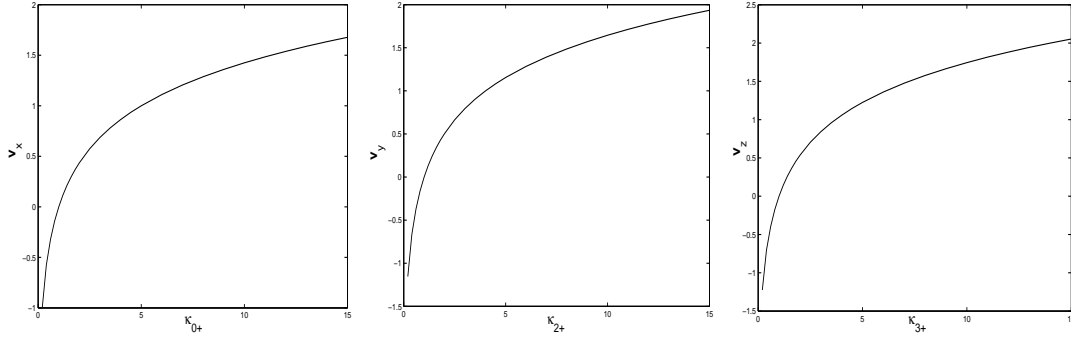


Fig. 5.3 Velocity components $\bar{v}_x(\kappa_{0+})$, $\bar{v}_y(\kappa_{2+})$, $\bar{v}_z(\kappa_{3+})$.

Let us now first fix $\bar{v}_y = \bar{v}_z = 0$ by the above conditions (ii) and (iii) respectively, and vary $\kappa_{0+} \in [0.2, 15]$ then we obtain \bar{v}_x as shown by the first of the Fig. 5.3. Similarly for varying κ_{2+} and κ_{3+} in the same domain we obtain the profiles respectively for \bar{v}_y and \bar{v}_z as shown by the second and third of the Fig. 5.3. As the temperature and bulk-velocity components are monotonically increasing with respect to the corresponding parameters, thus for required temperature and bulk velocities we can determine the corresponding parameters by the same method given by the Algorithm 3.1 in the chapter 3.

5.2 Solution of the Boltzmann equation

As a demonstration of the solution of the space homogeneous Boltzmann equation we present here (A) Comparison of the numerical solution with the exact solution of the Boltzmann equation due to Krook and Wu [51], (B) The relaxation problem.

5.2.1 The space homogeneous case

(A) Comparison with Exact solution

The exact solution of the space homogeneous Boltzmann equation for maxwell molecules is due to Wu and Krook [51] and is stated by the equation (3.3) in chapter 3. We compute the solution of the space homogeneous Boltzmann equation with the model M_1 and M_2 by using the fourth order Runge-Kutta scheme and this solution f_h is compared with the exact solution f for the two models.

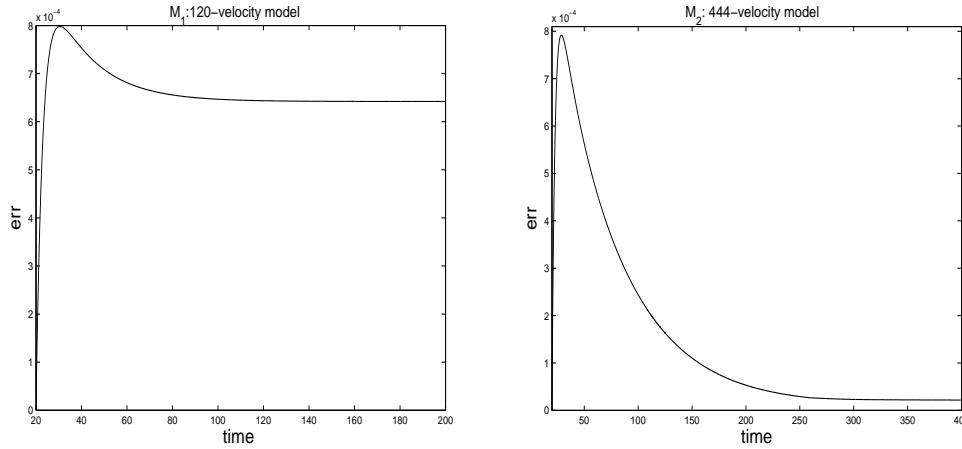


Fig. 5.4 Comparison with exact solution.

Fig. 5.4 shows the relative error

$$err = \frac{\|f - f_h\|_1}{\|f\|_1} \quad (5.3)$$

for the models M_1 and M_2 .

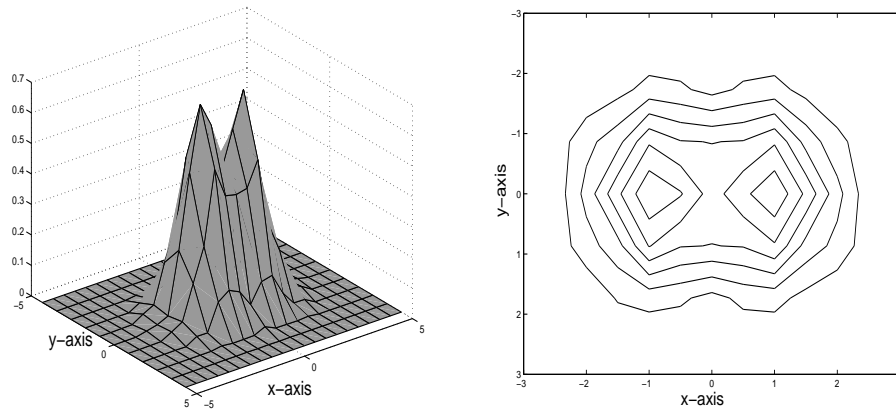
In both the cases we used the same temperature and as expected the error of M_2 is much less than that of M_1 . In large time, the error of M_2 is very near to zero and for both the models the errors are quite comparable with error which has been given by the equation 5.2 in the section 5.1.

(B) The Relaxation problem

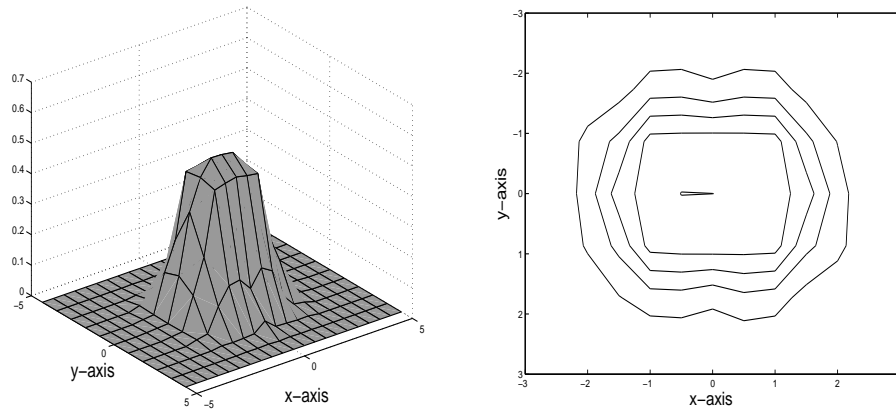
Our test case here concerns the relaxation of a spatially homogeneous distribution to its equilibrium. We consider a gas of identical hard sphere molecules so that, for each h-cubes H , the collision frequency

$$\gamma_H = \pi d^2 \times \text{diam}(H)$$

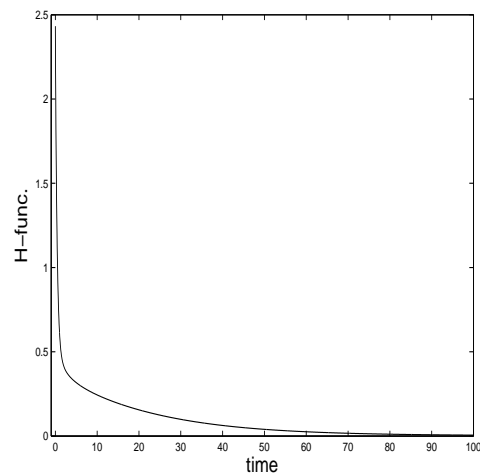
where d is the diameter of the molecules. The given value of the diameter d is related to determine the viscosity coefficient as well as the mean-free-path as already described by the equations (3.4), (3.5). We perform the relaxation of space homogeneous problem based on the 444-velocity model and verify the physical properties of the numerical solution. We have chosen the initial density (Fig. 5.5(a) shows the initial density restricted to the 0-level horizontal cut of the model) as the composition of two equilibria centered at two different points on the grid and of the same width. Fig. 5.5(b) shows the solution at final state restricted to the 0-level horizontal cut and Fig. 5.6 shows the time evolution of the H-functional.



(a) Initial state



(b) Solution at final state

Fig. 5.5 Relaxation problem based on the 444-velocity model.**Fig. 5.6** Time evolution of entropy in the relaxation problem.

These results are completely consistent with the basic features of kinetic theory

which has been described in chapter 4. i.e. Mass, momenta, kinetic energy are invariants and the time evolution of the H -functional is monotonically decreasing.

5.2.2 Space inhomogeneous case

We present the solution of the space inhomogeneous Boltzmann equation based on the 444-velocity model. We used hard sphere molecules and our test problem here is the heat transfer problem between two parallel plates. We used the classical operator-splitting method for the computation of the solutions which consists of splitting the equation into transport and collision steps. For the transport step we used a finite difference scheme and for the collision step we used the fourth order Runge-Kutta scheme.

Heat transfer between two parallel plates

We consider a hard sphere gas between two parallel infinite plates placed at a distance L and having uniform wall temperature $T_0 = 0.9$ and $T_1 = 1.35$ at $x = -L/2$ and $x = L/2$ respectively. We impose diffuse reflection boundary condition on both the walls with density $\rho = 1$ and bulk-velocity $\tilde{\mathbf{v}} = 0$. In our calculation, the discretization parameter of the velocity space $\Delta v = 1$, the Knudsen number $Kn = \lambda/L$, where λ is the mean free path.

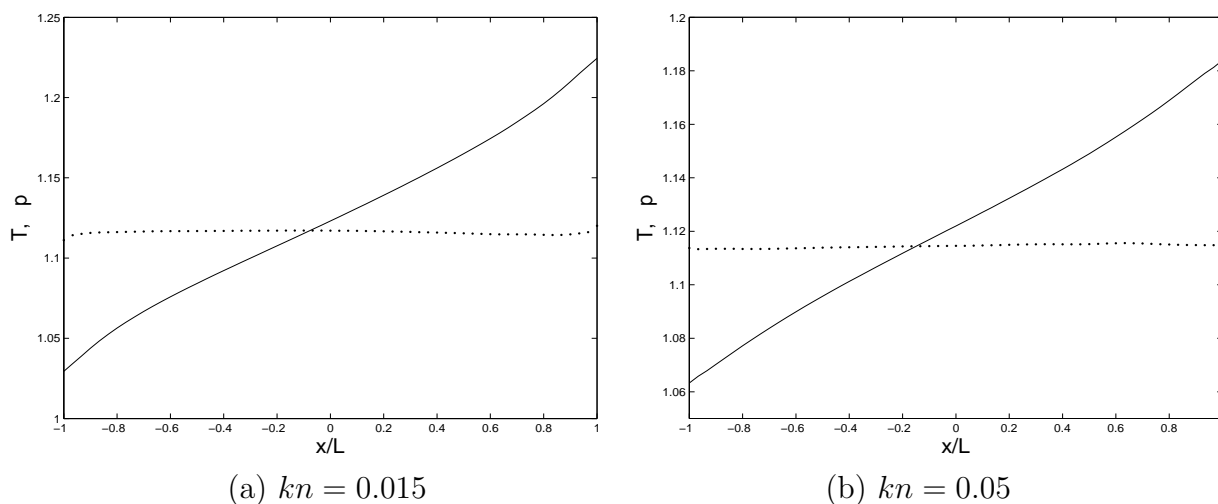


Fig. 5.7 Heat transfer problem by the 444-velocity model.

Fig. 5.7 shows the temperature profile (the solid line) and the pressure distribution (the dotted line). We know from the Navier-stokes theory that the temperature

profile between the two plates is a straight line connecting the two wall temperatures T_0 and T_1 . However, due to the description of the considered gas by kinetic equation and boundary conditions, we obtained the expected temperature jump as well as the kinetic boundary layers. As we also know from the theory of steady Couette flow (can be seen in [26], equation (2.3.6)) that the pressure is constant throughout the spatial domain between the plates, we obtained almost a constant pressure profile except little boundary effect. Thus we see that our 3D model is capable enough to determine the behavior of the test problems.

Appendix A

On the equilibria for the 3D model based on both binary and ternary collision law

We present here a lemma describing the property of equilibria restricted to the 0-level horizontal cut of a 81-velocity model. The proof the lemma is shown by symbolic calculation in maple.

Lemma A.1 *The equilibria $\mathbf{f} \in \mathcal{E}_{|v_z|=0}$ as presented by (4.88) of the 81-velocity model is a smooth four-dimensional manifold.*

Proof: The equilibria $\mathbf{f} \in \mathcal{E}_{v_z=0}$ is given by (4.88). We will show that $(r^{(k)}, \kappa_{0+}^{(k)}, \kappa_{2+}^{(k)}, k = 1, \dots, 7)$ can be uniquely parameterized by quadrupel $(\kappa_{0+}^{(1)}, \kappa_{2+}^{(1)}, r^{(1)}, r^{(2)})$. With this end, we search for common nodes in any two hexagons and then equate the densities at the common nodes and make all possible substitution for the rest of $(\kappa_{0+}^{(1)}, \kappa_{2+}^{(1)}, r^{(1)}, r^{(2)})$. We have as

$$5 \in H_1 \cap H_2,$$

$$\kappa_{2+}^{(2)} = \frac{r^{(1)}}{r^{(2)} \kappa_{2+}^{(1)}}, \quad (1.1)$$

$$0 \in H_1 \cap H_3,$$

$$\kappa_{0+}^{(3)} = \frac{r^{(3)}}{r^{(1)} \kappa_{0+}^{(1)}}, \quad (1.2)$$

$$13 \in H_2 \cap H_3, \text{ so solving } r^{(2)} \kappa_{1+}^{(2)} = r^{(3)} \kappa_{1-}^{(3)},$$

$$\kappa_{2+}^{(3)} = \frac{\kappa_{0+}^{(1)} \kappa_{2+}^{(1)}}{\kappa_{0+}^{(2)}}, \quad (1.3)$$

25 $\in H_3 \cap H_4$, solving $r^{(4)}\kappa_{2-}^{(4)} = r^{(3)}\kappa_{2+}^{(3)}$,

$$\kappa_{0+}^{(4)} = \frac{r^{(3)}}{r^{(1)}\kappa_{0+}^{(2)}}, \quad (1.4)$$

1 $\in H_1 \cap H_4$, solving $r^{(4)}\kappa_{1-}^{(4)} = r^{(1)}\kappa_{1+}^{(1)}$,

$$\kappa_{2+}^{(4)} = \frac{r^{(4)}\kappa_{0+}^{(2)}}{r^{(3)}\kappa_{0+}^{(1)}\kappa_{2+}^{(1)}}, \quad (1.5)$$

23 $\in H_3 \cap H_6$, solving $r^{(5)}\kappa_{0+}^{(5)} = r^{(3)}\kappa_{0+}^{(3)}$,

$$\kappa_{0+}^{(5)} = \frac{r^{(3)^2}}{r^{(1)}r^{(5)}\kappa_{0+}^{(1)}}, \quad (1.6)$$

33 $\in H_4 \cap H_6$, solving $r^{(5)}\kappa_{1+}^{(5)} = r^{(4)}\kappa_{0+}^{(4)}$,

$$\kappa_{2+}^{(5)} = \frac{r^{(4)}\kappa_{0+}^{(1)}}{r^{(3)}\kappa_{0+}^{(2)}}, \quad (1.7)$$

36 $\in H_4 \cap H_6$, solving $r^{(5)}\kappa_{2+}^{(5)} = r^{(4)}\kappa_{0-}^{(4)}$,

$$r^{(5)} = \frac{r^{(1)}\kappa_{0+}^{(2)^2}}{\kappa_{0+}^{(1)}}, \quad (1.8)$$

3 $\in H_1 \cap H_6$, solving $r^{(5)}\kappa_{0-}^{(5)} = r^{(1)}\kappa_{0-}^{(1)}$,

$$r^{(3)} = r^{(1)}\kappa_{0+}^{(2)^2}, \quad (1.9)$$

14 $\in H_2 \cap H_6$, solving $r^{(5)}\kappa_{1-}^{(5)} = r^{(2)}\kappa_{0-}^{(2)}$,

$$r^{(4)} = \frac{r^{(1)^2}\kappa_{0+}^{(2)^4}}{r^{(2)}\kappa_{0+}^{(1)^2}}, \quad (1.10)$$

12 $\in H_2 \cap H_6$, solving $r^{(5)}\kappa_{2-}^{(5)} = r^{(2)}\kappa_{0+}^{(2)}$

$$r^{(2)}\kappa_{0+}^{(2)} = r^{(2)}\kappa_{0+}^{(2)}, \quad (1.11)$$

From (1.8), \dots , (1.10) we substitute $r^{(5)}, r^{(3)}, r^{(4)}$ in the equations (1.2), \dots , (1.7) and we see that $(r^{(k)}, \kappa_{0+}^{(k)}, \kappa_{2+}^{(k)}, k = 1, \dots, 5)$ is parameterized by $(\kappa_{0+}^{(1)}, \kappa_{2+}^{(1)}, r^{(1)}, r^{(2)})$ with one additional parameter $\kappa_{0+}^{(2)}$. We proceed further,

as $36 \in H_4 \cap H_5$, solving $r^{(6)}\kappa_{0+}^{(6)} = r^{(4)}\kappa_{0-}^{(4)}$,

$$\kappa_{0+}^{(6)} = \frac{r^{(1)2}\kappa_{0+}^{(2)3}}{r^{(2)}r^{(6)}\kappa_{0+}^{(1)2}}, \quad (1.12)$$

$2 \in H_1 \cap H_5$, solving $r^{(6)}\kappa_{2-}^{(6)} = r^{(1)}\kappa_{2+}^{(1)}$,

$$\kappa_{2+}^{(6)} = \frac{r^{(6)}}{r^{(1)}\kappa_{2+}^{(1)}}, \quad (1.13)$$

$24 \in H_3 \cap H_7$, solving $r^{(7)}\kappa_{0+}^{(7)} = r^{(3)}\kappa_{1+}^{(3)}$,

$$\kappa_{0+}^{(7)} = \frac{r^{(1)}\kappa_{2+}^{(1)}\kappa_{0+}^{(2)3}}{r^{(7)}}, \quad (1.14)$$

$34 \in H_4 \cap H_7$, solving $r^{(7)}\kappa_{1+}^{(7)} = r^{(4)}\kappa_{1+}^{(4)}$,

$$\kappa_{2+}^{(7)} = \frac{r^{(1)2}\kappa_{0+}^{(2)5}}{r^{(2)2}\kappa_{0+}^{(1)5}\kappa_{2+}^{(1)2}}, \quad (1.15)$$

$43 \in H_5 \cap H_7$, solving $r^{(7)}\kappa_{2+}^{(7)} = r^{(6)}\kappa_{1+}^{(6)}$,

$$r^{(7)} = \frac{r^{(6)}r^{(2)}\kappa_{0+}^{(1)3}\kappa_{2+}^{(1)}}{r^{(1)}\kappa_{0+}^{(2)2}}, \quad (1.16)$$

$46 \in H_5 \cap H_7$, solving $r^{(7)}\kappa_{0-}^{(7)} = r^{(6)}\kappa_{1-}^{(6)}$,

$$r^{(6)} = \frac{r^{(1)2}\kappa_{0+}^{(2)4}}{r^{(2)}\kappa_{0+}^{(1)4}}, \quad (1.17)$$

$4 \in H_1 \cap H_7$, solving $r^{(7)}\kappa_{1-}^{(7)} = r^{(1)}\kappa_{1-}^{(1)}$,

$$\kappa_{0+}^{(2)} = \frac{\sqrt{r^{(1)}r^{(2)}}\kappa_{0+}^{(1)}\kappa_{2+}^{(1)}}{r^{(1)}}, \quad (1.18)$$

$13 \in H_2 \cap H_7$, solving $r^{(7)}\kappa_{2-}^{(7)} = r^{(2)}\kappa_{1+}^{(2)}$,

$$\sqrt{r^{(1)}r^{(2)}}\kappa_{0+}^{(1)} = \sqrt{r^{(1)}r^{(2)}}\kappa_{0+}^{(1)}, \quad (1.19)$$

Thus by (1.16), (1.17) we can substitute $r^{(6)}, r^{(7)}$ from (1.12), \dots , (1.15) and then by (1.18) we can substitute $\kappa_{0+}^{(2)}$'s from (1.3), \dots , (1.17). \square

Appendix B

On the equilibria for the 3D hexagonal model based on only binary collision law

In this appendix, we study the dimension of the equilibria for the model (in \mathbb{R}^3) based on only binary collision law. By making symbolic calculation in maple, first we find that the equilibria of a 120-velocity model is a eleven-dimensional manifold, then by using the equilibria of this 120-velocity as a basis, we find that the equilibria of a 177-velocity model (which is the composition of two 120-velocity model) is a seven-dimensional manifold and finally we find that the equilibria of a 216-velocity model (which is the composition of three 120-velocity model) is a five-dimensional manifold.

The list of basic, class-A and class-B h-cubes of a 120-velocity model M^0 denoted by M_0^0, M_A^0, M_B^0 is given by the array 2.1, 2.2, 2.3 respectively.

$$M_0^0 : = \left\{ \begin{array}{cccccccccccc} 0 & 1 & 2 & 3 & 4 & 5 & 6 & 7 & 8 & 9 & 10 & 11 \\ 12 & 13 & 14 & 0 & 15 & 16 & 17 & 18 & 19 & 20 & 21 & 22 \\ 23 & 24 & 25 & 26 & 1 & 14 & 27 & 28 & 29 & 30 & 31 & 32 \\ 26 & 33 & 34 & 35 & 36 & 2 & 37 & 38 & 39 & 40 & 41 & 42 \\ 3 & 36 & 43 & 44 & 45 & 46 & 47 & 48 & 49 & 50 & 51 & 52 \\ 53 & 4 & 46 & 54 & 55 & 56 & 57 & 58 & 59 & 60 & 61 & 62 \\ 63 & 15 & 5 & 53 & 64 & 65 & 66 & 67 & 68 & 69 & 70 & 71 \\ 72 & 73 & 74 & 75 & 76 & 77 & 78 & 79 & 80 & 6 & 18 & 68 \\ 75 & 81 & 82 & 83 & 84 & 85 & 86 & 87 & 88 & 47 & 7 & 59 \\ 89 & 90 & 91 & 92 & 81 & 74 & 93 & 94 & 95 & 37 & 28 & 8 \\ 96 & 97 & 98 & 99 & 100 & 101 & 9 & 51 & 42 & 102 & 103 & 104 \\ 105 & 106 & 107 & 96 & 108 & 109 & 20 & 10 & 32 & 110 & 111 & 112 \\ 113 & 108 & 101 & 114 & 115 & 116 & 69 & 61 & 11 & 117 & 118 & 119 \end{array} \right. \quad (2.1)$$

$$M_B^0 : = \begin{cases} 12 & 23 & 26 & 3 & 53 & 63 & 72 & 75 & 89 & 96 & 105 & 113 \\ 13 & 24 & 33 & 36 & 4 & 15 & 73 & 81 & 90 & 97 & 106 & 108 \\ 14 & 25 & 34 & 43 & 46 & 5 & 74 & 82 & 91 & 98 & 107 & 101 \\ 0 & 26 & 35 & 44 & 54 & 53 & 75 & 83 & 92 & 99 & 96 & 114 \\ 15 & 1 & 36 & 45 & 55 & 64 & 76 & 84 & 81 & 100 & 108 & 115 \\ 16 & 14 & 2 & 46 & 56 & 65 & 77 & 85 & 74 & 101 & 109 & 116 \\ 17 & 27 & 37 & 47 & 57 & 66 & 78 & 86 & 93 & 9 & 20 & 69 \\ 18 & 28 & 38 & 48 & 58 & 67 & 79 & 87 & 94 & 51 & 10 & 61 \\ 19 & 29 & 39 & 49 & 59 & 68 & 80 & 88 & 95 & 42 & 32 & 11 \\ 20 & 30 & 40 & 50 & 60 & 69 & 6 & 47 & 37 & 102 & 110 & 117 \\ 21 & 31 & 41 & 51 & 61 & 70 & 18 & 7 & 28 & 103 & 111 & 118 \\ 22 & 32 & 42 & 52 & 62 & 71 & 68 & 59 & 8 & 104 & 112 & 119 \end{cases} \quad (2.2)$$

$$M_A^0 : = \begin{cases} 19 & 27 & 28 & 8 & 6 & 18 & 73 & 74 & 89 & 1 & 14 & 0 \\ 8 & 37 & 38 & 49 & 47 & 7 & 81 & 82 & 92 & 36 & 2 & 3 \\ 68 & 6 & 7 & 59 & 57 & 67 & 76 & 85 & 75 & 4 & 5 & 53 \\ 22 & 20 & 10 & 11 & 69 & 70 & 15 & 5 & 0 & 108 & 109 & 113 \\ 11 & 9 & 51 & 52 & 60 & 61 & 4 & 46 & 3 & 100 & 101 & 114 \\ 32 & 30 & 41 & 42 & 9 & 10 & 1 & 2 & 26 & 97 & 107 & 96 \\ 12 & 24 & 34 & 44 & 55 & 65 & 78 & 87 & 95 & 102 & 111 & 119 \end{cases} \quad (2.3)$$

where each row of the array's represent a h-cube $H := (\pi_0^H, \pi_1^H, \pi_2^H, \pi_3^H, \pi_4^H, \pi_5^H, \pi_6^H, \pi_7^H, \pi_8^H, \pi_9^H, \pi_{10}^H, \pi_{11}^H)$. Let $H^{(k)}$, $k = 0, \dots, 31$, denote all the 32 h-cubes of the 120-velocity model, the first one in the array (2.1), ..., the bottom one in the array (2.3) respectively.

Proposition B.1 *The equilibria $\mathbf{f} \in \mathcal{E}_{|M^0}$ of a 120-velocity model is an 11-dimensional manifold.*

proof: Suppose $\mathbf{f} \in \mathcal{E}_{|M^0}$. Then from proposition 4.27, we have

$$f_{\pi_0^{H^{(k)}}} f_{\pi_3^{H^{(k)}}} = f_{\pi_1^{H^{(k)}}} f_{\pi_4^{H^{(k)}}} = f_{\pi_2^{H^{(k)}}} f_{\pi_5^{H^{(k)}}} = f_{\pi_6^{H^{(k)}}} f_{\pi_9^{H^{(k)}}} = f_{\pi_7^{H^{(k)}}} f_{\pi_{10}^{H^{(k)}}} = f_{\pi_8^{H^{(k)}}} f_{\pi_{11}^{H^{(k)}}} \\ \text{for } H^{(k)} \in M_0^0 \cup M_A^0 \cup M_B^0 \text{ for each } k = 0, \dots, 30. \quad (2.4)$$

Now, we make the ansatz

$$f_{\pi_0^{H^{(k)}}} := a_0^{(k)}, f_{\pi_3^{H^{(k)}}} := a_1^{(k)}, f_{\pi_1^{H^{(k)}}} := a_2^{(k)}, f_{\pi_2^{H^{(k)}}} := a_3^{(k)}, f_{\pi_6^{H^{(k)}}} := a_4^{(k)}, \\ f_{\pi_7^{H^{(k)}}} := a_5^{(k)}, f_{\pi_8^{H^{(k)}}} := a_6^{(k)} \text{ and consequently} \quad (2.5) \\ f_{\pi_4^{H^{(k)}}} := \frac{a_0^{(k)} a_1^{(k)}}{a_2^{(k)}}, f_{\pi_5^{H^{(k)}}} := \frac{a_0^{(k)} a_1^{(k)}}{a_3^{(k)}}, f_{\pi_9^{H^{(k)}}} := \frac{a_0^{(k)} a_1^{(k)}}{a_6^{(k)}}, \\ f_{\pi_{10}^{H^{(k)}}} := \frac{a_0^{(k)} a_1^{(k)}}{a_7^{(k)}}, f_{\pi_{11}^{H^{(k)}}} := \frac{a_0^{(k)} a_1^{(k)}}{a_8^{(k)}}.$$

There are common nodes among $H^{(k)}$'s. e.g. $\pi_0^{H^{(0)}} = \pi_3^{H^{(1)}}$ implies $a_1^{(1)} = a_0^{(0)}$, $\pi_1^{H^{(0)}} = \pi_4^{H^{(3)}}$ implies $a_2^{(2)} = (a_0^{(2)} a_1^{(2)})/a_2^{(0)}$ and so on. Implementing such ansatz successively in maple, it is seen that all the parameters $a_i^{(k)}$, $i = 0, \dots, 6$; $k = 0, \dots, 30$,

can be uniquely determined by the set of the eleven parameters:

$$\left\{ a_0^{(0)}, a_1^{(0)}, a_2^{(0)}, a_4^{(0)}, a_0^{(1)}, a_2^{(1)}, a_3^{(1)}, a_4^{(1)}, a_5^{(1)}, a_0^{(2)}, a_6^{(2)} \right\}.$$

Finally, re-denoting $a_i^{(0)} := a_i$, $a_i^{(1)} := b_i$, $a_i^{(2)} := c_i$, $\mathbf{f} = (f_i)_{i=0}^{119}$ is obtained in terms of the eleven parameters $\left\{ a_0, a_1, a_2, a_4, b_0, b_2, b_3, b_4, b_5, c_0, c_6 \right\}$ as

$$\begin{aligned} \mathbf{f} = & \left[a_0, a_2, \frac{a_2\sqrt{a_1}}{\sqrt{a_0}}, a_1, \frac{a_0a_1}{a_2}, \frac{\sqrt{a_1}a_0^{\frac{3}{2}}}{a_2}, a_4, \frac{\sqrt{a_0a_1}a_4}{a_0}, \frac{a_2a_4}{a_0}, \frac{a_0a_1}{a_4}, \frac{a_0^{\frac{3}{2}}\sqrt{a_1}}{a_4}, \frac{a_0^2a_1}{a_2a_4}, b_0, b_2, b_3, \frac{b_0a_0}{b_2}, \right. \\ & \frac{b_0a_0}{b_3}, b_4, b_5, \frac{a_2\sqrt{a_1b_0}a_4}{a_0a_1}, \frac{b_0a_0}{b_4}, \frac{b_0a_0}{b_5}, \frac{\sqrt{b_0}a_0^{\frac{3}{2}}\sqrt{a_1}}{a_2a_4}, c_0, \frac{a_2^3b_0}{a_0^3}, \frac{a_4^2b_0}{a_0^2b_3}, \frac{a_4^2b_0}{a_0^2c_0}, \frac{\sqrt{b_0}a_2^2a_4}{\sqrt{a_1}a_0^2}, \frac{\sqrt{b_0}a_2^2a_4^2}{\sqrt{a_1}a_0^2b_5}, c_6, \\ & \frac{a_2^2\sqrt{b_0}\sqrt{a_1}}{a_0a_4}, \frac{a_2^2\sqrt{b_0}\sqrt{a_1}b_5}{a_0a_4^2}, \frac{a_2^4b_0}{a_0^3c_6}, \frac{b_2a_1a_2^2}{a_0^3}, \frac{a_2^3b_0a_1^{\frac{3}{2}}}{a_0^{\frac{9}{2}}}, \frac{c_0a_1^2}{a_0^2}, \frac{a_2^2b_0a_1}{a_0^2b_2}, \frac{a_2^2b_4\sqrt{a_1}}{a_0^2\sqrt{b_0}}, \frac{a_2^2a_4\sqrt{b_0}a_1}{a_0^{\frac{7}{2}}}, \frac{a_2^6b_0^{\frac{3}{2}}a_4^2\sqrt{a_1}}{a_0^8c_6}, \\ & \frac{a_2^2b_0^{\frac{3}{2}}a_1^{\frac{3}{2}}}{a_0^3b_4}, \frac{a_2^2a_1\sqrt{b_0}}{a_0^{\frac{3}{2}}a_4}, \frac{a_0^3a_1^{\frac{3}{2}}c_6}{a_2^2a_4^2\sqrt{b_0}}, \frac{a_1^2b_0a_2^2}{a_0^3b_3}, \frac{a_1^3b_0}{a_0^3}, \frac{a_1^3b_2}{a_0a_2^2}, \frac{a_1^2b_3}{a_2^2}, \frac{b_0a_1a_4^2}{a_0^2b_4}, \frac{a_1^2b_0a_4^2}{b_5a_0^3}, \frac{a_2\sqrt{b_0}a_1^{\frac{3}{2}}a_4}{a_0^3}, \frac{a_1^3b_4}{a_0a_4^2}, \\ & \frac{a_1^2b_5}{a_4^2}, \frac{a_1^{\frac{5}{2}}\sqrt{b_0}}{a_2a_4}, \frac{b_0a_1}{c_0}, \frac{a_0a_1^3c_0}{a_2^4}, \frac{b_0a_1^3}{a_2^3}, \frac{a_0a_1^2b_0}{a_2^2b_3}, \frac{\sqrt{b_0}a_1^{\frac{3}{2}}a_4}{a_2^2}, \frac{b_5a_1^{\frac{5}{2}}\sqrt{b_0}}{a_0a_2^2}, \frac{a_2^2b_0a_1a_4^2}{a_4^2c_6}, \frac{a_1^{\frac{5}{2}}a_0\sqrt{b_0}}{a_2^2a_4}, \frac{a_1^{\frac{3}{2}}a_0^2\sqrt{b_0}}{a_2^2b_5}, \\ & \frac{a_1^3a_0^5c_6}{a_2^6a_4^2}, \frac{a_1a_0^3c_0}{a_2^4}, \frac{a_1^2a_0^2b_2}{a_2^4}, \frac{a_1^{\frac{3}{2}}a_0^{\frac{3}{2}}b_0}{a_2^3}, \frac{b_0^{\frac{3}{2}}a_4^2\sqrt{a_1}}{b_4a_2^2}, \frac{a_4\sqrt{a_0}a_1\sqrt{b_0}}{a_2^2}, \frac{a_0^4\sqrt{a_1}c_6}{a_2^4\sqrt{b_0}}, \frac{a_1^{\frac{3}{2}}a_0^3b_4}{a_2^2a_4^2\sqrt{b_0}}, \frac{a_1a_0^{\frac{5}{2}}\sqrt{b_0}}{a_2^2a_4}, \\ & \frac{a_1b_0\sqrt{a_1b_0}}{a_0c_6}, \frac{b_0^{\frac{3}{2}}a_2^2a_4^2}{\sqrt{a_1}a_0^3c_0}, \frac{\sqrt{b_0}a_2a_4^2}{\sqrt{a_1}a_0^2}, \frac{\sqrt{b_0}a_2^2a_4^2}{b_3\sqrt{a_1}a_0^2}, \frac{\sqrt{a_1}a_4^2c_0}{a_2^2\sqrt{b_0}}, \frac{\sqrt{b_0}a_4^2\sqrt{a_1}}{a_0a_2}, \frac{\sqrt{b_0}\sqrt{a_1}a_4^2b_3}{a_2^2a_0}, \frac{b_0a_4^3}{a_0^3}, \frac{b_0a_4^4}{a_0^3b_5}, \\ & \frac{b_0^{\frac{3}{2}}a_2^4a_4^4}{\sqrt{a_1}a_0^7c_6}, \frac{a_2^4b_2\sqrt{a_1}}{a_0^2\sqrt{b_0}}, \frac{a_2a_4^2\sqrt{b_0}a_1}{a_0^{\frac{7}{2}}}, \frac{a_1^{\frac{3}{2}}b_0^{\frac{3}{2}}a_2^2a_4^2}{a_0^5c_0}, \frac{a_1^{\frac{3}{2}}a_4^2b_0^{\frac{3}{2}}}{a_0^3b_2}, \frac{a_4^2a_1\sqrt{b_0}}{a_0^{\frac{3}{2}}a_2}, \frac{a_1a_4^2b_4}{a_0^3}, \frac{a_1^{\frac{3}{2}}a_4^3b_0}{a_0^{\frac{9}{2}}}, \frac{a_1a_4^2c_6}{a_2^2a_0}, \frac{\sqrt{b_0}a_2^2a_4^2}{\sqrt{a_1}a_0^3}, \\ & \frac{b_0^{\frac{3}{2}}a_2^4a_4^2}{\sqrt{a_1}a_0^5b_2}, \frac{\sqrt{a_1}\sqrt{b_0}a_2^2a_4^2b_3}{a_0^5}, \frac{a_2^2\sqrt{b_0}\sqrt{a_1}a_4^2}{a_0^4}, \frac{b_0^{\frac{3}{2}}a_2^2a_4^4}{\sqrt{a_1}a_0^5b_4}, \frac{\sqrt{a_1}\sqrt{b_0}a_2^2a_4^2b_5}{a_0^5}, \frac{a_2^3a_4^3b_0}{a_0^6}, \frac{a_1^{\frac{3}{2}}a_0^3c_0}{a_2^2\sqrt{b_0}a_4^2}, \frac{a_2\sqrt{b_0}a_1^{\frac{3}{2}}}{a_4^2}, \\ & \frac{b_3a_1^{\frac{5}{2}}\sqrt{b_0}}{a_0a_4^2}, \frac{a_1^{\frac{5}{2}}b_0^{\frac{3}{2}}a_2^2}{a_0^2a_4^2c_0}, \frac{a_1^{\frac{5}{2}}\sqrt{b_0}a_0}{a_2a_4^2}, \frac{a_1^{\frac{3}{2}}\sqrt{b_0}a_0^2}{a_4^2b_3}, \frac{a_1^3b_0}{a_4^3}, \frac{a_1^2a_0b_0}{a_4^2b_5}, \frac{a_1^{\frac{5}{2}}a_2^2b_0^{\frac{3}{2}}}{a_4^2a_0^2c_6}, \frac{b_0^{\frac{3}{2}}a_2^2\sqrt{a_1}}{a_4^2c_0}, \frac{a_2^2b_0^{\frac{3}{2}}\sqrt{a_1}}{a_4^2b_2}, \frac{a_2\sqrt{a_0}a_1\sqrt{b_0}}{a_4^2}, \\ & \frac{a_1^{\frac{3}{2}}a_0^3b_2}{a_2^2a_4^2\sqrt{b_0}}, \frac{\sqrt{b_0}a_1a_0^{\frac{5}{2}}}{a_2a_4^2}, \frac{a_1^2a_0^2b_4}{a_4^4}, \frac{b_0a_1^{\frac{3}{2}}a_0^{\frac{3}{2}}}{a_4^3}, \frac{a_1^2a_0^6c_6}{a_4^2a_4^4}, \frac{\sqrt{b_0}a_1^{\frac{3}{2}}a_0^3}{a_2^2a_4^2}, \frac{a_2^2a_1^{\frac{5}{2}}\sqrt{b_0}}{a_2^2a_4^2}, \frac{b_0^{\frac{3}{2}}a_1^{\frac{5}{2}}a_0^2}{a_2^2a_4^2b_2}, \frac{a_1^{\frac{5}{2}}\sqrt{b_0}a_0^3b_3}{a_4^2a_4^2}, \frac{b_0^{\frac{3}{2}}a_1^{\frac{5}{2}}a_0^2}{a_2^2a_4^2b_4}, \\ & \left. \frac{\sqrt{b_0}a_1^{\frac{5}{2}}a_0^3b_5}{a_2^2a_4^4}, \frac{b_0a_1^3a_0^3}{a_2^3a_4^3} \right] =: F^{(a,b,c)} \end{aligned} \quad (2.6)$$

The list of the basic h-cubes of the next two 120-velocity models with centers at the center of $H^{(1)}$ and $H^{(2)}$ respectively is given as in the following array.

$$M_0^1 : = \left\{ \begin{array}{cccccccccccc} 12 & 13 & 14 & 0 & 15 & 16 & 17 & 18 & 19 & 20 & 21 & 22 \\ 120 & 121 & 122 & 12 & 123 & 124 & 125 & 126 & 127 & 128 & 129 & 130 \\ 131 & 132 & 133 & 23 & 13 & 122 & 134 & 135 & 136 & 137 & 138 & 139 \\ 23 & 24 & 25 & 26 & 1 & 14 & 27 & 28 & 29 & 30 & 31 & 32 \\ 0 & 1 & 2 & 3 & 4 & 5 & 6 & 7 & 8 & 9 & 10 & 11 \\ 63 & 15 & 5 & 53 & 64 & 65 & 66 & 67 & 68 & 69 & 70 & 71 \\ 140 & 123 & 16 & 63 & 141 & 142 & 143 & 144 & 145 & 146 & 147 & 148 \\ 149 & 150 & 151 & 72 & 152 & 153 & 154 & 155 & 156 & 17 & 126 & 145 \\ 72 & 73 & 74 & 75 & 76 & 77 & 78 & 79 & 80 & 6 & 18 & 68 \\ 157 & 158 & 159 & 89 & 73 & 151 & 160 & 161 & 162 & 27 & 135 & 19 \\ 105 & 106 & 107 & 96 & 108 & 109 & 20 & 10 & 32 & 110 & 111 & 112 \\ 163 & 164 & 165 & 105 & 166 & 167 & 128 & 21 & 139 & 168 & 169 & 170 \\ 171 & 166 & 109 & 113 & 172 & 173 & 146 & 70 & 22 & 174 & 175 & 176 \end{array} \right. \quad (2.7)$$

$$M_0^2 : = \left\{ \begin{array}{cccccccccccc} 23 & 24 & 25 & 26 & 1 & 14 & 27 & 28 & 29 & 30 & 31 & 32 \\ 131 & 132 & 133 & 23 & 13 & 122 & 134 & 135 & 136 & 137 & 138 & 139 \\ 177 & 178 & 179 & 180 & 24 & 133 & 181 & 182 & 183 & 184 & 185 & 186 \\ 180 & 187 & 188 & 189 & 33 & 25 & 190 & 191 & 192 & 193 & 194 & 195 \\ 26 & 33 & 34 & 35 & 36 & 2 & 37 & 38 & 39 & 40 & 41 & 42 \\ 0 & 1 & 2 & 3 & 4 & 5 & 6 & 7 & 8 & 9 & 10 & 11 \\ 12 & 13 & 14 & 0 & 15 & 16 & 17 & 18 & 19 & 20 & 21 & 22 \\ 157 & 158 & 159 & 89 & 73 & 151 & 160 & 161 & 162 & 27 & 135 & 19 \\ 89 & 90 & 91 & 92 & 81 & 74 & 93 & 94 & 95 & 37 & 28 & 8 \\ 196 & 197 & 198 & 199 & 90 & 159 & 200 & 201 & 202 & 190 & 182 & 29 \\ 203 & 204 & 205 & 206 & 97 & 107 & 30 & 41 & 195 & 207 & 208 & 209 \\ 210 & 211 & 212 & 203 & 106 & 165 & 137 & 31 & 186 & 213 & 214 & 215 \\ 105 & 106 & 107 & 96 & 108 & 109 & 20 & 10 & 32 & 110 & 111 & 112 \end{array} \right. \quad (2.8)$$

The node enumeration of M_0^1 and M_0^2 is the same as M_0^0 , i.e $\pi_0^{M^1} = 12, \dots, \pi_{119}^{M^1} = 176$ and $\pi_0^{M^2} = 23, \dots, \pi_{119}^{M^2} = 112$. $M^0 \cup M^1$ is a 177-velocity model and $M^0 \cup M^1 \cup M^2$ is a 216-velocity model.

Proposition B.2 *The equilibria $\mathbf{f} \in \mathcal{E}_{|M^0 \cup M^1}$ of a 177-velocity model is a 7-dimensional manifold.*

proof: Suppose $\mathbf{f} \in \mathcal{E}_{|M^0 \cup M^1}$ be an equilibrium solution of the 177-velocity model $M^0 \cup M^1$. Then by corollary 4.28 \mathbf{f}_{M^0} and \mathbf{f}_{M^1} are the equilibrium solution for M_0 and M^1 respectively. Let $F^{(a',b',c')}$ denote the equilibria \mathbf{f}_{M^1} of the 2nd 120-velocity model (M^1), where $F^{(a,b,c)}$ is the equilibria \mathbf{f}_{M^0} of the first 120-velocity model (M^0) given by equation (2.6). Then the composition $M_0 \cup M^1$ contains 11 new parameters $a'_i, i = 0, \dots, 4; b'_j, j = 0, 2, 3, 4, 5; c'_k, k = 0, 6$. By exploiting the fact that there are some common h-cubes between M^0 and M^1 , the new eleven parameters as well as $b_j, j = 2, \dots, 5$ can be eliminated as follows.

$H_{|M^1}^0 = H_{|M^0}^1$ and so $F_{0,\dots,11}^{(a',b',c')} = F_{12,\dots,14,0,15,\dots,22}^{(a,b,c)}$ respectively. Therefore

$$\begin{aligned} a'_0 &= F_{12}^{(a,b,c)}, \quad a'_2 = F_{13}^{(a,b,c)}, \quad a'_1 = F_0^{(a,b,c)}, \quad a'_4 = F_{17}^{(a,b,c)} \quad (\text{thus all } a' \text{ 's are eliminated}) \\ b_3 &= \frac{a'_2 \sqrt{a'_1}}{\sqrt{a'_0}}, \quad b_5 = \frac{\sqrt{a'_0 a'_1 a'_4}}{a'_0}, \quad \text{and} \end{aligned} \quad (2.9)$$

$$F_8^{(a',b',c')} = F_{19}^{(a,b,c)} \implies b_4 = \frac{a_2 \sqrt{a_1 b_0 a_4 b_0}}{b_2 a_0 a_1}.$$

Again $H_{|M^1}^4 = H_{|M^0}^0$ and so $F_{3,36,43,\dots,52}^{(a',b',c')} = F_{0,\dots,11}^{(a,b,c)}$ respectively. Therefore

$$\begin{aligned} F_{36}^{(a',b',c')} = F_1^{(a,b,c)} &\implies b'_2 = \frac{a'_2{}^2 b'_0 a'_1}{a'_0{}^2 a_2}, \quad F_{43}^{(a',b',c')} = F_2^{(a,b,c)} \implies b'_3 = \frac{a'_1{}^2 b'_0 a'_2{}^2}{a'_0{}^3 F_2^{(a,b,c)}}, \\ F_{44}^{(a',b',c')} = F_3^{(a,b,c)} &\implies b'_0 = \frac{a'_0{}^3 F_3^{(a,b,c)}}{a'_1{}^3}, \quad F_{47}^{(a',b',c')} = F_6^{(a,b,c)} \implies b'_4 = \frac{b'_0 a'_1 a'_4{}^2}{a'_0{}^2 F_6^{(a,b,c)}}, \\ F_{48}^{(a',b',c')} = F_7^{(a,b,c)} &\implies b'_5 = \frac{a'_1{}^2 b'_0 a'_4{}^2}{a'_0{}^3 F_7^{(a,b,c)}} \quad (\text{thus all } b' \text{ 's are eliminated}) \end{aligned} \quad (2.10)$$

Now we eliminate c'_0 , c'_6 and b_2 from $H_{|M^1}^3 = H_{|M^0}^2$ and so $F_{26,33,\dots,36,2,37,\dots,42}^{(a',b',c')} = F_{23,\dots,26,1,14,27,\dots,32}^{(a,b,c)}$ respectively. Therefore

$$\begin{aligned} F_{26}^{(a',b',c')} = F_{23}^{(a,b,c)} &\implies c'_0 = \frac{a'_2{}^4 b'_0}{a'_0{}^3 F_{23}^{(a,b,c)}}, \quad F_{33}^{(a',b',c')} = F_{24}^{(a,b,c)} \implies b_2 = \frac{(b'_0{}^3 a'_1 a_0{}^2)^{\frac{1}{4}} a_2}{a_0 a_1} \\ F_{39}^{(a',b',c')} = F_{29}^{(a,b,c)} &\implies c'_6 = \frac{a'_2{}^6 b'_0{}^{\frac{3}{2}} a'_4{}^2 \sqrt{a'_1}}{a'_0{}^8 F_{29}^{(a,b,c)}} \end{aligned} \quad (2.11)$$

Equating the other common nodes between M^0 and M^1 we obtain identity. Thus we see that all the new 11 parameters a'_i, b'_i, c'_i as well as b_j , $j = 2, \dots, 5$ are eliminated. Thus the remaining parameters are only a_i , $i = 0, 1, 2, 4$; b_0, c_0, c_6 and $\mathbf{f} \in \mathcal{E}_{|177}$ is a 7-dimensional manifold.

Proposition B.3 *The equilibria $\mathbf{f} \in \mathcal{E}_{|M^0 \cup M^1 \cup M^2}$ of a 216-velocity model is a 5-dimensional manifold.*

proof: Suppose $\mathbf{f} \in \mathcal{E}_{|M^0 \cup M^1 \cup M^2}$ be an equilibrium solution of a 216-velocity model $M^0 \cup M^1 \cup M^2$. Then by corollary 4.28 \mathbf{f}_{M^0} , \mathbf{f}_{M^1} , \mathbf{f}_{M^2} are the equilibria in M^0 , M^1 M^2 respectively. Let $F^{(a',b',c')}$ denote the equilibria \mathbf{f}_{M^1} and $F^{(\tilde{a},\tilde{b},\tilde{c})}$ denote the equilibria \mathbf{f}_{M^2} , where $F^{(a,b,c)}$ is the equilibria \mathbf{f}_{M^0} given by equation (2.6). Then the composition $M^0 \cup M^1 \cup M^2$ contains 33 parameters a_i , $i = 0, 1, 2, 4$; b_j , $j = 0, 2, 3, 4, 5$; c_k , $k = 0, 6$; a'_i , $i = 0, 1, 2, 4$; b'_j , $j = 0, 2, 3, 4, 5$; c'_k , $k = 0, 6$ and \tilde{a}_i , $i = 0, 1, 2, 4$; \tilde{b}_j , $j = 0, 2, 3, 4, 5$; \tilde{c}_k , $k = 0, 6$. But in proposition B.2, it is

already shown that $M^0 \cup M^1$ reduced the first 22 parameters to the 7 parameters a_i , $i = 0, 1, 2, 4$; b_0, c_0, c_6 .

We observe further that $H_{|M^2}^0 = H_{|M^0}^2$ and so $F_{0,\dots,11}^{(\tilde{a},\tilde{b},\tilde{c})} = F_{23,\dots,26,1,14,27,\dots,32}^{(a,b,c)}$ respectively. Therefore

$$\begin{aligned} F_0^{(\tilde{a},\tilde{b},\tilde{c})} = F_{23}^{(a,b,c)} &\implies \tilde{a}_0 = F_{23}^{(a,b,c)}, & F_1^{(\tilde{a},\tilde{b},\tilde{c})} = F_{24}^{(a,b,c)} &\implies \tilde{a}_2 = F_{24}^{(a,b,c)}, \\ F_3^{(\tilde{a},\tilde{b},\tilde{c})} = F_{26}^{(a,b,c)} &\implies \tilde{a}_1 = F_{26}^{(a,b,c)}, & F_2^{(\tilde{a},\tilde{b},\tilde{c})} = F_{25}^{(a,b,c)} &\implies c_0 = \frac{(b_0^3 a_1^3 a_0^2)^{\frac{5}{4}} a_2^2}{a_0^4 a_1^4 b_0^3}, \\ F_6^{(\tilde{a},\tilde{b},\tilde{c})} = F_{27}^{(a,b,c)} &\implies \tilde{a}_4 = F_{27}^{(a,b,c)}, & F_8^{(\tilde{a},\tilde{b},\tilde{c})} = F_{29}^{(a,b,c)} &\implies c_6 = \frac{a_2^3 b_0^{\frac{3}{4}} a_4}{a_0^{\frac{7}{2}} a_1^{\frac{1}{4}}}, \end{aligned}$$

Thus \tilde{a} 's and c_0, c_6 are eliminated.

Now $H_{|M^2}^5 = H_{|M^0}^0$ gives $F_{53,4,46,54,\dots,62}^{(\tilde{a},\tilde{b},\tilde{c})} = F_{0,\dots,11}^{(a,b,c)}$ respectively, and so we have

$$\begin{aligned} F_{53}^{(\tilde{a},\tilde{b},\tilde{c})} = F_0^{(a,b,c)} &\implies \tilde{c}_0 = \frac{\tilde{b}_0 \tilde{a}_1}{a_0}, & F_{46}^{(\tilde{a},\tilde{b},\tilde{c})} = F_2^{(a,b,c)} &\implies \tilde{b}_3 = \frac{F_2^{(a,b,c)} \tilde{a}_2^2}{\tilde{a}_1^2}, \\ F_{55}^{(\tilde{a},\tilde{b},\tilde{c})} = F_4^{(a,b,c)} &\implies \tilde{b}_0 = \frac{F_4^{(a,b,c)} \tilde{a}_2^3}{\tilde{a}_1^3}, & F_{58}^{(\tilde{a},\tilde{b},\tilde{c})} = F_7^{(a,b,c)} &\implies \tilde{b}_5 = \frac{F_7^{(a,b,c)} \tilde{a}_0 \tilde{a}_2^2}{\tilde{a}_1^{\frac{5}{2}} \sqrt{\tilde{b}_0}}, \\ F_{59}^{(\tilde{a},\tilde{b},\tilde{c})} = F_8^{(a,b,c)} &\implies \tilde{c}_6 = \frac{\tilde{a}_2^2 \tilde{b}_0 \tilde{a}_1 \tilde{a}_4^2}{\tilde{a}_0^4 F_8^{(a,b,c)}}. \end{aligned}$$

From $H_{|M^2}^6 = H_{|M^0}^1$ we have

$$F_{64}^{(\tilde{a},\tilde{b},\tilde{c})} = F_{15}^{(a,b,c)} \implies \tilde{b}_2 = \frac{F_{15}^{(a,b,c)} \tilde{a}_2^4}{\tilde{a}_0^2 \tilde{a}_1^2}, \quad F_{66}^{(\tilde{a},\tilde{b},\tilde{c})} = F_{17}^{(a,b,c)} \implies \tilde{b}_4 = \frac{\tilde{b}_0^{\frac{3}{2}} \tilde{a}_4^2 \sqrt{\tilde{a}_1}}{\tilde{a}_2^2 F_{17}^{(a,b,c)}}$$

Thus all \tilde{a} 's, \tilde{b} 's, \tilde{c} 's are also eliminated. All other matching nodes gives identity. Therefore, the equilibria $\mathbf{f} \in \mathcal{E}_{|M^0 \cup M^1 \cup M^2}$ can be uniquely parameterized by the 5 parameters a_0, a_1, a_2, a_4, b_0 . \square

Bibliography

- [1] L. Arkeryd, C. Cercignani and R. Illner “*Measure solutions of the steady Boltzmann equation in a slab*”, *Comm. Math. Phys.*, 142: 285-296 (1991).
- [2] L. Arkeryd. “*On the Boltzmann equation*”, *Arch. Rat. Mech. Anal*, 45: 1-34 (1972).
- [3] L. S. Andallah, H. Babovsky. “*A discrete Boltzmann equation based on hexagons*”, *Math. Models Methods Appl. Sci.* vol. 13, No. 11 (2003)1-28 .
- [4] L. S. Andallah. “*On the generation of a hexagonal collision model for the Boltzmann equation*”, accepted for publication in *Comp. Meth. in Appl. Mathematics* Vol. 4, No. 3 (2004), pp 267-285.
- [5] H. Babovsky. “*Hierarchies of reducible kinetic models*”, in: *Discrete Modelling and Discrete Algorithms in Continuum Mechanics*, Th. Sonar and I. Thomas (Eds.), Logos Verlag, Berlin 2001.
- [6] H. Babovsky. “*Hexagonal kinetic models and the numerical simulation of kinetic boundary layers*”, Preprint M 12/03, Inst. f. Mathematik, TU Ilmenau, 2003.
- [7] H. Babovsky. “*A kinetic multiscale model*”, *Math. Models Methods Appl. Sci.*, 12:309-331, 2002.
- [8] H. Babovsky. “*Die Boltzmann-Gleichung*”, Teubner, Stuttgart, 1998.
- [9] H. Babovsky, “*A constructive approach to steady nonlinear kinetic equations*”, *J. of Comp. and Appl. Math.* , 89: 199-211 (1998).
- [10] H. Babovsky, “*A convergence proof for Nabu’s Boltzmann simulation scheme.*”, *Eur. J. Mech., B/Fluids*, 8:41-55, 1989.
- [11] H. Babovsky, “*Time average of simulation schemes as approximations to stationary kinetic equations.*”, *Eur. J. Mech., B/Fluids*, 11:199-212, 1992.
- [12] H. Babovsky, “*On a simulation scheme for the Boltzmann equation*”, *Math. Methods Appl. Sci.*, 8 (1986), pp. 223-233.

-
- [13] H. Babovsky, “*Discretization and numerical schemes for stationary kinetic model equations.* ”, *Comp. Math. Applic.*, 35(1/2): 29-40, 1998.
- [14] C. Bardos, R. E. Caflisch and B. Nicolaenko: “*The Milne and Kremers problem for the Boltzmann equation of a hard sphere gas*”, *Comm. pure Appl. Math.*, 39: 323-352 (1986).
- [15] G. A. Bird, “*Molecular Gas Dynamics and the direct simulation of gas flows* ”, Clarendon Press, Oxford, 1994.
- [16] A. Bobylev, A. Palczewski and J. Schneider. “*On approximation of the Boltzmann Equation by discrete velocity models* ”, *C. R. Acad. Sci. Paris*, I 320(5):639-644, 1995.
- [17] A. Palczewski, J. Schneider and A. Bobylev. “*A Consistency Result for a Discrete-Velocity Model of the Boltzmann Equation*”, *SIAM J. Numer. Anal.* vol. 34, No.5, pp. 1865-1883, October 1997.
- [18] L. Boltzmann. “*Weitere Studien über das Wärmegleichgewicht unter Gas-molekülen*”, *Sitzungsberichte der Akademie der Wissenschaften, Wien*, **66**, 275-370, 1872.
- [19] J. Broadwell, “*Study of a rarefied shear flow by discrete velocity model* ”, *J. Fluid Mech.*, 19 (1964), p. 367-370.
- [20] J. Broadwell, “*Shock structure in a simple discrete velocity gas*”, *Phys. of Fluids*, 7 (1964), p. 1243-1247.
- [21] C. Buet “*A Discrete-Velocity scheme for the Boltzmann Operator of Rarefied Gas Dynamics* ”, *Transport Theory and Statistical Physics*, 25(1),33-60(1996).
- [22] C. Buet, S. Cordier, P. Degond “*Regularized Boltzman Operator*”, *Compters Math. Applic.* Vol. 35, No 1/2, pp. 55-74, 1998 .
- [23] T. Carleman “*Problèmes mathématiques dans la théorie cinétique des gas* ”, *Publ. Sci. Inst. Mittag-Leffler, Almqvist-Wiksell*, Upsala, 1957.
- [24] C. Cercignani. “*The Boltzmann equation and its application*”, Springer-Verlag, New York, 1988.
- [25] C. Cercignani, R. Illner and M. Pulvirenti. “*The mathematical theory of Dilute gases*”, Springer-Verlag, New York, 1995.
- [26] C. Cercignani. “*Rarefied gas dynamics*”, Cambridge University Press, 2000.
- [27] C. Cercignani. “*Mathematical methods in kinetic theory*”, Plenum Press, New York and London 1990.

-
- [28] C. Cercignani. “*Temperature, Entropy, and Kinetic Theory*”, J. of Stat. Phys. vol. 87, Nos. 5/6, 1997.
- [29] A. J. Chorin, “*Numerical solution of Boltzmann’s equation*,” Comm. pure Appl. Math., 25(1972), p. 171-186.
- [30] J. H. Conway, N. J. A. Sloane. “*Sphere packings, Lattices and Groups*”, Springer, 1998.
- [31] F. Coron, F. Golse and C. Sulem “*A classification of well-posed kinetic layers problems*”, Comm. pure Appl. Math., 41(4): 409-435 (1988).
- [32] F. Coron and B. Perthame “*Numerical passage from kinetic to fluid equations*”, SIAM J. Numer. Anal., 28(1991), p. 26-42.
- [33] P. R. Cromwell “*Polyhedra*”, Cambridge university press, 1997.
- [34] L. Desvillettes and S. Mischler “*About the splitting algorithm for Boltzmann and BGK equations*,” Math. Models Methods Appl. Sci. 6(1996), pp. 1079-1101.
- [35] V. Garzó, M. López de Haro “*Nonlinear transport for a dilute gas in steady Couette Flow*”, Phys. Fluids, 9(3): 776, (1997).
- [36] R. Gatignol “*Théorie Cinétique des Gaz à Répartition Discrète de Vitesses*”, Springer Lecture Notes in Physics 36 (1975).
- [37] D. Görsch. “*Generalized discrete velocity models*”, Math. Models Methods Appl. Sci. 12(2002) 49-76.
- [38] D. Görsch. “*Numerics for generalized discrete velocity models*”, Preprint M 25/00, Inst. f. Mathematik, TU Ilmenau, November, 2000.
- [39] J. C. Hang and J. Y. Yang, “*Rarefied flow using nonlinear model Boltzmann equations*”, J. Comput. Phys., 120(1995), p. 323-339.
- [40] R. Illner and H. Neunzert, “*On simulation methods for the Boltzmann equation*”, Transport. Theory Statist. Phys., 16(1987), pp. 141-154.
- [41] T. Inamuro and B. Sturtevant, “*Numerical study of discrete velocity gases*”, Phys. Fluids A, 2(1990), pp. 2196-2203.
- [42] T. Inamuro, in “*Rarefied gas dynamics: Physical Phenomena*”, edited by E. P. Muntz, D. P. Weaver and D. H. Campbell (AIAA, Washington, DC, 1989), p. 418.
- [43] M. Junk, S. V. Raghurama Rao. “*A new discrete velocity method for Navier-Stokes equations*”, J. comp. Phys. vol. 155, 178-198, (1999).

-
- [44] M. Junk, A. Klar, L.-S. Luo. “*Asymptotic analysis of the lattice Boltzmann equation*”, Submitted to J. comp. Phys., 2004.
- [45] M. Junk, W.-A. Yong. “*Rigorous Navier-Stokes limit of the lattice Boltzmann equation*”, Asymptotic Analysis, 35:165-184, 2003.
- [46] M. Junk. “*A finite difference interpretation of the the lattice Boltzmann method*”, Num. meth. partial diff. equations 17:383-402, 2001.
- [47] M. Junk, A. Klar. “*Discretization for the incompressible Navier Stokes equations based on the lattice Boltzmann method*”, SIAM J. of Sci. Comp., 22, 1-19, 2000.
- [48] A. Klar. “*Relaxation scheme for a lattice Boltzmann-type discrete velocity model and numerical Navier-Stokes Limit* ”, J. of Comp. Phys. 148, 1-17, 1999.
- [49] C. S. Kim, J. W. Dufty, A. Santos and J. J. Brey “*Analysis of nonlinear transport in Couette flow*”, Phys. Rev., 40(A): 12, (1989).
- [50] J. M. Montanero, V. Garzó “*Nonlinear Couette Flow in a dilute gas: Comparison between theory and molecular-dynamics simulation*”, Phys. Rev., 58(E): 1836-1842, (1998).
- [51] M. Krook and T. T. Wu “*Formation of Maxwellian Tails*”, Phys. Rev. Lett. Vol. 36, p. 1107 (1976).
- [52] K. Nanbu, “*Direct simulation scheme derived from the Boltzmann equation. I. Monocomponent gases*”, J. Phys. Soc. Japan, 52(1983), pp. 2042-2049.
- [53] K. Nanbu, “*Interactions between various direct simulation methods for solving the Boltzmann equation.* ”, J. of the Physical Society of Japan, 52: 3382-3388, 1983.
- [54] N. A. Nurlybaev. “*Discrete Velocity Method in the theory of kinetic equations*”, Trans. Theo. and stat. Phys., 22(1):109-119, 1993.
- [55] H. Neunzert, and J. Struckmeier, “*Particle methods of the Boltzmann equation*”, Acta Numerica, p. 417-457, 1995.
- [56] T. Ohwada, “*Structure of normal shock waves: Direct numerical analysis of the Boltzmann equation for hard sphere molecules* ”, Phys. Fluid A, 5(1993), p. 217-234.
- [57] A. Palciewski and J. Schneider. “*Existence, stability and convergence of solutions of discrete velocity models to the Boltzmann equation* ”, J. Stat. Phys., 91(1/2):307-326, 1998.

-
- [58] T. Platkowski and R. Illner. “*Discrete Velocity Models of the Boltzmann Equation - A Survey on the Mathematical Aspects of the Theory*”, SIAM Review 30, pp. 213-255, June, 1988.
- [59] B. Perthame, “*Introduction to the theory of random particle methods for Boltzmann equation*”, in Advances in Kinetic Theory and Computing, B. Perthame, ed., World Scientific, River Edge, NJ, 1994.
- [60] D. Risso, P. Cordero “*Dilute gas Couette Flow : Theory and molecular dynamic simulation*”, Phys. Rev., 56(E): 489-498, (1997).
- [61] L. Pareschi and G. Russo. “*Numerical solution of The Boltzmann equation I : Spectrally accurate approximation of the collision operator*”, SIAM J. Num. Anal., 37:1217-1245, 2000.
- [62] F. Rogier and J. Schneider. “*A Direct Method for Solving the Boltzmann Equation*”, Trans. Theo. and stat. Phys., 23(1-3):313-338, 1994.
- [63] B. Shizgal and Ed. Weaver, D., “*Rarefied Gas Dynamics: Theory and Simulations*”, Washington, 1994.
- [64] Y. Sone, T. Ohwada and K. Aoki, “*Temperature jump and knudsen layer in a rarefied gas over a plan wall: Numerical analysis of the linearized Boltzmann equation for hard-sphere molecules*”, Phys. Fluids A, 1 (1989), p. 363-370.
- [65] D. R. Willis. “*Comparison of kinetic theory analysis of linearized Couette Flow*”, Phys. Fluids, 5(2): 127-135, (1962).

Zusammenfassung der Dissertationsschrift

In kompakter Form werden die Hauptergebnisse der diskreten Boltzmann-Gleichung basierend auf hexagonalen Elementen vorgestellt. Zwecks Lösung dieses Problems mittels des hexagonalen diskreten Geschwindigkeitsmodells, werden im \mathbb{R}^2 automatisch beliebig große Sechseckgitter generiert. Zur Identifikation jeder Sechseckstruktur wird gezeigt, dass der Mittelpunkt eines beliebigen regulären Hexagons entweder in die Mitte eines Basishexagons fällt oder ein Gitterknoten ist. Wir beweisen, dass bei Zugrundelegung des binären Stoßgesetzes der globale Stoßoperator in einem beschränkten Sechseckgitter in \mathbb{R}^2 nur eine künstliche Invariante besitzt, die auch aufgezeigt wird. Wir formulieren ein N -Schicht-Modell zum Aufstellen von generellen Formeln für alle möglichen regulären Hexagons auf dem Gitter G_N dieser Schicht und beweisen damit ihre Existenz. Dazu bestimmen wir den numerischen Aufwand (flops) zur Auswertung des Boltzmann Stoßoperator im N -Schicht-Modell.

Weiterhin entwickeln wir die kinetische Theorie der diskreten Boltzmann-Gleichung für eine hexagonale Diskretisierung in \mathbb{R}^3 . Das hexagonale Stoßmodell in \mathbb{R}^3 wird vorgestellt und das lokale Stoßmodell dazu ist ein 12-Geschwindigkeitsmodell entsprechend den 12 Ecken eines Kubischen Oktahedron ('hexagonaler Kubus' bzw. 'h-Kubus'). Die Berücksichtigung nur des binären Stoßgesetzes in dem lokalen Stoßmodell führt hier auf drei künstlichen Invarianten. Aber bei Einbeziehung des Drei-Teilchen-Stoßgesetzes wird das Auftreten dieser künstlichen Invarianten vermieden. Wir beweisen, dass das 3D-hexagonale Modell die grundlegenden Eigenschaften der klassischen kinetischen Theorie erfüllt. Schließlich zeigen wir noch, dass dieses 3D-Modell der genannten Theorie auch mit dem 2-Teilchen-Stoßgesetz ab dem 216-Geschwindigkeitsmodell genügt.

Wir präsentieren die Konstruktionen der Gleichgewichtsverteilung für das allgemeine 2D N -Schicht-Modell und für das 3D-Modell, wobei die Gleichgewichtsverteilung sich auf die Parameter von Masse, Momenten und kinetischen Energie beziehen. Wir geben dazu numerische Ergebnisse für das 2D als auch 3D hexagonale Modell an.

Abstract

We present briefly the main results of a discrete Boltzmann equation based on hexagons. In order to solve the Boltzmann equation by a hexagonal discrete velocity model, we generate a hexagonal grid in \mathbb{R}^2 which provides the basic as well as all possible larger hexagons (on which the local collision models are based) automatically. To identify all these regular hexagons, we prove that the centers of all regular hexagons constructed by the nodes of the hexagonal grid on \mathbb{R}^2 , is either a center of the regular basic hexagons or a node of the grid. We also prove that if we only include binary collision law, then the global collision operator based on any size of bounded hexagonal grid in \mathbb{R}^2 provides only one spurious invariant and this only spurious invariant is identified. We give notion of a N -layer model which is conducive to find general formulae for all possible regular hexagons contained in the grid \mathcal{G}_N of the N -layer model and we prove the existence of all these regular hexagons in the grid \mathcal{G}_N . We determine the computational costs (in floating point operation) for the evaluation of the Boltzmann collision operator based on the N -layer model.

We develop the kinetic theory of a discrete Boltzmann equation based on hexagonal discretization of \mathbb{R}^3 . A hexagonal collision model in \mathbb{R}^3 is introduced and the local collision model in \mathbb{R}^3 is a twelve-velocity model corresponding to the twelve vertices of a cub-octahedron (we call 'hexagonal cube' or abbreviated as 'h-cube'). The inclusion of only binary collision law in the local collision model produces three spurious invariants. Thus ternary collision law is imposed to avoid the spurious invariant. We prove that the 3D hexagonal model satisfies the basic features of the classical kinetic theory. Finally, we prove that the basic kinetic features are satisfied for the 3D hexagonal model based on only binary collision law and for this our basic regular collision model is a 216-velocity model.

We present constructions of the equilibrium distribution for the 2D (for the generalized N -layer model) and the 3D hexagonal model where the equilibria is described by the parameters characterizing mass, momenta and kinetic energy. We present numerical results based on both 2D and 3D hexagonal collision model.

Erklärung

Ich versichere, dass ich die vorliegende Arbeit ohne unzulässige Hilfe Dritter und ohne Benutzung anderer als der angegebenen Hilfsmittel angefertigt habe. Die aus anderen Quellen direkt oder indirekt bernommenen Daten und Konzepte sind unter Angabe der Quelle gekennzeichnet.

Weitere Personen waren an der inhaltlich-materiellen Erstellung der vorliegenden Arbeit nicht beteiligt. Insbesondere habe ich hierfür nicht die entgeltliche Hilfe von Vermittlungs- bzw. Beratungsdiensten (Promotionsberater oder anderer Personen) in Anspruch genommen. Niemand hat von mir unmittelbar oder mittelbar geldwerte Leistungen für Arbeiten erhalten, die im Zusammenhang mit dem Inhalte der vorgelegten Dissertation stehen.

Die Arbeit wurde bisher weder im In- noch im Ausland in gleicher oder ähnlicher Form einer Prüfungsbehörde vorgelegt.

Ich bin darauf hingewiesen worden, dass die Unrichtigkeit der vorstehenden Erklärung als Täuschungsversuch angesehen wird und den erfolglosen Abbruch des Promotionsverfahrens zu Folge hat.

Ilmenau, den 10. November 2004

Laek Sazzad Andallah